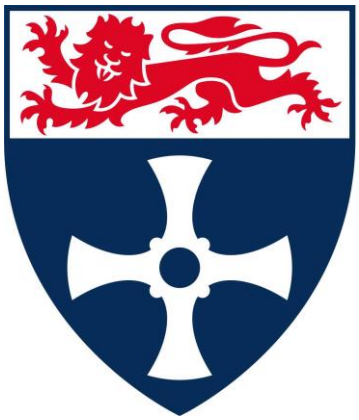

Mitochondrial DNA replication and biogenesis during embryonic development and in disease.

Phillippa Carling

(BSc Hons)

Thesis submitted to Newcastle University in candidature for the degree of Doctor of Philosophy

Institute of Genetic Medicine

Wellcome Trust Centre for Mitochondrial Research

June 2014

Abstract

Regulation of mtDNA content is critical to normal human health and is often abnormal in mitochondrial diseases. Only a proportion of a female's mtDNA is used to populate the oocytes she forms during embryogenesis. This mtDNA bottleneck can cause rapid shifts in heteroplasmy levels between generations in families with mtDNA mutations.

The heteroplasmy levels of several mtDNA mutations were analysed from mother-child pairs using previously validated pyrosequencing assays. Analysis of the shifts in heteroplasmy caused by the mtDNA bottleneck reveals that the inheritance of the pathogenic tRNA mutations m.3243A>G and m.8344A>G do not show selection bias. However, the distribution of m.8993T>G (in *MT-ATP6*) in offspring suggests this mutation is selected for during the mtDNA bottleneck. This finding is in agreement with meta-analysis performed on previously published data, which also reveals biased inheritance of the LHON mutations m.11778G>A and m.3460G>A, in Complex I genes. Selection for these mutations explains the higher prevalence of homoplasmy, as fixation can occur within fewer generations.

Crucial to formation of the mtDNA bottleneck is the dramatic increase in mtDNA replication rate that allows primordial germ cells (PGCs) to repopulate their mitochondrial genomes. Gene expression analysis during pre-implantation embryonic development has not revealed any other biological processes associated with regulation of mtDNA copy number. Upregulation of *Lrpprc* correlates with the expression of transcription factors as pre-implantation development progresses at this stage. The limited number of PGCs in the early stages of post-implantation development prevented sufficient quantity of high-quality RNA to be isolated for use with gene expression analysis.

The reduction of mtDNA copy number observed during the mtDNA bottleneck was modelled in myoblasts and fibroblasts, using ddC, a reverse transcriptase inhibitor. Although some gene expression changes were induced during repopulation of mtDNA, these were limited to below 3-fold change. Forcing reliance on oxidative phosphorylation through culture with galactose media could not increase the rate of mtDNA replication or induce greater gene expression responses.

Ragged-red fibres (RRFs) are a common hallmark of many mitochondrial diseases, caused by proliferation of mitochondria in the subsarcolemmal region of muscle tissue. Multiplex immunohistochemistry allowed fibre typing and identification of RRFs in muscle tissue from a patient with the m.8344A>G mutation. A novel technique was

established to ensure extraction of intact high-quality RNA from laser-microdissected muscle fibres. The RNA was used in a pilot microarray experiment to study the differences not only between control and patient tissue, but specifically within RRF, and has identified a multitude of potential signalling pathways involved in mitochondrial biogenesis and formation of RRFs.

This thesis reveals the complexity of mtDNA copy number regulation and, the critical involvement it has to human health and the inheritance and pathogenicity of mitochondrial diseases.

This thesis is dedicated to my Mum and Sister for their continued support and love, and to my Dad for my love of science.

Acknowledgements

I would firstly like to thank my supervisor Prof. Patrick Chinnery for the opportunity to undertake a PhD in his fantastic group and the guidance, encouragement and expert-knowledge I have received over the last four years. The freedom I was given over my project may have been my downfall at times, but has ignited a passion for further research and understanding in mitochondrial disease, which will stay with me forever. For that I am truly grateful.

I extend my thanks everyone who assisted me during my PhD, in particular Prof. Rob Taylor and Charlotte Alston at the NCG Mitochondrial Diagnostic Service (Newcastle), whose diligence and support have been instrumental to the success of two of my projects. I'd like to thank Mojgan Reza and the Neuromuscular Biobank for providing fibroblast and myoblast cell lines for my projects. Finally, I would like to acknowledge and thank all patients and individuals who contribute biological samples which have benefitted my projects.

My thanks go to all members of the PFC lab, who have helped me develop the techniques and comprehension of science and research that will hopefully remain useful to me throughout a career in academia. They have all made this PhD an enjoyable, exciting experience which I will remember forever. I would especially like to thank Dr Angela Pyle for her continued, caring support throughout my PhD, especially during the bumpy bits and the writing of this thesis. I would also like to thank Dr Gavin Hudson for always being willing to humour me during my crazier scientific hypothesising and for the thought-provoking conversations on science, life and anything.

My special thanks go to Dr Vivienne Neeve, the Fizz to my Pop. Never far from my side, I know I could not have accomplished anything during this PhD without her love, support and friendship. Being both completely different and yet completely the same and bonded through the trauma and excitement of studying for a PhD together, I know this is a unique friendship I won't find anywhere else.

I thank my new friends and work colleagues in Sheffield, who have also been essential in making the transition from PhD student to researcher as smooth as possible. The majority of this thesis was written whilst you supported me in my new home, and I am grateful for your open welcome and friendship.

My final thanks go to my family. Kathy is always there to help and support me, even when I don't know I need it. I know that things will always work out alright, because she is there for me. I am lucky to have someone to trust so completely with my well-being. Any achievements in my life have only been possible through the continued love and support I've received from my mother. She raised me to be enthusiastic about knowledge, and gave me the confidence to achieve what I want. Most importantly of all, I thank her for the mtDNA.

List of Contents

List of Figures

Chapter 1

Chapter 2

Chapter 3

Chapter 4

Chapter 5

List of Tables

Chapter 1

Chapter 3

Chapter 4

Chapter 5

Chapter 6

Author's Declaration

This thesis is submitted to the degree of Doctor of Philosophy in Newcastle University. The research detailed within was performed with the Mitochondrial Research Group within the Institute of Ageing and Health and Institute of Genetic Medicine, and is my own work unless otherwise stated. The research was carried out under the supervision of Professor Patrick Chinnery between October 2009 and October 2012.

I certify that none of the material offered in this thesis has been previously submitted by me for a degree or any other qualification at this or any other university.

Phillippa Carling

List of Publications

1. PJ Carling, LM Cree, PF Chinnery. (2011) “The implications of mitochondrial DNA copy number regulation during embryogenesis.”

   Mitochondrion. 2011 Sep;11(5):686-92. Review.

   PMID: 21635974

Abbreviations

ADP	Adenosine diphosphate
ANOVA	Analysis of variance
APS	Ammonium persulfate
aRNA	antisense RNA
ATP	Adenosine triphosphate
bp	Base pair
BSA	Bovine Serum Albumin
COX	Cytochrome c oxidase
Ct	Threshold cycle
DAB	Diaminobenzidine tetrahydrochloride
DAPI	4’-6-Diamidino-2-phenylindole
ddC	2'-3'-dideoxycytidine (Zalcitabine)
DEPC	Diethyl pyrocarbonate
dH_2O	Distilled water
D-loop	Displacement loop
DMEM	Dulbecco’s modified Eagle’s medium
DMSO	Dimethyl sulphoxide
DNA	Deoxyribonucleic acid
dNTPs	Deoxyribonucleotides
d.p.c.	Days post coitum
DPX	Distyrene-plasticizer-xylene
EDTA	Ethylene diamine tetra-acetic acid
EtBr	Ethidium bromide
ETC	Electron Transport Chain
FACS	Fluorescence-activated cell sorting
$FAD(H_2)$	Flavin adenine dinucleotide (reduced)

FBS	Fetal Bovine Serum
FITC	Fluorescein
hCG	Human chorionic gonadotrophin
HRP	Horseradish peroxidase
HSP	Heavy strand promoter
H-Strand	Heavy strand
IMM	Inner mitochondrial membrane
IMS	Intermembrane space
IPTG	Isopropyl β-D-1-thiogalactopyranoside
kDa	Kilodalton
kb	Kilobase (pairs)
LHON	Leber hereditary optic neuropathy
LMD	Laser Microdissection
L-Strand	Light strand
MELAS	Mitochondrial encephalopathy lactic acidosis and stroke-like episodes
MERRF	Myoclonic epilepsy and ragged-red fibres
mRNA	Messenger RNA
mtDNA	Mitochondrial DNA
$NAD(^{+}/H)$	Nicotinamide adenine dinucleotide (oxidised/reduced)
NBT	Nitroblue tetrazolium
NCR	Non-coding region
nDNA	Nuclear DNA
O_H	Heavy-strand origin of replication
O_L	Light-strand origin of replication
OCT	Optimum cutting temperature (medium)
OMM	Outer mitochondrial membrane
OXPHOS	Oxidative phosphorylation

PAGE	Polyacrylamide gel electrophoresis
PBS	Phosphate buffered saline
PCR	Polymerase chain reaction
PFA	Paraformaldehyde
PGCs	Primordial germ cells
Pi	Inorganic phosphate
PMS	Phenazine methosulphate
PMSF	Phenylmethylsulfonyl fluoride
PVDF	Polyvinyliden fluoride
Q	Ubiquinone (Coenzyme Q_{10})
QH_2	Ubiquinol (Dihydroquinone)
RFLP	Restriction fragment length polymorphism
RFU	Relative fluorescence units
RIN	RNA integrity number
RITOLS	Ribonucleotide incorporation throughout the lagging strand
RNA	Ribonucleic acid
ROS	Reactive Oxygen Species
RRF	Ragged-red fibres
rRNA	Ribosomal RNA
SDH	Succinate dehydrogenase
SDS	Sodium dodecyl sulphate
TAE	Tris-acetate EDTA
Taq	DNA polymerase from *Thermus aquaticus*
TCA Cycle	Tricarboxylic Acid cycle
TTBS	Tween-20 tris buffered saline
TEMED	Tetramethylethylenediamine
TIM	Translocase of the outer mitochondrial membrane

TLDA	TaqMan low density array
TOM	Translocase of the outer mitochondrial membrane
Tris-HCl	Tris(hydroxymethyl)aminomethane-Hydrochloride
Tris	2-amino-2-hydroxymethyl-propane-1,3-diol
tRNA	Transfer RNA
TTBS	Tween20-Tris buffered saline
UV	Ultra-violet
v/v	Volume/Volume
WT	Wild-type
w/v	Weight/volume
x g	Relative centrifugal force

Chapter 1. Introduction

Table of Contents

1.1 An Introduction to Mitochondria

1.1.1 The origins of mitochondria

The prokaryotic ancestors of eukaryotes

Mitochondria in eukaryotes are believed to be the result of an endosymbiosis between an oxidative bacterial cell and a primitive glycolytic cell (Margulis, 1971). Identification of mitochondrial heat shock protein-60 (Hsp60; *HSPD1*) genes in the nuclear genomes of seemingly amitochondriate 'archezoa' (Clark and Roger, 1995, Roger, 1999) and the identification of anaerobic homologue organelles, hydrogenosomes (Muller, 1993) and mitosomes (Tovar *et al.*, 1999), disproved the concept of an amitochondriate lineage of eukaryotes.

Phylogenetic analysis of both protein-coding and ribosomal RNA genes suggest the ancestor of mitochondria to be an α-proteobacteria (Gray, 1998). The host of the endosymbiotic event is more difficult to determine (Baldauf *et al.*, 1996, Harris *et al.*, 2003, Woese *et al.*, 1990). Reanalysis of phylogenetic trees, constructed from rRNA genes, using more appropriate models (accounting for composition heterogenetity), support the 'eocyte hypothesis', and propose *Crenarchaea* as the archaebacterial host of the endosymbiotic event (Cox *et al.*, 2008).

Phylogenetic sequence comparisons between endosymbiont-derived eukaryotic genes and eubacteria date the endosymbiotic event to approximately 1-2 billion years ago (Feng *et al.*, 1997, Sicheritz-Ponten *et al.*, 1998).

From the endosymbiotic event to modern eukaryotic mitochondria

The nuclear and mitochondrial genomes (nDNA and mtDNA respectively) in modern eukaryotes are highly diversified, and in most cases vary widely from that of the ancestral host or endosymbiont. This is a combination of genetic drift, reductive evolution, and gene transfer from the mitochondria to the nucleus.

Due to the uniparental inheritance of mtDNA and the bottleneck created during embryogenesis, mtDNA transmission shares many characteristics with the genomes of small asexual populations of intracellular obligates. Evolution of the genome is strongly affected by drift, Muller's ratchet and gene redundancy caused by the presence of the host genome leading to purifying selection (Andersson and Kurland, 1998).

The key difference between parasitic and organellar genome reduction is that organelles often still require the products of the genes on their genomes. However, since mtDNA has a high mutation rate, no recombination and is uniparentally inherited, it is advantageous to translocate genes to the more stable nDNA to improve cellular fitness (Timmis *et al.*, 2004). This may be achieved through incorporation of nucleic acid fragments into the nuclear genome, as a by-product of autophagy, followed by purifying selection (Berg and Kurland, 2000).

The reductive evolution of mtDNA in animals appears to have stopped, since all animal mtDNA contain the same 37 genes, with a few exceptions including: nematodes, bivalves and cnidarians (Boore, 1999). However, analysis of human nuclear DNA reveals fragments of mtDNA sequence (known as nuclear mitochondrial sequences, NUMTS) are being continually integrated into the nuclear genome, presumably by the same process, but without redundancy and removal of the gene encoded on the mtDNA (Mourier *et al.*, 2001).

Alongside transfer of genes to the nucleus, the nDNA evolved novel mitochondrial genes to complement the presence of the mitochondria. Studies of yeast mitochondrial proteins found that only half had prokaryotic homologues, with most mitochondrial regulatory and transport proteins evolving during development of eukaryotic lineages (Karlberg *et al.*, 2000).

The benefits of the endosymbiotic event

Arguably the largest benefit of the endosymbiotic event and acquiring mitochondria is a 200,000-fold increase in nuclear genome size compared to bacteria. Since expression of genes as proteins is highly energy-demanding, the development of a mitochondria allows cells a more diverse and highly expressed proteome in eukaryotes (Lane and Martin, 2010). This may explain why complex, multicellular life has been able to evolve in several eukaryotic groups, but never in prokaryotic lineages (Rokas, 2008).

1.1.2 Mitochondrial morphology and structure

The diversity of mitochondrial organelles

Mitochondria are diverse across eukaryotic lineages. The majority are aerobic mitochondria which, through consumption of oxygen and oxidative phosphorylation, efficiently produce ATP from supplied substrates. However, many eukaryotes live in

low oxygen or oxygen-free environments and have evolved anaerobic mitochondria. These systems still have an electron transport chain (ETC), but use substrates other than oxygen as their final electron acceptor, and consequently do not have H_2O as their end products. Some anaerobic mitochondria use environmentally available compounds as electron acceptors, such as NO_3^-, but some others use endogenously produced products such as fumarate. However, anaerobic respiration is much less efficient, producing only ~5 mol ATP per 1 mol glucose (compared to 36 mol using oxygen) (Tielens *et al.*, 2002). Hydrogenosomes are highly reduced mitochondrial homologues, found in some intracellular obligate parasites, which do not undergo oxidative phosphorylation and usually do not contain DNA. Instead, pyruvate:ferredoxin oxidoreductase (PFO) metabolises pyruvate to generate electrons, which are transferred to hydrogenase by ferredoxin, producing hydrogen and a small amount of ATP (~4 mol) (Embley *et al.*, 2003). Mitosomes are even further reduced, have never been found with a genome, and are only 0.2-0.5 µm in diameter. The ATP generating processes in eukaryotes containing mitosomes are situated in the cytosol, not in the mitosome itself, and ATP production is very low (~2-4 mol) (Aguilera *et al.*, 2008).

Aerobic mitochondrial structure in mammals

When mitochondria were first visualised by electron microscopy they were described as small, discrete vesicles with two membranes: the smooth outer membrane (OM) and invaginated inner membrane (IM), forming cristae. This compartmentalised the mitochondria into an intermembrane space (IMS), between the membranes, and the internal matrix contained by the IM (Palade, 1952). This led to the 'Baffle' model of mitochondrial structure, whereby the cristae of the inner membrane have wide openings into the intermembrane space, and stretch across the width of the matrix. However, the development of electron microscopic tomography allowed imaging of much thicker sections of tissue, at multiple angles. The cristae were more tubular in nature, with narrow joints to the inner membrane, called cristae junctions, suggesting that the cristae form separate pockets from the intermembrane space (Mannella *et al.*, 1994, Perkins *et al.*, 1997). Additionally, fluorescent microscope studies of human cultured cells revealed mitochondria as dynamic tubule networks, not discrete organelles (Bereiter-Hahn and Voth, 1994) (Figure 1.1A-C).

The IM is the site of oxidative phosphorylation (OXPHOS), but is also the site of many other components essential for mitochondrial function, including: mtDNA-containing nucleoids, mitoribosomes and the protein and solute transport machinery (Gilkerson *et al.*, 2003, Wang and Bogenhagen, 2006) (Figure 1.1D).

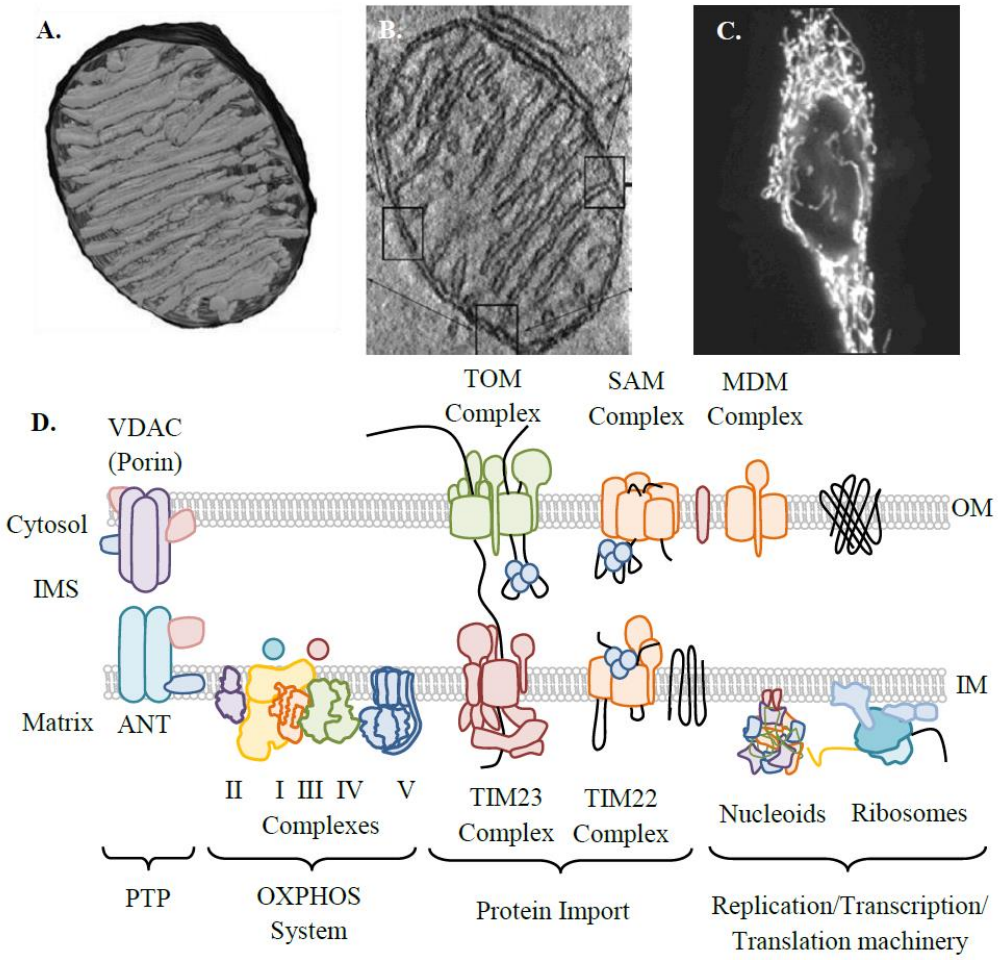

Figure 1.1 Mitochondrial structure and membrane components. (A) Computer generated 3D tomogram of a mitochondrion from chick cerebellum and (B) a single cross-section through the 3D tomogram allowing measurement of membrane dimensions (Adapted from Frey and Mannella, 2000). (C) Mitochondrial network morphology in wild-type HeLa cells (Benard *et al.*, 2007). (D) Major components of the mitochondrial outer membrane (OM) and inner membrane (IM) including (from left to right) the mitochondrial permeability transition pore (PTP), components of the OXPHOS system, protein import channels, nucleoids (comprising mtDNA and supporting proteins) and mitoribosomes involved in replication, transcription and translation.

1.1.3 An overview of mitochondrial functions

Energy metabolism is the primary function of mitochondria, but they also play a critical role in a number of other cellular processes.

Adaptive thermogenesis

In response to certain stimuli, such as cold temperatures or overfeeding, mitochondrial can increase energy expenditure, in a process known as adaptive thermogenesis. This is achieved by uncoupling the ETC from ATP synthesis, and dissipating the excess cellular energy as heat (Lowell and Spiegelman, 2000). In small mammals, this is mainly achieved by brown fat tissue; however, in humans this can be achieved in skeletal muscle (Wijers *et al.*, 2008). Adaptive thermogenesis is closely linked to the regulation of mitochondrial biogenesis and may present a therapeutic target to tackle obesity.

Calcium homeostasis

Cytosolic calcium ions (Ca^{2+}) must be maintained at extremely low concentrations to avoid toxicity. This achieved by both the endoplasmic reticulum (ER) and the mitochondria. Inositol 1,4,5-trisphosphate (IP_3) gated channels in the ER release Ca^{2+} in the vicinity of mitochondria, creating microdomains of high Ca^{2+} concentration, and stimulating uptake by mitochondria (Rizzuto *et al.*, 1993). Calcium homeostasis is important to the correct functioning of mitochondria. Intramitochondrial Ca^{2+} levels can alter the activity of key enzymes in the tricarboxylic (TCA) cycle (McCormack *et al.*, 1990), and is essential for maintenance of cellular bioenergetics in response to nutrient deprivation (Cardenas *et al.*, 2010). Apoptosis and necrosis are also regulated through alterations in mitochondrial Ca^{2+} concentrations (Chami *et al.*, 2004).

Apoptosis

The BCL-2 family of proteins regulate apoptosis ultimately through regulation of the permeability of the OM (Oltvai *et al.*, 1993). If apoptosis is triggered, OM permeability allows the release of intermembrane space proteins into the cytosol, including cytochrome c and apoptotic protease activation factor 1 (encoded by *APAF1*), forming the ‘apoptosome’. This subsequently activates the caspase cascade, responsible for the organised destruction of cellular content (Spierings *et al.*, 2005). Importantly, many of the proteins central to apoptosis regulation also have key functional roles in

mitochondrial bioenergetics, such as *BCL2* involvement in complex IV assembly, and apoptosis inducing factor 1 (*AIFM1*) as a protector from oxidative stress (Kilbride and Prehn, 2012).

Iron-sulphur (Fe-S) cluster and haem biogenesis

Several components of the ETC require Fe-S clusters or haem prosthetic groups to form redox centres within the complex structures. In addition, other mitochondrial proteins also require Fe-S clusters, such as mitochondrial aconitase (*ACO2*), participating in the TCA cycle, and glutaredoxin 2 (*GLRX2*), involved in redox signalling and oxidative stress. Furthermore, Fe-S clusters produced in the mitochondria are essential for many nuclear and cytosolic proteins such as ATP-binding cassette, sub-family E, member 1 (*ABCE1*), involved in ribosome assembly and xanthine dehydrogenase (*XDH*), functioning in purine metabolism (Gille and Reichmann, 2011). Mitochondrial Fe-S biogenesis also functions as a sensor for intracellular iron acquisition and distribution (Lill et al., 2012). The importance of Fe-S cluster biogenesis can be highlighted by the existence of mitosomes, ancient mitochondrial homologues that have lost all major functions except Fe-S cluster formation (Tovar et al., 2003).

1.2 Energy metabolism

1.2.1 Metabolic pathways prior to oxidative phosphorylation

OXPHOS requires specific substrates first generated by downstream metabolic processes. Glycolysis is a 10-step cytosolic process, which converts one molecule of glucose to two molecules of pyruvate (Figure 1.2). The first phase consumes ATP to convert glucose into two glyceraldehyde-3-phosphate (G3P) molecules. The second phase, converts the G3P into pyruvate, producing both a small amount of ATP and NADH.

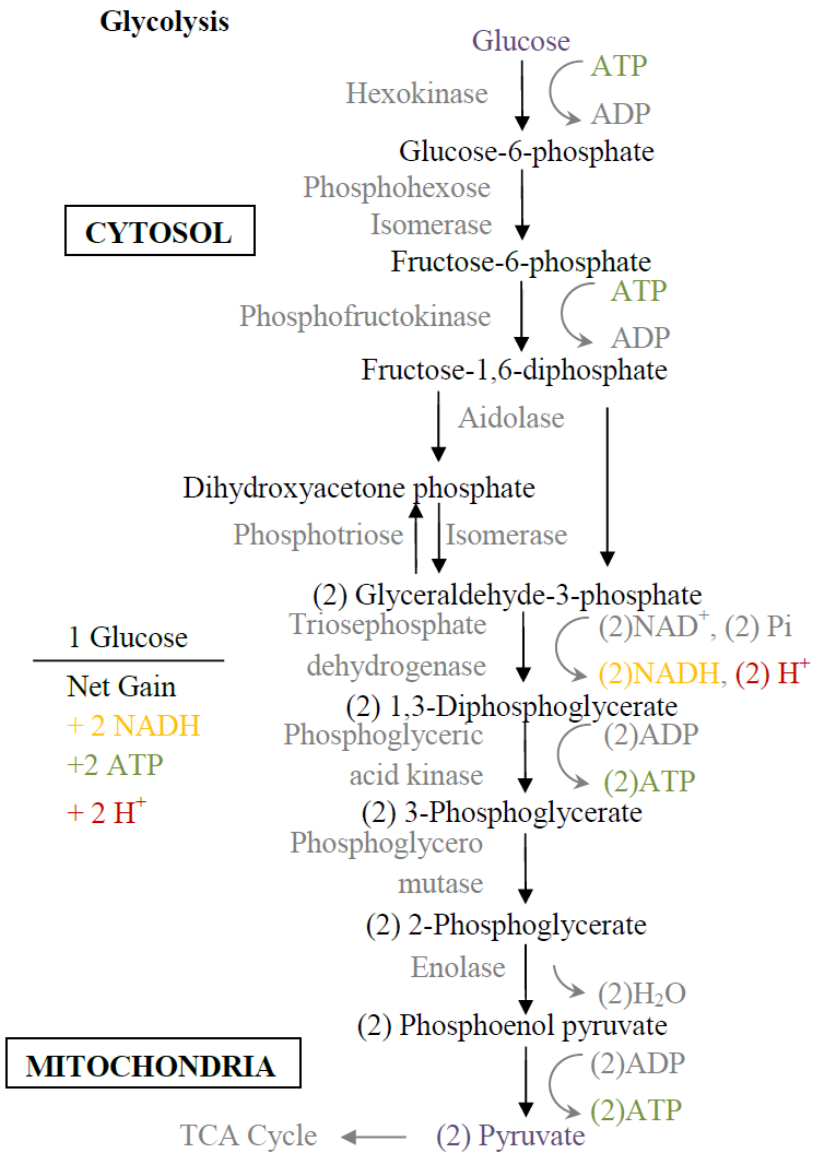

Figure 1.2 An overview of glycolysis. The metabolic pathway converting glucose to pyruvate. Many other carbohydrates can enter glycolysis at alternative stages to contribute to the TCA cycle and ultimately oxidative phosphorylation. From each molecule of glucose there is a net gain of two NADH and two ATP molecules.

The pyruvate is then transported to the mitochondria, where pyruvate dehydrogenase converts it to acetyl-CoA, which then partakes in the tricarboxylic acid (TCA) cycle (Figure 1.3). The main products of the TCA cycle are NADH, utilised by Complex I (NADH dehydrogenase) and $FADH_2$, used by Complex II (Succinate dehydrogenase; also partaking in the TCA cycle).

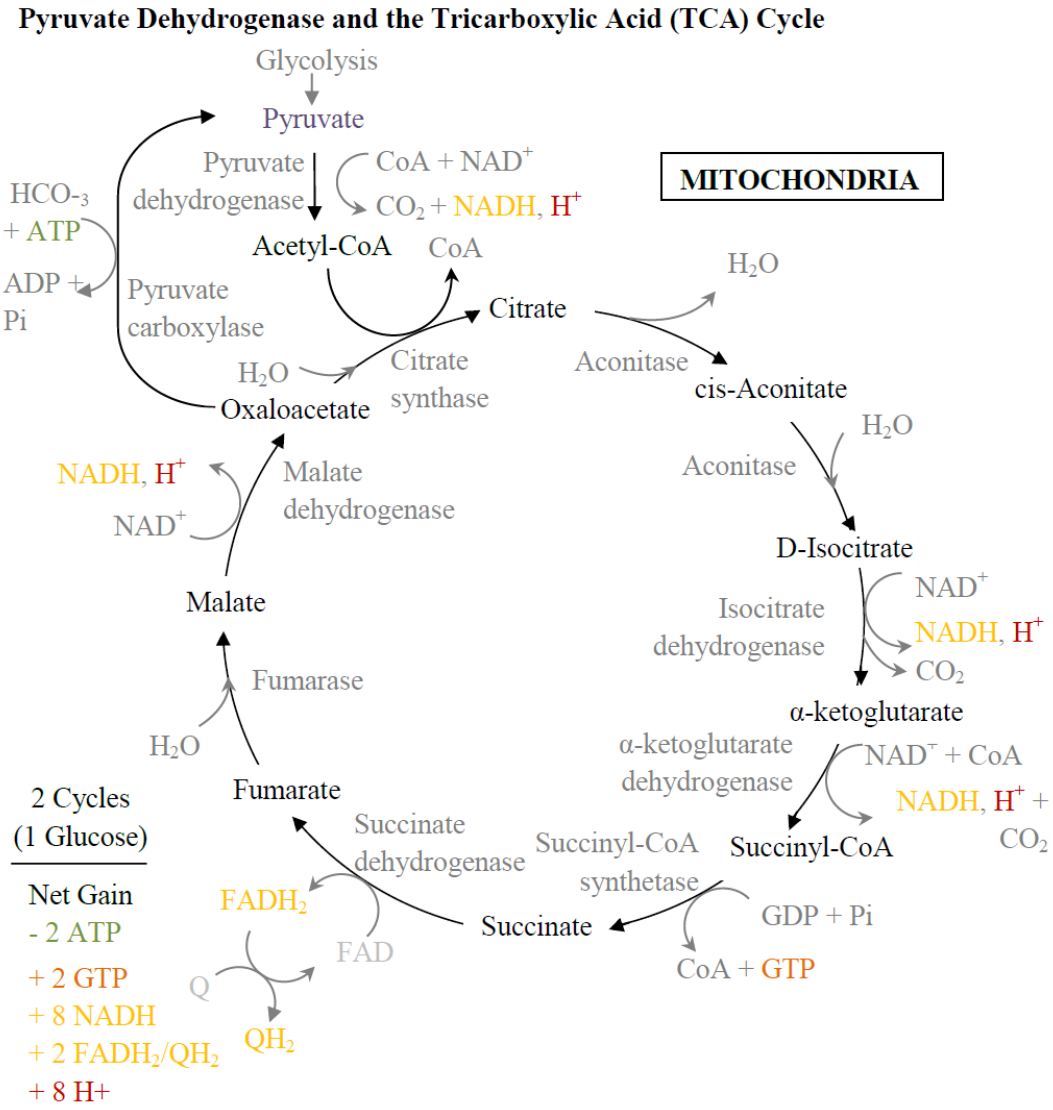

Figure 1.3 An overview of pyruvate dehydrogenase and the TCA cycle. The metabolic pathway converting pyruvate generated from glycolysis into acetyl-CoA, which is utilised by the TCA cycle to produce a net gain of eight NADH and two $FADH_2$ molecules for input into the ETC.

Although the initial step of glycolysis requires glucose, other nutrients enter these pathways at various points to contribute to energy production in mitochondria. By various processes nutrient components can be converted to substrates of glycolysis or the TCA cycle (Table 1.1).

Table 1.1. Alternative nutrient entry points into glycolysis and the TCA cycle. The carbohydrate, lipid and protein components that can be metabolised into substrates of either glycolysis or the TCA.

Nutrient	Molecule	Entry Substrate
Carbohydrate Components	Glycogen/Galactose	Glucose-6-phosphate
	Fructose/Mannose	Fructose-6-phosphate
Lipid Components	Glycerol	Dihydroxyacetone phosphate
	Fatty Acids	Acetyl-CoA
Protein Components*	L, K, F, W, Y, I, T	Pyruvate
	A, C, G, S, T, T,W	Acetyl-CoA
	D, N	Oxaloacetate
	D, N, Y, F	Fumarate
	I, M, V, T	Succinyl-CoA
	Q, R, P, H, E	a-Ketoglutarate

*Amino acid symbols listed.

Amino acids are an alternative source of cellular energy. Glucogenic amino acids can be converted to a gluconeogenic or TCA cycle intermediates and can be used to synthesise glucose. Ketogenic amino acids can only be converted to acetyl-CoA, acetoacetyl-CoA or acetoacetate but cannot be used to synthesise glucose.

Many lipid molecules consist of a glycerol with three bound fatty acid chains (triglyceride). β-oxidation is the process whereby fatty acids are shortened to acetyl-CoA to be used in the TCA cycle as a source of energy. Long-chain fatty acids are activated in the cytosol by conversion to acyl-CoA molecules which are reacted with carnitine to be transported into the mitochondria. Short-chain acyl-CoA molecules can diffuse across the membrane. In a 4-step process, an acetyl-coA molecule is removed from the acyl-CoA chain; this is repeated until the final products are two acetyl-CoA molecules (Wanders *et al.*, 2010). This process produces NADH and $FADH_2$ molecules used by the entry point enzymes of the electron transport chain (Figure 1.4A). Glycerol is phosphorylated to glycerol-3-phosphate which can be converted to DHAP by mitochondrial glycerol-3-phosphate dehydrogenase, producing $FADH_2$ and ubiquinol (QH_2) (Guo *et al.*, 1993, MacDonald, 1981) (Figure 1.4B).

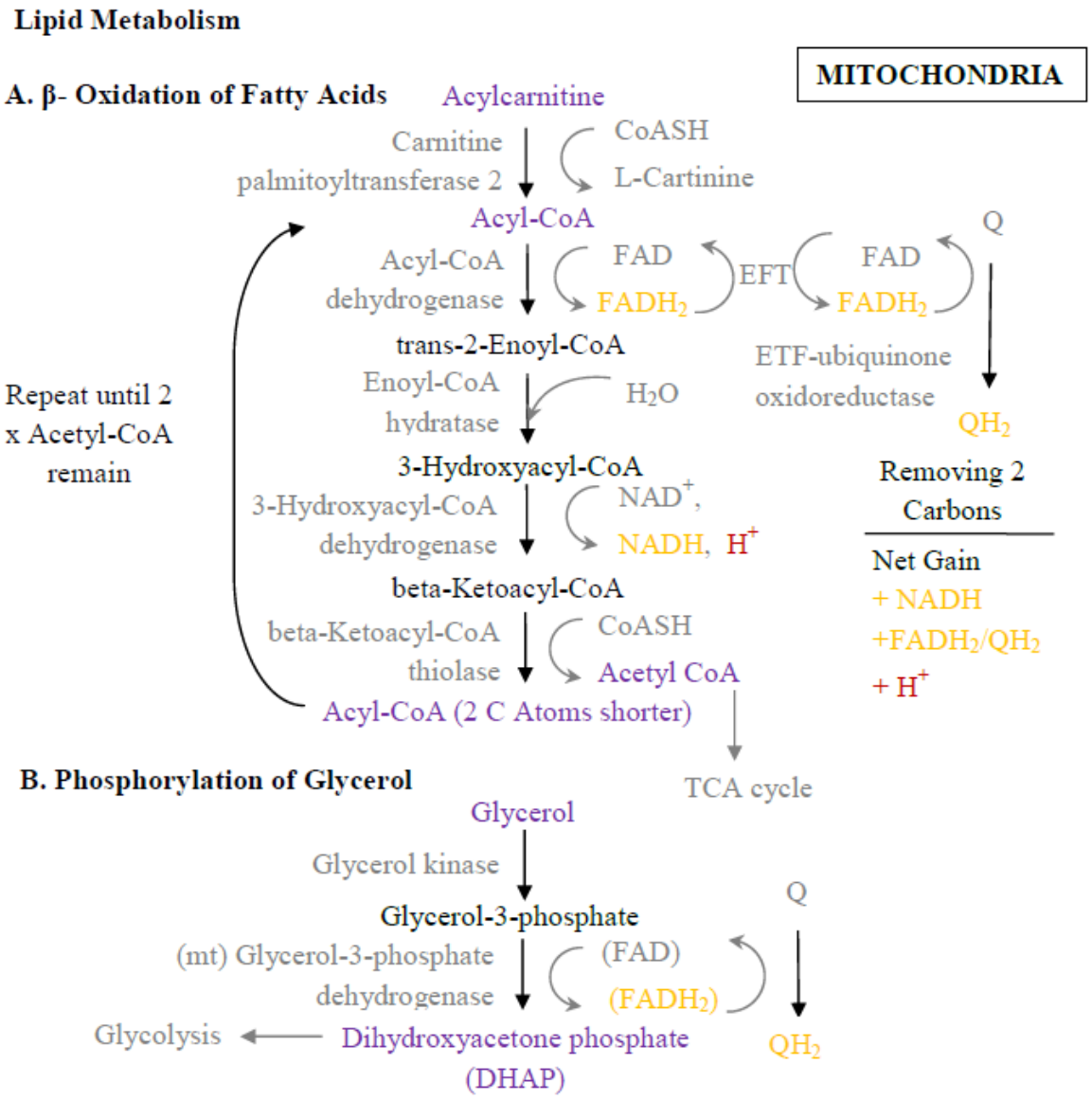

Figure 1.4 Lipid metabolism in mitochondria. The metabolism of lipid components (fatty acids and glycerol) generating NADH, $FADH_2$ and QH_2 which contribute to the ETC.

1.2.2 Oxidative Phosphorylation (OXPHOS)

The OXPHOS system uses the reducing capacity of the coenzymes NADH and $FADH_2$, produced during glycolysis, the TCA cycle and β-oxidation of fatty acids, to pass electrons between redox centres in the ETC complexes. This translocates H^+ ions from the matrix to the IMS and creates an electric potential ($\Delta\psi$) and a chemical (and pH) potential ($\Delta\mu_H^+$) gradient. This gradient is then utilised to induce conformational changes in Complex V (ATP synthase), catalysing the conversion of ADP and Pi to ATP (Figure 1.5).

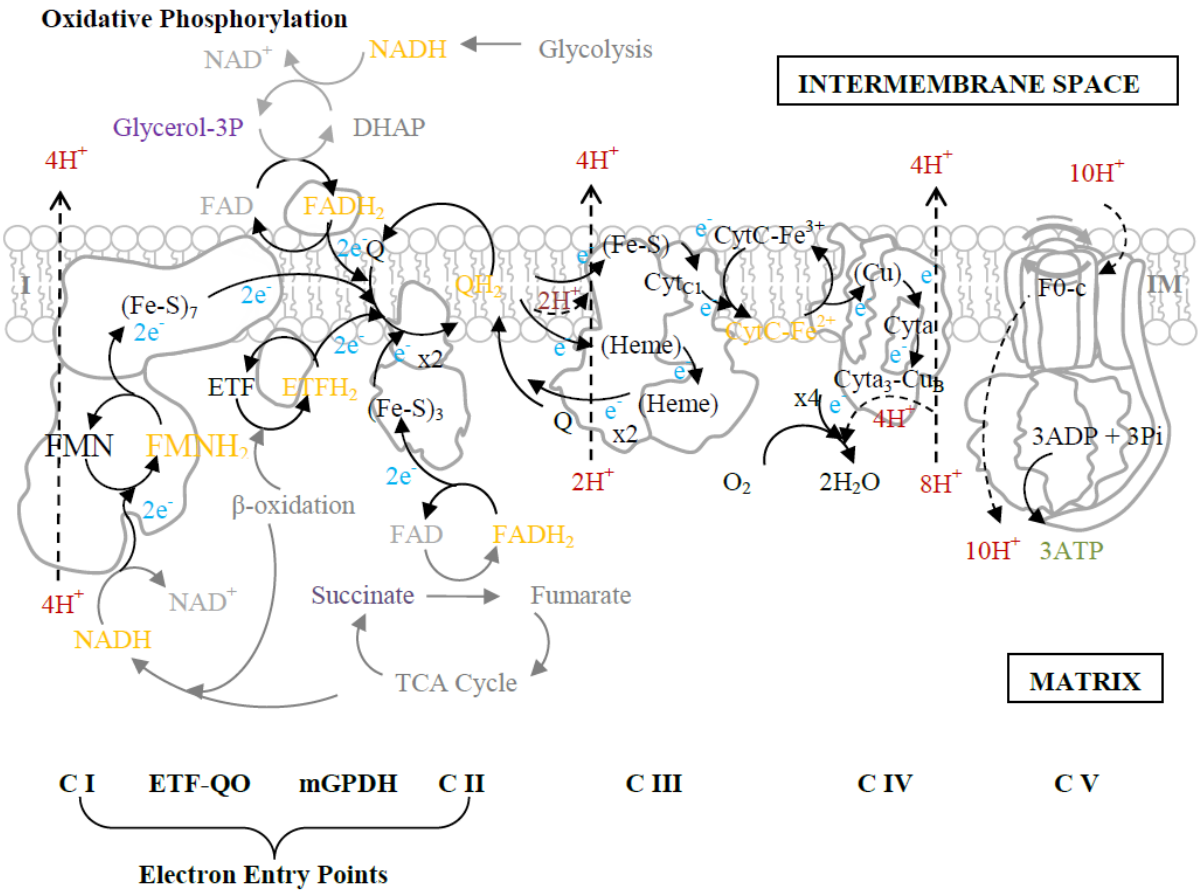

Figure 1.5 An overview of the OXPHOS system. Glycolysis and the TCA cycle produce substrates utilised by the ETC to move H^+ ions from the matrix to the intermembrane space. The electrochemical gradient (potential) drives ATP synthase (CV) to convert ADP and Pi into ATP.

Complex I

The coenzyme NADH is produced at many stages during glycolysis and the TCA cycle. Complex I, NADH:ubiquinone reductase (or NADH dehydrogenase), oxidises NADH to NAD^+ and transfers the H^+ ions and electrons (e^-) to the first redox prosthetic group, flavine mononucleotide (FMN). The electrons are then passed from $FMNH_2$ along a chain of seven iron-sulphur (Fe-S) clusters and are finally used to reduce ubiquinone (CoQ/Q) to ubiquinol (QH_2). In addition, this process is predicted to induce an indirect conformational change leading to the translocation of four protons (H^+) from the matrix to the intermembrane space (Friedrich, 2001, Galkin *et al.*, 1999).

To date, the most in-depth study of complex I is from bovine heart mitochondria, which identified 46 protein subunits (Carroll *et al.*, 2003). The complex core comprises 14 subunits containing all the critical redox centres (Weidner *et al.*, 1993). There are two

distinct groups of core proteins: seven hydrophobic proteins, containing transmembrane domains, encoded by mtDNA; and seven hydrophilic proteins, containing binding motifs for redox prosthetic groups, encoded by nDNA (Fearnley and Walker, 1992). Complex I contains an additional 32 accessory subunits. The exact function of the additional subunits remains unclear, though it has been proposed that some may have a role in the assembly of the complex, iron-sulphur cluster formation, rhodanese activity (cyanide detoxification), proapoptoic function and fatty acid metabolism (Brandt, 2006).

Complex II

Succinate dehydrogenase (SDH; complex II) is part of both the TCA cycle and the ETC. During the TCA cycle, SDH oxidises succinate to fumarate, and reduces FAD to $FADH_2$. In the ETC, it oxidises $FADH_2$, passing electrons through three Fe-S clusters and reducing Q to QH_2 (Rutter *et al.*, 2010).

SDH is comprised of four subunits, all encoded by nDNA. The enzyme has a hydrophilic domain (protruding into the matrix), containing the catalytic core of the enzyme and a hydrophobic domain, embedded in the inner membrane (protruding slightly into the intermembrane space) (Sun *et al.*, 2005).

Alternative entry to the ETC

Each cycle of β-oxidation of fatty acids removes two carbon units (acetyl-CoA) from long-chain acyl-CoA esters, ultimately resulting in two acetyl-CoA molecules. Each step in the process is catalysed by a FAD-containing dehydrogenase (Watmough and Frerman, 2010). There are nine acyl-CoA dehydrogenases and two enzymes of mitochondrial one-carbon metabolism (Hoskins and Mackenzie, 1961), which utilise the electron transfer flavoprotein (ETF) as an electron acceptor entry point to the respiratory chain (Crane and Beinert, 1956). ETF is then reduced by electron transfer flavoprotein-ubiquinone oxidoreductase (ETF-QO), which transfers electrons via a FAD and Fe-S cluster domain to ultimately reduce Q to QH_2 (Ruzicka and Beinert, 1977).

NADH produced by glycolysis cannot be transported into the mitochondria from the cytosol. The glycerol phosphate shuttle is a system allowing this NADH to contribute to oxidative phosphorylation through a paired redox reaction (Shen *et al.*, 2006). Cytosolic glycerol-3-phosphate dehydrogenase (*cGPDH*) converts dihydroxyacetone phosphate (DHAP) to glycerol-3-phosphate (glycerol-3-P) and oxidises one molecule of NADH to

NAD^+. The DHAP is then converted back to glycerol-3-P by mitochondrial glycerol-3-phosphate dehydrogenase (mGPDH), embedded in the outer surface of the inner mitochondrial membrane (Chowdhury *et al.*, 2005, Klingenberg, 1970). This conversion also reduces a bound FAD group to $FADH_2$, which is sequentially used to reduce Q to QH_2.

Complex III

Coenzyme Q: cytochrome c - oxidoreductase is the third complex of the respiratory chain. It has 11 subunits of both mitochondrial and nuclear genetic origin (Iwata *et al.*, 1998). Initially, it binds and oxidises two QH_2 molecules, produced by either Complex I, Complex II, ETF-QO or mGPDH, back to Q and releases two H^+ ions into the intermembrane space. An electron is transferred to cytochrome c_1 and then onto cytochrome c, and another single electron reduces a Q to ubisemiquinone (QH). After a further round of reactions, another cytochrome c is reduced, and the QH from the previous reactions is fully reduced to QH_2 and released back into the pool. The overall reaction results in two molecules of cytochrome c reduced, to be used by Complex IV, two H^+ ions picked up from the matrix and four H^+ ions released into the intermembrane space, contributing to the proton gradient required for ATP synthase function (Crofts, 2004).

Complex IV

Cytochrome c oxidase is Complex IV of the respiratory chain. It has 13 subunits, three of which are encoded by mtDNA. It accepts an electron at a Cu_A site from each of the four cytochrome c molecules reduced by Complex III. These electrons are then transferred through a cytochrome a and an a_3-Cu_B binuclear centre to a molecule of oxygen, which binds four H^+ and forms two molecules of H_2O. In the process, four H^+ ions are transported across the mitochondrial membrane to contribute to generation of the proton gradient (Babcock and Wikstrom, 1992, Tsukihara *et al.*, 1995).

Supercomplexes

The original concept of the organisation of mitochondrial complexes was the liquid state model, whereby each complex was free to move independently throughout the mitochondrial inner membrane, with reactions occurring by random collisions during diffusion (Hackenbrock *et al.*, 1986). However, blue native polyacrylamide

electrophoresis (BN-PAGE), allowed isolation and characterisation of mitochondrial supercomplexes (respirasomes). These supercomplexes were found, existing in different combinations of Complex I, Complex III and Complex IV monomers (Cruciat *et al.*, 2000, Schagger *et al.*, 2004, Schagger and Pfeiffer, 2000).

Advancement in electron microscopy allowed mapping of first the 2D and 3D structure of mitochondrial supercomplexes, confirming that they were not simply an artefact of the solubilisation process but function in substrate channelling between complexes (Schafer *et al.*, 2007, Schafer *et al.*, 2006).

Complex V

Complex V utilises the electrochemical (H^+) gradient generated by the ETC to drive synthesis of ATP from ADP and Pi. The complex is composed of two regions, F_0, embedded in the inner mitochondrial membrane and F_1, which protrudes in the matrix of the mitochondria. The F_0 portion forms a 'proton pore', where a ring of c-subunits translocates H^+ ions across the inner membrane, and rotates in the process of doing so. Subunit γ is an asymmetric stalk attached to the c-ring, and protrudes into the centre of the $\alpha_1\beta_1$ subunit trimer that forms the catalytic site of the F_1 portion. The catalytic core is stabilised by other subunits of ATP synthase. As the stalk rotates with the c-ring, it causes a conformational change in each of the $\alpha_1\beta_1$ heterodimers. At any one time, one dimer will be in an "open" state, where any previously made ATP is released and ADP and Pi can bind, another will be in a "loose" state, and the other in a "tight" state, where ADP and Pi are bound tightly and ATP is produced. The cycle repeats so each dimer is continuously producing ATP (Gresser *et al.*, 1982).

1.3 Mitochondrial Genetics

1.3.1 Mitochondrial DNA (mtDNA)

Human mtDNA is ~16.7 kb in length, and contains 37 genes: 13 protein coding, 22 tRNA and two rRNA genes (Figure 1.6). mtDNA was first sequenced in 1981 and later revised as the 'revised Cambridge Reference Sequence (rCRS)' (Anderson *et al.*, 1981, Andrews *et al.*, 1999). Since the rCRS is of contemporary European origin, it has been recently suggested that its use results in inconsistencies, misinterpretations, and errors in medical, forensic, and population genetic studies.

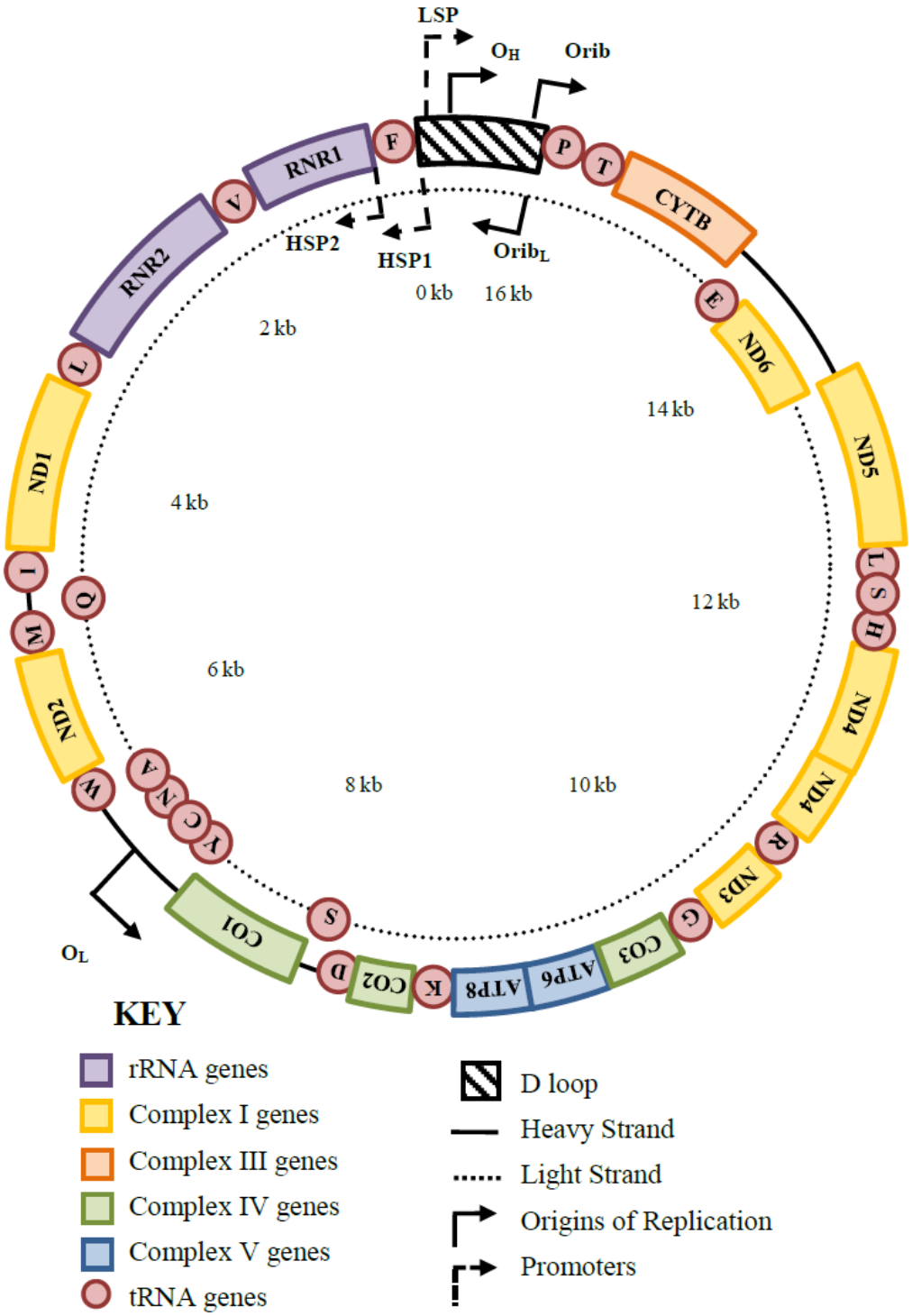

Figure 1.6 Mitochondrial genome map. A map of the heavy and light strand of mitochondrial DNA identifies the D-loop or non-coding region (NCR), transcription promoters, the origins of replication and genes locations. Genes are colour coded depending on which OXPHOS complex they contribute to, or if they are an rRNA or tRNA gene.

There are several prevailing models which attempt to explain why mtDNA has been retained, despite mass transfer of the majority of mitochondrial genes to the nDNA.

Hydrophobic membrane proteins are difficult to localise correctly and import into the mitochondria, with the possibility of misdirecting proteins into the membrane of the endoplasmic reticulum (ER) (Popot and de Vitry, 1990, von Heijne, 1986). This is supported by higher eukaryote mtDNA encoding only central membrane-embedded respiratory chain subunits, and recombinant peptide experiments showing the inability of the mitochondria to import proteins with more than 3-4 transmembrane helices (Claros *et al.*, 1995). Further theories include the necessity for rapid expression regulation of particularly important genes by the redox state of the mitochondria (Allen, 1993), or the possible cytosolic toxicity of mitochondrial translation products (Martin and Schnarrenberger, 1997). The disparity between the genetic codes used to translate nuclear and mitochondrial genes must also factor into the ability of mitochondrial genes to be transferred to the nDNA.

Due to the high importance of mitochondrial function, it might be expected that mitochondrial genes would be under a lot of constraint; however, mtDNA appears to evolve 5-10 times faster than single copy nDNA (Brown *et al.*, 1979). Mitochondrial DNA likely has high mutation rates due to a combination of proximity to damaging free-radical production (Balaban *et al.*, 2005), continuous replication of mtDNA, meaning higher base misincorporation (Johnson and Johnson, 2001) and diminished repair systems (Mason and Lightowlers, 2003).

1.3.2 Haplogroups

As mtDNA mutation rate is high, there is vast variation between human mtDNA sequences. Analysis of European populations identified 10 major haplogroups of mtDNA sequences (H, I, J, K, M, T, U, V, W, and X), defined by specific sequence polymorphisms (Torroni *et al.*, 1996). Updating the phylogenetic tree with the further analysis of ~4000 publically available mtDNA sequences revealed the complexity of haplogroups subtypes, and allowed the SNP definition of each haplogroup to be refined (van Oven and Kayser, 2009). Mitochondrial haplogroups are of particular significance as they can be used to track population distribution (Torroni *et al.*, 2006), and have been associated with the occurrence or severity of many clinical disorders (Herrnstadt and Howell, 2004).

1.3.3 Inheritance and the mtDNA bottleneck

Mitochondrial DNA in humans is maternally inherited (Giles *et al.*, 1980). Despite the contribution of ~100 mtDNA from the sperm to the fertilised egg, the paternal mtDNA is tagged for destruction by ubiquitin, and is degraded before or during the third embryonic cleavage (Sutovsky *et al.*, 1999). In one case, mutated mtDNA from the father caused myopathy in a patient (Schwartz and Vissing, 2002); however, this appears to be an extremely rare event (Taylor *et al.*, 2003).

Nucleated mammalian cells contain multiple copies of mtDNA, dependent upon cellular energy demand. When all of the molecules are identical, the situation is known as homoplasmy. However, cells can contain a mixture of mtDNA with different genotypes, and this is called heteroplasmy (Larsson and Clayton, 1995).

Heteroplasmic, pathogenic mutations generally do not result in a phenotypic effect until a specific threshold level (Taylor and Turnbull, 2005). Heteroplasmic variants are heritable; however, the level of heteroplasmy can vary dramatically between a mother and her children. The shift in heteroplasmy levels is purportedly explained by the 'mitochondrial bottleneck hypothesis' (Howell *et al.*, 1992a). It is theorised that the bottleneck provides an evolutionary mechanism for the removal of deleterious mtDNA variants from the population, thus protecting the human species from the mutational meltdown predicted by Muller's Ratchet (Bergstrom and Pritchard, 1998, Felsenstein, 1974, Muller, 1964).

1.4 Mitochondrial Biogenesis

Mitochondrial biogenesis is a synergistic process, requiring the simultaneous upregulation and coordination of both nDNA and mtDNA encoded mitochondrial proteins, along with replication of the mtDNA. The nuclear-encoded mitochondrial proteome is estimated as >1000 proteins which contribute to mitochondrial function (Lythgow *et al.*, 2011, Pagliarini *et al.*, 2008).

1.4.1 Protein transport

All but the 13 proteins encoded on the mtDNA must be transcribed and translated in the nucleus and cytosol, and transported into the mitochondria. This includes not only the remaining complex subunits but all structural and regulatory proteins as well (Anderson *et al.*, 1981, Andrews *et al.*, 1999).

Proteins in the cytosol are maintained in a precursor form, often bound by chaperone proteins (such as Hsp70 and Hsp90) or containing the mitochondrial signalling peptide sequences. The N-terminal presequence, also known as the matrix-targeting sequence (MTS), does not necessarily share the same primary sequence but tends to form conserved amphiphilic helical structures (Roise *et al.*, 1988).

The chaperones or presequences are recognised by components of the translocase of the outer membrane (TOM) complex, which activates transport of the protein into the intermembrane space (Abe *et al.*, 2000, Young *et al.*, 2003). Several β-barrel proteins require insertion into the outer mitochondrial membrane, and this is mediated by the sorting and assembly machinery (SAM) complex (Paschen *et al.*, 2003).

Some proteins are targeted for the IMS or integration into the IMS side of the inner membrane by addition of a hydrophobic sorting domain accompanying the N-terminal MTS. This prevents translocation into the matrix, instead causing the protein to be inserted into the membrane by translocase of the inner membrane (TIM) 23 (Meier *et al.*, 2005, Rojo *et al.*, 1998). A special group of cysteine-containing IMS proteins, which do not contain N-terminal targeting sequences, are instead transported into the mitochondria by the disulphide relay (Deponte and Hell, 2009).

Carrier proteins to be integrated into the inner mitochondrial membrane are escorted from the TOM complex by small Tim proteins, which are thought to prevent unwanted interactions in the IMS (Vergnolle *et al.*, 2005). This allows the protein to associate with the TIM22 complex, enabling the insertion of the carrier protein into the inner membrane (Sirrenberg *et al.*, 1996).

Proteins destined for the mitochondrial matrix are passed onto the TIM23 complex, which recognises the MTS and facilitates the transport of proteins across the inner membrane (Schulz *et al.*, 2011). The targeting presequences are then cleaved off, usually by the mitochondrial processing peptidase (MPP) (Braun and Schmitz, 1997, Vogtle *et al.*, 2009).

1.4.2 Transcription

The initiation of mitochondrial transcription was originally thought to begin with mitochondrial transcription factor A (TFAM) binding to mtDNA promoters, which in turn recruited the transcription complex, containing RNA polymerase (POLRMT) and

transcription factors B1 or B2 (TFB1M/2M) (Bonawitz *et al.*, 2006). More recently, it was shown TFB2M is primarily responsible for transcription, with TFB1M functioning mainly in the methylation of *12S RNA* (Cotney *et al.*, 2009, Cotney *et al.*, 2007).

Recent *in vitro* modelling revealed that transcription can occur in the absence of TFAM but is enhanced at LSP and HSP1 by optimal TFAM concentrations (Shutt *et al.*, 2010). This implies a two-component transcription system, also observed in lower eukaryotes, with TFAM providing a method of complex regulation specific to mammals (Figure 1.7).

The regulated, two-component transcription system

The human RNA polymerase, POLRMT, was first identified through its homology to those in lower eukaryotes (Tiranti *et al.*, 1997). Eukaryote polymerases show high levels of conservation to those of T3/T7 bacteriophages (Masters *et al.*, 1987). The C-terminal domain (CTD) contains the conserved motifs essential for the catalytic activity of the enzyme, and the N-terminal domain (NTD) functions in promoter binding and recognition. An N-terminal extension region contains the mitochondrial targeting sequence and novel pentatricopeptide repeat (PPR) motifs. The function of the PPR domain is currently unknown, but it is essential for initiation of promoter-directed transcription (Ringel *et al.*, 2011). Suggested roles, based on the functional properties of other PPR domain proteins, include RNA processing and linking transcription to translation (Aphasizheva *et al.*, 2011, Lightowlers and Chrzanowska-Lightowlers, 2008). Unlike bacteriophage polymerase, POLRMT requires additional factors for initiation of transcription.

TFB2M was identified, alongside its paralogue TFB1M, as rRNA dimethyltransferase homologues with the capability of interaction with POLRMT and essential for initiation of transcription (Falkenberg *et al.*, 2002, McCulloch *et al.*, 2002).

In vitro, the use of 'bubble templates', created using non-complementary sequences, simulates 'pre-melted' promoter regions. POLRMT can initiate promoter-specific transcription from these templates without TFB2M, suggesting the main function of this protein is promoter melting (Sologub *et al.*, 2009). This study also found, through crosslinking and catalytic autolabelling, that TFB2M interacts with the templating nucleotide and priming substrate (NTP), suggesting that TFB2M functions to maintain

the upstream edge of the open transcription site and the position of the template nucleotide and priming substrate for POLRMT.

TFAM was identified as a member of the high-mobility-group (HMG) of proteins, capable of wrapping, bending and unwinding mtDNA, and mediating transcription from POLRMT (Fisher and Clayton, 1988, Fisher *et al.*, 1992, Parisi and Clayton, 1991). The HMG-box motifs are known for their ability to bend DNA, whereas the C-terminal end of the protein has been proven essential for transcription enhancing through interaction with TFB2M (Dairaghi *et al.*, 1995, McCulloch and Shadel, 2003). TFAM is unique in its ability to bind DNA non-specifically in addition to recognising specific sequences within promoter regions, known as TFAM responsive elements (TREs). Nonspecific binding packages mtDNA into nucleoids, facilitating mtDNA replication and transcription, and provides protection from DNA damage (Alam *et al.*, 2003, Kaufman *et al.*, 2007).

TFAM functions through induction of U-turns in mtDNA structures, which have been shown to be distorted to a higher degree in TREs at promoter regions compared to nonspecific mtDNA sequences (Malarkey *et al.*, 2012, Ngo *et al.*, 2011). The U-turn bend at TREs enables the C-terminal end to approach the promoter site and interact with TFB2M to enhance transcription at LSP and HSP1 (Rubio-Cosials *et al.*, 2011).

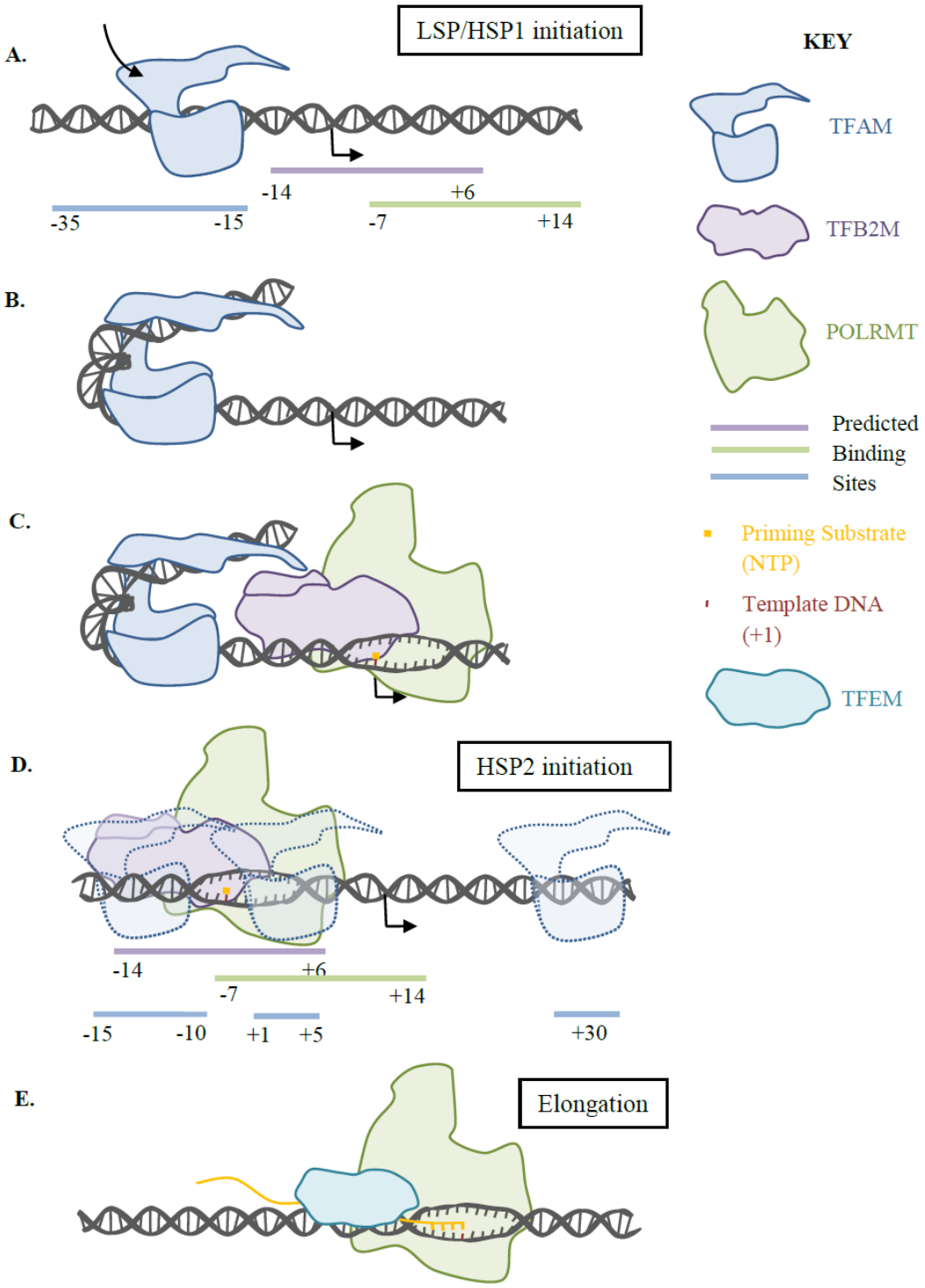

Figure 1.7 An overview of mitochondrial transcription initiation. Initiation at HSP1 and LSP consists of (A) TFAM binding and (B) bending mtDNA at TREs in the promoter region. (C) POLRMT and TFB2M form the initiation complex (IC) and assemble onto promoter sequences. TFAM C-terminal domain enhances transcription initiation. TFB2M is responsible for promoter melting and aligning the priming substrate and DNA template for POLRMT processing. (D) Transcription from HPS2 can be inhibited by TFAM due to overlapping binding sites. (E) Extended transcription elongation requires TEFM to increase processivity of POLRMT.

Regulation of transcription initiation

Each strand is transcribed as a long, polycistronic precursor mRNA molecule. Light strand transcription initiates from a single promoter (LSP), but heavy strand transcription initiates from two promoters, HSP1 and HSP2 (Montoya *et al.*, 1982, Montoya *et al.*, 1983). Integral to regulation of transcription initiation are the varied gene products transcribed by each promoter. Transcription from HSP2 begins at the 5' end of *MT-RNR1* (*12S rRNA*), and transcribes all but the $tRNA^{Phe}$ gene (meaning it transcribes all subunits of the OXPHOS system except *MT-ND6*). HSP1 transcription includes only the $tRNA^{Phe}$, *MT-RNR1*, $tRNA^{Val}$ and *MT-RNR2* before terminating, meaning it can independently upregulate transcription of rRNA, essential for translation, without transcribing unnecessary OXPHOS components. Transcription from LSP produces the eight tRNA genes and *MT-ND6* encoded on the light strand; however, it also generates the RNA primers essential for initiation of replication (Chang and Clayton, 1985). This enables maintenance of OXPHOS components by HSP2 and biogenesis by HSP1/LSP to be regulated separately. As previously stated, TFAM is not essential for initiation of transcription (*in vitro*), but conveys an additional layer of regulation onto expression from the independent promoters.

Each promoter responds differently to varying concentrations of TFAM (Figure 1.8). HSP1 transcription has a higher basal rate of transcription, but requires higher concentrations of TFAM for maximal activity compared to LSP (Shutt *et al.*, 2010). Despite enhancing transcription from HSP1 and LSP, transcription from HSP2 is actually repressed by even low concentrations of TFAM (Lodeiro *et al.*, 2012, Zollo *et al.*, 2012). This explains how previous attempts to transcribe from HSP2 using conditions suitable for LSP or HSP1, containing TFAM, have been unsuccessful (Litonin *et al.*, 2010). DNase I footprinting at HSP2 reveals predicted TFAM binding sites overlapping with POLRMT/TFB2M binding sites, suggesting competitive repression by TFAM. This principle is supported by higher concentrations of POLRMT and TFB2M overcoming small concentrations of TFAM (Lodeiro *et al.*, 2012). Overall, this means that an absence of TFAM favours HSP2 transcription, low TFAM concentration favours LSP transcription and high TFAM concentration favours HSP1 transcription.

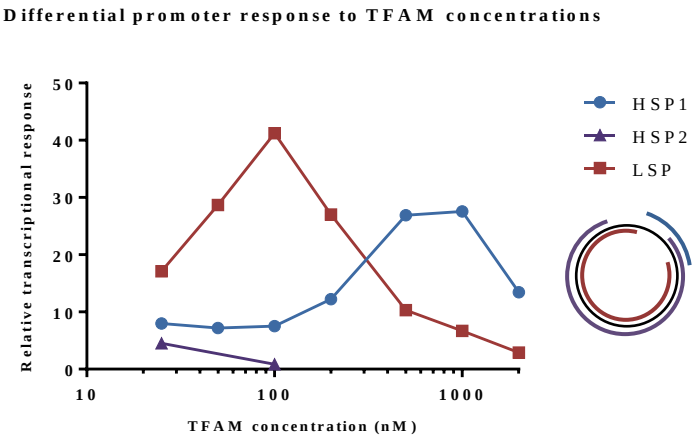

Figure 1.8 Differential promoter response to TFAM concentrations. Graphical representation of the response from the different promoters to variable concentrations of TFAM. HSP1 and HSP2 have higher transcription levels in the absence of TFAM; however, low levels of TFAM stimulate full activation of LSP whilst inhibiting HSP2. Higher concentrations of TFAM inhibit transcription from LSP whilst enhancing transcription from HSP1. Concentrations above 1000 nM inhibit transcription from all promoters. (Compiled using data from Lodeiro *et al.*, 2012, Shutt *et al.*, 2010)

This may explain the heterogenic nature of nucleoids. TFAM is responsible for packaging the mtDNA into nucleoids, and at full capacity has 450 binding sites on mtDNA (Kaufman *et al.*, 2007). It has been previously noted that the TFAM content of nucleoids is variable and not always co-localising with replicating mtDNA, which could be perceived as either coincidental or a possible regulation mechanism (Wai *et al.*, 2008).

Recently, photoactivated localization microscopy (PALM/iPALM) has been used to obtain super-resolution images of mitochondrial nucleoids based on their TFAM incorporation (Brown *et al.*, 2011). This study demonstrated not only the wide range of nucleoid sizes and shapes, but that TFAM distribution is not always even.

Transcription elongation

Independently, POLRMT can only transcribe short species of RNA (approximately 25-75 nt in length) (Wanrooij *et al.*, 2008). *In vitro* modelling has shown that transcription elongation factor, mitochondrial (TEFM) binds the catalytic subunit of POLRMT and increases the enzyme processivity, allowing generation of longer templates. *In vivo*, disruption of TEFM leads of loss of transcripts distal to the promoters, suggesting premature failing of mitochondrial transcription (Minczuk *et al.*, 2011). This study also reveals RNA-dependent complexes formed containing TEFM, POLRMT,

pentatricopeptide repeat domain 3 (PTCD3) and DEAH-box polypeptide 30 (DHX30), but noticeably with neither initiation factors TFAM and TFB2M.

Extensive study of PTCD3 revealed it is not essential for mitochondrial transcription, but is required for mitochondrial translation, suggesting a function in linking transcription to translation (Davies *et al.*, 2009).

DHX30 is a DEAH-box RNA helicase, previously shown to localise to mitochondria but with unknown function (Wang and Bogenhagen, 2006). Since further analysis of DHX30 function has not been completed to date, it is possible that this protein functions directly in transcription elongation; however, the typical roles of other mitochondrial helicases, such as SUPV3L1 (formally SUV3), would suggest a role in mtRNA metabolism or maintenance (Szczesny *et al.*, 2010).

Excision repair cross-complementing rodent repair deficiency, complementation group 6 (ERCC6; previously CSB) has also been recently implicated in mitochondrial transcription elongation (Berquist *et al.*, 2012). The major functions of this protein are nuclear transcription-coupled nucleotide excision repair (TC-NER) and enhancing transcription elongation from nuclear RNA polymerases (Orren *et al.*, 1996, Selby and Sancar, 1997). ERCC6 has previously been shown to localise to the mitochondria and is involved with base excision repair (BER) of mtDNA (Aamann *et al.*, 2010). Recent data has shown that ERCC6 assists POLRMT in transcription, through dissociating non-specifically bound TFAM from mtDNA during elongation (Berquist *et al.*, 2012). This study reveals defective ERCC6 causes loss of transcripts distal to the promoter region, but increasing concentrations of ERCC6, *in vitro*, causes a general reduction in transcription, presumably through loss of TFAM stimulation at promoters. What is not considered by this study is the separate action of HSP1 and HSP2. With evidence of TFAM repressing HSP2 *in vitro* (Lodeiro et al., 2012), decreased levels of protein-coding transcripts in ERRC6-deficient cells could be, in part, due to increased TFAM repression at HSP2 and not simply deficient removal of non-specific TFAM.

Transcription termination

The first mitochondrial transcription termination factor identified was mitochondrial termination factor 1 (*MTERF1*) (Kruse *et al.*, 1989). The crystal structure revealed it binding duplex DNA and causing duplex melting and inversion of three bases (Jimenez-Menendez *et al.*, 2010, Yakubovskaya *et al.*, 2010). To date, it is the only factor

required for termination at the $tRNA^{Leu}$ from both HSP1 and LSP, with a higher affinity for termination of light-strand transcription (Asin-Cayuela *et al.*, 2005, Shang and Clayton, 1994). Additional binding sites have been found in the HSP1 promoter region, leading to the model whereby simultaneous binding of MTERF1 to the termination site at $tRNA^{Leu}$ and HSP1 causes a looping out of the bridging DNA segment, and can stimulate HSP1 transcription through the ease in recycling the transcription complex when they are brought in close proximity (Martin *et al.*, 2005) (Figure 1.9A). Manipulation of MTERF1 expression affects relative amounts of anti-sense transcripts around the $tRNA^{Leu}$ site, suggesting MTERF1 also plays a crucial role in the termination of light-strand transcription (Hyvarinen *et al.*, 2010) (Figure 1.9B). This is of critical importance as there are no genes on the light-strand downstream of the $tRNA^{Leu}$ site, but generation of anti-sense rRNA transcripts could interfere with ribosomal biogenesis. Weaker MTERF1 binding sites have been identified in the non-coding region (NCR), suggesting a role for MTERF1 in termination from HSP2 transcripts also; however, there is yet to be conclusive evidence supporting the model of HSP2 transcription termination (Hyvarinen *et al.*, 2007).

As previously discussed, transcription of the light-strand is essential for generation of primers for heavy-strand replication (Chang and Clayton, 1985). One model for production of replication primers involves post-transcriptional cleavage of RNA transcripts through a generated ‘R-loop’ (Lee and Clayton, 1998). However, a more recent model predicts premature termination of transcription on the light-strand by formation of four-stranded G-quadruplex structures in nascent RNA transcribed from the conserved sequence block II (CSBII) downstream of the LSP site (Wanrooij *et al.*, 2010). The presence of the G-quadruplex structure in the nascent RNA and presence of a downstream poly-dT region, which enhances termination at CSBII, is reminiscent of rho-independent prokaryotic termination using hair-pin loops (d'Aubenton Carafa *et al.*, 1990) (Figure 1.9C).

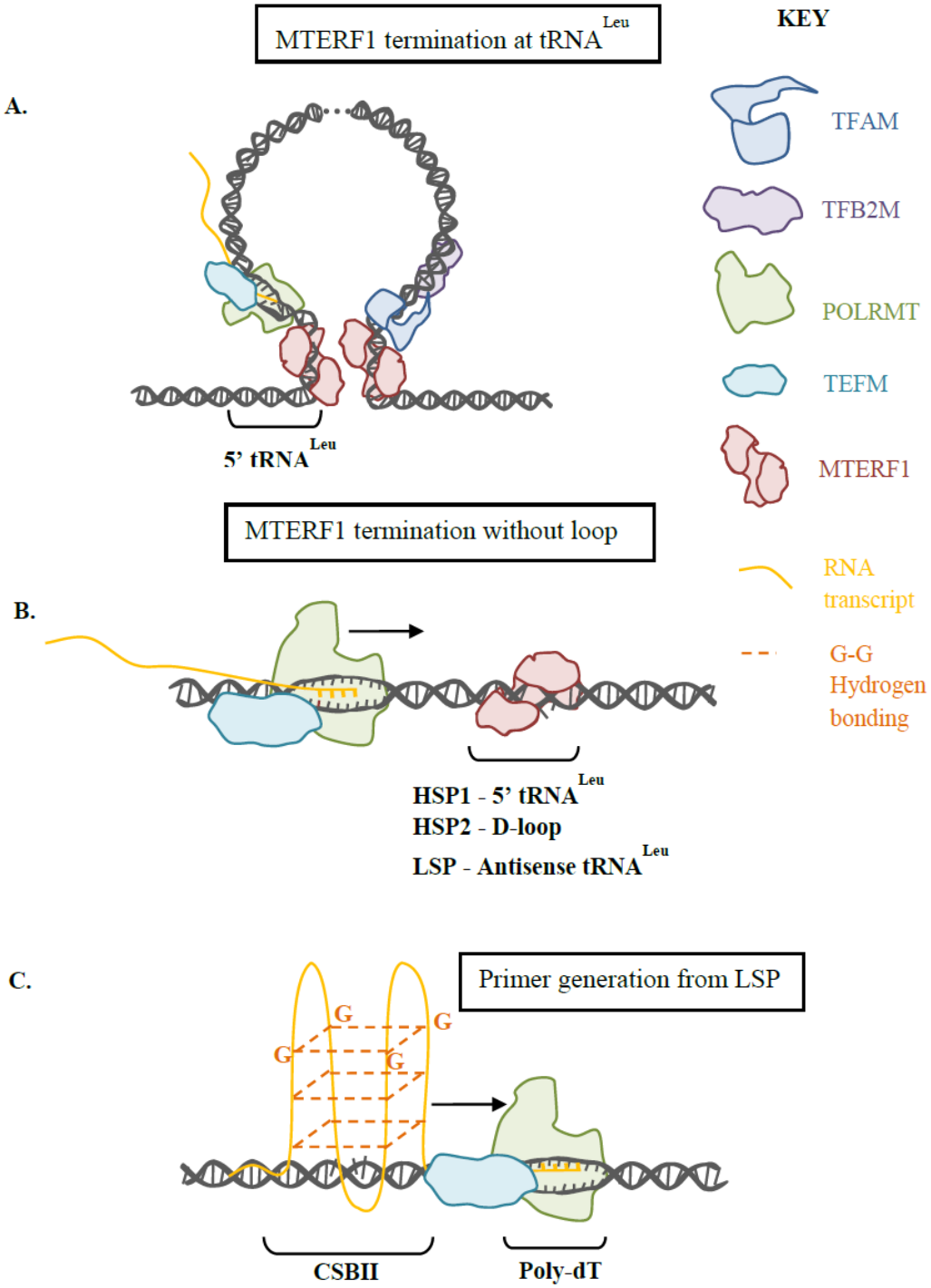

Figure 1.9 An overview of predicted transcription termination mechanisms. Several predicted termination models have been suggested. (A) Termination at $tRNA^{Leu}$ from HSP1 and LSP requires looping of the promoter region to the termination site, joined by binding of MTERF1. (B) MTERF1 can terminate transcription from any promoter without looping either at the $tRNA^{Leu}$ site or within the NCR. (C) Premature termination from LSP to generate replication primer oligos requires formation of G-quadruplex structures in the conserved sequence block II (CSBII).

Phylogenetic analysis and similarity studies led to identification of three additional proteins related to MTERF1, consequently named MTERF2-4 (Linder *et al.*, 2005). However, despite being structurally similar to MTERF1, they do not seem to function in transcription termination, although sufficiently thorough characterisation has not been completed and there have been conflicting reports on their functions. MTERF2 and MTERF3 seem to have functions relating to regulation of transcription or replication (Huang *et al.*, 2011, Park *et al.*, 2007), whereas MTERF4 deficiency impairs translation despite an increase in mitochondrial transcripts (Camara *et al.*, 2011).

Post-transcriptional modification

Perhaps the first and most important post-transcriptional modification is processing of the polycistronic transcripts generated from the heavy and light strands into individual mRNA, tRNA or rRNA molecules. This led to the proposition of the 'punctuation model' of processing, where tRNA genes mark cleavage sites which separate the individual transcripts (Ojala *et al.*, 1981). 5' tRNA processing is achieved by the RNase P complex, consisting of RNase P protein 1-3 (MRPP1-3) (Holzmann *et al.*, 2008, Rossmanith and Holzmann, 2009). 3' tRNA processing is achieved by RNase Z complex, consisting of elaC homologue 2 (ELAC2) and pentatricopeptide repeat domain 1 (PTCD1) (Sanchez *et al.*, 2011, Takaku *et al.*, 2003).

After cleavage, tRNAs are matured by the addition of CCA sequence to the 3' by ATP(CTP):tRNA nucleotidyltransferase, allowing for the addition of the amino acid (Nagaike *et al.*, 2001). tRNAs are further processed by nucleoside modification. There have been 16 species of nucleoside modification identified, three of which are specific to mitochondria, and are essential for correct tRNA folding or function (Suzuki *et al.*, 2011).

mRNAs from the heavy strand are polyadenylated at their 3' end, by mitochondrial poly(A) polymerase (MTPAP) forming the functional stop codon in seven of the heavy strand genes (Nagaike *et al.*, 2005, Tomecki *et al.*, 2004). There is no unanimous function for the polyA tail on mRNA transcripts. Removal of the polyA tail has been achieved by either MTPAP silencing (Piechota *et al.*, 2006), mitochondrial targeting of cytosolic poly(A)-specific exoribonuclease (PARN) (Wydro *et al.*, 2010) or overexpression of mitochondrial poly(A)-specific exoribonuclease, phosphodiesterase 12 (PDE12) (Poulsen *et al.*, 2011, Rorbach *et al.*, 2011). These studies demonstrate

poly(A) tail removal causes increase in ND1, ND2 and ND5 transcripts whilst decreasing the stability of ATP8/6, CO1 and CO2 (Poulsen *et al.*, 2011, Rorbach *et al.*, 2011).

rRNA is also subject to post-transcriptional modification. Two adenines in the 3' stem-loop of 12S rRNA are N6-dimethylated by TFB1M (Seidel-Rogol *et al.*, 2003). Methylation at these positions is critical for assembly of the mitoribosomes and essential for efficient translation of mitochondrially-encoded proteins (Metodiev *et al.*, 2009). Further methylation sites have not been confirmed in humans, but appear in hamster mtDNA in both 12S and 16S, functioning mainly in ribosomal assembly or function (Rorbach and Minczuk, 2012).

1.4.3 Replication

Replication of mtDNA is essential to maintain a stable and sufficient copy number throughout cell division and as part of mtDNA turnover (degradation and replacement of mtDNA molecules). mtDNA replication occurs continuously within tissues, even in post-mitotic cells, and is not limited to a particular phase of the cell cycle (Bogenhagen and Clayton, 1977).

Proteins of the mitochondrial replisome

Polymerase Gamma (Pol γ) is the only mitochondrial polymerase, and consists of one catalytic subunit (encoded by *POLG*) and a dimer of accessory subunits (encoded by *POLG2*) (Gray and Wong, 1992, Lim *et al.*, 1999). The catalytic subunit has DNA polymerase, 3'→5' exonuclease and 5'-deoxyribose phosphate (dRP) lyase activity, whilst the accessory subunits promote processivity by enhancing DNA binding (Johnson *et al.*, 2000). The exonuclease activity conveys proof-reading activity, and is required for degradation of newly incorporated nucleotides. The dRP lyase activity is important for base excision repair (BER) of mtDNA (Longley *et al.*, 1998). Pol γ can utilise many different substrates as templates, including RNA, suggesting the enzyme has reverse transcriptase activity (Murakami *et al.*, 2003). Although Pol γ preferentially incorporates deoxyribonucleotides over ribonucleotides during DNA replication, it has been shown that it can incorporate stretches of RNA into DNA, and can differentiate between the different ribonucleotide triphosphates (Kasiviswanathan and Copeland, 2011, Murakami *et al.*, 2003).

Pol γ cannot use dsDNA as a template, and therefore requires DNA to be unwound before replication can occur. *Twinkle* helicase (encoded by *C10orf2*) has sequence homology to T7 phage helicase, but lacks primase activity, and can exist as a hexamer or heptamer (Spelbrink *et al.*, 2001, Ziebarth *et al.*, 2010). *Twinkle* may be involved with initiation of replication or primer extension, as it can bind circular dsDNA without aid of an additional loading protein (Jemt *et al.*, 2011). *Twinkle* helicase requires single-stranded binding protein (SSBP1) to unwind more than short stretches of DNA (Korhonen *et al.*, 2004).

SSBP1 forms nucleoprotein fibrils within single-stranded regions of mtDNA (Van Tuyle and Pavco, 1985). SSBP1 forms tetramers, which wrap DNA around them through electropositive sites (Li and Williams, 1997, Yang *et al.*, 1997). SSBP1 stimulates the activity of Pol γ, and is essential for the replication of long stretches of DNA, increasing the replication processivity of Pol γ and *Twinkle* from 2 kb to 16 kb lengths of DNA (Genuario and Wong, 1993, Korhonen *et al.*, 2004). Mutational analysis of *SSBP1* reveals that separate domains of the protein are responsible for the stimulatory effect of Pol γ and *Twinkle*, and mutations affecting interaction with one does not necessarily affect the other (Oliveira and Kaguni, 2011).

Additional proteins have been implicated in mtDNA replication, though do not form essential components of the 'minimal replisome'. Topoisomerases relieve stress from supercoiled DNA, generated as DNA is unwound. There are two topoisomerases known to function within the mitochondria, mitochondrial topoisomerase 1 (TOP1MT) (Zhang *et al.*, 2001) and topoisomerase IIIα (TOP3A). TOP1MT cleavage sites are mapped to the NCR, and primarily affect transcription, with only a knock-on effect with replication (Dalla Rosa *et al.*, 2009, Zhang and Pommier, 2008). TOP3A functions in both the nucleus and the mitochondria, with alternative start codon usage providing a mitochondrial targeting sequence for some isoforms of the protein (Wang, 2002). Little is known about TOP3A in humans; however, research in trypanosomes and bacteria suggest the protein is needed to resolve junction intermediates at the end stage of replication (Scocca and Shapiro, 2008, Suski and Marians, 2008).

RNASEH1 removes long stretches of RNA/DNA hybrids and has been proven important for maintenance of mtDNA levels (Cerritelli *et al.*, 2003). Human telomerase (TERT) has been shown to localise to mitochondria, and copurifies with mtDNA and

known nucleoid proteins (Sharma *et al.*, 2012). Knockdown of TERT in mice leads to mtDNA depletion, and overexpression can increase mtDNA copy number after depletion by ethidium bromide, suggesting a role for TERT in mtDNA maintenance (Sahin *et al.*, 2011). TERT accumulates in the mitochondria during oxidative stress (Ahmed *et al.*, 2008), which may support a role for TERT in mtDNA replication, but there is also a possibility the protein functions in double-strand break (DSB) repair, which can use RNA subsequently converted to DNA to repair damage (Storici *et al.*, 2007).

Replication models

There are three models of mtDNA replication: the strand asynchronous displacement model, the strand-coupled bidirectional model and the ribonucleotide incorporated throughout the lagging strand (RITOLS) model.

Strand asynchronous replication is initiated at the H-strand origin (O_H) in the non-coding region (NCR), primed by transcription products from the light-strand (Chang and Clayton, 1985, Robberson *et al.*, 1972). After replication of two-thirds of the H-strand, the L-strand origin (O_L) is exposed in the 'WANCY' tRNA region (Figure 1.10A-B). Further analysis of the NCR revealed a second H-Strand replication origin, known as Ori-b, which, though a strong promoter site, is poorly understood (Yasukawa *et al.*, 2006, Yasukawa *et al.*, 2005).

L-strand replication is initiated by synthesis of an RNA primer by POLRMT (Fuste *et al.*, 2010, Wanrooij *et al.*, 2008, Wong and Clayton, 1985). These studies demonstrated that when O_L becomes single-stranded, it forms a hair-pin loop, allowing short primer synthesis by POLRMT, which is then utilised by Pol γ for lagging-strand DNA synthesis. SSBP1 overexpression causes a reduction in primer synthesis but an increase in DNA replication, suggesting the hair-pin loop functions to prevent binding of SSBP1 to O_L. This allows primer synthesis by POLRMT, but prevents non-O_L binding elsewhere, which could inhibit replication progression (Wanrooij *et al.*, 2008). POLRMT only requires the polyT stretch within the hair-pin loop and does not require additional factors, such as TFB2M, presumably because the template is already single-stranded (Fuste *et al.*, 2010). (Figure 1.10C-D).

.

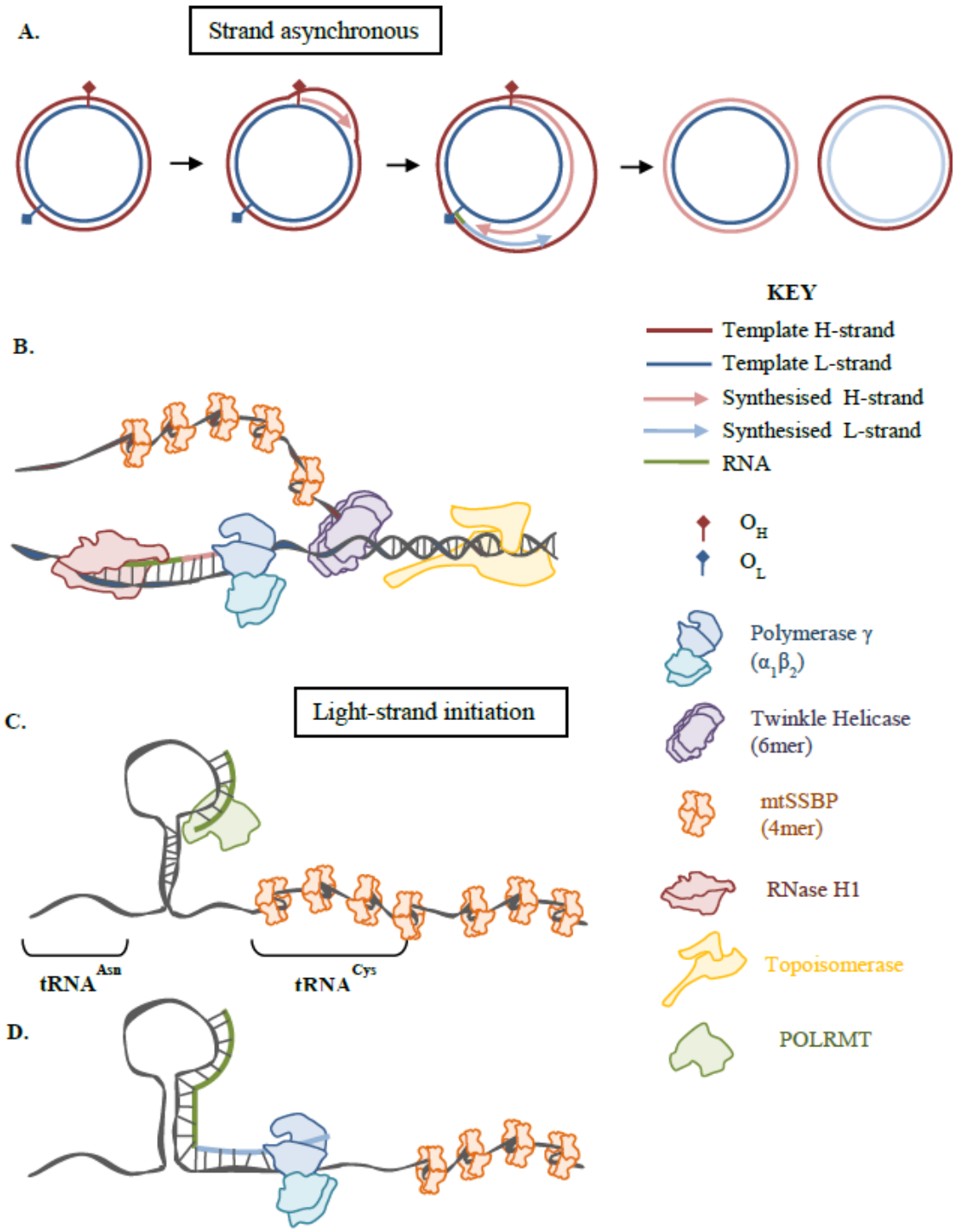

Figure 1.10 The strand asynchronous model. (A) Schematic for replication via the strand asynchronous mechanism. (B) Initiation of heavy-strand replication at O_H, primers from transcription bind the replication origin, Pol γ extends the primer with DNA synthesis. *Twinkle* helicase and topoisomerases unwind DNA which is bound by SSBP1. RNASEH1 degrades the RNA primer. (C) O_L forms a hair-pin loop which prevents SSBP1 binding, allowing primer synthesis by POLRMT. (D) Pol γ extends the RNA primer by DNA synthesis.

This model has been adapted to the RITOLS model, whereby replication occurs in the same manner, except the displaced parental H-strand is not single-stranded, but instead coated with RNA fragments (Yasukawa *et al.*, 2006) (Figure 1.11A). Since the RNA stretches on the displaced strand are prone to degradation, this was proposed to account for the observation of the single-stranded replication intermediates which led to the strand-asynchronous model of replication (Yang *et al.*, 2002). There are two proposed theories to how the RNA intermediates arise. Firstly, that the RNA fragments are generated by POLRMT directly on the displaced strand, since this can prime lagging-strand synthesis, creating Okazaki fragments (Wanrooij *et al.*, 2008) (Figure 1.11B). Secondly, pre-existing fragments of RNA, perhaps generated during transcription, are annealed to the displaced strand, and then processed into small fragments (the bootlace model) (Yasukawa *et al.*, 2006) (Figure 1.11C). In the RITOLS model, after exposure of $O_{L,}$ the lagging-strand RNA is matured into DNA. This is likely to be dependent on Pol γ, as inhibition or mutation of the catalytic subunit prevents maturation of RNA intermediates (Wanrooij *et al.*, 2007) (Figure 1.11D). This is supported by the reverse transcriptase function of Pol γ (Murakami *et al.*, 2003).

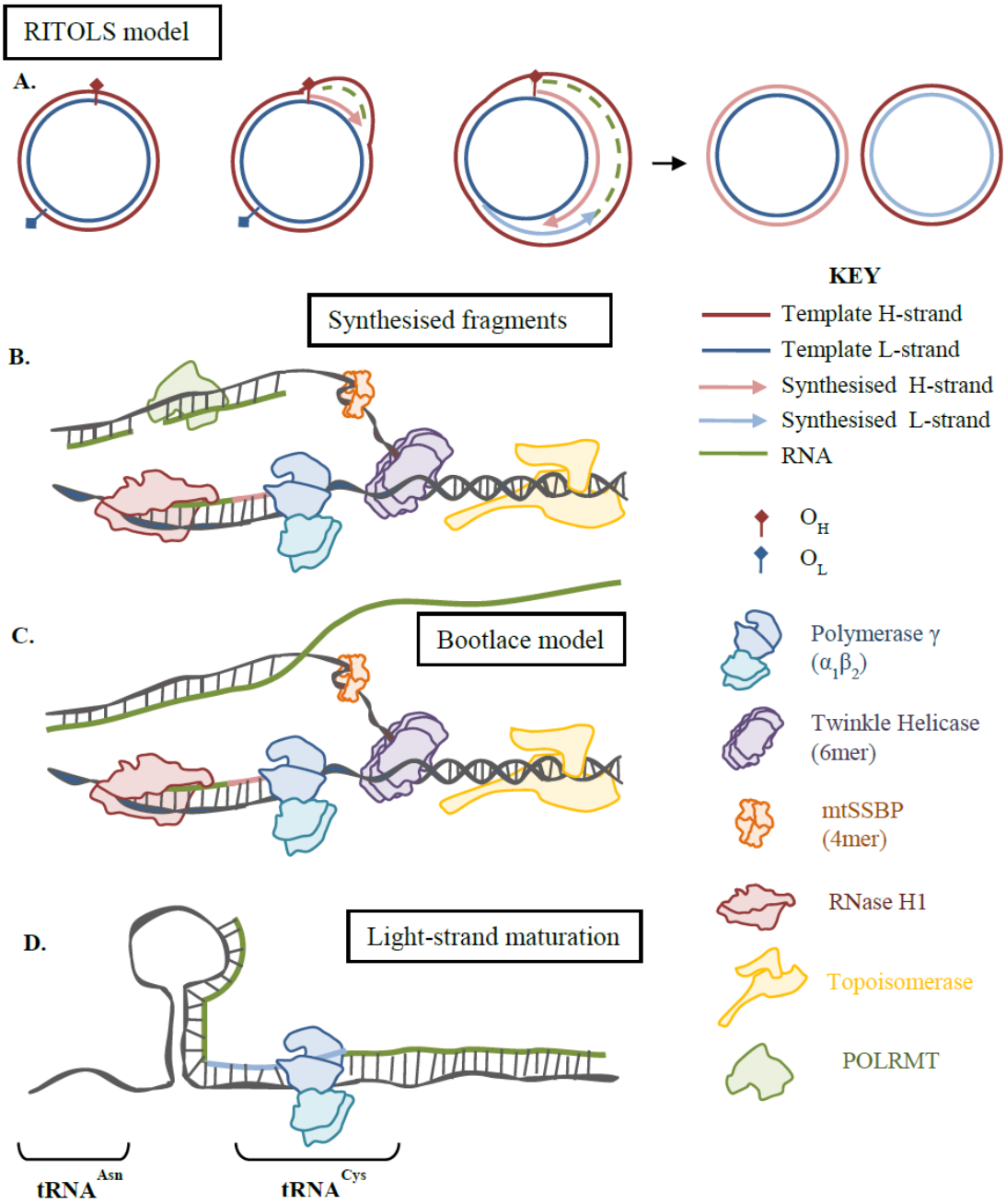

Figure 1.11 The RITOLS model of mtDNA replication. (A) Schematic for replication via the RITOLS mechanism. (B) Initiation of heavy-strand occurs in the same manner as the strand asynchronous mechanism, with the addition that the displaced strand has short RNA fragments synthesised along its length or (C) is bound by long premade RNA fragments. (D) Light strand replication initiation is primed between $tRNA^{Asn}$ and $tRNA^{Cys}$, where a hairpin loop structure forms.

Analysis of replication intermediates revealed that although some are single-stranded or coupled to RNA, presumably resulting from asynchronous replication, others were fully double-stranded, suggesting simultaneous replication of both strands (Holt *et al.*, 2000).

This mechanism of replication resembles nuclear DNA replication, and thus has been called 'conventional, strand-coupled Okazaki fragment associated (COSCOFA)' replication (Figure 1.12A). Initiation occurs bidirectionally, downstream of O_H in the 'initiation zone', but is halted in one direction upon reaching O_H (Bowmaker *et al.*, 2003, Yasukawa *et al.*, 2005). As Pol γ can only replicate DNA in a 5' → 3' direction, leading strand synthesis is continuous, but the lagging strand must be synthesised in short fragments, primed by RNA (Okazaki fragments) (Figure 1.12B). Processing of Okazaki fragments occurs by the same means as in nuclear replication, with specialised helicases and flap-endonucleases (Holt, 2009). PIF1 is a helicase which unwinds short flaps, containing the 5' RNA primers for each Okazaki fragment (Futami *et al.*, 2007). SSBP1 can bind to the DNA in the flap to moderate the association of the flap endonclueases DNA2 and FEN1, which cleave the 5' of the flap, and process the remaining nucleotides respectively (Liu *et al.*, 2008, Zheng *et al.*, 2008) (Figure 1.12C-D). A DNA ligase, potentially ligase III, must then join each fragment to form a continuous strand.

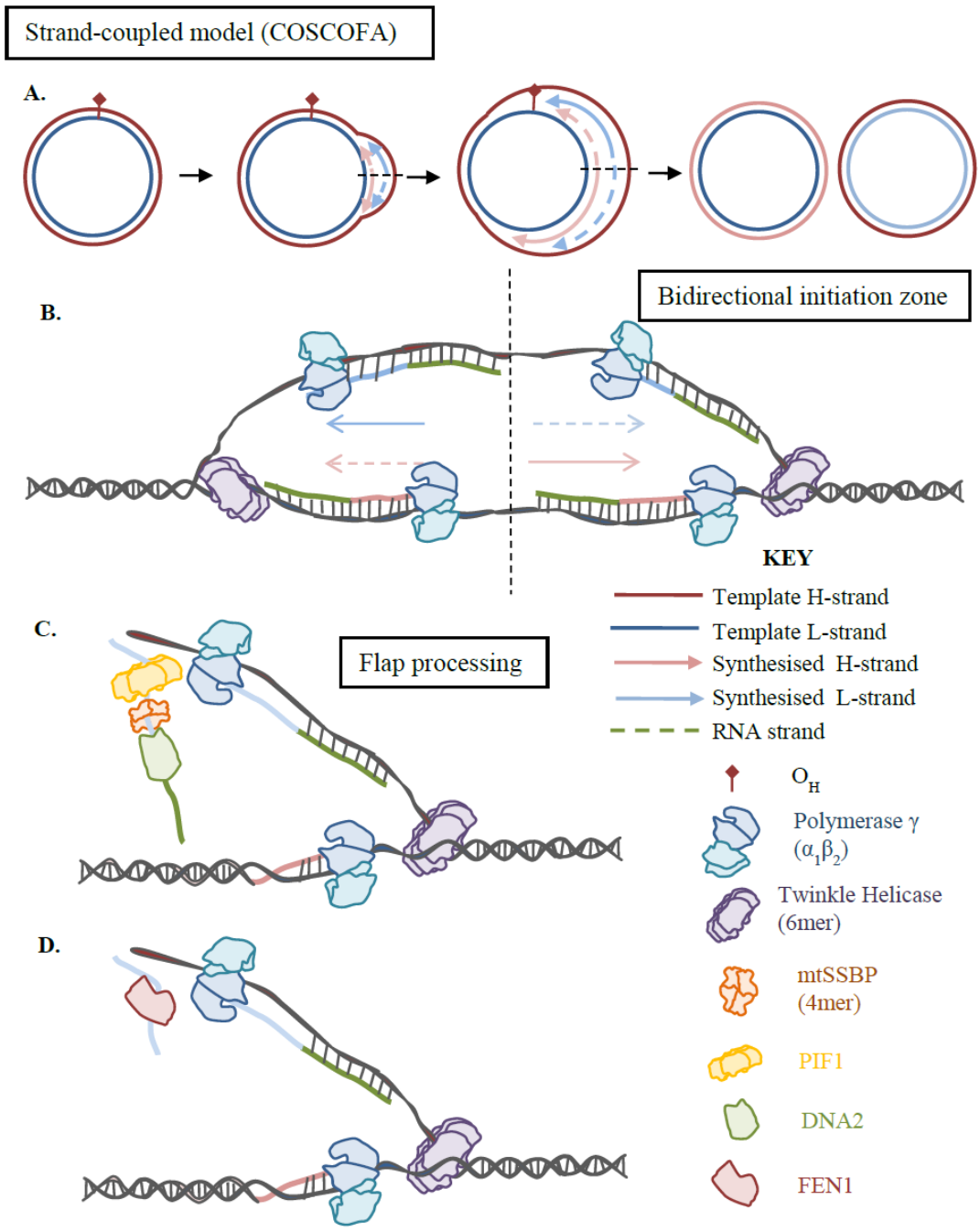

Figure 1.12 The COSCOFA model of mtDNA replication. (A) Schematic for replication via the conventional, strand-coupled Okazaki fragment associated (COSCOFA) mechanism. (B) Initiation of replication occurs bidirectionally at the 'initiation zone', with lagging-strand synthesis occurring alternately in each direction. (C) RNA primers for formation of Okazaki fragments are cleaved off, and (D) the remaining flaps removed by flap endonucleases.

The relative abundance of intermediates from different replication modes vary between tissue types, with RITOLS intermediates predominating in cultured cells, liver and kidney tissue, and COSCOFA intermediates being highest in skeletal muscle, heart and cultured cells recovering from depletion (Pohjoismaki and Goffart, 2011).

Pausing and Termination

The replication machinery has been shown to pause at particular positions on the mtDNA, which is enhanced in regions of MTERF binding (Hyvarinen *et al.*, 2007). Replication pausing may serve to facilitate the passage of transcription and replication machinery, particularly at the $tRNA^{Leu}$ position regulating the highly transcribed region of rRNA genes.

As previously stated, one direction of COSCOFA replication terminates prematurely at O_H, whilst the other direction continues around the entire genome, until meeting again at the NCR. Although not much is known of replication termination, it has been shown that 4-way junctions are formed in this region (Bowmaker *et al.*, 2003). *Twinkle* and members of the MTERF family seem to be necessary for resolution of these molecules (Hyvarinen *et al.*, 2011).

Repair

Originally it was thought that mitochondria had no DNA repair mechanisms; however, there are now several repair pathways identified which act in mitochondria (Stuart and Brown, 2006). This repertoire has been expanded to include base excision repair (BER), mismatch repair, and homologous/nonhomologous end-joining (Liu and Demple, 2010). Importantly, replication enzymes such as Pol γ and flap processing enzymes DNA2 and FEN1 are involved in BER. SSBP1 has been shown to prevent processing of damaged bases, such as excision of uracil, whilst DNA remains single stranded (Wollen Steen *et al.*, 2012). Ensuring DNA is double-stranded ensures no nicks being formed in DNA.

1.4.4 Nucleoids

As previously stated, mtDNA is not as unprotected as once thought, but is contained within protein aggregates known as nucleoids. Limitations in labelling and microscopy have made estimating numbers of nucleoids and the mtDNA content of each nucleoid difficult (Bogenhagen, 2012). Recent advances in imaging have led to a conservative estimate of 1-3 mtDNA molecules per nucleoid, tightly packed into an average volume

of 830,000 nm^3 (Brown *et al.*, 2011, Kukat *et al.*, 2011). TFAM facilitates this compaction by nonspecific binding and bending of the mtDNA within nucleoids (Kaufman *et al.*, 2007). TFAM occupies a 22bp region of DNA when bound the HSP; however, the ratio of TFAM molecules to mtDNA is still under debate, and may vary widely between species, tissue types and gene expression conditions (Cotney *et al.*, 2007, Ngo *et al.*, 2011, Rubio-Cosials *et al.*, 2011). Aldehyde cross-linking and immunoaffinity purification established that the core components of the transcription and replication machinery, such as Pol γ and TFB2M, as well as a diverse range of proteins involved in mtDNA maintenance, are contained within nucleoids (Bogenhagen *et al.*, 2008, Wang and Bogenhagen, 2006). This includes several mitochondrial ribosomal proteins, suggesting association of nucleoids with translational machinery. Immunoprecipitation using ribosomal recycling factor (a translational protein) identified well-known nucleoid proteins, further supporting the notion of linked transcription and translation (Rorbach *et al.*, 2008).

1.4.5 Translation

The 13 protein coding genes of the mtDNA require translation by an independent system located in the mitochondria. An overview of this process can be seen in Figure 1.13.

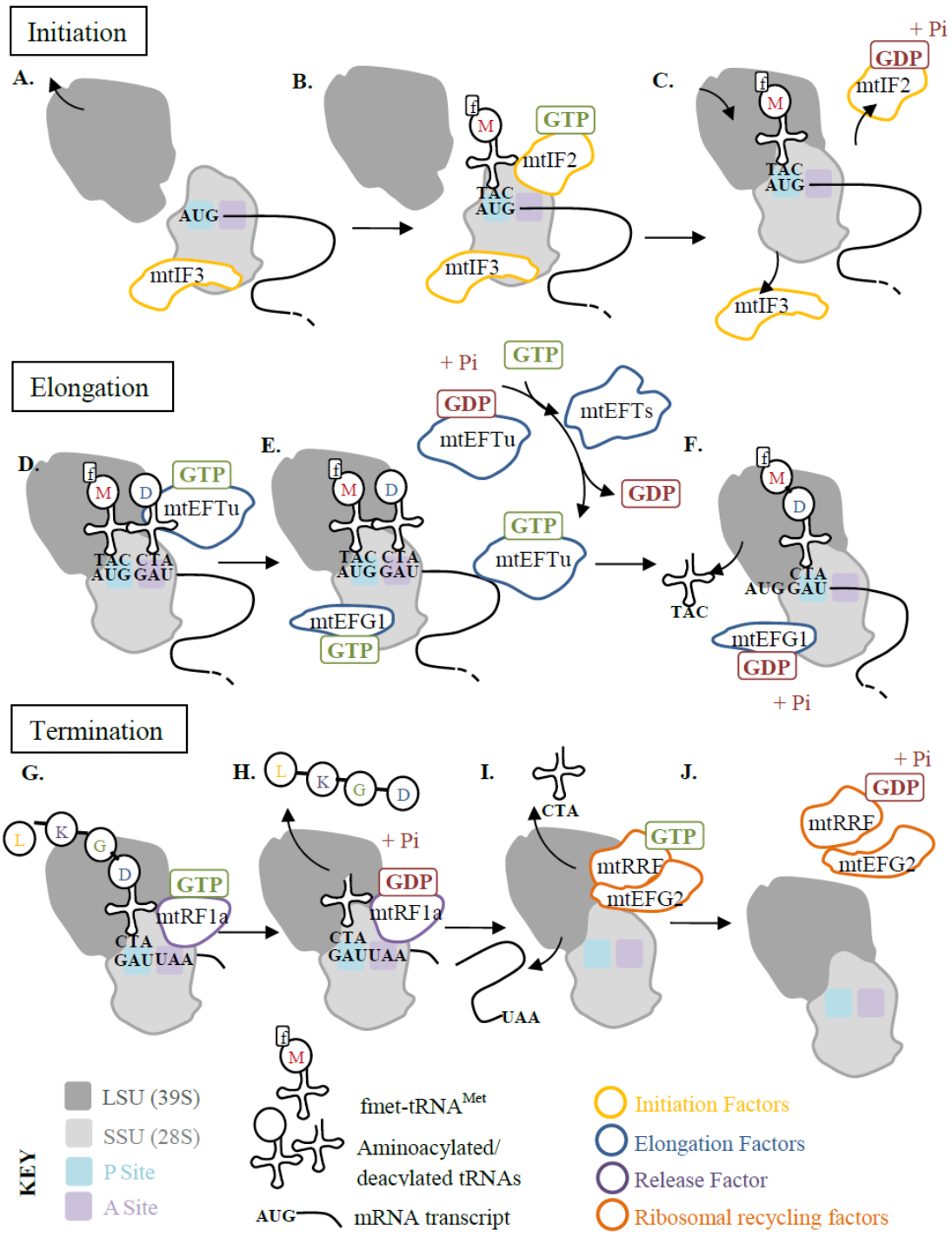

Figure 1.13 An overview of mitochondrial translation. Mitochondrial translation begins with initiation. (A) mtIF3 dissociates the LSU and mRNA transcripts bind the LSU. (B) mtIF2 recruits fMet-tRNA^{Met} to the p site. (C) mtIF2 is removed from the mitoribosome. (D) mtEFTu recruits the next aminoacylated tRNA. (E) mtEFTu is removed, mtEFTs exchanges GDP for GTP to recycle mtEFTu and mtEFG1 binds. (F) A peptide bond forms between the amino acids, a conformational change shifts the tRNA/mRNA along and the deacylated tRNA exits. (G) When a stop codon is encountered, mtRF1a binds. (H) The ester bond between the nascent peptide and tRNA is hydrolysed. (I) mtRRF and mtEFG2 are recruited to remove the mRNA and deacylated tRNA. (J) mtRRF and mtEFG2 leave the mitoribosome.

The mitochondrial translation system uses a different genetic code to cytoplasmic translation, with even a universal stop codon (UGA) being used instead as a tryptophan codon (Osawa *et al.*, 1992). The codon recognition system is simplified to allow recognition of all codons by only the 22 tRNAs encoded by the mtDNA (Barrell *et al.*, 1980). The mRNA transcripts generated from transcription of mtDNA also differ, with little to no 5' UTR sequence (Montoya *et al.*, 1981) or 5' 7-methylguanylate (m^7G) cap (Grohmann *et al.*, 1978) and with the polyA tail directly following, and sometimes forming, the stop codon (Ojala *et al.*, 1981).

Mitochondrial tRNAs

Mitochondrial tRNAs form clover-leaf secondary and L-shaped tertiary structures, similar to cytosolic tRNAs, though there are small structural variations (Helm *et al.*, 2000). They are more heavily reliant on post-transcriptional modification for structural stability and function (Helm, 2006). For example, initiation of translation requires formylated methionyl-tRNA (fMet-$tRNA^{Met}$). In cytosolic and bacterial translation, there are two independent methionyl-tRNAs, but in mitochondria there is just one, where a proportion is formylated by mitochondrial methionyl-tRNA transformylase (MTFMT) (Mikelsaar, 1983, Takeuchi *et al.*, 1997).

Mitoribosomes

The mitoribosomes (55S) contain the two rRNAs (12S and 16S), encoded by the mtDNA, and approximately 81 mitochondrial ribosomal proteins (MRPs), encoded by the nuclear DNA (Smits *et al.*, 2007). They lack some rRNA components compared to bacterial ribosomes, but have additional protein subunits. These, however, do not compensate for the lacking rRNA but form their own mitochondrial specific functions (Sharma *et al.*, 2003).

Translation initiation

Initiation is the first stage of translation. There are two mitochondrial translation initiation factors (IFs), mtIF2 and mtIF3 (Koc and Spremulli, 2002, Ma and Spremulli, 1995). They are orthologous to prokaryotic IFs, except that mtIF2 has a 37-amino acid insertion that allows it to function as IF1 does in bacteria, aiding the formation of the initiation complex (Gaur *et al.*, 2008). mtIF3 begins initiation by dissociating the mitoribosome complex (55S) into the small (SSU; 28S) and large (LSU; 39S) ribosomal

subunits, thereby allowing the initiation complex to assemble (Figure 1.13A) (Christian and Spremulli, 2009). Despite lacking the 5' m^7G-cap or 5'UTR guidance sequences, the mRNA is bound to the SSU in a sequence-independent manner (Laursen *et al.*, 2005). This aligns the start codon (AUG) to the peptidyl (P) site of the mitoribosome. mtIF2, enhanced with GTP, is required for binding of fmet-$tRNA^{Met}$ to the SSU (Figure 1.13B) (Liao and Spremulli, 1990, Ma and Spremulli, 1996). Recombination of the LSU to the SSU complex triggers release of initiation factors (Figure 1.13C) (Haque *et al.*, 2008).

Translation elongation

There are three elongation factors: mtEFTu; mtEFTs and mtEFG1 (Hammarsund *et al.*, 2001, Ling *et al.*, 1997, Xin *et al.*, 1995). There is a homologue of mtEFG1, mtEFG2, which appears to have a role in ribosomal recycling rather than translocation (Tsuboi *et al.*, 2009). Elongation begins with mtEFu binding GTP and an aminoacylated tRNA and determines whether the tRNA has been aminoacylated correctly (Figure 1.13D) (Nagao *et al.*, 2007). This complex then moves to the A site, where the mitoribosome hydrolyses the GTP to release mtEFTu-GDP. This is then recycled by mtEFTs, which converts the bound GDP back to GTP (Figure 1.13E). A peptide bond forms between the amino acid in the P site and the newly added amino acid at the A site. Hydrolysis of GTP bound to mtEFG1 causes a conformation change in both mtEFG1 and the mitoribosome, translocating the mRNA and bound tRNA across, so the last amino acid is in the P site. The previous tRNA then exits the mitoribosome complex and the elongation cycle repeats (Figure 1.13F) (Smits *et al.*, 2010b).

Translation termination

There are three factors responsible for termination of mitochondrial translation. Originally, mtRF1 was deemed a release factor, but it has been shown to lack release factor activity, with mtRF1a being the only release factor required for termination at the UAA and UAG stop codons (Nozaki *et al.*, 2008, Soleimanpour-Lichaei *et al.*, 2007, Zhang and Spremulli, 1998). Although AGA and AGG were considered stop codons in MT-CO1 and MT-ND6 transcripts, it was shown that these codons actually cause ribosome stalling and frameshifting to produce a UAG stop codon, terminated by mtRF1a (Temperley *et al.*, 2010). Class II release factors in bacteria are responsible for dissociation of the release factors from the ribosome, but it remains unclear whether a

mitochondrial equivalent exists (Bertram *et al.*, 2001). Stop codons are recognised by mtRF1a bound to GTP, and triggers hydrolysis of the ester bond joining the tRNA and nascent peptide at the P site (Figure 1.13G-H). After termination, the mRNA and deacylated tRNA must be removed from the ribosomal complex; this is achieved by the ribosomal recycling factors (mtRRF and mtEFG2/RRF2) (Figure 1.13I). GTP hydrolysis then enables release of the recycling factors from the ribosomes (Figure 1.13J) (Rorbach *et al.*, 2008, Tsuboi *et al.*, 2009).

Regulation of translation

There is much unknown about regulation of mitochondrial translation. One possible mechanism involves the negative feedback system generated by the ATP-dependent m-AAA protease, essential for quality control of inner membrane proteins (Nolden *et al.*, 2005). When the m-AAA protease processes MRPL32, it forms a tight association with the inner membrane. If excess respiratory subunits accumulate, they could block the m-AAA protease, preventing processing of MRPL21 and decreasing the translation rate of new proteins.

Several potential COXI specific regulators of translation have been identified. Mutations in *TACO1* have shown lower levels of COXI being produced despite normal levels of *COXI* transcript (Weraarpachai *et al.*, 2009). Leucine-rich PPR-motif (LRPPRC) may also function in COXI translation regulation by stabilising *COXI* and *COXIII* transcripts (Xu *et al.*, 2004); however, it has also been thought to function in concert with heterogeneous nuclear ribonucleoprotein K (HnRNP K) and POLRMT in coupling transcription and translation (Shadel, 2004).

Post-translational processing

After translation, mitochondrial proteins are bound by chaperones such as HSP60 and HSP70, to prevent aggregation and ensure correct folding. HSP100/Clp chaperones disturb protein aggregates and process misfolded proteins by targeting them for refolding or degradation where appropriate (Voos and Rottgers, 2002). Proteases are responsible for quality control and degradation of aberrant proteins. Lon and Clp-like proteases are located in the matrix of the mitochondria, whereas AAA-proteases are positioned either side of the inner membrane (i-AAA (intermembrane space) and m-AAA (matrix) (Koppen and Langer, 2007).

Mitoribosomes are directly associated with the inner membrane (Liu and Spremulli, 2000), which allows for co-translational insertion of nascent peptides directly into the inner membrane. Several proteins are implicated in this process, including: Oxa1 (Bonnefoy *et al.*, 2009, Stuart, 2002); Mba1, Mrp20 and Mrpl40 homologues MRPL45, MRPL23 and MRPL24 respectively (Jia *et al.*, 2003, Jia *et al.*, 2009, Ott *et al.*, 2006). LETM1, a homologue to yeast Mdm38, has also been implicated in this process through its interaction with MRPL36 (Piao *et al.*, 2009). This would allow for efficient transition of peptides between translation machinery and addition to assembling complexes.

The majority of identified assembly factors have been associated with Complex I or IV (Fernandez-Vizarra *et al.*, 2009); however, assembly factors have been identified for all complexes, such as: NDUFA1 for Complex I (Vogel *et al.*, 2005); SDHAF1 for Complex II (Ghezzi *et al.*, 2009); BSC1L for Complex III (Pecina *et al.*, 2004); SURF1 for Complex IV and ATP11 for Complex V (Wang *et al.*, 2001). Correct assembly into supercomplexes is also essential for efficient mitochondrial function, and explains how assembly defects for one complex can cause combined respiratory deficiency by secondary instability of other complexes (Schagger *et al.*, 2004). There are also proteins essential for stability of particular supercomplexes. Tafazzin (encoded by *TAZ*) participates in cardiolipin metabolism, an inner membrane phospholipid, and mutations in this gene cause cardiolipin deficiency and instability of the $I/III_2/IV$ supercomplex (McKenzie *et al.*, 2006).

1.4.6 Regulation of biogenesis

Regulation of the demand for energy is not dependent on a singular rate-limiting step, and is reliant on many factors such as enzyme content, concentration of intermediate substrates and the steady-state energy levels in each tissue (Fell, 1992). These parameters can contribute to the understanding of how different specialised organs regulate mitochondrial bioenergetics in a different manner (Pfeiffer *et al.*, 2001). Mitochondrial biogenesis is an orchestrated process requiring the synthesis and import of proteins and lipids co-ordinated with the replication of mtDNA (Figure 1.14).

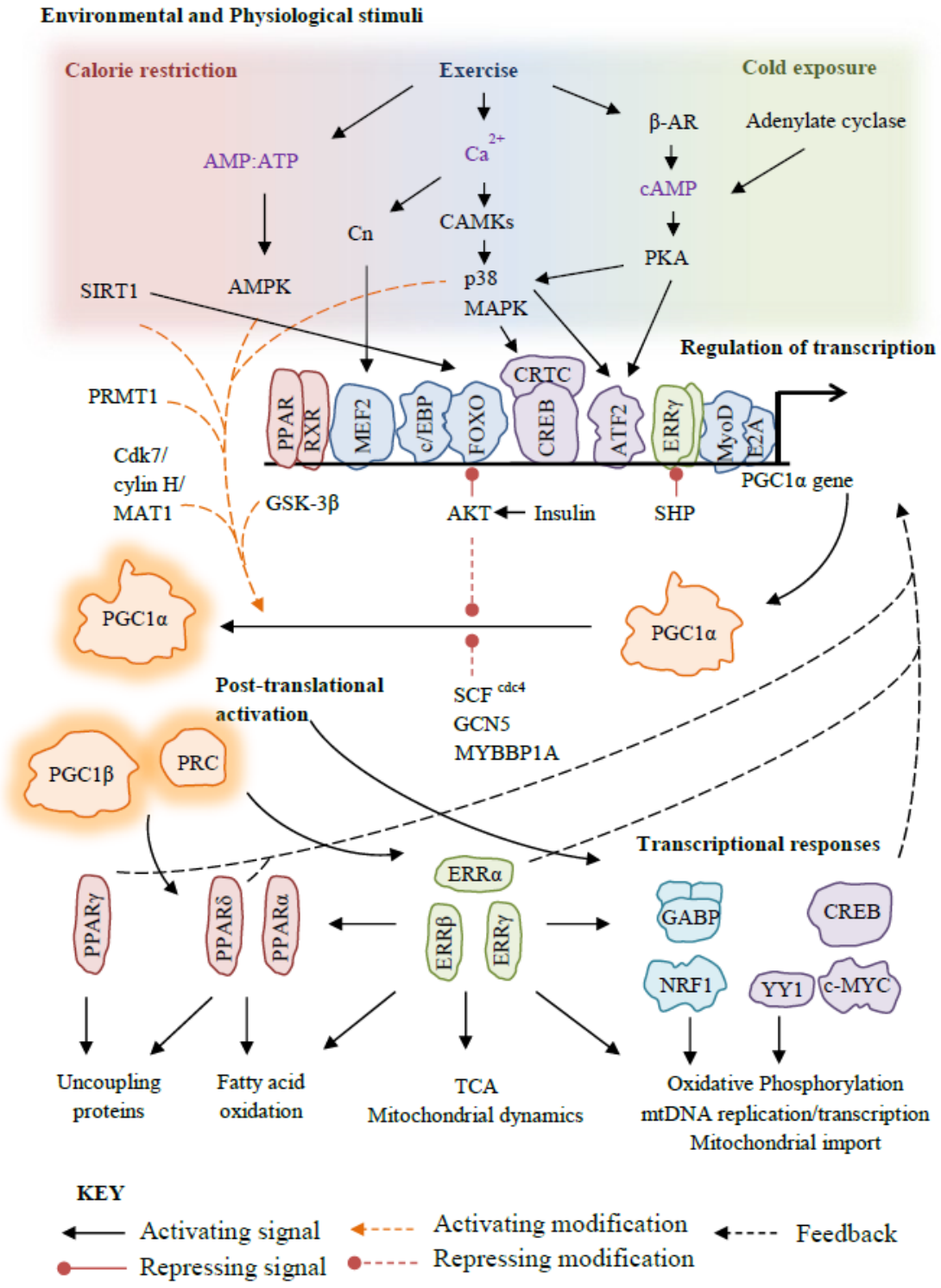

Figure 1.14 An overview of regulation of mitochondrial biogenesis. Temperature, exercise and calorie restriction can stimulate transcription factors responsible for upregulation of PGC1α expression and the post-translational modifications that regulate its activity. PGC1α induces downstream transcriptional responses to upregulate mitochondrial biogenesis (Adapted from Hock and Kralli, 2009).

Transcriptional co-regulators: The PGC1 family

Mitochondrial biogenesis can be stimulated by numerous methods, both through environmental or physiological stimuli or molecular metabolic processes. Co-ordination of this vast number of interconnecting pathways is achieved mainly through the PPARγ coactivator 1 (PGC1) family of proteins. These proteins have integral transcription activation domains, the ability to interact with numerous different transcription factors, and sites of post-translational modification, all of which allow a deeper level of complexity to its interaction with regulatory proteins (Hock and Kralli, 2009).

The predominant member of the family is peroxisome proliferator-activated receptor-γ coactivator 1 α (PGC1α; encoded by *PPARGC1A*), first identified through its interaction with PPARγ (Puigserver *et al.*, 1998). This led to the subsequent identification of PGC1β and PRC through their sequence homology to PGC1α (Andersson and Scarpulla, 2001, Lin *et al.*, 2002)

Upregulation of PGC1α and PGC1β in skeletal muscle causes increased mtDNA content, mitochondrial gene expression and improved exercise ability (Calvo *et al.*, 2008). Inactivation of either gene causes decreased mitochondrial expression and mitochondrial activity, with mild phenotypic impairment such as poor response to cold temperatures and weakened exercise capacity (Lelliott *et al.*, 2006, Leone *et al.*, 2005). PGC1α and PGC1β induce similar, but not identical, transcriptional responses and thus can compensate for mutational loss or downregulation of each other. However, in mice, if both genes are knocked out simultaneously there is a synergistic impact on mitochondrial function, with severe respiratory defects and death shortly after birth (Lai *et al.*, 2008).

Regulation of the PGC1 family is first achieved through tissue-specific transcriptional control of these gene products. Expression is inducible through environmental and physiological stimuli such as response to cold and exercise (Handschin and Spiegelman, 2006). Beyond transcriptional control, there is complicated regulation of PGC1α activity through post-translational regulation such as phosphorylation, acetylation, arginine methylation and ubiquitination (Jager *et al.*, 2007, Lerin *et al.*, 2006, Olson *et al.*, 2008, Teyssier *et al.*, 2005).

Receptor-interacting protein 140 (RIP140) is the major repressor for mitochondrial biogenesis, and acts in opposition to the PGC1 family members. It interacts with similar

targets to PGC1α/β, and recruits additional corepressors such as CtBP and histone deacetylases (HDACS) (Christian *et al.*, 2006, White *et al.*, 2008). Gene silencing or knock-out of RIP140 in mice leads to increased mitochondrial gene expression and biogenesis, and acts, at least in part, through interaction with ERRα (Leonardsson *et al.*, 2004, Powelka *et al.*, 2006). Like PGC1α, RIP140 is also regulated through post-translational modifications, such as sumoylation, acetylation and arginine methylation (Ho *et al.*, 2008, Mostaqul Huq *et al.*, 2006, Rytinki and Palvimo, 2008).

Physiological stimuli

Endurance training and exercise is known to stimulate mitochondrial biogenesis as a response to rising cellular energy demand. Signals induced by physical activity include increased muscle contraction-induced Ca^{2+} levels, and cellular response to energy deficit through AMP-activated protein kinases (AMPKs). Exercise can also stimulate the sympathetic nervous system causing adrenergic and cAMP signalling (Rockl *et al.*, 2008).

Adaptive thermogenesis in response to cold also activates the sympathetic nervous system inducing adrenergic stimulation with an increase of cAMP signalling (Klingenspor, 2003). This ultimately induces uncoupling proteins which cause the proton gradient produced through the ETC to generate heat rather than ATP (Cao *et al.*, 2004).

In situations of long-term calorie restriction, energy substrates for respiration are limited and therefore mitochondria must become more efficient to maintain cellular energy levels. Calorie restriction was thought to increase mitochondrial biogenesis through pathways required to increase energy production efficiency, such as AMPK, Sirtuin 1 (SIRT1) and endothelial nitric oxide synthase (eNOS) signalling (Lopez-Lluch *et al.*, 2006, Nisoli *et al.*, 2005). However; recent evidence suggests that mitochondrial efficiency is increased without upregulation of mitochondrial mass (Lanza *et al.*, 2012) and that calorie restriction merely preserves mitochondrial biogenesis during aging to extend lifespan (Picca *et al.*, 2013).

Molecular signalling pathways

Partial control of mitochondrial biogenesis relies on the balance between ATP production and ATP consumption, mirrored by the respective levels of AMP (adenine

monophosphate) compared to ATP. When the AMP/ATP ratio is high, AMPKs are triggered, which send downstream signals to block energy-demanding processes whilst enhancing metabolic processes to generate ATP (Hardie, 2007). A downstream target of AMPKs is SIRT1, which deacetylates downstream targets such as PGC1α, forkhead box O1 and O3 (FOXO1/FOXO3a) (Greer *et al.*, 2007). These proteins and their downstream targets represent the major pathways connecting external physiological stimuli to regulation of mitochondrial biogenesis.

Ca^{2+} signalling induces mitochondrial biogenesis through calcineurin (a Ca^{2+}-dependent phosphatase), Ca^{2+}/calmodulin dependent kinases (CAMKs) and p38 MAPK (Rockl *et al.*, 2008). These signalling molecules act upon the PGC1α promoter, in conjunction with transcription factors of the MEF2 and CREB/ATF2 families, to induce expression of PGC1α (Akimoto *et al.*, 2008, Akimoto *et al.*, 2005, Handschin *et al.*, 2003, McGee and Hargreaves, 2004). p38 MAPK also stimulates PGC1α activity through phosphorylation (Puigserver *et al.*, 2001).

Adrenergic stimulation and cAMP signalling has been implicated in the regulation of mitochondrial biogenesis (Miura *et al.*, 2007). The cAMP response-element binding protein (CREB) can induce gene expression in some genes directly through promoter binding, or indirectly through upregulation of PGC1α. It has also been shown to translocate to the mitochondria and cause the upregulation of mitochondrially-encoded genes (De Rasmo *et al.*, 2009).

Another mechanism of stimulation, is inducing the expression of eNOS, increasing intracellular nitric oxide (NO) levels, and further stimulating mitochondrial biogenesis through increased expression of PGC1α (Nisoli *et al.*, 2005, Niwano *et al.*, 2006). PPARγ and PGC1α expression has also been enhanced by induction of neuregulins, which can activate ErbB tyrosine kinases and increase mitochondrial expression and oxidative capacity (Canto *et al.*, 2006, Lebrasseur *et al.*, 2003).

c-Myc binds to the promoter regions of 107 nuclear-encoded mitochondrial genes and can activate expression of PGC1β (Kim *et al.*, 2008, Zhang *et al.*, 2007). Although further study is required, the other functions of c-Myc would suggest a possible link between cellular proliferation and mitochondrial biogenesis. Similarly, YY1 transcription factor (YY1) has been shown to complex with PGC1α in muscle, dependent on mammalian target of rapamycin (mTOR) (Cunningham *et al.*, 2007).

Since mTOR promotes cellular growth in the presence of sufficient nutrients, it is conceivable that YY1 regulates mitochondrial biogenesis in response to nutrient levels and with subsequent cellular growth patterns.

Downstream transcription factor responses

Nuclear respiratory factor 1 (NRF1) was first identified through its binding with cytochrome c promoter; however, binding sites for NRF1 have been identified in the promoter regions of many mitochondrial genes (including *TFAM, TFB1M* and *TFB2M*) (Scarpulla, 2008, Virbasius *et al.*, 1993a). *NRF1* expression can be regulated through phosphorylation or interaction with PGC1 family proteins (Wu *et al.*, 1999). Its activity is repressed by cyclin D1, linking mitochondrial biogenesis to cell cycle progression (Wang *et al.*, 2006). *NRF1* expression does not regulate mitochondrial biogenesis alone, as upregulation of *NRF1* transcripts does increase the expression of some of its targets, but does not increase the capacity for respiration (Baar *et al.*, 2003). Overexpression of *NRF1* in adipocytes increases mtDNA copy number but decreases lipid content and does not stimulate an increase in ATP production in cells. Furthermore, in addition to mitochondrial metabolic changes, continuous *NRF1* overexpression alters cellular proliferation, apotosis and inflammatory response and eventually leads to insulin resistence in adiopocytes (van Tienen *et al.*, 2010).

NRF2, more correctly known as GA repeat -binding protein (GABP) is a heterotetramer comprised of two subunits, GABPα (encoded by *GABPA*) and GABPβ1 or β2 (encoded by *GABPB1* and *GABPB2* respectively) (Virbasius *et al.*, 1993b). It also has promoter binding sites in many nuclear mitochondrial genes, including a subset downregulated in diabetes (Mootha *et al.*, 2004). With the addition of host-cell factor 1 (*HCF1*), phosphorylated GABP can recruit PGC1α and PGC-1-related coactivator (PRC) to further increase its transcriptional activity (Vercauteren *et al.*, 2008).

Peroxisome proliferator-activated receptors (PPARα, PPARγ, and PPARδ) are predominantly involved in lipid homeostasis and each is highly abundant in different tissues (Evans *et al.*, 2004). They also regulate the expression of uncoupling proteins (UCPs) which allows adaptive responses to external stimuli such as exercise and cold temperatures in a tissue-specific manner (Puigserver *et al.*, 1998). A PPAR response element (PPRE) has been identified in the promoter PGC1α, allowing PPARs to enhance the activity of the transcriptional co-activtors (Tanaka *et al.*, 2003).

Estrogen-related receptors (ERRα, ERRβ, and ERRγ) are not regulated by estrogen, but instead are regulated by interaction with coactivators such as SRC or the PGC1 family, which can activate transcription of mitochondrial genes (Giguere, 2008, Schreiber *et al.*, 2003). ERRs bind to ERR response elements (ERREs) in the promoters of genes involved in fatty acid oxidation, components of OXPHOS, the TCA cycle, mitochondrial dynamics and stress response. In concert with receptor-interacting protein 140 (RIP40), ERRs can become negative repressors of transcription, causing downregulation of genes typically upregulated by PGC1 coactivators (White *et al.*, 2008). They also have indirect stimulatory effect on biogenesis through upregulation of GAPBα and PPARα (Huss *et al.*, 2004, Mootha *et al.*, 2004).

Mitochondrial dynamics and degradation

The mitochondrial network is continuously fluctuating, resulting from multiple fission and fusion events. Key proteins responsible for mitochondrial dynamics are OPA1, MFN1, MFN2, FIS1 and DRP1. Mutations in these genes result in defects in mitochondrial dynamics leading to compromised energy production (Chen *et al.*, 2005). Recent evidence also suggests that mitochondrial dynamics can contribute to the regulation of ATP production in normal physiological situations. In times of stress, cells can undergo stress-induced mitochondrial hyperfusion (SIMH) which is accompanied by an increase in cellular ATP content (Tondera *et al.*, 2009). Since mitochondria are heterogeneous in terms of shape, structure, position and the distribution of internal respiratory components (Wikstrom *et al.*, 2009), fusion events could promote functional complementation across the mitochondrial network to prevent loss of ATP production in particular regions of the network (Nakada *et al.*, 2001). This is corroborated by the evidence that MFN2 is upregulated in situations of high energetic demand, and overexpression of MFN2 stimulates mitochondrial biogenesis and glycolysis (Bach *et al.*, 2005, Bach *et al.*, 2003).

Mitochondrial dynamics are also responsible for maintenance of mitochondrial function through selective separation of dysfunctional segments of the mitochondrial network, which are then targeted for degradation through mitophagy (Twig *et al.*, 2008).

1.5 Genetic Variation and Disease

In 1962, investigation of a female patient with severe hypermetabolism identified morphologically abnormal mitochondria in her muscle biopsy and an uncoupling of

mitochondrial oxidation and phosphorylation (Luft *et al.*, 1962). In the 1970s there were several more cases with mitochondrial dysfunction reported, leading eventually to the first classification of mitochondrial diseases based on which area of metabolism they affected (DiMauro *et al.*, 1985). Mitochondrial disorders can usually be classified more specifically into well-defined syndromes, but often show high levels of phenotypic overlap.

1.5.1 Overview of mitochondrial disease phenotypes

Mitochondrial disorders are often multisystemic, typically having dysfunction in organs with high energy demands. The diverse range of clinical phenotypes associated with mitochondrial diseases is highlighted in Table 1.2.

Table 1.2 Clinical features in mitochondrial disorders. The clinical phenotypes common to mitochondrial disorders in adults and children listed by the affected system of the body (Adapted from Taylor and Turnbull, 2005).

System	Adult	Paediatric
Neurological	Migraine, strokes, epilepsy, dementia, myopathy, peripheral neuropathy, diplopia, ataxia, speech disturbances, sensorineural deafness	Epilepsy, myopathy, psychomotor retardation, ataxia, spasticity, dystonia, sensorineural deafness
Gastrointestinal	Constipation, irritable bowel, dysphagia	Vomiting, failure to thrive, dysphagia
Cardiac	Heart failure, heart block, cardiomyopathy	Biventricular hypertrophic cardiomyopathy, rhythm abnormalities
Respiratory	Respiratory failure, nocturnal hypoventilation, recurrent aspiration, pneumonia	Central hypoventilation, apnoea
Endocrinal	Diabetes, thyroid disease, parathyroid disease, ovarian failure	Diabetes, adrenal failure
Ophthalmological	Optic Atrophy, cataract, ophthalmoplegia, ptosis	Optic atrophy
Haematological	-	Anaemia, pancytopaenia
Renal	-	Renal tubular defects
Liver	-	Hepatic failure

A core set of symptoms are used to classify each disease, but additional clinical presentations are common and variable. For example, myoclonic epilepsy with ragged-red fibres (MERRF) is diagnosed based on myoclonus, ataxia and seizures but is frequently observed with a combination of psychomotor regression, peripheral neuropathy, short stature and sensorineural hearing loss (DiMauro and Schon, 2001).

1.5.2 Primary mtDNA mutations

The first mtDNA point mutation discovered was m.11778G>A, in the protein coding gene *MT-ND4*, associated with Leber's Hereditary Optic Neuropathy (LHON) (Wallace *et al.*, 1988). This was shortly followed by the discovery of mtDNA macrodeletions of up to 7kb in patients with general mitochondrial myopathy (Holt *et al.*, 1988). The first tRNA mutations, m.8344A>G and m.3243A>G, were identified in 1990 as the cause of myoclonic epilepsy with ragged-red fibres (MERRF) and mitochondrial encephalomyopathy, lactic acidosis, and stroke-like episodes (MELAS) respectively (Goto *et al.*, 1990, Shoffner *et al.*, 1990).

Scoring systems have been developed to determine the probability of newly discovered mutations in either RNA or protein-coding genes being pathogenic (McFarland *et al.*, 2004, Mitchell *et al.*, 2006). The pathogenicity of all reported mtDNA mutations was assessed by Hellebrekers and colleagues (2012), and used to determine the possibility of pathogenic heteroplasmic mutation carriers having healthy children through preimplantation genetic diagnosis (PGD) (Hellebrekers *et al.*, 2012).

Mutations affecting protein synthesis

Mutations disrupting mitochondrial protein synthesis can be either single deletions or point mutations in tRNA or rRNA genes. Mitomap (http://mitomap.org) lists 30 confirmed (248 reported) pathogenic point mutations in tRNA/rRNA genes (correct as of 12/05/2014).

Since any defects in protein synthesis will affect expression of all mitochondrial encoded proteins, disorders can be multisystemic. Additionally, defects in protein synthesis will generally cause lactic acidosis and mitochondrial proliferation, evidenced by the appearance of ragged-red fibres (RRFs) on muscle biopsy (DiMauro and Schon, 2001).

More than 50% of the identified pathogenic mutations are in tRNA genes, despite them only covering ~10% of the mitochondrial genome (Levinger *et al.*, 2004). Mutations in tRNA genes can cause misfolding, prevent correct base modification, cause instability or affect aminoacylation (Scaglia and Wong, 2008). The majority of pathogenic mutations occur on the stem structures of tRNAs, particularly in the anticodon and aminoacyl acceptor stems (McFarland *et al.*, 2004).

Of the two rRNA genes, pathogenic mutations have only ever been identified in the gene encoding 12S rRNA (*RNR1*). These mutations are typically associated with sensorineural deafness, the most common mutation being m.1555A>G (Rotig, 2011). In many cases, the mutation induces sensitivity to aminoglycosides, with variable clinical phenotypes when not exposed to the drug (Prezant *et al.*, 1993). Penetrance can be variable, and there is evidence that genes involved in post-transcriptional modification of 12S rRNA can act as nuclear modifiers of the m.1555A>G mutation (discussed further in Section 1.5.3) (Bykhovskaya *et al.*, 2004b, Guan *et al.*, 2006).

Mutations in protein-coding genes

The mitochondrial genome encodes subunits for Complex I, III, IV and V. Mitomap lists 29 confirmed (226 reported) pathogenic point mutations in these genes (correct as of 12/05/14). The majority of these mutations are heteroplasmic, with the homoplasmic mutations seemingly modified by tissue-specific nuclear genes (Wong, 2007).

Mutations have been found in all seven Complex I genes (*MT-ND1-6, MT-ND4L*), usually, but not exclusively, causing LHON, MELAS or Leigh syndrome (Brown *et al.*, 1995, Kirby *et al.*, 2004, Lebon *et al.*, 2003). Mutations in the only Complex III subunit, *MT-CYTB*, cause a more diverse set of clinical symptoms, but most commonly include exercise intolerance, myoglobinuria, hypertrophic cardiomyopathy and mitochondrial encephalopathy (Andreu *et al.*, 1999). Mutations in any of the three Complex IV genes (*MT-CO1-3*) cause a wide range of clinical phenotypes, most commonly including myopathy, exercise intolerance, rhabdomyolysis, and severe early-onset Leigh syndrome (Horvath *et al.*, 2005, Shoubridge, 2001). The majority of mutations in the two Complex V genes (*MT-ATP6, MT-ATP8)* cause Leigh syndrome, though cases with bilateral striatal necrosis (BSN) and neuropathy, ataxia, retinitis pigmentosa (NARP) have been identified (De Meirleir *et al.*, 1995, Enns *et al.*, 2006).

mtDNA rearrangements

Mitomap lists 133 deletions ranging in size from 4 to 10987 bases, and six small insertions ranging from 4 to 266 bp (correct as of 12/05/14). There has even been a case of a small, 7 bp inversion in the *ND1* gene causing mitochondrial myopathy (Musumeci *et al.*, 2000).

Whereas multiple deletions arise from nuclear mutations in genes involved in mtDNA maintenance, single mtDNA mutations arise from clonally expanded, sporadic events (Suomalainen and Kaukonen, 2001). Single mtDNA deletions are estimated to account for a quarter of adult mitochondrial diseases, and also to cause some cases of paediatric disease (Chinnery *et al.*, 2000a). One mechanism suggests that homologous base pairs on alternative strands align and loop out regions of the mtDNA molecule during asynchronous replication (Shoffner *et al.*, 1989), another suggests that the deletions occur during double-strand break repair (Krishnan *et al.*, 2008).

The common mtDNA deletion removes 4977 bp of DNA, containing several protein-coding genes and many tRNA genes, whilst retaining the ability to replicate (Barritt *et al.*, 1999, Chan *et al.*, 2005, Chen *et al.*, 1995). Although a diverse range of phenotypes occur due to single deletions, the most commonly associated syndromes are Pearson marrow-pancreas syndrome (PMPS), Kearns–Sayre syndrome (KSS) and Progressive external ophthalmoplegia (PEO) (Pitceathly *et al.*, 2012).

1.5.3 nDNA mutations

The first nuclear mutation affecting mitochondrial function was described in a subunit of Complex II, causing Leigh Syndrome (Bourgeron *et al.*, 1995).

Structural subunit genes

The most common mutations discovered in nuclear encoded OXPHOS subunits are in Complex I genes. Usually, mutations in nuclear Complex I subunits result in Leigh Syndrome (Loeffen *et al.*, 1998), but others have been identified in patients with hypertrophic cardiomyopathy and encephalomyopathy (Benit *et al.*, 2003). Complex II subunit mutations have also resulted in Leigh Syndrome (Bourgeron *et al.*, 1995) but most often result in paragangliomas (Baysal *et al.*, 2000). Complex III and IV mutations are more rare, with variable associated phenotypes such as hypoglycaemia and lactic acidosis (Haut *et al.*, 2003) and infantile encephalomyopathy respectively (Massa *et al.*, 2008). To date, there has been no complex V nuclear subunit mutations identified.

mtDNA maintenance and mitochondrial depletion syndromes (MDS)

Maintenance of mtDNA levels requires a diverse set of proteins surrounding replication of the mitochondrial genome. This includes Pol γ, both the catalytic and accessory subunits (encoded by *POLG and POLG2* respectively), along with additional proteins

involved with replication such as the helicase *Twinkle* (encoded by *C10orf2*). It also involves maintenance of a stable dNTP pool to supply Pol γ during replication. Mutations in genes responsible for dNTP pool maintenance often lead to induced point mutations, deletions and mtDNA depletion (Copeland, 2008, Saada, 2004).

The first mutation identified in *POLG* was associated with progressive external opthalmoplegia (PEO) with classical appearance of mtDNA deletions (Van Goethem *et al.*, 2001). Since then, further mutations have been found commonly associated with Alpers' syndrome (Naviaux and Nguyen, 2004) and several types of ataxia-neuropathy such as sensory ataxic neuropathy, dysarthria and ophthalmoparesis (SANDO) (Van Goethem *et al.*, 2001).

Later, a mutation was identified in *POLG2*, causing a phenotype similar to that caused by *POLG* mutations in PEO, presumably through failure to enhance processivity of Pol γ (Longley *et al.*, 2006). Mutations in *C10orf2* (*Twinkle*) have also been found associated with PEO (Spelbrink *et al.*, 2001) and SANDO (Spelbrink *et al.*, 2001). Solute carrier family 25 (mitochondrial carrier; adenine nucleotide translocator), member 4 (SLC25A4; formerly adenine nucleotide transporter 1, ANT1), has also been found to cause PEO when mutated (Kaukonen *et al.*, 2000).

There are several genes regulating dNTP pools implicated in mitochondrial diseases. Mutations in thymidine phosphorylase (encoded by *ECGF1*) are commonly associated with mitochondrial neurogastrointestinal encephalomyopathy (MNGIE) (Nishino *et al.*, 1999). Mutations in mitochondrial thymidine kinase (*TK2*) cause dysfunction mainly in skeletal muscle, where *TK2* expression is the highest (Saada *et al.*, 2003), causing fatal myopathy and mitochondrial depletion in infants (Saada *et al.*, 2001). Deoxyguanosine kinase (*DGUOK*) mutations cause severe hepatocerebral forms of mitochondrial depletion syndrome (MDS) (Mandel *et al.*, 2001). Further genes affected by mutations causing MDS in various forms include: deoxynucleotide carrier (*SLC25A19*) (Rosenberg *et al.*, 2002); succinyl-coA subunits (*SUCLG1/SUCLA2*) (Elpeleg *et al.*, 2005, Ostergaard *et al.*, 2007); *MPV17* (Spinazzola *et al.*, 2006) and p53-inducible ribonucleotide reductase (*RRM2B*) (Bourdon *et al.*, 2007).

Several mutations were identified in *OPA1*, a mitochondrial fusion gene, as causing dominant optic atrophy plus (DOA+) (Amati-Bonneau *et al.*, 2008, Hudson *et al.*, 2008). Though the condition mainly affects the ocular system, it was later established

that mutations in *OPA1* usually cause multi-system neurological dysfunction (Yu-Wai-Man *et al.*, 2010). Later, in patients suffering with optic atrophy, axonal sensorimotor neuropathy and cerebellar ataxia, mutations in another mitochondrial fusion gene, *MFN2*, were identified (Rouzier *et al.*, 2012). Mutations in both *OPA1* and *MFN2* cause accumulation of somatic mtDNA deletions, and the disease mechanism is suspected to be either increased rate of *de novo* mutation formation or accelerated clonal expansion of pre-existing mutations (Yu-Wai-Man and Chinnery, 2012).

Translation factors

Since mitochondrially-encoded proteins require their own translation machinery, it is inevitable that mutations in genes encoding these proteins will affect mitochondrial function. Mutations have been identified in proteins covering a broad range of translational functions. Mutations in mitoribosomal protein genes, such as *MRPS16*, cause fatal neonatal lactic acidosis (Miller *et al.*, 2004). Mutations in genes encoding elongation factors, such EFTu or EFG1, can cause severe lactic acidosis and progressive, fatal encephalopathy (Valente *et al.*, 2007). There is also a wide range of tRNA processing proteins essential for mitochondrial translation. The first group are tRNA synthetases, responsible for aminoacylation of the tRNAs. Mutations in *DARS2* were found in 30 families with Leukoencephalopathy with brain stem and spinal cord involvement and lactate elevation (LBSL) (Scheper *et al.*, 2007). TRMU is responsible for 2-thiolation of the wobble bases in tRNA-Lys, tRNA-Gln, and tRNA-Glu, and mutations can cause acute liver failure in infancy (Zeharia *et al.*, 2009). PUS1 converts uridine to pseudouridine in tRNAs, thought to stabilise the tertiary structure and aid the peptidyl transferase, and mutations in *PUS1* cause mitochondrial myopathy, lactic acidosis and sideroblastic anaemia (MLASA) (Bykhovskaya *et al.*, 2004a). Paraplegin is a protein of the m-AAA protease, involved in quality control and ribosomal processing. A mutation has been found in this gene causing hereditary spastic paraplegia (Casari *et al.*, 1998).

Import proteins

Defects in mitochondrial import can have widespread phenotypic consequences due to the diverse nature of proteins requiring import into mitochondria. Mutations in *TIMM8A*, a component of the inner membrane translocase complex, have been identified as causing deafness-dystonia syndrome (DDS; also known as Mohr-

Tranebjaerg syndrome, MTS) and Jensen Syndrome (Jin *et al.*, 1996, Tranebjaerg *et al.*, 2000). Mutations in TIM23 complex protein *DNAJC19* cause dilated cardiomyopathy with ataxia (DCMA) syndrome (Davey *et al.*, 2006).

Complex assembly factors

Many mutations have been found in assembly factors for Complex I, III, IV and V. Mutations in Complex I assembly factor gene, *NDUFAF*, cause decreased Complex I activity leading to progressive encephalopathy (Ogilvie *et al.*, 2005). Mutations in Complex III assembly factor *BCS1L* have been associated with hepatic failure, tubulopathy and encephalopathy (de Lonlay *et al.*, 2001). Complex IV assembly factor mutations are the most abundant, such as *SURF1* mutations causing Leigh Syndrome (Tiranti *et al.*, 1998), and *SCO1/SCO2* mutations causing neonatal hepatic failure, encephalopathy and neonatal cardioencephalomyopathy (Papadopoulou *et al.*, 1999, Valnot *et al.*, 2000). Despite no mutations in Complex V nuclear subunit genes, mutations in ATP12, a complex V assembly gene, have been described as causing early-onset encephalopathy and lactic acidosis (De Meirleir *et al.*, 2004).

Nuclear modifiers of mtDNA mutations

Some mtDNA mutations require nDNA mutations acting in concert to produce distinct phenotypes. In 90% of cases with LHON, 1 of 3 mtDNA mutations are present, m.3460G>A, m.11778G>A or m.14484T>C. However, the presence of any of the mutations alone is not sufficient to cause LHON, with only 50% of males and 10% of females with a homoplasmic mutation developing a clinical phenotype (Man *et al.*, 2003). This suggests a nuclear modifying mutation is required for expression of the disease phenotype, which is yet to be identified (Hudson *et al.*, 2010, Hudson *et al.*, 2011).

The mtDNA mutation m.1555A>G in 12S rRNA is associated with maternally inherited deafness, and several nuclear gene mutations have been found which modify the phenotypic expression of this mutation. This includes some of the proteins responsible for methylation of 12S rRNA, TRMU and TFB1M (Bykhovskaya *et al.*, 2004b, Guan *et al.*, 2006).

1.5.4 Accumulation of mtDNA mutations with age

Approximately 90% of available tissue oxygen is consumed by mitochondria, 1-5% of which is leaked as oxygen radicals ($O_2 \cdot^-$), by Complex I and III (Richter *et al.*, 1995). These reactive oxygen species (ROS) are typically converted to hydrogen peroxide (H_2O_2) by manganese-superoxide dismutase (MnSOD), then subsequently detoxified by catalase (CAT) or glutathione peroxidase (GPx) (Fridovich, 1997). However, some ROS evade detoxification and can cause damage to nearby proteins and mtDNA molecules.

Many mitochondrial proteins are susceptible to oxidative damage, including proteins directly involved in energy metabolism, such as glutamate dehydrogenase (GDH) and support proteins such as prohibitin (PHB), which prevents protein misfolding (Conrad *et al.*, 2001, Schleicher *et al.*, 2008).

Pathogenic mutations affecting OXPHOS capacity have been shown to exacerbate the leak of oxygen radicals from mitochondrial complexes (Piccolo *et al.*, 1991, Smits *et al.*, 2010a). Although somatic mutations can be introduced onto individual mtDNA molecules, the accumulation of high enough heteroplasmy levels to cause loss of mitochondrial activity is more likely occur from clonal expansion of mtDNA mutations present at birth (Elson *et al.*, 2001), as studies show affected cells to have a single mutation type. There is evidence of tissue-specific 'hot spots' where mutations are frequently discovered, particularly in the 407-411 region of mtDNA (Corral-Debrinski *et al.*, 1992, Nekhaeva *et al.*, 2002), though age-related mutations can accumulate across the whole genome (Kraytsberg *et al.*, 2006, Michikawa *et al.*, 1999). Accumulation of mtDNA macrodeletions has also been observed in aged tissues (Cortopassi *et al.*, 1992).

The consequence of mtDNA mutations in aged tissues is evidenced by the mosaic loss of COX-activity in some tissues (such as muscle), strikingly similar to that of mitochondrial disease (Brierley *et al.*, 1998, Muller-Hocker *et al.*, 1992).

1.5.5 Mitochondrial involvement in common complex disease

mtDNA variants are also causative or associated with common complex diseases. Diabetes is the most common metabolic disease, and several mtDNA variants have been found to be the cause in a small number of cases (Lowell and Shulman, 2005). There is also accumulating evidence for mtDNA variants in the predisposition of common diseases such as diabetes, Alzheimer's disease and Parkinson's disease (Lin and Beal,

2006). Several studies have identified associations between particular haplogroups and the occurrence of common diseases; however, results often contradict one another, leaving the relevance of any identified association unclear (Chagnon *et al.*, 1999, Ross *et al.*, 2003, van der Walt *et al.*, 2004, van der Walt *et al.*, 2003).

Some mutations in nuclear-encoded mitochondrial genes are thought to cause tumours, such as fumarate hydratase mutations in uterine leiomyomas and renal cell carcinomas (Lehtonen *et al.*, 2004), and Complex II subunit mutations in paraganglioma formation (Astuti *et al.*, 2001, Baysal *et al.*, 2000). Increased ROS production is implicated in the pathogenesis of tumour formation, as MnSOD knockout in mice increased cancer incident by 100% (Van Remmen *et al.*, 2003), and many tumours have reduced MnSOD activity (Xu *et al.*, 1999). Accumulation of somatically acquired mtDNA mutations in cancers have also been observed, suggesting a possible link between risk of cancer and aging (Petros *et al.*, 2005).

1.5.6 Treatment of mitochondrial disease through manipulation of biogenesis

In most cases, mitochondrial disease cannot be prevented and treatment options are limited; however, several therapeutic strategies are being developed to combat a diverse range of mitochondrial disorders. These include replacement of defective gene products, scavenging toxic intermediates, optimising ATP synthesis and bypassing defective OXPHOS components (Wenz *et al.*, 2010).

Manipulation of Ca2+ concentration has potential therapeutic uses, as increases in mitochondrial Ca2+ concentration can stimulate dehydrogenases partaking in the TCA cycle with increased downstream ATP synthesis (Visch *et al.*, 2004).

Another method of increasing ATP synthesis to alleviate mitochondrial dysfunction is to stimulate biogenesis, so increasing the overall number of OXPHOS subunits. This principle was demonstrated to be successful by transgenic overexpression of PGC1α, which increased mitochondrial mass, improved energy production and rescued the myopathy phenotype caused by COX deficiency (Wenz *et al.*, 2008). Upregulation of PGC1α/β in human cultured cells with either Complex III/IV deficiency or the m.3243A>G mutation improves OXPHOS function and respiratory capacity (Srivastava *et al.*, 2009). This can be adapted from mice to benefit humans by exercise-induced stimulation of biogenesis through AMPK and Ca2+ signalling (Benton *et al.*, 2008, Wenz *et al.*, 2009).

Pharmacological agents have been developed to stimulate biogenesis without the need for exercise, which can be challenging for some patients with mitochondrial disease. Bezafibrate treatment has been shown to ameliorate mitochondrial myopathy in mouse models with COX deficiency (Wenz *et al.*, 2008), and restore OXPHOS capacity in human cell lines with various complex deficiencies or tRNA mutations (Bastin *et al.*, 2008, Wenz *et al.*, 2011).

Modulation of mitochondrial biogenesis as a therapeutic strategy has a wider scope of use than solely in mitochondrial disease. Glycogen synthase kinase-3 (GSK) inhibitors can restore mitochondrial biogenesis to neurones suffering oxygen-glucose deprivation (OGD) as a result of ischemic stroke (Valerio *et al.*, 2011). Natural polyphenolic compounds, commonly found in food, have been shown to be potent stimulators of mitochondrial biogenesis. The benefits of a Mediterranean diet in reduction of cardiovascular disease are attributed in part to hydroxytryrosol (HT), found in olive oil, which has been shown to stimulate expression of PGC1α and increase mitochondrial biogenesis (Hao *et al.*, 2010). Resveratrol (RSV) is found in grape skins, and the treatment of mice with RSV significantly increased their aerobic capacity and prevented diet-induced obesity and insulin resistance (Lagouge *et al.*, 2006).

1.6 The aims of this study

This PhD endeavours to understand the regulation of mitochondrial biogenesis and the relevance of these processes during embryonic development, to inheritance and in mitochondrial disease.

1.6.1 Chapter 3: Investigating the inheritance of pathogenic mtDNA mutations

Due to the mtDNA bottleneck, heteroplasmy levels can rapidly shift between generations. The central aim of this project is to improve our understanding of the variance in heteroplasmy inheritance in the population. I will assay the heteroplasmy levels in a large cohort of mother-child pairs for three common pathogenic mtDNA mutations, m.3243A>G, m.8344A>G and m.8993T>G. I will use these to calculate the change in heteroplasmy beween each mother and her children and establish whether any mutations show selection bias as they pass through the mtDNA bottleneck.

I will compare these results to a meta-analysis of previously published studies for these, and two additional mutations, m.11778G>A and m.3460G>A.

Summary

1. Assess the most reliable method for measuring mtDNA heteroplasmy values, testing restriction fragment length polymorphism (RFLP) analysis and pyrosequencing.
2. Measure the heteroplasmy of mother-child pairs for three mutations: m.3243A>G, m.8344A>G and m.8993T>G.
3. Use mother-child pairs to generate data for variance caused by the mtDNA bottleneck, establishing whether any mutation has skewed selection.
4. Collate heteroplasmy data from available published resources for five mtDNA mutations: m.3243A>G; m.3460G>A; m.8344A>G; m.8993T>G; m.11778G>A.

1.6.2 Chapter 4: Gene expression during murine embryogenesis

The mechanism for how the mtDNA bottleneck skews heteroplasmy values between generations has not yet been fully elucidated. Crucial to formation of the bottleneck is the dramatic increase in mtDNA replication rate that allows primordial germ cells (PGCs) to repopulate their mitochondrial genomes. Analysis of mtDNA copy number during embryogenesis has been undertaken in many laboratories, including our own. I

aim to monitor the expression of genes related to mitochondrial biogenesis and replication at critical stages of embryonic development, allowing identification of the stage at which mtDNA replication rate increases. As this area is novel in our group, this project will also involve setting up and optimising gene expression analysis on tissue which is very limited.

Summary

1. Selection of a gene panel suitable for studying mitochondrial related-gene expression during murine embryogenesis.
2. Gene expression analysis during pre-implantation embryogenesis.
3. Optimising gene expression analysis from PGCs during post-implantation embryogenesis.

1.6.3 Chapter 5: Identification of mtDNA copy number regulatory factors

To complement the investigation of mitochondrial gene expression during murine embryogenesis, I will establish a human cell culture model to mimic the regulation of mtDNA copy number observed during the bottleneck. This will allow identification of regulated genes, crucial to the process of recovering mtDNA copy number in dividing cells. There are many therapeutic agents which target components of the mitochondrial biogenesis pathways. These offer the potential to investigate how modulation of mtDNA replication and biogenesis may affect mtDNA copy number repopulation during embryogenesis, and the subsequent impact on heteroplasmy variance observed between generations.

Summary

1. Selection of the most suitable drugs and concentrations to test for depletion of mtDNA and optimisation of the repopulation assay.
2. Assay the gene expression patterns of several known mitochondrial biogenesis replication factors (*TFAM; NRF1; POLG; POLG2*) during repopulation of cellular mtDNA copy.
3. Identify the most suitable experimental technique for further in-depth analysis of mitochondrial gene expression.

4. Assess techniques to alter gene expression of key genes identified during depletion/repopulation as a potential method for modulating the mtDNA bottleneck *in vivo*.

1.6.4 Chapter 6: Gene expression analysis in MERRF muscle fibres

Ragged-red fibres (RRFs) are a common hallmark of many mitochondrial diseases, caused by proliferation of mitochondria in the subsarcolemmal region of muscle tissue. This provides a unique model to study mitochondrial biogenesis relevant to human disease. Previously, gene and protein expression in RRFs have only been visualised by immunohistochemistry or *in situ* hybridisation. In this chapter, I will first develop methods to visualise RRF in tissues, and allow extraction of intact RNA for broad analysis of mitochondrial-related gene expression in isolated populations of fibres.

Summary

1. Investigation of techniques to identify ragged-red fibres in muscle sections.
2. Optimise a protocol to ensure RNA quality remains high during tissue preparation and identification of RRF.
3. Optimise a protocol for RNA extraction from laser-microdissected muscle fibres.
4. Gene expression analysis from isolated populations of muscle fibres.

Chapter 2. Materials and Methods

Table of Contents

2.1 Primer Design

Gene reference sequences were identified using RefSeq (Maglott *et al.*, 2000, Pruitt *et al.*, 2009). Primer oligonucleotides for polymerase chain reaction (PCR) were designed using Primer3 (Rozen and Skaletsky, 2000) and tested using UCSC In Silico PCR (Fujita *et al.*, 2011) to ensure the product was specific to the region of interest. When designing primers for cDNA gene expression analysis, special care was taken to design primer pairs around exon boundaries, to exclude the possibility of genomic DNA amplification. In genes where alternative splicing is present, primer sets were designed to amplify products for all known transcript variants. Primer pairs were typically designed at the 3' end of the transcript, to limit the effect of any undetected RNA degradation on the qPCR signal.

2.2 Primary PCR and agarose gel electrophoresis

PCRs were performed using a Veriti® 96-well Thermal Cycler (Applied Biosystems, Life Technologies, Paisley, UK).

2.2.1 GoTaq® reaction

GoTaq® DNA Polymerase reaction (All reagents from Promega, Southampton, UK): 1 U GoTaq® polymerase, 1x GoTaq® Buffer (1.5mM $MgCl_2$), 2mM dNTPs (dATP, dTTP, dCTP and dGTP), 0.25 µM forward and reverse primers, with ~30 ng DNA template and deionised water (d.H_2O) to 30 µL. PCR program: 94 °C 4 min; 94 °C 1 minute, 60 °C 1 min, 72 °C 1 min for 30 cycles followed by a 72 °C for 10 min extension. Unless specified, all PCR reactions were cycled with an annealing temperature of 60 °C.

2.2.2 Immolase™ reaction

Immolase™ DNA Polymerase reaction (All reagents from Bioline, London, UK): 1 U Immolase™ polymerase, 1X ImmoBuffer, 2 mM dNTPs (dATP, dTTP, dCTP and dGTP), 0.25 µM forward and reverse primers, with ~30 ng DNA template and d.H_2O to 25 µL. PCR program: 95 °C 10 min; 95 °C 45 s, 60 °C 45 s, 72 °C 1 min for 30 cycles followed by a 72 °C for 10 min extension. Unless specified, all PCR reactions were cycled with an annealing temperature of 60 °C.

2.2.3 Agarose gel electrophoresis

The PCR product was analysed on an agarose gel. The PCR product (typically 5 µL) was mixed with one volume Orange G loading buffer (50% Glycerol, 50% H_2O, Orange G (Sigma-Aldrich). Unless specified otherwise, agarose gels were made with 1.5% (w/v) Seakem® LE agarose (Helena Bioscience, Gateshead, UK) and 0.4 µg Ethidium Bromide (Sigma-Aldrich, Dorset, UK) in 1X TAE buffer. The gels were electrophoresed in 1X TAE at 50-70 V for 45 min to 2 h depending on the expected fragment sizes. One volume DNA ladder (Hyperladder I-V, Bioline) was electrophoresed alongside PCR product to aid in sizing DNA fragments.

Agarose gels were imaged under UV and analysed using the GelDoc-It® Imager (UVP, Cambridge, UK).

2.3 Bacterial Cloning

2.3.1 Ligation and transfection

Ligation templates were created by amplifying fragments of DNA from the region of interest using a standard GoTaq Polymerase reaction (Section 2.2.1). The PCR product was ligated into the plasmid vector overnight at 4 °C following the standard pGEM-T Easy Vectors protocol (Promega). 50 µL JM109 (Promega) competent cells were used for transformation with 2 µL ligation product. The cells were placed on ice for 20 min, followed by heat-shock at 55 °C for 45-55 s, and then returned to ice.

2.3.2 Bacterial culture

Lysogeny broth (LB) culture media was prepared with bacto tryptone (1%; w/v), yeast (0.5%; w/v) and NaCl (1%; w/v). LB agar was prepared by the addition of bacterial culture agarose (1.5%; w/v), X-gal (75 mg/ mL), IPTG (0.5 µL/ mL) and Ampicillin (50 mg/ mL) to LB culture media (All from Sigma-Aldrich). Under sterile conditions, LB media was poured whilst molten into culture dishes and allowed to cool. To increase bacterial population, 475 µL LB media was added to the transformation mixture and incubated for 1.5 h at 37 °C.

With variable ligation efficiency, multiple dilutions of cells were spread onto agar plates under sterile conditions to obtain optimal yield for individual colonies. If the ligation efficiency was expected to be low, the cells were centrifuged for 5 min at 1000 x *g* and the pellet resuspended in 100 µL LB media. The total volume was spread onto an agar

plate under sterile conditions. All plates were incubated overnight at 37 °C, including a negative control to exclude the possibility of contamination.

The following day, individual white colonies (transfected with plasmids containing the desired insert) were picked and streaked across new plates and left to culture for 8 h at 37 °C to expand the population. Blue colonies indicate successful transfection, but plasmids without successful ligation of the PCR product. Samples from streaks were harvested and placed in 5 mL LB Agar (with the addition of 50 mg/ mL Ampicillin) and left to culture overnight at 37 °C with shaking.

The following day, DNA was extracted using the QIAprep Spin Miniprep Kit (QIAGEN, Manchester, UK) standard protocol (Section 2.8.2).

2.4 Restriction Fragment Length Polymorphism (RFLP) Analysis

2.4.1 Last cycle fluorescent polymerase chain reaction (PCR)

PCR was completed using the standard GoTaq Protocol (Section 2.2.1) with one modification. The program was paused before the last cycle and a mix (0.5 µL) with a fluorescently labelled primer was added: 0.5U GoTaq® polymerase, 1x GoTaq® Buffer (1.5mM $MgCl_2$), 2mM dNTPs (dATP, dTTP, dCTP and dGTP), 2 µM forward and reverse primers (one standard, one fluorescent). The program was continued with one further cycle of 94°C 1 min, 58 °C 1 min, 72 °C 1 min followed by a 72 °C for 10 min extension.

2.4.2 Restriction digest

The digest reaction mix was 10 U restriction enzyme, compatible 1X restriction buffer, with ~10-20ng PCR product and d.H_2O to 20 µL. The reaction was incubated overnight at 37 °C (All reagents from New England BioLabs, Hitchin, UK).

2.4.3 Mapping and analysis

For analysis of the digested fragments, 2 µL digest product was loaded onto a 96-well PCR plate with Hi-Di® (8.5 µL) and Rox-500 size standard (0.5 µL). The plate was analysed on an ABI 3130xl Genetic Analyser, using a fragment analysis program to read the lengths of DNA fragments tagged with fluorescent primers. RFLP analysis was performed using GeneMapper® Software v4.1 (all reagents and equipment supplied by Applied Biosystems, Life Technologies).

2.5 Pyrosequencing Analysis

2.5.1 Assay and primer design

Primers for both primary and sequencing reactions were designed using PyroMark® Assay Design SW 2.0 (QIAGEN). Selected primer sets were deemed to be 'high quality', indicating the software identified no problems or concerns and the primers were compatible.

Assays for specific primer sets were created using the PyroMark® Q24 Software (QIAGEN).

2.5.2 Primary PCR with biotinylated primers

The primary PCR was a 25 µL GoTaq® Hot Start Polymerase (Promega) reaction: 1 U GoTaq® Hot Start polymerase, 1x Colourless GoTaq® Flexi Buffer (1.5mM $MgCl_2$), 2mM dNTPs (dATP, dTTP, dCTP and dGTP), 0.25 µM forward and reverse primers, with ~30 ng DNA template and d.H_2O to 30 µL. PCR program: 95 °C 10 min; 94 °C 30 s, 60 °C 30 s, 72 °C 30 s for 30 cycles followed by a 72 °C for 10 min extension.

2.5.3 Product clean-up and pyrosequencing

After assessment of PCR product quality and quantity using agarose gel electrophoresis (Section 2.2.3), 5-20 µL PCR product was added to the binding solution (40 µL binding buffer, 2 µL streptavidin-coated Sepharose® beads) with 18-33 µL H_2O to a total volume of 80 µL. The samples were agitated for 10 min to bind the DNA to the beads. Using the hand-held vacuum tool, the DNA was washed with Ethanol (70%), followed by Denaturation Solution and Wash Buffer. The product was eluted from probes in 25 µL annealing solution (annealing buffer containing 0.3 µM sequencing primer; all reagents from QIAGEN).

The pyrosequencing was completed on a PyroMark® Q24 (QIAGEN).

2.5.4 Analysis of results

Analysis was performed using PyroMark® Q24 Software. Any reads flagged as low quality were repeated until satisfactory. Percentage heteroplasmy was automatically calculated by the software.

2.6 Sanger Sequencing

Primary PCR products were generated using the Immolase PCR reaction described in Section 2.2.2.

2.6.1 ExoSAP-IT treatment of primary PCR products

ExoSAP-IT (GE Healthcare, Amersham, UK) contains the enzymes Exonuclease I and Shrimp Alkaline Phosphatase. It removes unincorporated dNTPS and primers and is an essential pre-sequencing treatment. Approximately 10-20 ng of primary PCR product (dependent on fragment length) was added to 2 µL ExoSAP-IT. It was incubated at 37 °C for 30 min, followed by enzyme inactivation at 80 °C for 15 min.

2.6.2 BigDye® terminator v3.1 cycle sequencing

For the 20 µL sequencing reaction, BigDye® Cycle Sequencing RR-100 (1 µL), 1X BigDye® Terminator v3.1 Sequencing Buffer and 0.5 µM forward or reverse primer (specific to each reaction) were combined with the ExoSAP-IT treated PCR product and d.H2O to 20 µL). Reactions were cycled under the following conditions: 96 °C 1 min, 25 cycles of 96 °C for 10 s, 50 °C for 5 s and 60 °C for 4 min.

2.6.3 Ethanol precipitation

To precipitate DNA fragments, 3 M Sodium Acetate (2 µL) (Sigma-Aldrich), 125 mM EDTA (2 µL) (Sigma-Aldrich) and 100% Ethanol (70 µL) were added to the cycle sequenced product, mixed gently, and incubated at room temperature in the dark for 15 min to allow for DNA precipitation. Following precipitation, it was centrifuged at 2000 x *g* for 30 min. After centrifugation, the solution was removed by inverting and centrifuging on the lowest setting for 15 s. To wash the pellet, 70% ethanol (100 µL) was added and the samples were centrifuged again at 1650 x *g* for 15 min. The ethanol was removed again, and the pellets were left to dry at room temperature in the dark for 20 min.

2.6.4 Sequence analysis

The DNA pellets were resuspended in 10 µL Highly de-ionised (Hi-Di®) formamide, heated to 95°C for 2 min and then cooled on ice. Capillary sequencing was completed on the ABI 3130xl Genetic Analyser. The resulting raw data was then analysed using SeqScape® v2.1.1 software (All supplied by Applied Biosystems, Life Technologies).

Mitochondrial DNA sequences were compared to the revised Cambridge Reference Sequence (rCRS) (NC_012920; http://www.ncbi.nlm.nih.gov/genbank/). Any potential changes identified were confirmed by sequencing in reverse.

2.7 Tissue Culture

To prevent contamination, primary cell culture was performed in a Heraeus HERAsafe HS-12 class II biohazard hood (Fisher Scientific, Loughbourough, UK). Reagents were prewarmed to 37°C before use with cultured cells. Cells were grown in either CELLSTAR® Cell Culture Flasks (25/75/225 cm^2) or 6-well Cell Culture Plates (Greiner Bio-one, Stonehouse, UK) at 37°C in a humidified Heracell 150i cell culture incubator (Fisher Scientific, UK) containing 5% CO_2.

2.7.1 Media change and subculture

Primary myoblasts were cultured using Skeletal Muscle Cell Growth Medium with addition of the Supplement Mix (Promocell, Heidelberg, Germany), 10% or 15% Fetal Bovine Serum (FBS), 2 mM L-Glutamine, 50 µg/ mL uridine and 30 µg/ mL Gentamicin (All reagents Gibco, Life Technologies).

Primary fibroblasts were cultured using Dulbecco's Modified Eagle Medium (DMEM; Gibco, Life Technologies) containing 25mM D-glucose, 1 mM sodium pyruvate, 2 mM L-glutamine with the addition of 10% FBS, 50 µg/ mL uridine, Penicillin (500 U/mL) and Streptomycin (500µg/ mL) (All from Gibco/ Life Technologies).

Medium was changed at least every third day of culture. Before addition of new medium, the old medium was aspirated away and the cells washed with sterile phosphate buffered saline (PBS; Oxoid, Basingstoke, UK).

To subculture cells, the old medium was first removed by aspiration, and the cells washed with PBS. To dissociate the cells from the flask, enough 1x Trypsin-EDTA solution (0.05% trypsin) (diluted in PBS) was added to create a thin layer over the cells. The flasks were then incubated at 37°C for 3-5 minutes, making sure all cells were detached before adding two volumes of medium to neutralise the trypsin. Cells were then pelleted by centrifugation at 1200 rpm for 5 min. The old media was aspirated off, and the cell pellet was then re-suspended in fresh media, and new flasks were re-seeded at the required cell density.

2.7.2 Freezing cells for storage

For long-term storage, cell pellets were re-suspended in 1 mL 'freezing medium' consisting of 70% (v/v) DMEM, 20% FBS and 10% dimethyl sulfoxide (DMSO; Sigma-Aldrich). The cryovial was placed in a Nalgene® Mr. Frosty isopropanol bath (Sigma-Aldrich) and then in a -80 °C freezer, allowing a gradual cooling rate of 1°C/min. After 48 hr at -80 °C, cryovials were moved to liquid nitrogen ($L.N_2$) for long-term storage.

2.7.3 Cell counting

Estimates of cell number were made using an Improved Neubauer Cell Counting Chamber (Hawksley, Lancing, UK). Cell pellets were resuspended in 1 mL PBS, then 50 µL was transferred to a clean 200 µL Eppendorf tube and mixed in equal volumes with Trypan Blue (Sigma-Aldrich). 20 µL of this solution was loaded into each side of the cell counting chamber. The number of viable (unstained) cells in the four corner squares (1 mm^2; volume 0.1 µL) of each side were counted and an average taken. This number was multiplied by 10^4 to calculate the total number of viable cells in 1 mL of resuspension media.

2.7.4 Pelleting cells for extraction

Cells to be used for downstream applications, such as DNA/RNA/Protein extractions, were pelleted by centrifugation at 1200 rpm for 5 min, the old medium was removed by aspiration and the cells re-suspended in 1 mL PBS to wash away medium traces. The cells were centrifuged again under the same conditions, the PBS supernatant removed and the cell pellets frozen at -80°C.

2.7.5 Mycoplasma detection

Cell cultures were tested when initially removed from storage, monthly, or before being frozen down by the MycoAlert® Mycoplasma Detection Kit (Lonza, Basel, Switzerland). All reagents were brought to room temperature before use. The old medium from cell culture was centrifuged at 1500 rpm for 5 min to pellet any cells or debris. 100 µL of supernatant was transferred into a 96-well white-walled plate well, and 100µL MycoAlert® Reagent was added and incubated at room temperature for 5 min. This control 1-second integrated reading was taken (Read A). The MycoAlert® substrate was then added and incubated at room temperature for 10 min. Another

reading was then taken (Read B), and the ratio between the first and second reading calculated (Read B/Read A). As the substrate is processed only by mycoplasma uninfected cells have a ratio <1, whereas infected cells have a ratio >1.

2.7.6 Differentiation of myoblasts into myotubes

To differentiate myoblasts, they were first grown to full confluency, then the medium was changed to DMEM containing 25mM D-glucose, 1 mM sodium pyruvate, 2 mM L-glutamine with the addition of 2% horse serum, and 30 µg/mL gentamicin (All from Life Technologies). Cells were not subcultured, only the medium was changed and cells were left to differentiate for at least five days.

2.7.7 Gelatin-coating coverslips for immunocytochemistry

Cells to be used for immunocytochemistry required growing on removable glass coverslips. However, some cell types have poor adherence to glass, so the coverslips were first coated in gelatin. A 0.1% gelatin (Sigma-Aldrich) in d.H_2O solution was autoclaved, and used to cover sterile coverslips in 6-well plates. The plates were chilled overnight at 4 °C, then the gelatin was removed by aspiration and the wells washed with sterile PBS. Plates were stored at 4 °C with PBS for later use or used immediately.

2.8 DNA Extraction

2.8.1 DNA extraction from cultured cells

DNA was extracted from frozen cell pellets using the DNeasy Blood & Tissue Kit (QIAGEN) which lyses cells and binds total DNA (nuclear and mitochondrial) to the column membrane, and with centrifugation and washing, removes contaminants and enzyme inhibitors. The DNA was then eluted into 30-100 µL low-salt Tris buffer supplied (Buffer EB).

2.8.2 DNA extraction from bacterial cells

Bacterial cultures were incubated overnight at 37 °C with shaking and then centrifuged to create a pellet. The DNA was extracted using the QIAprep Spin Miniprep Kit (QIAGEN), which uses alkaline lysis and high salt conditions to absorb only DNA onto a silica membrane. The membrane was washed to remove endonucleases and salts, then the DNA was eluted into 30-100 µL low-salt Tris buffer (Buffer EB).

2.9 RNA Extraction and Quality Control

2.9.1 Solution preparation

Laboratory water may contain ribonucleases (RNases), which will degrade the RNA in samples if not first inactivated. Autoclaving alone is not generally enough to permanently inactivate RNases, as the enzymes renature once cooled. All water used in RNA handling was pre-treated with 0.1% diethylpyrocarbonate (DEPC; Sigma-Aldrich), incubated at room temperature overnight, and then autoclaved to inactivate the chemical. Any solutions requiring water, such as 70% ethanol, were made using DEPC-treated water.

2.9.2 RNA extraction from cultured cells

RNA was extracted from cultured cells using the RNeasy® Mini Kit (QIAGEN). Cells were first lysed, and then homogenised using a guanidine-thiocyanate based lysis buffer provided (Buffer RLT with β-mercaptoethanol) and QIAshredders, a biopolymer spin column designed to reduce viscosity caused by cellular debris. Addition of ethanol allowed binding of RNA to the RNeasy® spin columns, which were then washed in high-salt buffers to remove contaminants. The RNA was typically eluted in 30-50 µL RNase-free H_2O supplied.

2.9.3 RNA extraction from muscle tissue

RNA extraction from small samples, such as laser microdissected cells, was done using the Arcturus® PicoPure® RNA Isolation Kit (Life Technologies). It uses high-recovery MiraCol™ purification columns to bind RNA, and stringent washes to remove impurities. RNA was typically eluted in 10-15 µL low ionic strength buffer provided (Buffer EB).

2.9.4 Ethanol precipitation of RNA

RNA is soluble in water due to the polarity of both water and the phosphate groups in RNA. Ethanol is non-polar and, in combination with positive salt ions, allows the precipitation of RNA out of solution, which can be pelleted and redissolved in a smaller amount of liquid for a high concentration sample. After RNA extraction, samples were combined and 0.1 volume 3 M sodium acetate (Sigma-Aldrich) and 2.2 volumes of 100% ice cold ethanol were added. The samples were centrifuged at 4 °C, 10,000 x *g* for

10 min. The ethanol was then removed carefully, without disturbing the RNA pellet, and replaced with 500 µL ice cold 70% ethanol. The samples were centrifuged again at 4 °C, 10,000 x *g* for 5 min. The ethanol was removed again and the RNA pellet allowed to air dry for 15 min. The RNA was dissolved in a lower volume of RNase-free H_2O. Concentration was analysed on the NanoDrop 2000 UV-Vis Spectrophotometer (Thermo Scientific) and Agilent 2100 Bioanalyzer (Agilent Technologies, Cheadle, UK).

2.9.5 RNA quality control

The purity of RNA samples was measured using the NanoDrop 2000 UV-Vis Spectrophotometer with absorbance at 260 nm. The 260/230 and 260/280 ratios determine whether any contaminants such as phenol or protein are present in the sample. The 260/230 ratio should be between 2-2.2 and the 260/280 ratio should be between 1.8-2.

The RNA integrity was analysed on the Agilent 2100 Bioanalyzer using the RNA 6000 Pico Kit. A RIN score of 7-10 is acceptable, any RNA samples with a RIN score less than 7 was discarded and not used for gene expression analysis.

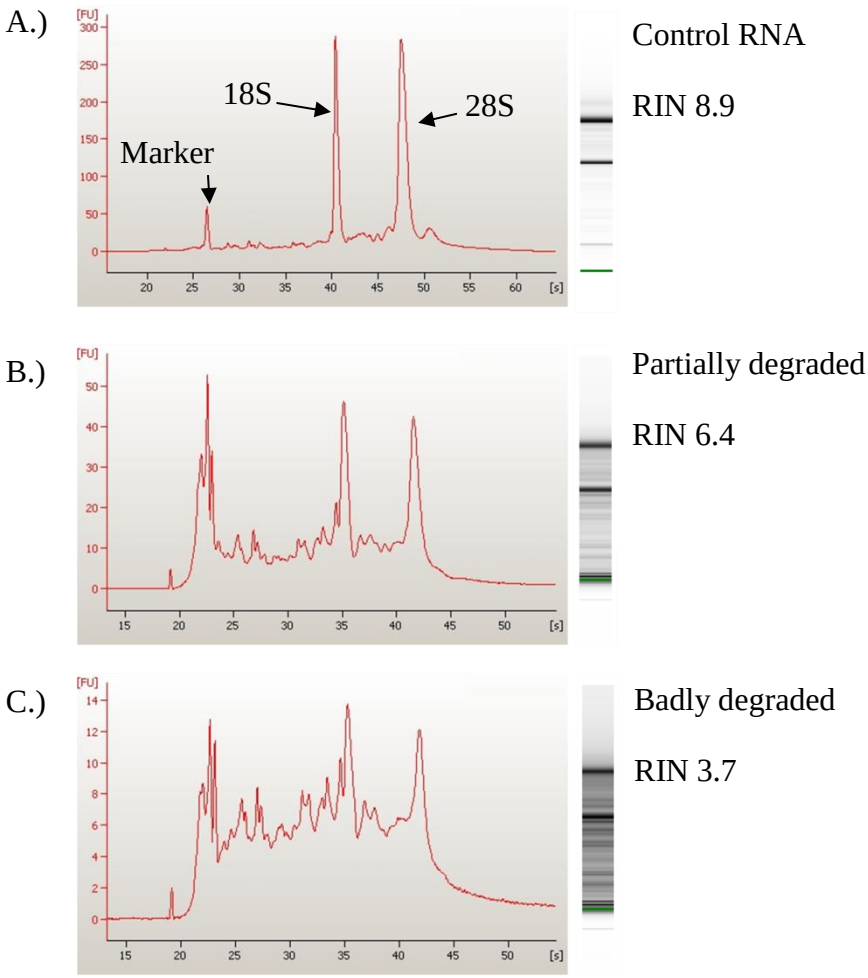

Figure 2.1 Examples of RNA samples with varying degradation. A.) RNA with low degradation with a 8.9 RIN. B.) RNA with partial degradation with a 6.4 RIN. C.) RNA with severe degradation with a 3.7 RIN.

2.10 RNA amplification

RNA amplification was achieved using the Arcturus® RiboAmp® HS PLUS RNA Amplification Kit. The kit is designed to produce microgram quantities of amplified antisense/amplified RNA (aRNA) from low (100 pg) quantities of total cellular RNA.

The first reaction generated single-stranded cDNA (from mRNA transcripts) with an incorporated T7 promoter sequence. This was converted to double-strand cDNA which was purified using MiraCol™ Purification Columns. *In vitro* transcription was performed using a T7 RNA polymerase, which yields antisense RNA (aRNA), also purified using MiraCol™ Purification Columns. This aRNA can be used for a second round of amplification.

2.11 cDNA Synthesis

SuperScript III First-Strand Synthesis System (Invitrogen)

SuperScript III synthesises first-strand cDNA from 1 pg to 5 µg of total RNA. First the primers are annealed to the template. Oligo dTs were used to amplify mRNAs only and random hexamers were used to amplify both rRNA and mRNA, depending on which the situation required. Oligo dTs are more efficient than random hexamers at generating templates for qPCR, therefore random hexamers were only used when rRNA genes were also being assessed or if targets were not polyadenylated.

WT-Ovation® RNA Amplification and One-Direct Systems (NuGEN)

The WT-Ovation® RNA Amplification System is designed for use with an input of 5 to 50 ng total RNA. The WT-Ovation® One-Direct Amplification System is designed for use with either cell lysates, or 10 to 500 pg of total RNA.

Both systems rely on Ribo-SPIA (Single Primer Isothermal Amplification) technology. First-strand cDNA was prepared with reverse transcription using primers targeted to either the polyA tail or randomly across the transcript, with a unique RNA tag at the 5' end of the primer. The RNA in this cDNA/RNA heteroduplex was fragmented to generate priming sites for DNA polymerase, and the second-strand was synthesised, leaving a DNA/RNA tag at one end. The SPIA® amplification utilised by these systems is a linear isothermal DNA amplification process. RNase H was used to degrade the RNA in the unique tag sequence, exposing the DNA segment of the tag, allowing for binding of a second RNA/DNA primer. This primer was then extended by DNA polymerase, displacing the existing strand. The cycle was repeated several times to amplify the cDNA up to 1,500-fold with the minimum RNA requirement.

2.12 Quantitative Real-time PCR

Quantitative real-time PCR (qPCR) utilises a double-strand DNA intercalating dye (SYBR) to measure fluorescent intensity relative to the amount of PCR product produced at each cycle. The PCR reactions were performed on a MyIQ™ thermocycler (Bio-Rad, Hemel Hempstead, UK). The raw data was analysed on iQ5™ optical system software v.2.0 (Bio-Rad), to determine at which cycle the fluorescence units pass a set threshold level for each sample, known as the threshold cycle (Ct). This allowed

comparison of the relative amounts of different genes or mRNA transcripts. All the qPCR preparation steps were performed in a UV-sterilised Aura PCR workstation.

2.12.1 qPCR reaction

The qPCR reaction was 25 µL for each sample, made with 1X iQ™ SYBR® Green, 0.5 µM forward and reverse primer with 1 µL template and d.H_2O to 25 µL. All reactions were prepared in a UV-sterilised Aura PCR workstation (Bioair Instruments, Milan, Italty) to avoid any cross-contamination.

The PCR program was: 95 °C, 3 min; 95 °C for 10 sec followed by 62.5 °C for 1 min for 40 cycles; 95 °C 1 min; and a melt curve. The melt curve was performed by monitoring loss of fluorescence signal after each of the 10-second incubation steps, rising from 65 °C to 95 °C in 0.5 °C increments.

2.12.2 Quality control

The efficiency of each reaction was measured using standard curves generated using 1 in 10 serial dilutions of either control cDNA or purified DNA templates. As the amount of DNA should double with every PCR cycle, the C_t value of each 10-fold dilution should be 3.3 cycles apart. The 'no template control' should be no lower than 35 cycles (Figure 2.2A). The threshold must be set during the log phase, where each curve appears as a straight line stretch (in log view) (Figure 2.2B). When the standards are plotted, the efficiency of the reaction (represented as E) should be >95%, the R^2 should be > 0.98 (indicating accurate dilutions and pipetting), and the slope between -3.2 to -3.5. Melt curve analysis, which distinguishes between product sizes and G-C content, should show a single peak for each expected amplification product (Figure 2.2D-F).

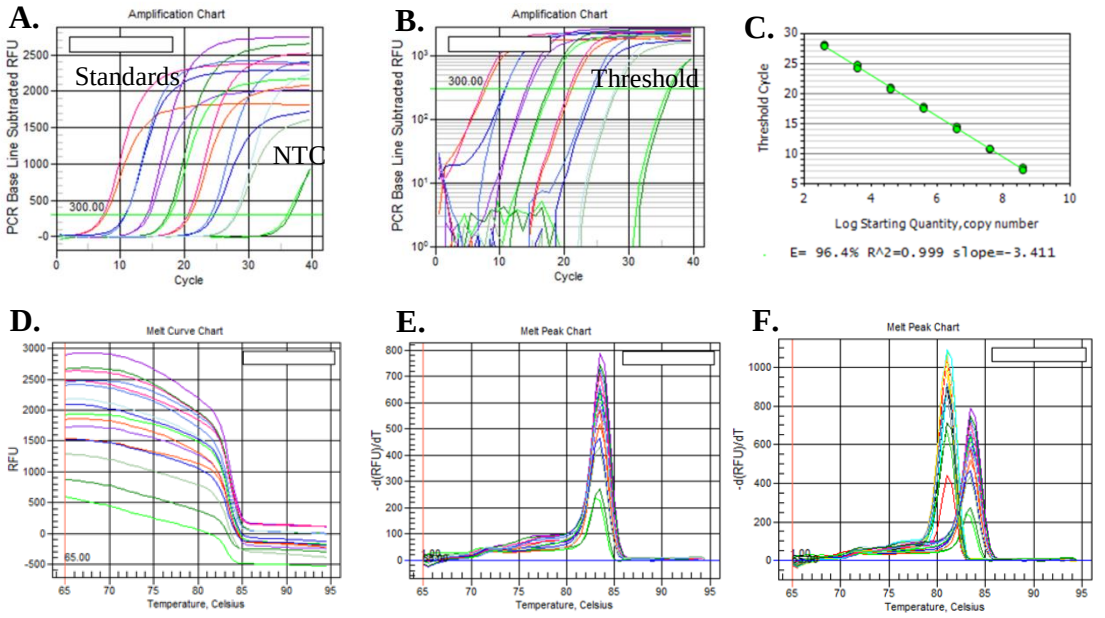

Figure 2.2 Quality control of real-time qPCR. Standard curves generated using 10-fold dilution of PCR template. (A) Amplification chart shows uniform spacing of each set of dilutions. (B) Logarithmic (log) view of amplification curve, with the threshold set during the log phase. (C) When the C_t values of the standards are plotted, the efficiency of the reaction is 96.4%, the R^2 is 0.999, and the slope -3.411 (D) Melt curve analysis distinguishes between product sizes and G-C content. (E) Melt peak for a single product is sharp with only one peak. (F) Melt peaks for different amplification reactions shows two distinguishable peaks indicating two different products.

Each standard was analysed in duplicate and each sample was analysed in triplicate. The standard deviation between each sample triplicates was <0.25, or was repeated.

2.13 TaqMan® Low Density Array (TLDA) cards

The TaqMan® Custom Array is a 384-well micro fluidic card which allows 384 simultaneous real-time PCR reactions for up to eight samples. The assays are pre-loaded in each of the wells with only the addition of cDNA and TaqMan® Universal PCR Master Mix into each port on the card.

2.13.1 Designing the TLDA cards

Custom TLDA cards are designed using Applied Biosystem's configuration tool. Each 384-well microfluidic card can be designed to analyse between 1-8 samples and 12-384 assays, depending on the format chosen. Each port (8 in total) requires 50 µL of cDNA. Depending on the format chosen, one sample may require two or more ports, which must be taken into consideration.

2.13.2 Loading the TLDA cards

The TLDA cards were incubated for 15 minutes prior to loading the sample. For each port to be used, 50 µL of cDNA was mixed gently with 50 µL of TaqMan® Universal PCR Master Mix before loading.

Once loaded, cards were fitted to custom TaqMan® card holders and buckets for the Multifuge 1S-R Benchtop Refrigerated Centrifuge (Heraeus, Thermo Scientific, Waltham, USA). With a ramp up/down rate of 9, the cards are centrifuged at 1200 rpm (331 x g) for two separate sessions of one minute. The wells of the card were sealed using the TaqMan® Array Micro Fluidic Card Sealer, which depresses the foil within the main fluid distribution channels of the card. The ports were then cut away.

The cards were analysed on the 7900HT Fast Real-Time PCR System (Applied Biosystems). The TaqMan® Array Micro Fluidic Card Thermal Cycling Block and correct plate adapter must be fitted to the PCR instrument tray for use with TLDA cards.

The plate setup was loaded from the Array Information CD provided with the cards. The correct cycling conditions were: 45 °C 10 min, 94 °C for 10 min, and 45 cycles of 94 °C for 30 s followed by 60 °C for 1 min.

2.13.3 Analysis of results

Results were generated from the 7900HT Fast Real-Time PCR System (Applied Biosystems) using the compatible SDS 2.4 software. Analysis of the results file was completed using RQ manager. The automatic baseline and a threshold of 0.2 were used for analysis of each plate. Any outliers or failed wells were omitted from the analysis.

2.14 SDS-PAGE and Western Blotting

2.14.1 Protein extraction from fibroblast pellets

Cells were washed with PBS before centrifugation and the pellets were stored at -80 °C.

Cell pellets were defrosted on ice for 5 min and then lysed in 50 µL lysis buffer. The lysis buffer mix is 50 µL 1 M Tris (pH 7.5) (Sigma-Aldrich), 26 µL 5 M NaCl (BDH), 4 µL 0.5 M $MgCl_2$ (BDH), 10 µL 100 mM PMSF (Sigma-Aldrich), 10 µL Triton X-100 (Sigma-Aldrich). The lysis mix containing cells was vortexed for 30 s to homogenise the suspension. To remove cellular debris, the tubes were centrifuged at 2500 rpm for 2 min at 4 °C and the supernatant removed to a clean tube. Protein concentration was

determined using the NanoDrop 2000 UV-Vis Spectrophotometer, measuring at 280 nm. Protein was diluted to 2.5 µg/ µL using protease inhibitor (Pi) mix (Roche) with an addition of 5 µL 100 mM PMSF. The protein solution was mixed with an equal volume of loading dye. The loading dye mix is: 5 mL 0.5 M Tris-HCl (pH 6.8), 2 mL glycerol, 0.4 g SDS, and 0.01 g bromophenol blue (all reagents from Sigma-Aldrich). Protein aliquots were frozen for later use at -80 °C or used directly in SDS-PAGE.

2.14.2 SDS-PAGE

Before use, the protein samples required the addition of 15 U benzonase nuclease (Novagen®, Merck Millipore, Watford, UK) per 20 µL sample, and were incubated at 37 °C for 30 min to prevent COXI aggregation.

SDS-PAGE was performed using Mini-Protean Tetra Cell apparatus (Bio-Rad). Polyacrylamide separating gels were made to either 14% or 8%, depending on the size of the proteins to be separated. Gel mixes (14%/ 8%) include (4.66/ 2.68 mL) 29:1 30% bisacrylamide (Amresco, Solon, USA) and (4.11/ 6.11 mL) H_2O, 1 mL 3.75 M Tris-HCl (pH 8.5) (Sigma-Aldrich), 100 µL 10% SDS solution (Sigma-Aldrich), 10 µL TEMED (Sigma-Aldrich) and 100 µL 10% APS solution (Sigma-Aldrich). After loading the gel solution into the casting cassette, a layer of isopropanol was added to ensure a smooth upper gel line and to prevent evaporation during the polymerisation process.

Once the separating gel has polymerised, the isopropanol was removed and the 4% stacking gel can be added (approximately 3 cm layer). The 4% gel mix is 0.625 mL 29:1 30% bisacrylamide (Amresco), 3.025 mL H_2O, 1.25 mL 0.5 M Tris/HCl (pH 6.8) (Sigma-Aldrich), 50 µL 10% SDS solution (Sigma-Aldrich), 5 µL TEMED (Sigma-Aldrich) and 50 µL 10% APS solution (Sigma-Aldrich). The comb is inserted before the stacking gel was allowed to polymerise.

Once the stacking gel was set, the gels were placed in the tank with 1X running buffer: 3.03 g Trizma® base, 14.4 g glycine and 1 g SDS in 1 L d.H_2O (All reagents from Sigma-Aldrich). The comb was removed and the protein loaded at two different concentrations to control for saturation. Novex® Sharp Pre-stained protein ladder (Invitrogen, Life Technologies) was added to the first lane to check the sizing of proteins.

The gel was electrophoresed at 10 mA through the stacking gel, and 25 mA through the separating gel for varying lengths of time, depending on the proteins to be separated.

2.14.3 Western Blotting

After electrophoresis, the gel was equilibrated in 1X transfer buffer for 10 min. The transfer buffer was made with 3.03 g Trizma® base, 14.4 g glycine and 0.2 g SDS and 10% methanol in 1 L dH_2O. The polyvinylidene difluoride (PVDF) membrane was activated in methanol for 20 s then washed in 1X transfer buffer for 1 min. The gel and membrane were both inserted between filter paper and sponges in the transfer cassette, and transferred in 1X transfer buffer at max mA for 1 h or 30 V/ 120mA overnight at 4 °C.

2.14.4 Probing the blot

Non-specific binding sites were blocked by incubating the blot for 1 h at room temperature with either 5% milk (Marvel, Premier Foods, St. Albans, UK) or 5% BSA (Sigma-Aldrich) in Tris-buffered saline with Tween20® (TTBS), to block non-specific binding sites. Primary antibodies were incubated for either 1 h at room temperature or overnight at 4 °C with shaking. After primary antibody probing, the blot was washed with TTBS for three periods of 10 min. TTBS was prepared with 20 mL 1 M Tris (pH 7.0) (Sigma-Aldrich), 29.2 g NaCl (VWR, Lutterworth, UK) and 1 mL Tween20® (Sigma-Aldrich) up to 1 L with $d.H_2O$.

After the TTBS washes, the blot was probed for 1 h with HRP-conjugated secondary antibody using the appropriate species to match the primary antibody used. This was followed with three more 10 min TTBS washes.

2.14.5 Visualisation of the blot

To visualise the blot, 1 mL solution A was added to 25 µL of solution B from the ECL Plus Western Blotting Detection Reagents (GE Healthcare, Little Chalfont, UK). The solution was evenly distributed over the surface of the blot and incubated in the dark for 4 min. The excess ECL-Plus mix was removed, and the blot protected in a plastic wallet.

The blots were visualised on a BioSpectrum® Imaging System (UVP). White-light images of the blot were used to align the ladder to the protein band images to ensure the protein bands observed were the expected size.

Quantification of bands was completed using Fiji imaging software (http://fiji.sc/wiki/index.php/Fiji), calculating the ratio between the intensity area of the protein of interest and a reference protein (such as β-Actin).

2.15 Immunocytochemistry on cultured cells

2.15.1 Cell fixation

Cells were washed with PBS to remove traces of media and then incubated with 4% paraformaldehyde (PFA) at room temperature for 30 min. The PFA was then removed and the cells washed with PBS for 3 x 5 min. The cells can be stored at 4 °C in 0.1% sodium azide solution for up to two weeks or used directly for antibody staining.

2.15.2 Antibody staining

After fixing cells with 4% PFA in PBS, the cells were incubated with 0.1% TritonX 100 (Sigma-Aldrich) for 15 min to permeabilise the membrane. The cells were blocked with 5% BSA for one hour, then incubated with the primary antibody for 1 h. After removal of the antibody, the cells were washed with PBS for 3 x 5 min. The cells were incubated with the appropriate fluorochrome-conjugated secondary antibody for 1 h and washed again with PBS for 3x 5 min.

2.15.3 Microscopy

Fluorescent images were captured using an Axio Imager microscope with an attached ApoTome and AxioCam HRc digital camera. Images were analysed using the compatible AxioVision software (All from Carl Zeiss).

2.16 Cryosectioning of muscle tissue

Muscle blocks to be sectioned were snap frozen in L.N_2-cooled-isopropanol and mounted on filter paper using OCT. Before sectioning, they were allowed to equilibrate to -20 °C in the cryostat. Sections were typically cut between 8-20 µM and mounted onto either glass or PEN-membrane slides. Slides were frozen at -80 °C for later use or allowed to air dry for 30 min before processing.

2.17 Histochemistry on muscle sections

2.17.1 Combined COX-SDH

Each solution was made fresh and used immediately with a final volume of 1 mL.

The stain for COX activity was prepared with 4 mM 3,3'-diaminobenzidie tetrahydrochloride (DAB), 100 mM cytochrome c and a few crystals of catalase (All reagents from Sigma-Aldrich). The sections were incubated for 40-45 min at 37 °C, then washed three times with 0.1 M PBS.

The stain for SDH activity was made with 1.5 mM nitroblue tetrazolium (NBT), 0.13 M Sodium Succinate, 0.2 mM phenazine methosulfate (PMS) (All reagents from Sigma-Aldrich). The sections were incubated for 35-40 min at 37 °C then washed three times with 0.1 M PBS.

The sections were dehydrated and mounted or taken for further processing (see Section 2.17.3).

2.17.2 Modified Gomori trichrome

Modified Gomori trichrome was used to identify ragged-red fibres (RRF). Stained nuclei will appear red-purple, normal muscle myofibrils will appear green, and intermyofibrillar muscle membranes will appear red. Abnormal mitochondria accumulate in the subsarcolemma region of muscle and have a distinct 'Ragged-Red' appearance. The solution was made using 0.6% Chromotrope 2R 0.3% Fast Green FCF, 0.6% Phosphotungstic acid (All Sigma-Aldrich) and 1% glacial acetic acid in distilled water. The pH was adjusted to 3.4 using 1 M NaOH. Sections cut no thicker than 12 µm were first stained with Harris Haematoxylin (Sigma-Aldrich) for 5 min then rinsed in distilled water. They were stained with modified Gomori trichrome stain for 10 min. The stain was differentiated from purple to green using three successive washes in 0.2% acetic acid solution. The sections were dehydrated and mounted or taken for further processing (see Section 2.17.3).

2.17.3 Section dehydration and mounting

Sections on glass slides are dehydrated in progressively more concentrated ethanol solutions (70%, 2 min; 90% 2 min; 100%, 2 min; 100%, 10 min), immersed in Histo-Clear® (Fisher Scientific) for 2 min (2 x 1 min sessions) and then mounted with distyrene plasticizer and xylene (DPX; VWR). Sections on membrane slides for laser microdissection required rapid processing in ice cold ethanol (70% 2 min; 100% 2 min), do not need Histo-Clear® treatment and were not mounted.

2.18 Laser Microdissection

Laser microdissection was performed using a Leica AS LMD laser microscope (Leica Microsystems, Germany). This system uses contact-free UV-laser microdissection and gravity capture into the caps of individual 0.5 mL tubes. Tissue sections were mounted facing downwards towards the cap lid. Tissue was dissected into both dry caps and caps with added lysis buffer. If fluorescent microscopy was required for visualisation of staining, the software was switched to fluorescent mode and the appropriate filter chosen for the fluorophore in use.

2.19 Statistical analysis

All statistical analyses were performed using GraphPad Prism® v.6 statistical software (GraphPad Software Inc., La Jolla, USA).

To determine the significance of differences in the means of two independent groups with equal variance an unpaired t-test at a confidence level of 95% was employed. Results were considered significant if the p-value < 0.05 (*), <0.01 (**), <0.001 (***).

Chapter 3. Investigating Inheritance of Pathogenic mtDNA Mutations

Table of Contents

3.1 Introduction

Mutations on mtDNA are a major cause of human disease, affecting at least 1 in 5000 of the population (Chinnery *et al.*, 2000a, Schaefer *et al.*, 2008). In a study of mtDNA sequences in the cord blood from clinically unaffected live-births, common pathogenic mtDNA mutations were detected in 0.5% of individuals (Elliott *et al.*, 2008).

Homoplasmic mutations are typically associated with an organ-specific, mild biochemical phenotype, such as m.1555A>G in 12S rRNA causing isolated sensori-neural deafness (Prezant *et al.*, 1993). Many pathogenic mtDNA mutations are heteroplasmic, where mutant load tends to correlate with the severity of the disease and explains the clinical heterogeneity between siblings of the same family (Chinnery *et al.*, 1997, Chinnery *et al.*, 1998, White *et al.*, 1999a).

mtDNA deletions are not frequently transmitted, with a risk of approximately 1 in 24 chance of an affected mother having an affected child (Chinnery *et al.*, 2004). However, the majority of point mutations are readily transmitted from mother to child and inheritance is dependent on the type of mutation (Elson *et al.*, 2009). There are rapid shifts in m.8993T>G/C heteroplasmy levels between generations, leading to smaller pedigrees as the mutation is rapidly lost or fixed (White *et al.*, 1999a). In contrast, large shifts in m.8344A>G heteroplasmy are rare, causing the mutation to persist through many generations (Larsson *et al.*, 1992).

Analysis of heteroplasmy in 82 single primary oocytes from a woman carrying m.3243A>G suggested a random genetic drift mechanism of inheritance (Brown *et al.*, 2001). However, selection of m.3243A>G may be dependent on the mother's mutant load, as women with heteroplasmy >50 % tend to have children with the same or lower heteroplasmy (Uusimaa *et al.*, 2007).

Random genetic drift does not appear to be the mechanism by which the m.8993T>G mutation is inherited. Seven oocytes from a woman with approximately 50 % m.8993T>G heteroplasmy were assayed for the mutation; one was found to have 0 % and the others all had greater than 95 % (Blok *et al.*, 1997).

By creating homozygous knock-in mice that express a proof-reading-deficient version of the polymerase gamma catalytic subunit, a mouse model was developed with increased levels of mtDNA point mutations and deletions (Trifunovic *et al.*, 2004). Backcrossing allowed removal of the mutant *Polg* gene, whilst maintaining a

heteroplasmic state of several mtDNA mutations (Stewart *et al.,* 2008).The mice from six successive generations were assayed for mtDNA heteroplasmy levels of each mutation. It was discovered that non-synonmyous changes in protein coding genes were rapidly lost from mouse pedigrees, suggesting a strong purifying selection against deleterious mutations in the mouse germ line. Further evidence for purifying selection was achieved through the introduction of two mtDNA mutations into the female germ line of mice, a severe frameshift mutation in *MT-ND6* and more mild, mis-sense mutation in *MT-CO1* (Fan *et al.*, 2008). The severe mutation was rapidly lost within four generations, but the mild mutation was retained over successive generations.

It is possible that the mtDNA bottleneck and the process of purifying selection are linked, but they could also occur independently. The mechanism of selection could be at the organellar or cellular levels, explaining how even low levels of heteroplasmy could be selected against. There is evidence that defective mitochondria are separated and targetted for degradation through autophagy (Twig *et al.,* 2008).

3.1.1 Research aims

Different techniques and laboratories have variable accuracy and sensitivity when measuring heteroplasmy levels in DNA samples. To eliminate the sources of technical variability, the heteroplasmy levels of three common mtDNA mutations (m.3243A>G, m.8344A>G and m.8993T>G) will be assessed in a large cohort of mother-child pairs. This will establish whether the inheritence of pathogenic mtDNA mutations is dictated purely by random genetic drift, or whether some or all mutations are positively or negatively selected.

These results will then be compared to meta-analyis of previously published data for these and two further mutations (m.11778G>A and m.3460G>A) to establish whether these results have been corroborated.

3.2 Materials and Methods

3.2.1 DNA samples

This study had the relevant institutional approval, and written informed consent was obtained from all of the subjects involved. DNA samples for mother-child pairs were collated from NCG Mitochondrial Diagnostic Service (Newcastle, England), Division of Molecular Neurogenetics, Istituto Nazionale Neurologico C. Besta (Milan, Italy),

Medizinisch Genetisches Zentrum (MGZ) (Munich, Germany), The Centre for Mitochondrial Medicine (Bergen, Norway) and Dipartimento di Scienze Neurologiche, Università di Bologna (Bologna, Italy) (Table 3.1).

Table 3.1 DNA samples collated for heteroplasmy measurements. DNA samples (n=147) extracted from blood from individuals with either m.3243A>G, m.8344A>G or m.8993T>G were collated from Newcastle (n=89), Milan (n=24), Munich (n=11), Bergen n=10) and Bologna (n=13). All samples included are in unrelated mother-child pairs.

Mutation	Cohort Source	Individuals	Pedigrees	Transmissions
m.3243A>G	Newcastle (England)	70	26	44
	Milan (Italy)	14	7	7
	Bergen (Norway)	10	4	6
	Total	*94*	*37*	*57*
m.8344A>G	Newcastle (England)	19	8	11
	Milan (Italy)	10	5	5
	Munich (Germany)	4	1	3
	Total	*33*	*14*	*19*
m.8993T>G	Munich (Germany)	7	3	4
	Bologna (Italy)	13	5	8
	Total	*20*	*8*	*12*

3.2.2 Generation of heteroplasmic controls

The disease control DNA sample for each mutation was selected from a patient with known high heteroplasmy levels to make isolation of the mutation during cloning more efficient. Control DNA did not have any of the mutations studied here. Amplicons from these samples were generated using a standard GoTaq PCR reaction (Section 2.2.1), using the primer sets in Table 3.2. The amplicons were ligated and transformed into competent bacterial cells following the standard cloning protocol (Section 2.3). Plasmid DNA was extracted following the QIAprep Spin Miniprep Kit (QIAGEN). Extracted DNA was sequenced using Big-Dye Terminator Cycle Sequencing (Section 2.6), using the same primers in Table 3.2 to identify whether the clone was mutant or wild-type at each relevant position.

Table 3.2 Primers for ligation templates. Primer sequences to create templates for ligation into plasmid vectors for the MELAS fragment (m.3243A>G), MERRF fragment (m.8344A>G), and LS/NARP fragment (m.8993T>G).

Mutation	Primer Sequence	Position	Size (bp)
m.3243A>G	F-TGTAAAACGACGGCCAGTCAGCCGCTATTAAAGGTTCG R-CAGGAAACAGCTATGACCGGAGGGGGGTTCATAGTAG	3017-3374	357
m.8344A>G	F-TGTAAAACGACGGCCAGTACAGTTTCATGCCCATCGTC R-CAGGAAACAGCTATGACCGTATAAGAGATCAGGTTCGTC	8196-8740	544
m.8993T>G	F-TGTAAAACGACGGCCAGTACCACCCAACAATGACTAATC R-CAGGAAACAGCTATGACCGTTGTCGTGCAGGTAGAGG	8656-9201	545

3.2.3 Creation of heteroplasmic templates

To assess the reliability of heteroplasmy measurement techniques, standards were made with heteroplasmy levels varying between 0 and 100%. The concentration of plasmid DNA collected was determined using the Nanodrop Spectrophotometer ND-1000. Dilutions were made so that both wild-type and mutant DNA had the same concentration (~20 ng/ µL). Heteroplasmy templates were prepared by mixing different volumes of the wild-type and mutant DNA clones yielding mixes between 5% and 95%.

3.2.4 Restriction Fragment Length Polymorphism (RFLP)

The primary PCR for RFLP analysis was a 30 µL GoTaq reaction (Section 2.2.1). Primers used in the PCR reaction are shown in Table 3.3. RFLP was carried out following the standard protocol (Section 2.4).

Table 3.3 Primers for amplification of fragment for RFLP analysis. The primer sequences used to amplify products for RFLP analysis of m.3243A>G mutation indicating the position on the mtDNA covered and which are 6-FAM fluorescently tagged (*).

Mutation (Position)	Primer Sequence	Position of Primer	Size (bp)
MELAS (m.3243A>G)	*F-CACAAAGCGCCTTCCCC R-GCGATTAGAATGGGTACAAT	3155-3353	198

The products generated from primary PCR amplification are then digested with a restriction enzyme which has had a restriction site removed or added by the presence of the mutation, yielding different fragment lengths for mutant and wild-type. The restriction enzymes used for each mutation and the cut site information are shown in Table 3.4.

Table 3.4 Restriction enzymes for RFLP analysis. The restriction enzyme required to differentiate between wild-type and mutant mtDNA for the MELAS (m.3243A>G) mutation, the cut site and the size of the fluorescently labelled fragment.

Mutation (Position)	Restriction Enzyme	Restriction Buffer	Cut Site	Fragment Sizes
MELAS (m.3243A>G)	HaeIII	2	GG / CC CC / GG	A (WT) 160 G (Mut) 86

3.2.5 Pyrosequencing analysis of heteroplasmic mutations

The primary PCR for pyrosequencing analysis was a 30 µL GoTaq Hot Start Polymerase (Promega) reaction (Section 2.5.2). Primers used in the primary PCR (F- and R-) and sequencing (Seq-) reactions are shown in Table 3.5.

Table 3.5 Primary PCR and sequencing primers for pyrosequencing. Primary PCR and sequencing primers for pyrosequencing. Showing size and position of primers or fragments. *BIO indicates biotinylated primers.

Primer	Sequence and Modification	Position of Primer	Size (bp)
(m.3243A>G)	F-*BIO-TAAGGCCTACTTCACAAAGCG R- GCGATTAGAATGGGTACAATGAG	3142-3353	211
	Seq-ATGCGATTACCGGGC	3258-3244	-
(m.8344A>G)	F-*BIO-CATGCCCATCGTCCTAGAAT R- TTTTTATGGGCTTTGGTGAGG	8203-8495	292
	Seq-TAAGTTAAAGATTAAGAGA	8325-8343	-
(m.8993T>G)	F-AGGCACACCTACACCCCTTA R-*TGTGAAAACGTAGGCTTGGAT	8919-9171	252
	Seq-CATTCAACCAATAGCCC	8976-8922	-

3.2.6 Compilation of published heteroplasmy data

Blood heteroplasmy data was collated by myself and Dr. Passorn Wonnapinij from published studies for five mtDNA mutations: m.3243A>G, m.8344A>G, m.8993T>G, m.11778G>A and m.3460G>A (Appendix B.1). When possible, muscle heteroplasmy levels were also recorded for comparison to blood heteroplasmy levels; however, were not used to generate O-M values to study variance.

3.2.7 Statistical analysis

Descriptive statistics were calculated for each frequency distribution, including: the minimum and maximum values; inter-quartile ranges; mean and median and standard deviation (Std. Dev) and standard error of the mean (SEM).

The selected normality test was the D'Agostino & Pearson omnibus. It first computes the skewness and kurtosis to quantify how far from Gaussian the distribution is in terms of asymmetry and shape. The normality test was passed if the combined p-value < 0.05.

A one-sample t-test was performed to assess whether the data were sampled from a Gaussian population with a mean equal to the hypothetical value of 0 (no selection bias). Results were considered significant if p-value < 0.05 (*), <0.01 (**), <0.001 (***).

3.3 Assay development

There are several methods for quantifying mtDNA heteroplasmy level, which rely on either mutation-specific restriction enzyme digestion or sequencing. I have chosen to assess fluorescent restriction fragment length polymorphism (RFLP) and pyrosequencing, to determine which is the most sensitive and reliable technique.

3.3.1 Optimisation of quantification of mtDNA heteroplasmy

Both techniques require PCR amplification of a template surrounding the mutation site. If all available templates do not amplify reliably at each cycle, this could introduce shifts in heteroplasmy from the true value. Therefore a standard curve across the full range of m.3243A>G heteroplasmy levels was generated and assayed in triplicate from independent PCR reactions.

The m.3243A>G mutation introduces an additional cut site for the HaeIII restriction enzyme, meaning the wild-type sequence generates a 160 bp tagged fragment, but the mutant sequence generates an 86 bp tagged fragment. Using a capillary DNA analyser, the relative fluorescence of each peak can be measured and used to quantify the heteroplasmy level (Figure 3.1A).

Pyrosequencing can distinguish between nucleotides at a particular position in a sequence through sequential addition of dNTPs, which release pyrophosphate (PPi) when incorporated into a DNA fragment. The PPi is converted to ATP by ATP sulfurylase which is used in a luciferase-mediated reaction to generate light. Detection of the light signal after each dNTP addition allows quantification of each base at the mutation site (Figure 3.1B).

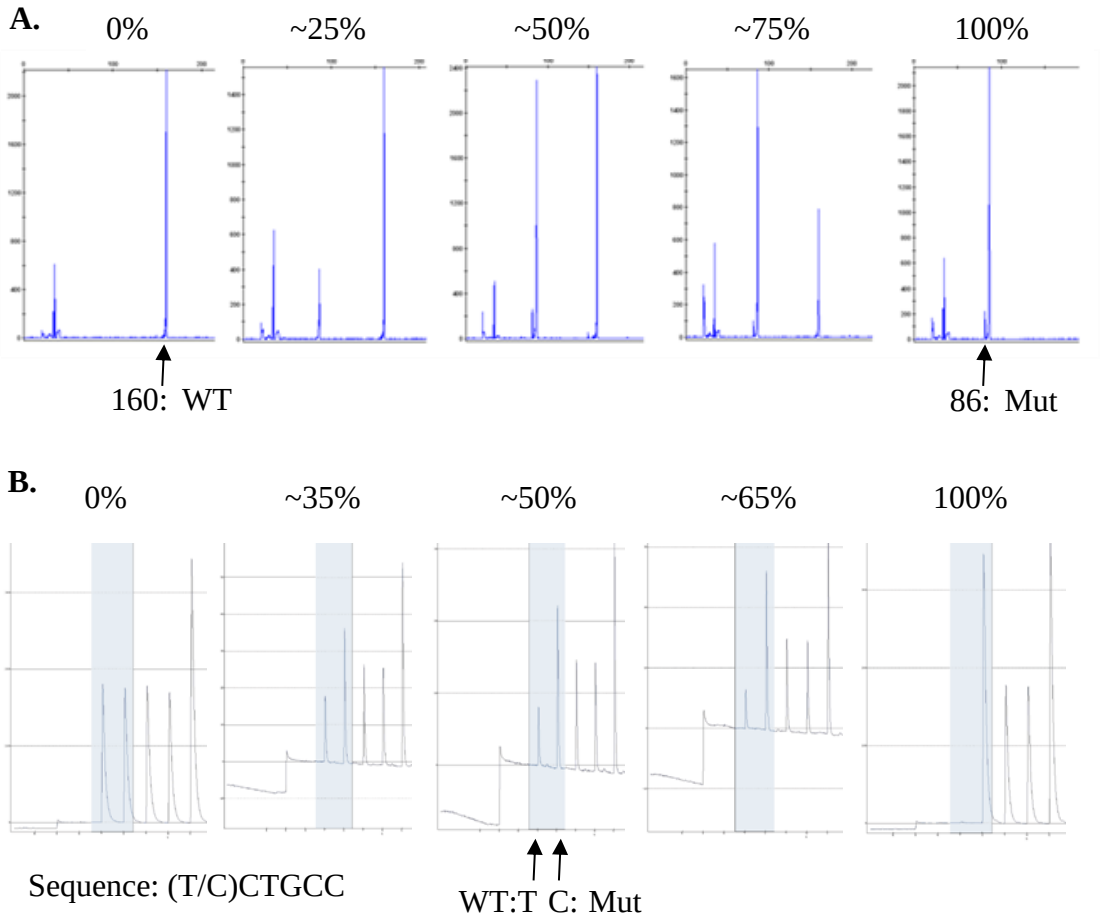

Figure 3.1 m.3243A>G heteroplasmic control standards. m.3243A>G heteroplasmy quantification using (A) fluorescent RFLP and (B) pyrosequencing in artificially generated standard samples with known mutation load.

There is mild deviance from the expected heteroplasmy (indicated by the black lines) when using both RFLP (Figure 3.2A) and pyrosequencing (Figure 3.2B). However, the measured heteroplasmy levels correlate well with each other (Figure 3.2C), and the deviance from the expected heteroplasmy is therefore likely to be introduced during dilution of the wild-type and mutant clones. Although both techniques provide accurate quantification of heteroplasmy levels, pyrosequencing has better reproducibility between technical replicates.

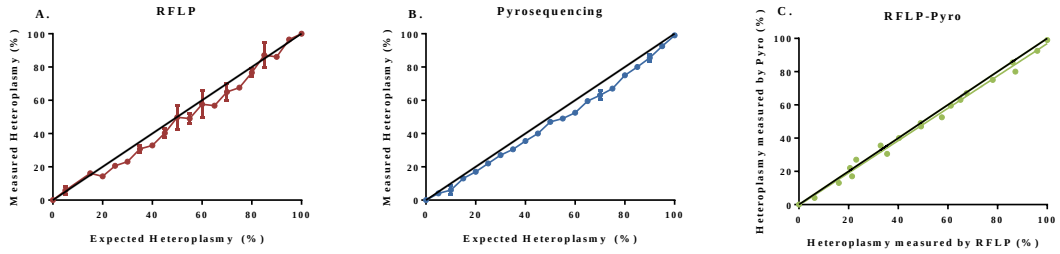

Figure 3.2 Comparison of RFLP and pyrosequencing heteroplasmy measurements. The graph shows the scatter of measured heteroplasmy for both (A) RFLP and (B) pyrosequencing in triplicate, compared to the predicted heteroplasmy values. Error bars represent the SD of triplicate reactions.

3.3.2 Correction of blood heteroplasmy measurements

The heteroplasmy level of m.3243A>G measured in blood has been consistently lower than that measured in post-mitotic tissues such as skeletal muscle and brain (Ciafaloni *et al.*, 1991). Measurement of m.3243A>G heteroplasmy level at two time points showed a decrease in mutation load over time in 28 of 29 patients assayed across two studies (Pyle *et al.*, 2007, Rahman *et al.*, 2001, t Hart *et al.*, 1996). The greatest decrease in mutant load is observed in younger patients, consistent with an exponential loss of mutated DNA in blood leukocytes. The proposed mechanism is selection against haematopoietic (precursor) cells with high mutation loads.

By simulating the segregation of mtDNA in precursors cells, Rajasimha and colleagues derived an equation to correct for the loss of the m.3243A>G mutation in blood (Rajasimha *et al.*, 2008).

Published data from individuals with heteroplasmy measurements made in both blood and muscle were compared for three mtDNA mutations: m.3243A>G; m.8344A>G and m.8993T>G. As expected, the uncorrected heteroplasmy level of m.3243A>G in blood correlates poorly with that measured in muscle (blood mean, 33.41; muscle mean, 64.86; $p < 0.0001$ unpaired t test).The correlation is improved by age-correction using the formula derived by Rajasimha and colleagues (Figure 3.3A) (blood-corrected mean, 58.42; ns). Exclusion of patients with <15% mutation load measured in blood further improved the correlation between blood and muscle heteroplasmy levels (blood >15% uncorrected, 66.97, ns), suggesting there may be a threshold effect where blood precursor cells with a low mutation load are no longer strongly selected against (Figure 3.3B).

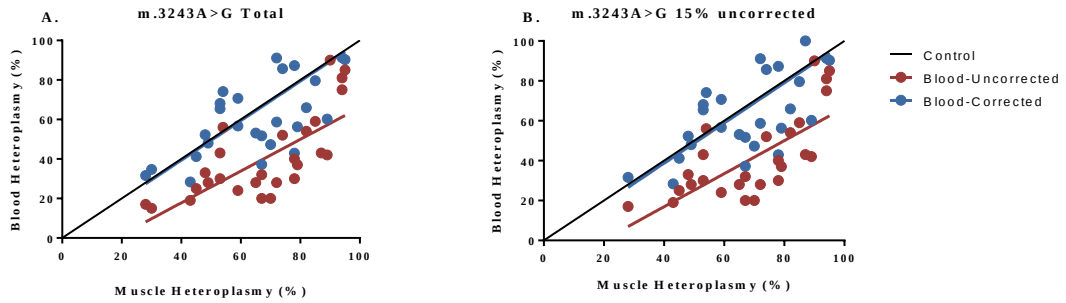

Figure 3.3 Correction of m.3243A>G heteroplasmy level in blood. The mutation load of m.3243A>G measured in both blood and muscle (A) correlate well with each other when age-corrected and (B) is improved through exclusion of those with <15% measured blood heteroplasmy.

Although there are some cases where the m.8344A>G blood heteroplasmy level is lower than that measured in muscle, the majority correlate well with each other (blood mean, 65.25; muscle mean, 77.78; $p < 0.05$ unpaired t test) (Figure 3.4A). There are few incidences where both blood and muscle heteroplasmy have been measured in an individual patient, but heteroplasmy levels remain consistent between tissue (blood mean, 86.5; muscle mean, 89.2; ns).

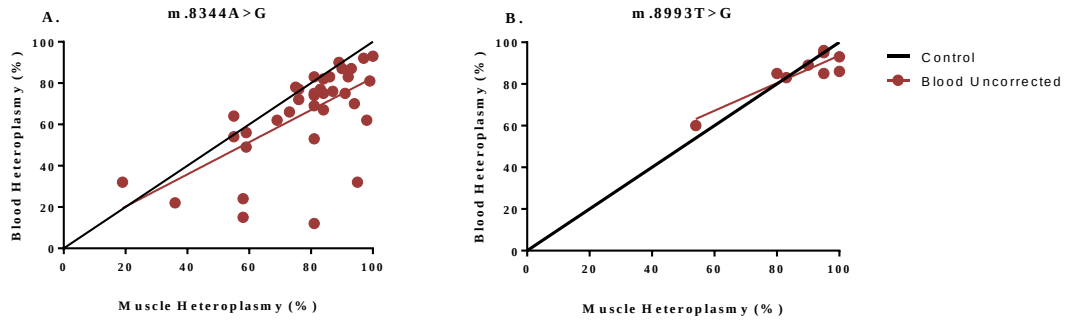

Figure 3.4 Uncorrected m.8344A>G and m.8993T>G heteroplasmy levels in blood. The mutation load of (A) m.8344A>G and (B) m.8993T>G is more consistent between blood and muscle.

Data including heteroplasmy measurements from both blood and muscle are limited, since usually only one tissue is assayed in each study. However, the reduction in m.3243A>G mutant load in blood during aging is also evident when plotting blood heteroplasmy against the patient's age at sampling (Figure 3.5A). The distribution of corrected m.3243A>G heteroplasmy across age groups is comparable to that of m.8344A>G and m.8993T>G (Figure 3.5B-D). Analysis of the published data for the

LHON mutations demonstrates that high m.11778G>A heteroplasmy levels are maintained in patients above 80 years of age (Figure 3.5E), but there is an apparent decline of mutant load in blood with aging for the m.3460G>A mutation (Figure 3.5F).

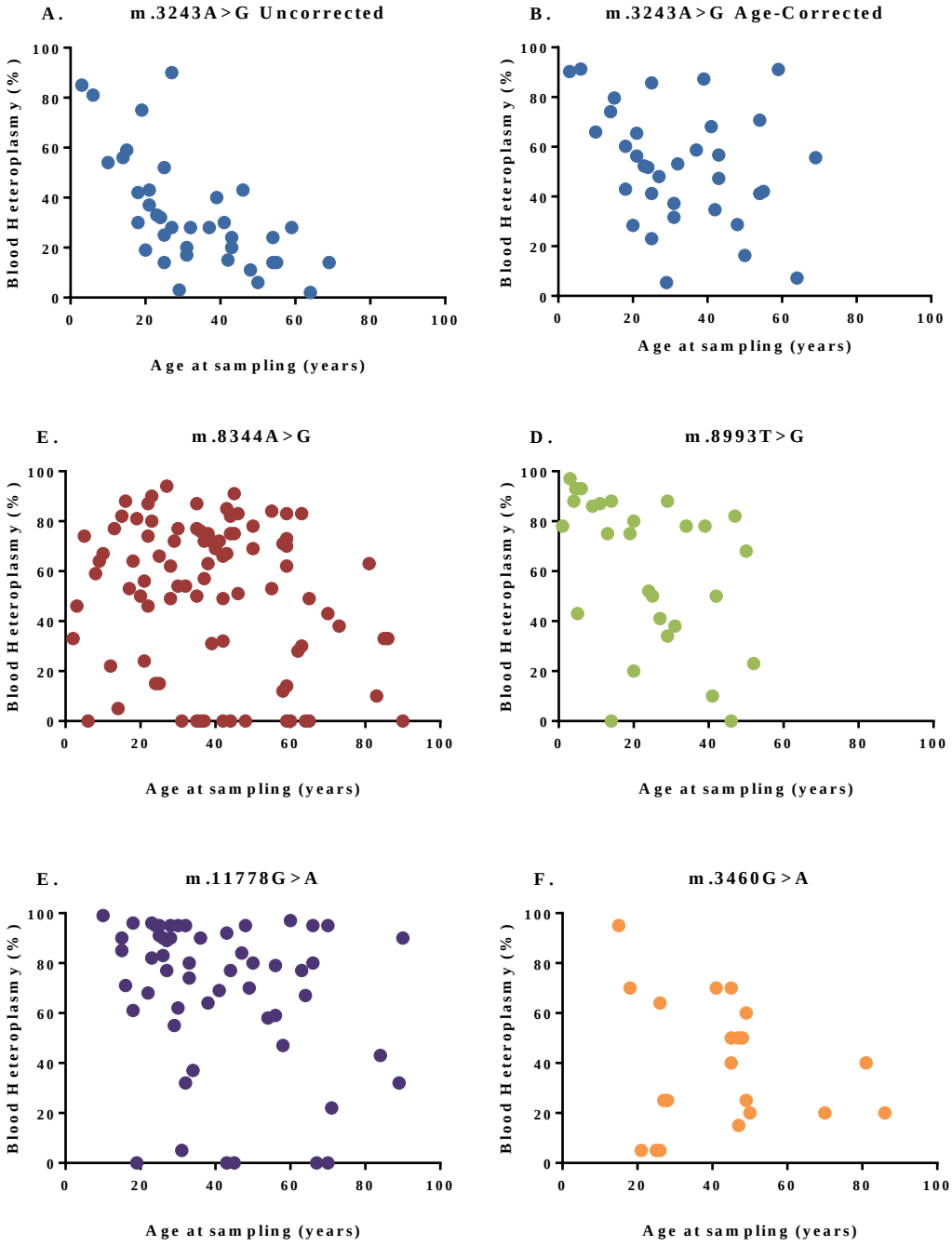

Figure 3.5 Heteroplasmy level distribution across patient ages. The mutant load of (A) m.3243A>G, (B) m.3243A>G age-corrected, (C) m.8344A>G, (D) m.8993T>G, (E) m.11778G>A and (F) m.3460G>A in patients across varying ages in published studies.

There are two possible explanations for the reduced m.3460G>A heteroplasmy level observed in older individuals. If heteroplasmy levels correlate to clinical severity, it is plausible that those with lower mutant load will survive longer than those with high mutant load, seeming to suggest a decrease in heteroplasmy with age. The aetiology of LHON is complex, with strong indication that other genetic and/or environmental factors influence penetrance of the mtDNA mutations. Although unaffected individuals may be homoplasmic for m.3460G>A, the mutant load in affected individuals has been discovered to affect manifestation of the disease phenotype (Black *et al.*, 1996).

In an analysis of tissue segregation patterns in 27 members of a family with m.3460G>A, 18 had >95% mutation load in all tissues, and the other nine had lower heteroplasmy levels in blood than in hair follicles (Kaplanova *et al.*, 2004). This discrepancy leads to seemingly skewed segregation patterns when analysing heteroplasmy levels from blood but not hair follicles. Decreasing blood m.3460G>A heteroplasmy was confirmed by a longitudinal study of five heteroplasmic individuals from one maternal pedigree, showing a decrease of ~1% year (Howell *et al.*, 2000).

As m.3460G>A is a rare mutation, it has not been fully established whether heteroplasmy levels decrease in blood across a wide range of pedigrees, and no correction method has been established. This will have to be taken into consideration when interpreting any segregation data for this mutation.

3.4 Results and Discussion

3.4.1 Analysis of O-M variance in measured heteroplasmy data

The shift in heteroplasmy level between generations is calculated by subtracting the mother's mutant load from that of her child (O-M value). If plotted on a frequency histogram, a mutation with inheritance governed by random drift will be normally distributed around a mean of 0. Frequency histograms were generated for the m.3243A>G (n=57), m.8344A>G (n=19) and m.8993T>G (n=12) (Figure 3.6).

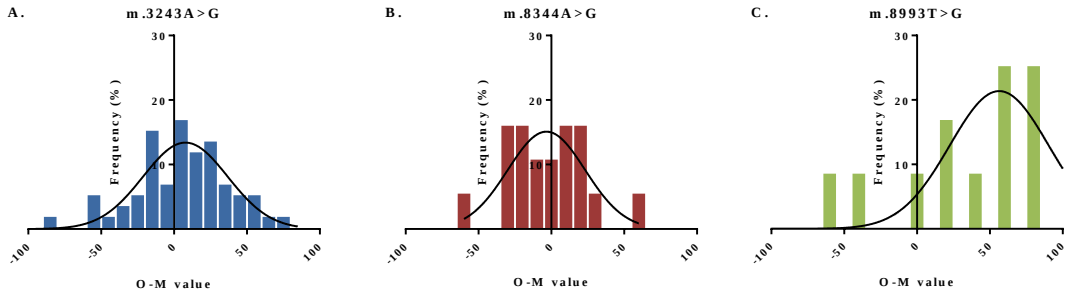

Figure 3.6 Frequency histograms of O-M values for m.3243A>G, m.8344A>G and m.8993T>G transmissions. O-M values represent the shift in heteroplasmy between generations of (A) m.3243A>G, (B) m.8344A>G and (C) m.8993T>G.

The descriptive statistics for each mutation are listed in Appendix A.1. The mean O-M values for the tRNA mutations are close to 0 (m.3243A>G, 5.77 %; m.8344A>G, -3.15 %) but the mean for m.8993T>G is 33.33 %. There is greater potential for an increase than decrease in heteroplasmy for the transmissions measured for the m.8993T>G mutation (Min, -50.3 %; Max, 89.3 %). Although heteroplasmy can either increase or decrease to a similar degree for the tRNA mutations, there is greater potential for change with m.3243A>G (min, -84.3 %; max, 79.2 %) than for m.8344A>G (min, -57 %; max, 55.3 %). This may reflect a different width of mtDNA bottleneck. If a smaller proportion of the mother's total mtDNA repopulates the oocyte, there is a greater potential for change in heteroplasmy level.

Each distribution was subjected to D'Agostino-Pearson omnibus test for normality. The distribution for m.8993T>G shows the greatest level of skew (-0.86), but all mutation distributions passed the normality test (Appendix A.2). A one-sample t-test shows that m.3243A>G and m.8344A>G do not significantly differ from a theoretical mean of 0. The discrepancy -33.03 ($p < 0.05$ one-sample t test) for the m.8993T>G mutation is significant; however, the 95% confidence interval is large, with a minimum value of just 3.25 (Appendix A.3).

There are several sources of bias which might affect the reliability of the results. There is a potential for ascertainment bias, since all samples used in the study have been brought to the attention of clinicians through diagnosis of an affected individual (proband). Any transmissions including the proband case have been removed from the m.3243A>G data set, to determine whether ascertainment bias has affected the distribution of O-M values (Figure 3.7B).

Where inheritance of mtDNA is governed by random genetic drift, the heteroplasmy variance is critically dependent on the initial heteroplasmy level in the mother. This means that mothers with ~50% heteroplasmy may have greater shifts in mutant load than mothers with extreme heteroplasmy values (close to 0 or 100 %). Previously, any measured variance in heteroplasmy has been normalised by the mother's heteroplasmy levels to avoid misinterpretation of data (Samuels *et al.*, 2010). However, in this study the variance within a population is not being measured. Instead, the transmissions where heteroplasmy has shifted in one direction to a greater degree than it could potentially shift in the other direction have been removed (Figure 3.7C).

As previously determined from analysis of published data, the age-based correction method for blood heteroplasmy levels may not work as reliably when the measured mutant load is below 15 %. Any transmission where either the mother or child have a measured heteroplasmy below 15 % was removed (Figure 3.7D).

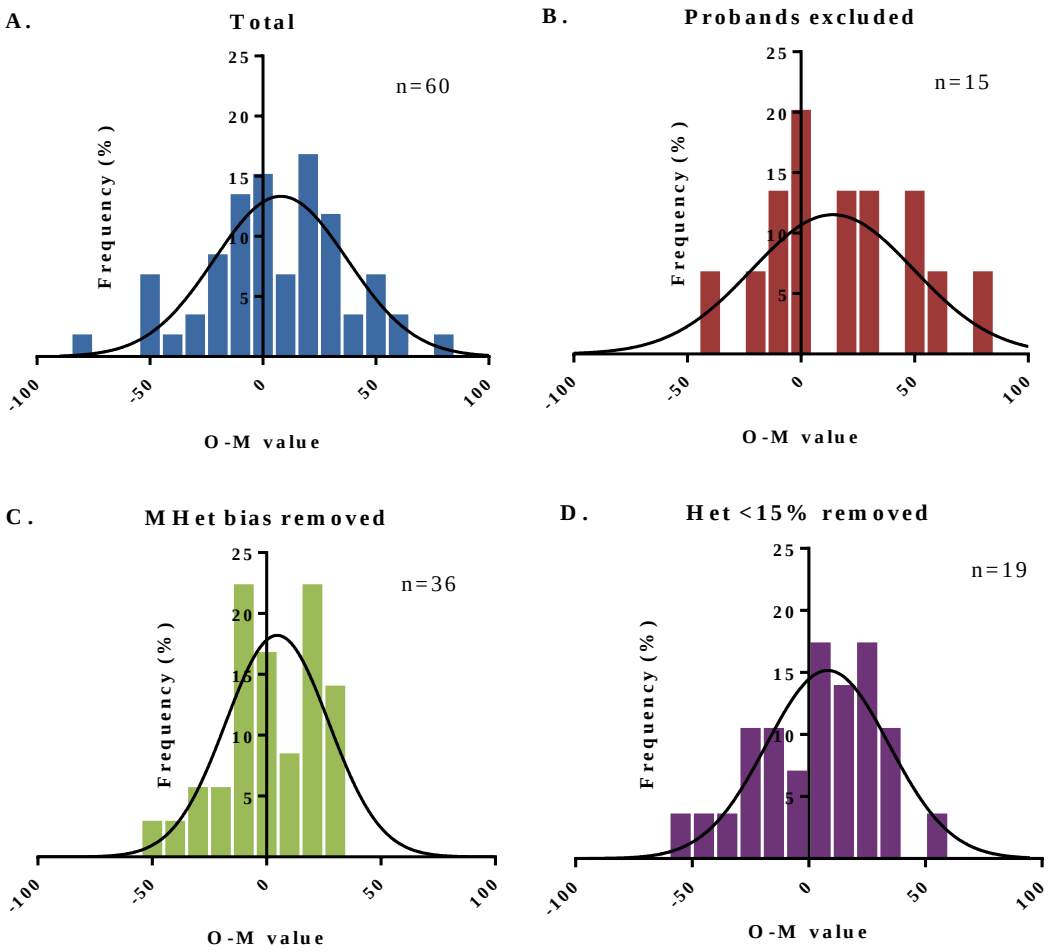

Figure 3.7 Removal of potential bias influencing transmission data for m.3243A>G. Comparison of frequency distributions between (A) total m.3243A>G transmission data and after (B) exclusion of transmissions containing probands, (C) removal of bias caused by differences in mothers' heteroplasmy levels and (D) removal of any transmission including individuals with a measured heteroplasmy below 15 %.

The descriptive statistics for each distribution after removal of potential sources of bias are listed in Appendix A.4. The largest difference was between the total data set and upon exclusion of the proband cases (total mean, 5.77 %; excl. probands, 16.71 %). In this data set, 13 transmissions included mothers (6 individuals) who were probands and 11 transmissions contained children who were probands. After removal of proband cases, there was only 1 of 11 mothers with heteroplasmy levels >50 %, as the women with the highest heteroplasmy values tended to be the affected proband. Removal of the proband cases did not have the same effect on the remaining children (9/15 > 50 %), since siblings of proband cases could also have high heteroplasmy levels and remain included in the study.

All distributions pass the D'Agostino-Pearson omnibus test for normality ($p > 0.05$) and have low values of skewness and kurtosis (Appendix A.5). The one-sample t-tests show none of the distributions differ significantly from a mean of 0 ($p > 0.05$) (Appendix A.6).

3.4.2 Meta-analysis of published heteroplasmy data

Heteroplasmy data for mother to child transmissions were compiled from published studies for five mutations: m.3243A>G (n=111), m.8344A>G (n=96), m.8993T>G (n=118), m.11778G>A (n=118) and m.3460G>A (n=74). The blood heteroplasmy for m.3243A>G was corrected as previously stated and the O-M values for all mutations were generated. Frequency histograms were plotted for each mutation, and a Gausssian curve fitted to each plot (Figure 3.8).

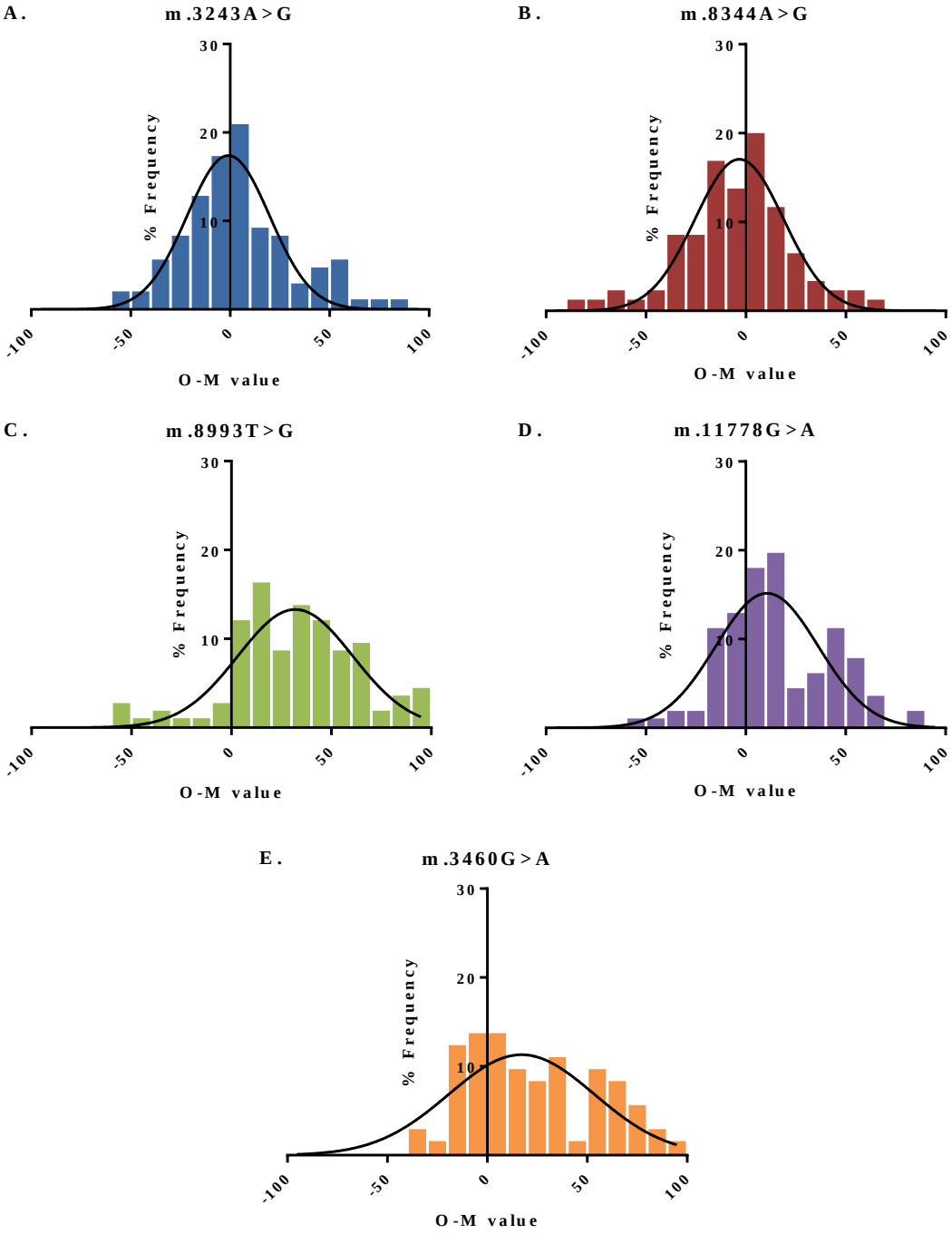

Figure 3.8 Frequency histograms of O-M values for transmission of five heteroplasmic mutations generated from meta-analysis of published data. O-M values represent the shift in heteroplasmy between generations of (A) m.3243A>G (n=111), (B) m.8344A>G (n=96) and (C) m.8993T>G (n=118), (D) m.11778G>A (n=118) and (E) m.3460G>A (n=74) compiled from previously published studies.

The mean values of the distributions measured by pyrosequencing are remarkably similar to those compiled from published data (m.3243A>G measured, 5.77 %; m.3243A>G published, 3.32 %; m.8344A>G measured, -3.15 %; m.8344A>G published, -4.96 %; m.8993T>G measured, 33.33 %; m.8993T>G published, 32.67 %). The mean value for m.11778G>A is 15.4 % and the mean for m.3460G>A is 22.02 %. Further descriptive statistics for the frequency distributions from published data can be found in Appendix B.2.

The only distribution which did not pass the D'Agostino-Pearson omnibus normality test was that of m.3460G>A ($p < 0.01$) (Appendix B.3). The one-sample t-test shows the distributions for the tRNA mutations, m.3243A>G and m.8344A>G, do not significantly differ from a theoretical mean of 0. However, the mutations in protein-coding genes, m.8993T>G, m.11778G>A and m.3460G>A, have distributions which all significantly differ from 0 ($p < 0.0001$ one-sample t test) (Appendix B.4).

The apparent selection for mutations in protein-coding genes is evident in the fixation frequency in the mother-child pairs from published data. For the purposes of this analysis and due to limitations in the techniques for measuring heteroplasmy in some studies, fixation has been defined as instances where heteroplasmy ≤ 30 %, ≤ 60 % and ≤ 90 % in the mother has increased to ≥ 95 % in the child. The mutations were also lost during some transmissions, defined as instances where heteroplasmy ≥ 10 %, ≥ 40 % and ≥ 70 % heteroplasmy in the mother has decreased to ≤ 5 % heteroplasmy in the child. Transmissions in which fixation was not reached have been defined as either a negative change (lower heteroplasmy in child than in mother), neutral ± 5 % (the common sensitivity on most techniques) or positive (higher heteroplasmy in child than in mother).

Fixation rate for the tRNA mutations was low (m.3243A>G, 1.8 %; m.8344A>G, 0 %) but was higher for all three protein-coding gene mutations (m.8993T>G, 21.2 %; m11778G>A, 23.7 %; m.3460G>A, 23.0 %) (Figure 3.9). Loss of the mutation was highest in m.8344A>G (17.3 %), with moderately high levels of m.3243A>G (9.0 %) and m.3460G>A (9.5 %) loss. Frequency of m.8993T>G and m.11778G>A loss was lower, at only 3 % and 0.8 % respectively.

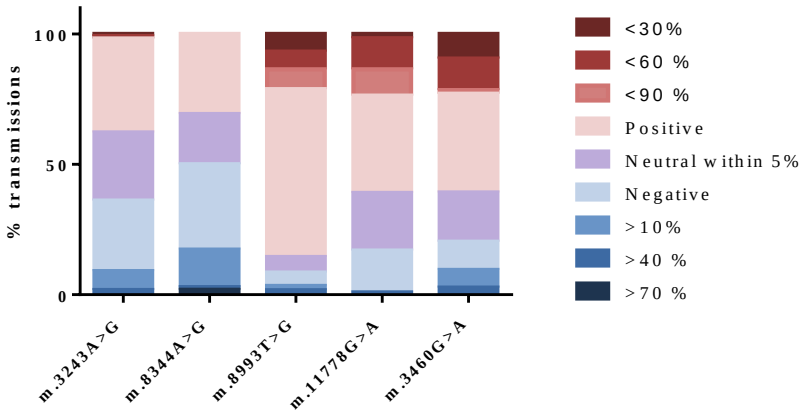

Figure 3.9 Fixation rate of mutations from published transmissions. Mutations were categorised by whether there was a negative, neutral or positive change between mother and child. Positive changes were further characterised by fixation to over 95 % heteroplasmy in the child from a heteroplasmy of under 30 %, between 30-60 % and between 60-90 % in the mother. The tRNA mutations m.3243A>G (~2 %) and m.8344A>G (0 %) have a low frequency of fixation but the protein-coding mutations m.8993T>G, m.11778G>A and m.3460G>A have ~20% frequency of fixation.

From the published studies, individuals were only included if there was recorded data of transmission from a heteroplasmic mother to her child. In addition to these individuals, there are those without their mother's heteroplasmy measurements and those who are homoplasmic for the mtDNA mutation. The rate of fixation is evident in the mutant load in the total participants (Figure 3.10). Homoplasmy frequency (≥95 %) is low for tRNA mutations (m.3243A>G blood, 11.7 %; m.3243A>G muscle, 9.4 %; m.8344A>G, 6.2 %). The higher rate of m.3243A>G homoplasmy in blood compared to muscle is likely due to imperfect age-based correction of measured blood heteroplasmy levels. There is a higher frequency of individuals who are homoplasmic (≥95 %) for protein-coding mutations (m.8993T>G, 33.3 %; m.11778G>A, 81.3 %; m.3460G>A, 46.5 %).

There is a high frequency of wild-type homoplasmy for m.8344A>G (23.8 %), m.8993T>G (34.6 %) and m.3460G>A (18.0 %). There is a moderately high frequency of m.3243A>G homoplasmy in blood (15.8 %) which is not observed in muscle (1.9 %) and lower frequency of homoplasmy for m.11778G>A (3.0 %).

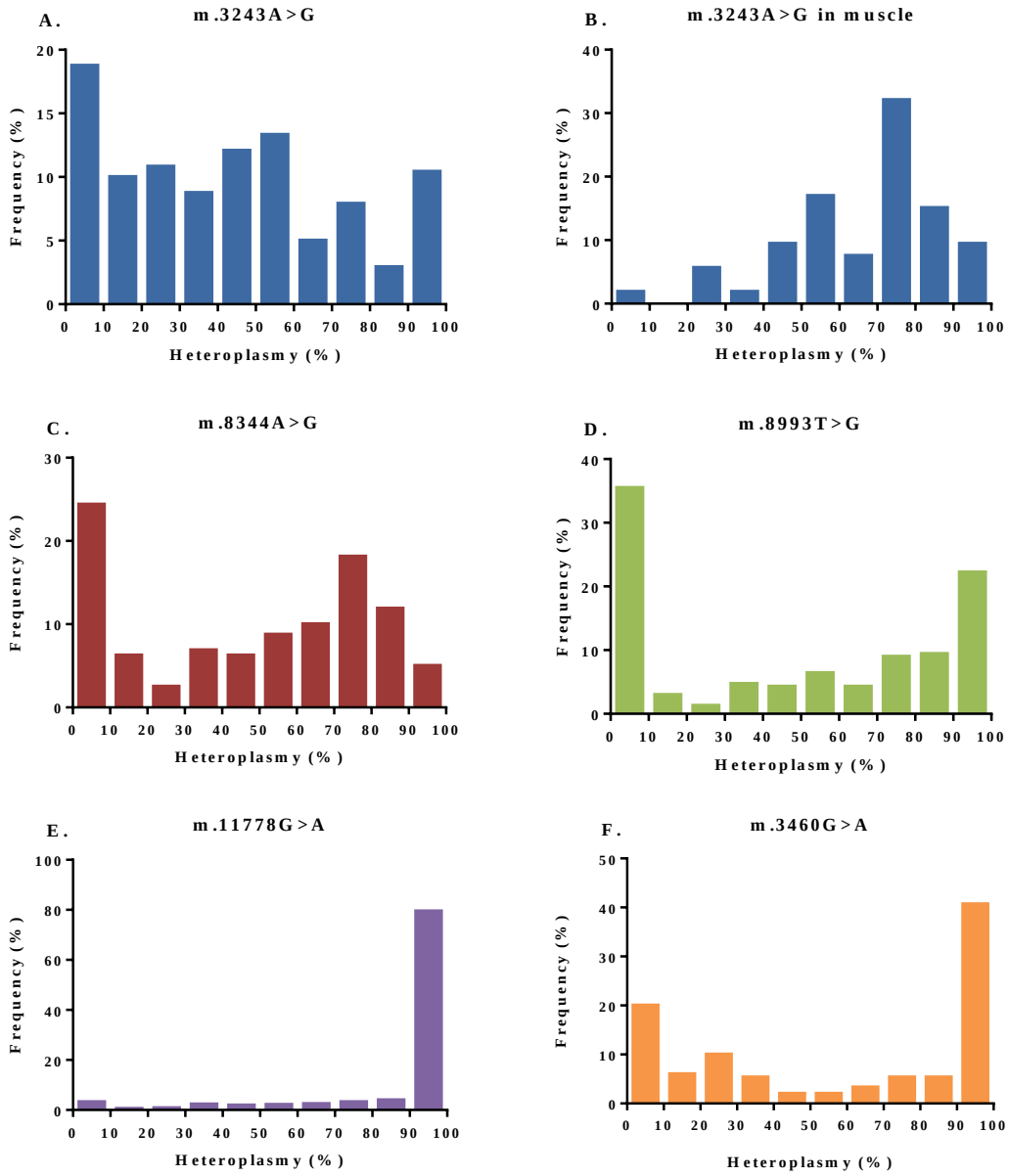

Figure 3.10 Heteroplasmy levels of mtDNA mutations in published data. The heteroplasmy levels reported in published studies of (A) m.3243A>G in blood (B) m.3243A>G in muscle, (C) m.8344A>G, (D) m.8993T>G, (E) m.11778G>A and (F) m.3460G>A. Higher levels of homoplasmy are evident in the protein-coding mutations, which showed a significant deviance away from neutral transmission.

The severity of the tRNA mutations prevents survival of those with near homoplasmic mutant load, explaining why the frequency for m.3243A>G in muscle and m.8344A>G peaks at 70-80 % but declines above this threshold. Despite having the largest discrepancy in distribution mean, m.8993T>G has the lowest homoplasmy frequency of the protein-coding mutations. This is also likely due to the relative severity of the

mutations. The high numbers of individuals with 0 % m.8993T>G in the published studies are mostly from pedigrees where the mutation has occurred *de novo* on one lineage, rather than a loss of mutation from a heteroplasmic female. Both m.11778G>A and m.3460G>A cause Leber's Hereditary Optic Neuropathy (LHON), but with incomplete penetrance. LHON typically presents during mid-life as acute or subacute bilateral visual loss, occasionally with additional clinical presentations (Nikoskelainen *et al.*, 1995). In this study, there are heteroplasmic individuals for both of these mutations above the age of 80, including those with heteroplasmy > 90 % above the age of 70. The m.8993T>G mutation can cause Leigh Syndrome (LS) or neuropathy, ataxia, and retinitis pigmentosa (NARP), and disease severity broadly correlates to heteroplasmy level (White *et al.*, 1999a). Disease onset is earlier, with a wide variety of clinical presentations, and often causes premature death. In this study, the oldest recorded patient studied for m.8993T>G was 52, and all individuals with >90 % heteroplasmy level were below 10 years of age. Thus, although m.8993T>G transmission is most offset from neutral, the opportunity to assay homoplasmic individuals is limited, as those with highest heteroplasmy have the worst prognosis.

3.4.3 Absence of m.3243A>G heteroplasmy decline in blood.

The heteroplasmy level of m.3243A>G was investigated extensively in the blood and muscle of seven families with variable clinical phenotypes (Hammans *et al.*, 1995). In one of these families, all four members had higher than expected heteroplasmy level in blood. Upon sequencing, a homoplasmic mutation was identified in the $tRNA^{Leu}$ gene, m.3290T>C, in addition to m.3243A>G. When the age-correction formula is applied to these individuals, all of their estimated heteroplasmy levels correct to above 100 % (107, 149, 164 and 279 %). It was postulated that the additional mutation was affecting the clinical phenotype. In light of more recent evidence that the mutation load of m.3243A>G decreases in age with blood, this mutation may also modify selection against the mutant molecules in blood precursor cells.

Correction of all publicised blood heteroplasmy data revealed a further three families from independent studies which correct to above 100 % (Campos *et al.*, 1995, Iwanishi *et al.*, 1995, Morovvati *et al.*, 2002). Some of these studies include more than one pedigree, yet all members of one family and none of the others correct to above 100 %,

suggesting strong evidence of a genetic basis of resistance to purifying selection in blood.

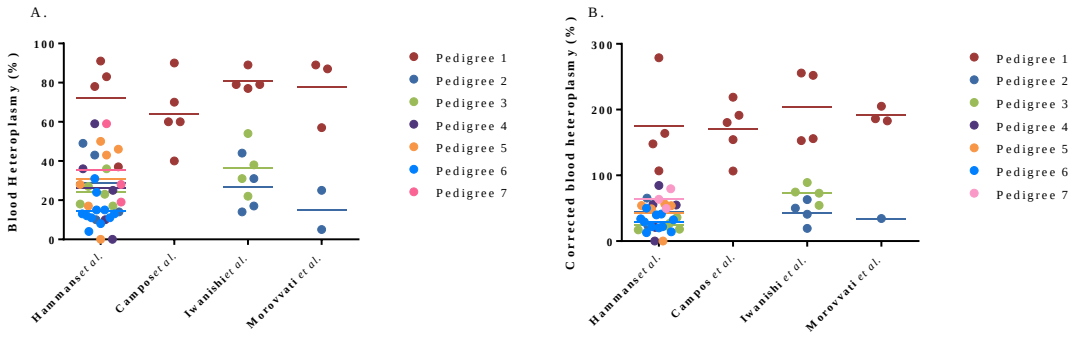

Figure 3.11 Over-correction of blood m.3243A>G heteroplasmy in published data. The m.3243A>G heteroplasmy data from four published studies showing (A) a family in each with higher than normal mutant load in blood which (B) over-corrects to above 100 %.

In two of the studies, there was no further sequence analysis completed to identify evidence of modifying mutations; however, Morovvati and colleagues (2002) identified two mutations specific to the family which had higher than expected m.3243A>G heteroplasmy levels. These were m.1520T>C in the 12S rRNA gene and m.12153C>T in the $tRNA^{His}$ gene. Both mutations are listed as rare SNPs (>0.2 % of total GenBank sequences) on www.mitomap.org. Aside from mtDNA changes, it is also plausible that a nuclear factor is instead providing protection for these mutations and allowing maintenance of high levels of heteroplasmy in blood cells.

From the samples whose heteroplasmy was measured locally by pyrosequencing, only one corrected to above 100 %. This was a 54 year-old woman with two children. Her measured heteroplasmy level was 40.7 %, which age-corrects to 119.8 %. Her children's heteroplasmy levels were only 20.7% (at age 27 corrected to 35.5 %) and 30.7 % (at age 22 corrected to 47.6 %). Although their heteroplasmy levels do not correct to above 100 %, it is possible they have always had lower heteroplasmy levels which have remained constant.

The mother's mtDNA was sequenced to identify any additional mutations which may be modifying the behaviour of the mutant mtDNA molecules in blood precursor cells. Sequence changes from the rCRS in the RNA and protein-coding genes are listed in Table 3.6.

Table 3.6 mtDNA sequence changes in a female with m.3243A>G. The mtDNA coding and RNA sequence variants in a female with m.A3243A>G whose measured blood heteroplasmy over-corrects to above 100%. The loci and effect on amino acid coded for is given for each sequence variant. The SNP status and GenBank Frequency were collated from www.mitomap.org. Haplogroup associations were collated from www.phylotree.org and identifies the woman as haplogroup K.

Base	Nucleotide Change	Loci	Syn?	SNP	GenBank Frequency	%	Haplogroup Association
994	A>G	12S RNA	-	Y	1	<0.01	-
1189	T>C	12S RNA	-	Y	323	1.8	K1
1438	A>G	12S RNA	-	Y	749	4.1	
1811	A>G	16S RNA	-	Y	1450	7.9	U2-8 (K)
2706	A>G	16S RNA	-	Y	13893	75.7	
3243	A>G	tRNA Leu (H)	-	N	-	-	-
3480	A>G	ND1	Y	Y	951	5.2	Ub8 (K)
4646	T>C	ND2	Y	Y	240	1.3	K1b1a1a
4769	A>G	ND2	Y	Y	17964	97.8	
5913	G>A	COI	Asp>Asn	Y	109	0.6	K1b
7028	C>T	COI	Y	Y	14259	77.7	
8860	A>G	ATP6	Thr>Ala	Y	18178	99.0	
9055	G>A	ATP6	Ala>Thr	Y	997	5.4	Ub8 (K)
9698	T>C	COIII	Y	Y	961	5.2	U8 (K)
9962	G>A	COIII	Y	Y	57	0.3	K1b1
10289	A>G	ND3	Y	Y	75	0.4	K1b2
10398	A>G	ND3	Thr>Ala	Y	7972	43.4	K1
10550	A>G	ND4L	Y	Y	915	5.0	K
11299	T>C	ND4	Y	Y	1045	5.7	K
11467	A>G	ND4	Y	Y	2465	13.4	U (K)
11719	A>G	ND4	Y	Y	13641	74.3	
11923	A>G	ND4	Y	Y	47	0.3	K1b1a
12308	A>G	tRNA Leu	-	Y	2454	13.4	U (K)
12372	G>A	ND5	Leu>Leu	Y	2654	14.5	U (K)
13967	C>T	ND5	Thr>Met	Y	79	0.4	K1b1a1
14053	A>G	ND5	Thr>Ala	Y	80	0.4	
14167	C>T	ND6	Y	Y	920	5.0	Ub8 (K)
14766	C>T	CYTB	Thr>Iso	Y	13539	73.7	
14798	T>C	CYTB	Phe>Leu	Y	1472	8.0	K
15257	G>A	CYTB	Asp>Asn	Y	242	1.3	K1b1a
15326	A>G	CYTB	Thr>Ala	Y	18123	98.7	
15946	C>T	tRNA Thr	-	Y	38	0.2	K1b1

The majority of sequence changes are associated with haplogroup K and its subtypes (K1b1a1a), identified using www.phylotree.org. All sequence changes are listed as SNPs on www.mitomap.org, excluding m.3243A>G. There is one sequence on

GenBank which has identical RNA and protein-coding sequence changes to this female (JQ704057.1) and only some alternative changes in the D-loop (data not shown) and the m.3243A>G mutation. This suggests a moderately close genetic relationship, with no additional pathogenic mutations evident.

In the published pedigrees, the additional mutations which may have influenced selection against m.3243A>G were in the $tRNA^{Leu}$ gene itself (Hammans *et al.*, 1995), and 12S rRNA or $tRNA^{His}$ (Morovvati *et al.*, 2002). Although lacking an additional mutation in the $tRNA^{Leu}$ gene, there is a rare SNP in the 12S rRNA gene, m.994A>G.

A longitudinal study of heteroplasmy levels in the individuals of this pedigree is needed to determine whether their mutant load is stable in blood, before any conclusion can be drawn on the significance of the presence of m.994A>G.

3.5 Concluding Remarks

The heteroplasmy levels of m.3243A>G, m.8344A>G and m.8993T>G from mother-child pairs were accurately measured by pyrosequencing. The tRNA mutations showed Gaussian distributions centred around a mean transmission of 0, suggesting neutral transmission governed by random drift. The transmission of the *MT-ATP6* mutation, m.8993T>G, had a mean significantly different to 0 (33.33 %, $p < 0.05$ one-sample t test), suggesting there may be positive selection of this mutation. These results were corroborated by analysis of previously published data, which show positive deviance from 0 for m.8993T>G and also two other protein-coding mutations, m.11778G>A and m.3460G>A.

m.8993T>G and m.11778G>A show high frequencies of fixation to ≥95 % heteroplasmy and have low frequencies of mutation loss to ≤ 5 % heteroplasmy, supporting the notion of selection in favour of these mutations.

Although m.3460G>A has a high frequency of fixation, it also shows moderate frequency of mutation loss. This suggests a narrow bottleneck with a greater capacity for change in mutation load, but does not necessarily support positive selection. The deviance from 0 in the mean O-M variance could be artefactual, caused by the apparent decrease in blood heteroplasmy with age, which could not be corrected.

The means of O-M variance for both the tRNA mutations, m.3243A>G and m.8344A>G, are not significantly different from 0 and are normally distributed (one-

sample t test). Although both mutations show higher frequencies of mutation loss than mutation fixation, high mutation loads of m.3243A>G and m.8344A>G are not tolerated and will therefore not be measurable in the population.

In addition to the family mentioned in observed by Hammans and colleagues (1995), a further three pedigrees with m.3243A>G have been identified from independent studies which show higher than normal blood heteroplasmy levels. The heteroplasmy of these individuals over-correct to above 100 % when the age-based formula is applied, which does not occur in any individual from other pedigrees from these studies. This strongly suggests a genetic factor rather than a technical artefact. Additional mutations in $tRNA^{Leu}$, 12S rRNA and $tRNA^{His}$ were identified in these families.

Only one individual's heteroplasmy measured by pyrosequencing age-corrected to over 100 %. No additional $tRNA^{Leu}$ mutations were identified in this individual; however, there was a rare homoplasmic SNP in 12S rRNA (m.994A>G). Further study is needed to establish whether this mutation influences the selection of m.3243A>G in blood precursor cells.

Future study in this field would benefit from increased avaialability of DNA samples from tissue other than blood, such as muscle. Since preimplantation genetic diagnosis (PGD) is becoming a more widely used diagnostic tool, it allows the possibility to study the transmission of different heteroplasmy mutations across many embryos from individual females (Sallevelt *et al.*, 2013).

Chapter 4. Gene Expression During Murine Embryogenesis

Table of Contents

4.1 Introduction

The mtDNA bottleneck was first hypothesised after observations of a homoplasmic mtDNA mutation occurring in a proportion Holstein cows dispersed across a single lineage (Hauswirth and Laipis, 1982, Olivo *et al.*, 1983). The mutation is unlikely to have occurred multiple times independently across the lineage. Consequently they proposed that the founder female contained both the wild-type and mutant mtDNA genotypes, and random segregation or unequal amplification accounted for the fixation to either genotype in subsequent generations.

Since then, much work has been undertaken to identify the mechanism and timing by which heteroplasmy values shift between generations. The majority of this work has relied upon mice as a model organism, where embryogenesis is comparable to humans, and transgenic lines allow identification and manipulation of the germ line (Payer *et al.*, 2006, Sugimoto and Abe, 2007).

Many stages of embryonic development and germ-line formation provide potential sites for the mtDNA bottleneck. Unequal partitioning of mtDNA during cleavage of the pre-implantation embryo, or reduction in mtDNA copy number in PGCs during post-implantation development, could account for a prenatal mtDNA bottleneck. Replication of a sub-population of mtDNA genomes during maturation of primary oocytes could potentially cause shifts in heteroplasmy during postnatal development. Understanding mouse embryogenesis and development of the female germ-line is critical to uncovering the timing and mechanism of the mtDNA bottleneck, and the implications it has for transmission of mitochondrial disease.

4.1.1 Mouse embryogenesis

After fertilisation of the oocyte, the embryo undergoes a series of cellular cleavages (Figure 4.1A). The embryo remains a constant size, but contains a progressively higher numbers of smaller blastomeres (Cockburn and Rossant, 2010). Once the embryo reaches the 8-cell stage compaction occurs, where there is increased intracellular adhesion and cells become flattened, but continue to divide. Once at the 32-cell stage, the cells closest to the outside become committed to the trophectoderm lineage. Within the embryo a fluid-filled blastocoele cavity forms, allowing development of the inner cell mass (ICM) (Pedersen *et al.*, 1986). The formed blastocyst develops over the following 24 hours, and implants in the uterine wall by 4.5 d.p.c.

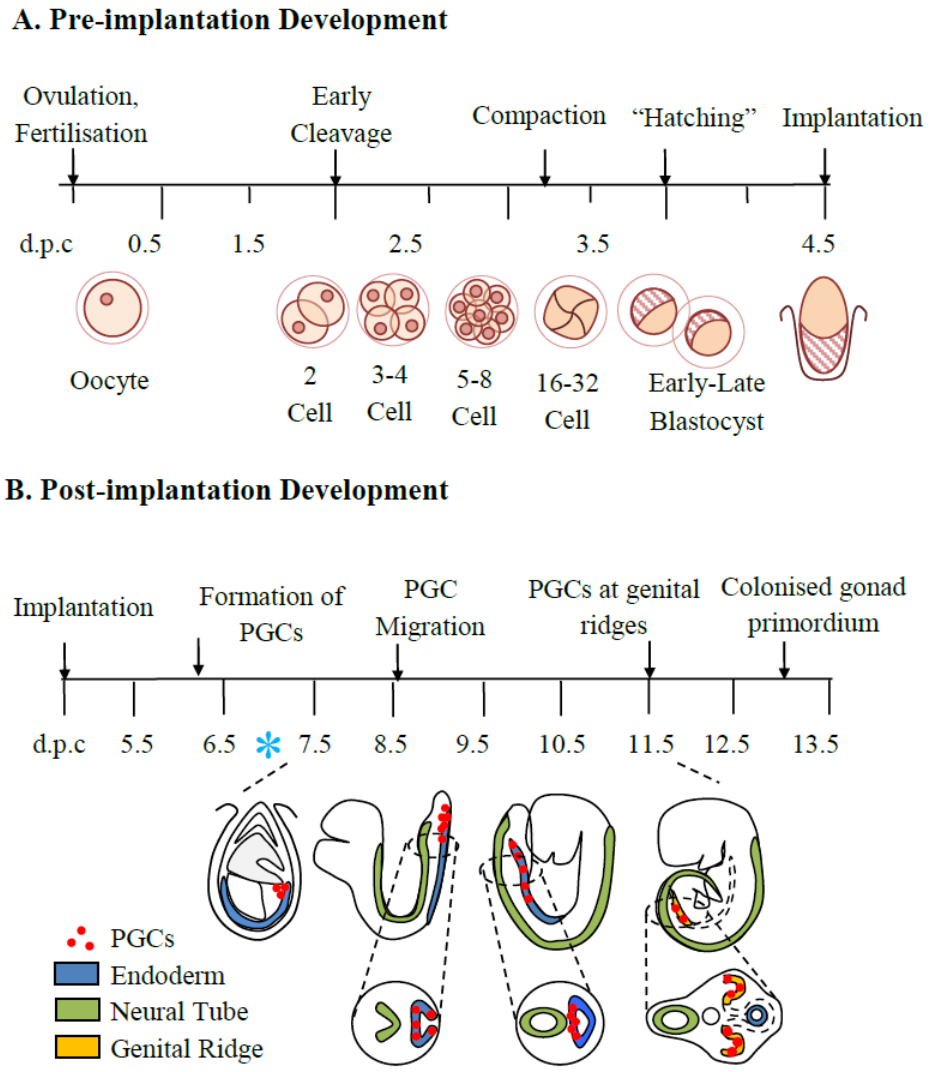

Figure 4.1 An overview of early mouse embryogenesis. After fertilisation of the oocyte (A) pre-implantation begins with cleavage of the embryo, dividing into more blastomeres until compaction and formation of the blastocyst at ~ 3.5 d.p.c. At 4.5 d.p.c. the blastocyst implant in the uterine wall and begin (B) post-implantation development. At 6.25 d.p.c. the first cells form that will become lineage-restricted to PGCs, and by 7.25 d.p.c. the population has expanded to ~40 cells and express the germ-cell specific marker, Stella *(Dppa3).* As the PGC population expands, the PGCs migrate from the endoderm to the genital ridges. After mitosis they form germ-cysts and eventually colonise the gonad primordium, as oogonia, by 13 d.p.c. * Prenatal bottleneck predicted by Cree and colleagues (2008) and supported by Freyer and colleagues (2012).

Gastrulation occurs within the first 48 h of post-implantation development (Figure 4.1B), and embryos can be staged by morphological landmarks relating to the formation of the primitive streak and the development of the different germ layers (endoderm, ectoderm and mesoderm) (Downs and Davies, 1993). At 6.25 d.p.c., a subset of pluripotent proximal epiblast cells respond to signals from the extra-embryonic ectoderm and the visceral endoderm, and begin to express Fragilis *(Ifitm3)* (Saitou *et al.*,

2002). Of these, ~6 cells will begin to express Blimp1 *(Prdm1)* and become lineage-restricted to PGC precursors (Ohinata *et al.*, 2005). By 7.25 d.p.c., the PGC population has expanded to ~40 cells and expression of Stella (*Dppa3)* is detectable (Saitou *et al.*, 2002). At 8.5 d.p.c. the endoderm invaginates, and the PGCs migrate along the length of the forming hindgut. By 9.5 d.p.c., the PGCs are directed from the hindgut to the dorsal body wall, until eventually colonising the genital ridges (McLaren, 2003). At this stage they begin expressing other PGC-specific biomarkers, such as Vasa (*Ddx4*) (Toyooka *et al.*, 2000), germ cell nuclear antigen 1 *(Gcna1)* (Enders and May, 1994) and Germ cell-less homolog 1 *(Gmcl1)* (Kimura *et al.*, 1999).

Once at the genital ridge, PGCs undergo mitosis and cluster together, forming germ-cysts containing many oogonia (Figure 4.2A). At 13.5 d.p.c. the oogonia enter meiotic prophase, becoming oocytes, and arrest in diplotene at 18.5 d.p.c., near the time of birth.

At this point, ~30% the oocytes in the clusters begin to form primordial follicles, gaining a surrounding layer of granulosa cells; the remainder are destroyed through apoptosis (atresia) (Pepling *et al.*, 2010). The primordial follicles remain inactive until selected through initial recruitment for follicle maturation. Thecal cells are recruited to secondary follicles and further stimulate growth and maturation to antral follicles, at which point there is a surge in gondadotrophin (particularly luteinising hormone (LH)) secretion (Figure 4.2B). This induces ovulation, and the oocyte is released from the follicle, ready for fertilisation. The follicle, stimulated by LH, differentiates into a corpus luteum, essential for the early stages of pregnancy (Uzumcu and Zachow, 2007).

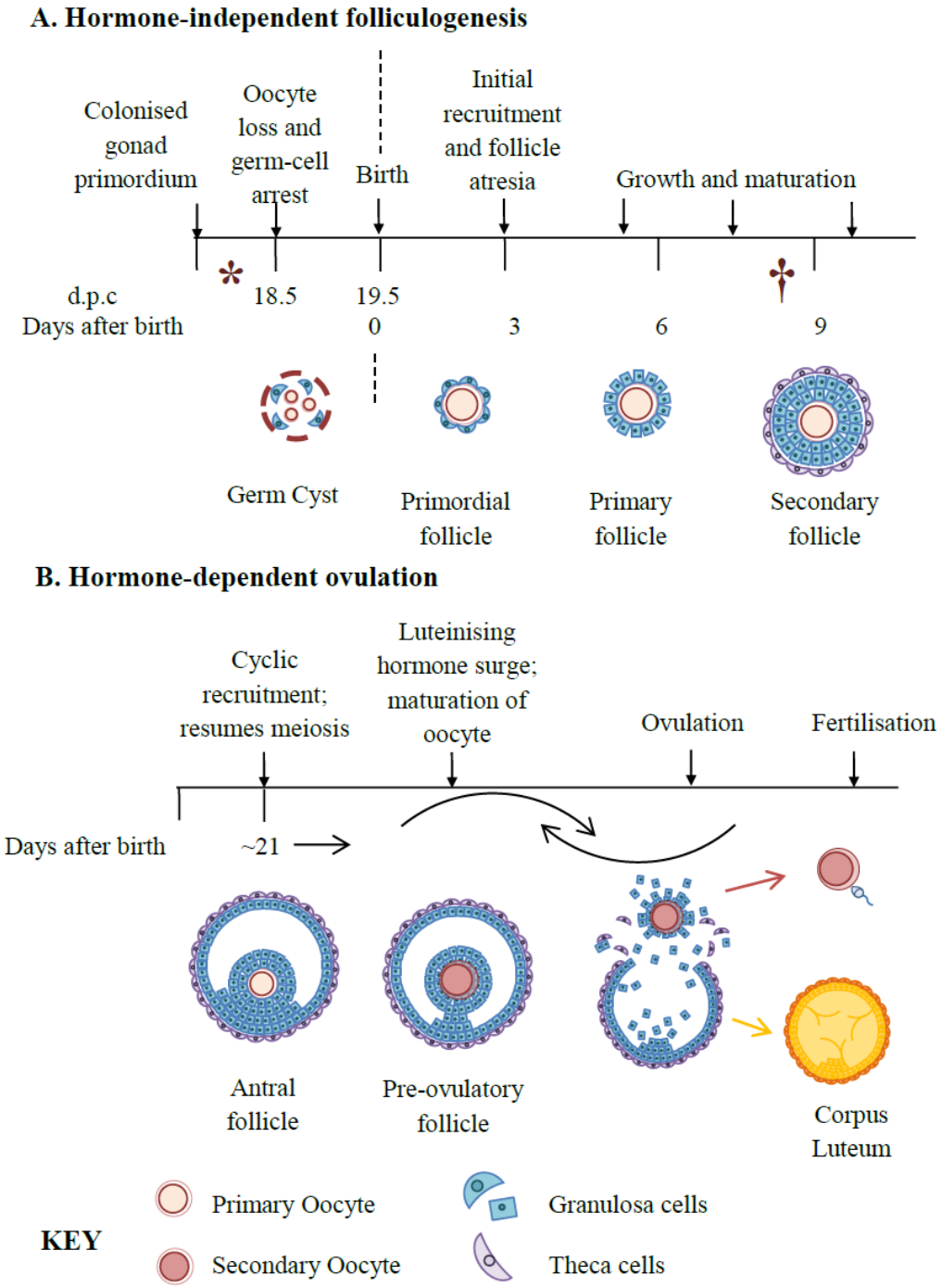

Figure 4.2 An overview of mouse folliculogenesis and ovulation. At the genital ridges (A) a proportion of formed oogonia are selected for formation of primordial follicles. These recruit first granulosa cells, then thecal cells as the follicles grow and mature. (B) Once at the antral stage, a surge in gonadotrophin (LH) secretion stimulates maturation of the primary to a secondary oocyte and it is released for fertilisation. * Jenuth and colleagues (1996) predict a mtDNA bottleneck caused by unequal segregation during expansion of the oogonia population. † Marchington and colleagues (1997) support the hypothesis that heteroplasmic variation has formed by oocyte maturation.

4.1.2 Mechanisms of the mtDNA bottleneck

To test these hypotheses, Jennuth and colleagues (1996) generated mice with heteroplasmic polymorphisms by electrofusing cytoplasts from one mouse breed into the one-cell embryo of another breed. A post-fertilisation mtDNA bottleneck was eliminated through comparison of mature, unfertilised oocytes to progeny of the same female, finding no difference in variance of heteroplasmy levels. Similarly, comparison of immature primary oocytes and mature secondary oocytes from the same mouse showed similar variance in heteroplasmy, suggesting the mtDNA bottleneck has occurred by folliculogenesis at postnatal day 3. PGCs isolated at 8.5 d.p.c. showed little heteroplasmic variance. They proposed that this indicated the mtDNA bottleneck is caused by unequal segregation during the mitotic divisions undergone by the oogonial population prior to primary oocyte formation. By modelling the divisions required to generate this population of oogonia and the variance achieved, they estimated the number of independent segregating units to be 185. This calculated value is remarkably close to the primitive estimate of 200, based upon mitochondria per oogonia (40) and average number of genomes per mitochondria (5) (Nass, 1969, Nogawa *et al.*, 1988).

Variance in the heteroplasmy of polymorphic tracts in mature human oocytes supported the conclusion that at least part of the heteroplasmic variance is generated by oocyte maturation (Marchington *et al.*, 1997). By assaying polymorphic tracts and mtDNA rearrangements, they calculated the number of segregating units for a single selection point to be ~9, but if accounting for 23 divisions, it would be 210 segregating units (Marchington *et al.*, 1998). Although ~200 segregating units accounts for how heteroplasmy levels shift due to genetic drift, it would not allow *de novo* mutations to reach the high heteroplasmy levels often seen (Lebon *et al.*, 2003). This suggests the estimates of the number of segregating units are only a mean value, and mtDNA copy number in individual cells may vary greatly, including some cells with extremely low heteroplasmy values.

Although alluding to the timing and size of the bottleneck, these studies did not uncover the mechanism, or mechanisms, by which the mtDNA bottleneck is formed (Figure 4.3).

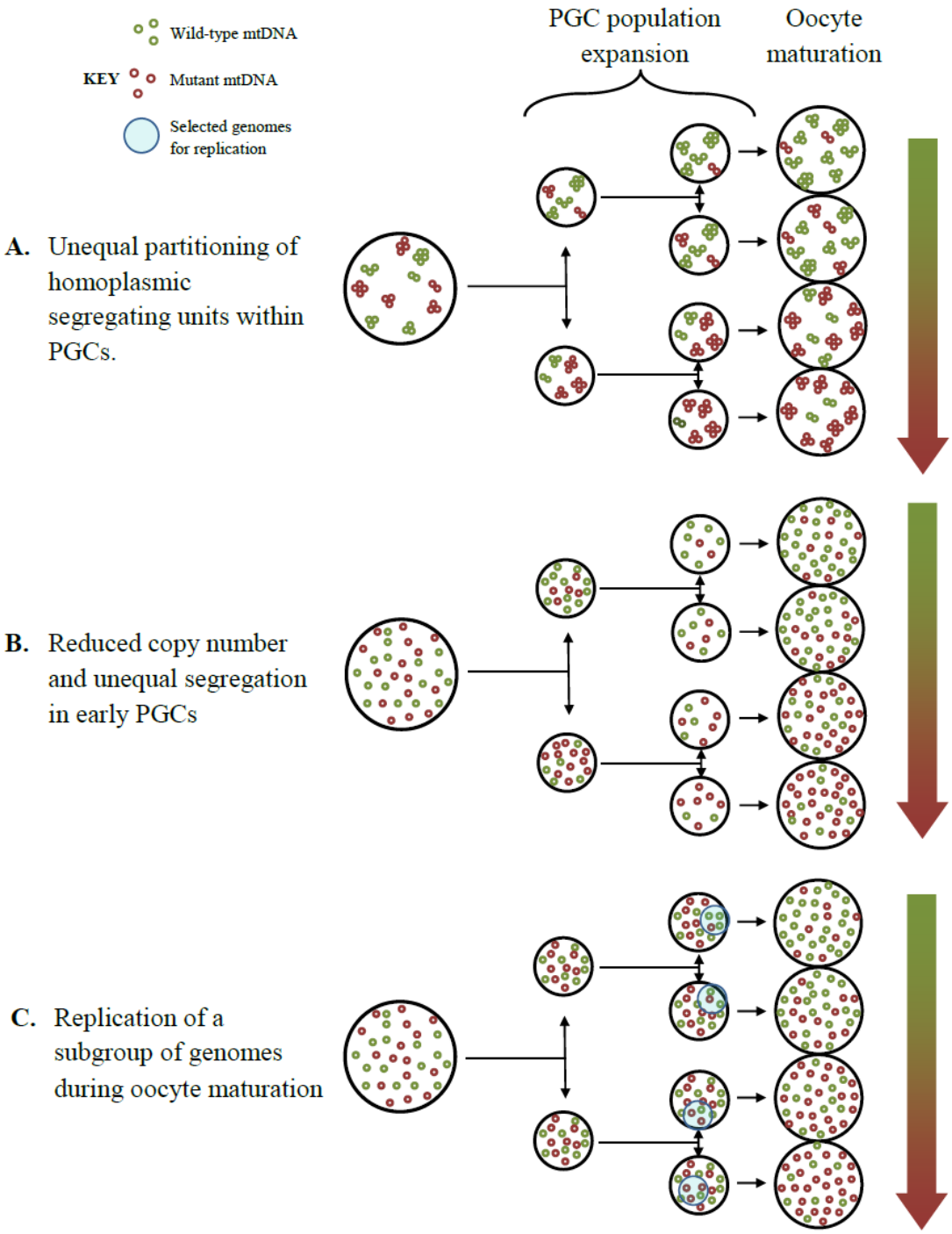

Figure 4.3 Proposed mechanisms for generation of heteroplasmy variance (the mtDNA bottleneck). Potential mechanisms for formation of the mtDNA bottleneck include (A) unequal segregation of homoplasmic nucleoids, (B) reduced mtDNA copy number followed by unequal segregation of single mtDNA molecules and (C) replication of a subpopulation of mtDNA causing a skew in heteroplasmy levels.

Rather than relying on statistical modelling to estimate the size of the mtDNA bottleneck, Cao and colleagues (2007) directly measured mtDNA copy number in

mouse cells from developing embryos using qPCR techniques. During pre-implantation, the mtDNA copy number per blastocyst halved at each cell division, but remained constant in the overall embryo. The majority of cells had a measured copy number of over 620 genomes. When assaying PGCs, identified by alkaline phosphatase staining, from 7.5 to 13.5 d.p.c. they found few cells with lower than 600 genomes per cell, which remained consistent as the PGC population expanded. Their evidence led them to conclude that the mtDNA bottleneck occurs without a reduction in mtDNA copy number, and that limiting the number of segregating units occurs through aggregation of mtDNA genomes into homoplasmic nucleoids or through replication of a sub population of genomes (Figure 4.3A).

This finding was later disputed by a further two studies which independently measured a dramatic reduction in mtDNA copy number in the early PGC population (Cree *et al.*, 2008, Wai *et al.*, 2008). As alkaline phosphatase was shown to interfere with mtDNA copy number measurements, these studies instead used PGC-specific GFP-reporter transgenic mice to identify and separate PGCs from somatic cells. Using an adapted population genetic model, Cree and colleagues (2008) calculated that the reduction in mtDNA copy number observed at 7.5 d.p.c. can account for 70% of the heteroplasmy variance observed in the progeny of heteroplasmic mice, with the remaining 30% generated through massive mitochondrial proliferation as the PGC population expands (Figure 4.3B). However, Wai and colleagues (2008). analysed heteroplasmic PGCs at various stages of prenatal oogenesis, and reported no increase in heteroplasmy variance during oogenesis. By using the thymidine analogue 5-bromo-2'-deoxyuridine (BrdU), they demonstrated only a small percentage of mtDNA molecules in primary oocytes are replicating, and suggested this as the major mechanism responsible for generation of heteroplasmic variance (Figure 4.3C). These results were further disputed (Samuels *et al.*, 2010), and there is therefore a need to confirm the precise timing of the bottleneck using an independent, validated technique.

Mice with defective polymerase gamma (Pol γ) (D257A PolgA exo− or mtDNA-mutator mice) allowed generation of mouse lines with a range of mtDNA mutations (Trifunovic *et al.*, 2004). This included a mouse line with heteroplasmic levels of the pathogenic mutation m.3875delC in tRNAMet, found to remain stable across all tissues of the body and through inheritance to further generations (Freyer *et al.*, 2012). There was an absence of mice with >86% mutation level, and no reduction in fecundity in

female mice with higher heteroplasmy, indicating a purifying selection before formation of the offspring. By crossing these mice with the GFP-Stella reporter line (Payer *et al.*, 2006), they were able to isolate heteroplasmic PGCs at 13.5 d.p.c. Measurements of the mutation levels in these PGCs demonstrated that the heteroplasmic variance observed in oocytes and live offspring is already generated by 13.5 d.p.c. in PGCs. These findings support the hypothesis of a prenatal bottleneck caused by the dramatic reduction in mtDNA copy number during early post-implantation development.

4.1.3 mtDNA replication during embryonic development

For the mtDNA copy number to increase dramatically as the PGC population expands, the rate of mtDNA replication must be greatly increased compared to pre-implantation development. The mtDNA copy number in a total embryo does not vary throughout embryonic development (McConnell and Petrie, 2004, Thundathil *et al.*, 2005). However, the use of BrdU identified mtDNA replication occurring in fertilised oocytes and in 2-cell mice embryos, indicating a higher turnover rate at these stages (McConnell and Petrie, 2004). Contrary to this, Thundathil and colleagues (2005) measured increased expression of known replication-related genes (*Polg-A*, *Polg-B*, *Ssb* and *RNase MRP*) from the 8-cell stage to the blastocyst stage. Measuring the transcript levels of *mt-Nd2* and *mt-Nd6* transcripts demonstrated higher expression of mitochondrial genes at the morulae (compaction) and blastocyst stages. This correlated with an increase in *Tfam* expression, but not with increased expression of *Nrf1*, *Tfb2m* and *Tfb1m*. This agreed with the original measurements of mitochondrial transcripts made by Piko and Taylor (1987), who determined the egg and 2-cell embryo are transcriptionally silent relative to cleavage stages.

The expression of mitochondrial replication genes has also been correlated to mtDNA accumulation during oocyte growth, with *Tfam*, *Polg* and *Polg2* expression being highest between 12-15 days and then decreasing as oocyte growth halts and mtDNA replication rate lowers (Mahrous *et al.*, 2012).

4.1.4 Research Aims

Recent research supports a prenatal mtDNA bottleneck forming before 13.5 d.p.c. (Freyer *et al.*, 2012). Since expression of mtDNA replication factors is critical to regulation of mtDNA copy number, we will assess the expression of these genes during pre- and post-implantation development to determine the stage at which mtDNA

replication rate increases. We will expand the scope of genes assessed, and explore how mitochondrial dynamics, replication, transcription, and biogenesis contribute to regulation of mtDNA copy number during embryogenesis.

4.2 Materials and Methods

4.2.1 Mouse tissue isolation

Sample isolation was performed by Dr L.M. Cree or Dr. V. Floros under license (Institute of Genetic Medicine, Newcastle University) and in accordance with the UK Home Office Animal Act (1986).

C57BL/6J.CBA females were mated with Stella-GFP BAC–homozygous C57BL/6J.CBA males (Payer *et al.*, 2006). For collection of pre-implantation zygotes, females were superovulated with pregnant mares' serum (PMS) (Sigma- Aldrich) and human chorionic gonadotrophin (hCG) (Sigma-Aldrich). Single-cell embryos were recovered by flushing the oviducts with pre-warmed M2 medium (Sigma-Aldrich) and transferred to pre-warmed M16 media (Sigma-Aldrich). Embryos were incubated at 37 °C in a humidified atmosphere containing 5 % CO_2 until they reached the required cleavage stage. For each sample, 15 embryos were pooled and transferred to sterile PCR tubes and lysed in TRIzol® Reagent (Invitrogen, Life Technologies) and stored at -80 °C until extraction.

For isolation of PGCs from post-implantation samples, Stella-GFP heterozygous embryos were collected in supplemented DMEM, (Invitrogen, Life Technologies) at 7.5, 8.5, 9.5 and 11.5 d.p.c. (counting from midnight on the evening of mating). The posterior region of the 7.5, 8.5, and 10.5 d.p.c. embryos and the genital ridges of 11.5 d.p.c. embryos were dissected, pooled and dissociated. The tissue was resuspended in one volume of FBS and then centrifuged at low speed. The final pellet was resuspended in further supplemented DMEM and kept on ice until fluorescence-activated cell sorting (FACS). PGCs were uni-directionally sorted using a BD FACSAria (Becton Dickinson) into TRIzol® Reagent (Invitrogen, Life Technologies) to a total of 150 cells in each biological replicate. Samples were stored at -80 °C until extraction.

4.2.2 RNA isolation, amplification and cDNA synthesis

RNA isolation was performed was performed by Dr L. M. Cree (Institute of Genetic Medicine, Newcastle University) using PureLink® RNA Mini Kit (Ambion, Life Technologies), which can extract ultrapure total RNA from samples lysed with TRIzol® Reagent using silica-based spin columns. RNA extraction was performed as described in the PureLink® RNA Mini Kit manual using chloroform (Sigma-Aldrich) to separate organic, interphase and aqueous layers and RNase-Free DNase (QIAGEN) for the optional on-column DNase treatment.

The purity and quality of the extracted RNA was analysed on the NanoDrop 2000 UV-Vis Spectrophotometer and Agilent 2100 Bioanalyzer respectively, as described in Section 2.9.5).

RNA extracted from pre-implantation samples was converted to cDNA exclusively using WT-Ovation® RNA Amplification System (NuGEN). Post-implantation sample cDNA synthesis was tested with both WT-Ovation® RNA Amplification and One-Direct Systems (NuGEN) and SuperScript III First-Strand Synthesis System (Invitrogen, Life Technologies) described in Section 2.11. The post-implantation RNA samples were also amplified using Arcturus® RiboAmp® HS PLUS RNA Amplification Kit (Section 2.10).

4.2.3 TaqMan Low Density Array (TLDA) cards

The selected card layout for these experiments was ‘Format 32’, allowing measurement of 31 target assays in addition to the mandatory internal reference gene (*18S rRNA*). All measurements were made in triplicate, allowing for four unique samples per card (one sample in two ports). Gene selection was based on previously published studies. The details for the Taqman® assays used are shown in Table 4.1.

Table 4.1 Assay information for mouse gene expression TLDA cards. The 31 selected genes (and reference gene) on the TLDA cards, including information on the sequence, assay ID and the amplicon positional information.

Gene Symbol	Accession Number	Assay ID	Location	Exons	Position*	Amplicon Length
Gapdh	NM_008084.2	Mm99999915_g1	75	1-1	5'	107
18S	X03205.1	Hs99999901_s1	609	--	3'-M	187
B2m	NM_009735.3	Mm03003532_u1	160	2-2	5'-M	247
Bax	NM_007527.3	Mm00432051_m1	592	5-6	3'	84
Dnm1l	NM_001025947.1	Mm01342903_m1	1707	13-14	3'	71
Fis1	NM_001163243.1	Mm00481580_m1	445	2-3	3'	60
Hif1a	NM_010431.2	Mm01283758_g1	791	3-4	M	141
Hist2h2	NM_013549.1	Mm00501974_s1	47	1-1	5'	57
Lrpprc	NM_028233.2	Mm00511512_m1	3546	30-31	3'	64
Mfn1	NM_024200.4	Mm00612599_m1	980	7-8	M	88
Mfn2	NM_133201.2	Mm00500120_m1	622	4-5	5'-M	61
Nrf1	NM_001164226.1	Mm00447996_m1	632	4-5	M	69
Opa1	NM_001199177.1	Mm00453879_m1	2270	21-22	M	80
Pdx1	NM_008814.3	Mm00435565_m1	523	1-2	M	74
Peo1	NM_153796.3	Mm00467928_m1	1815	1-2	5'	74
Phb2	NM_007531.2	Mm00476104_m1	443	3-4	5'	102
Polg	NM_017462.2	Mm00450527_m1	975	2-3	5'	99
Polg2	NM_015810.2	Mm00450161_m1	577	1-2	5'	132
Polrmt	NM_172551.3	Mm00553272_m1	216	2-3	5'	118
Pop5	NM_026398.4	Mm00503231_m1	422	3-4	3' M	102
Pparg	NM_001127330.1	Mm01184322_m1	757	5-6	3'	101
Ppargc1a	NM_008904.2	Mm00447187_g1	2036	9-10	3'	81
Ppargc1b	NM_133249.2	Mm01258518_m1	2734	9-10	3'	83
Pprc1	NM_001081214.1	Mm00521078_m1	4406	9-10	3'	123
Rnaseh1	NM_011275.2	Mm00488036_m1	328	2-3	5'	68
Sirt5	NM_178848.3	Mm00663721_m1	656	5-6	M	70
Sod2	NM_013671.3	Mm00449726_m1	433	2-3	5'	67
Sp1	NM_013672.2	Mm00489039_m1	1940	4-5	3'	75
Tfam	NM_009360.4	Mm00447485_m1	327	2-3	5'	81
Tfb1m	NM_146074.1	Mm00524825_m1	669	5-6	3'	88
Tfb2m	NM_008249.4	Mm01620397_s1	41	1-1	5'	125
Txn1	NM_011660.3	Mm00726847_s1	668	5-5	3'	113

*M=Middle.

4.2.4 Gene expression analysis

As the samples of the study are five independent stages of embryogenesis, the C_t values generated for reference and target genes were used to calculate the expression of the target gene as a percentage of the reference.

$$Target\ \%\ of\ reference\ gene = 100(10^{(-\Delta Ct/3.333)})$$

4.2.5 Real-Time qPCR

For assessing the relative quantity of RNA transcripts in mouse samples, a standard 25 µL qPCR reaction mix (Section 2.12.1) was used with the following primers in Table 4.2.

Table 4.2 Mouse gene expression primers. *β-actin* gene expression primers to assess the quantity of cDNA in post-implantation samples.

Primer	Sequence	Fragment Size
Actb	F-TTGCTGACAGGATGCAGAAG R-CTCCTCCTGAGCGCAAGTAC	86 bp

4.3 Assay Development

4.3.1 Selection of reference genes

The TLDA cards are designed with an assay for *18S rRNA* as a control gene. In addition to *18S rRNA*, three other genes were selected as reference genes to allow the option of selecting the most stably expressed gene as the reference. The additional genes selected were beta-2-microglobulin (*B2m*), glyceraldehyde-3-phosphate dehydrogenase (*Gapdh*) and histone cluster 2, H2aa1(*Hist2h2aa1*).

To assess the reliability and stability of the gene expression for each gene the C_t values for all four reference genes were subjected to BestKeeper analysis (Pfaffl *et al.*, 2004). This software uses pair-wise correlations to calculate the stability of C_t values for each 'reference gene' across all experimental conditions, on the assumption that equal amounts of total RNA/cDNA have been loaded into the reaction. It also generates an averaged index value between all samples for genes deemed stably expressed. If normalising against a control sample using the ΔΔCt method to generate a fold change value, this index can be used as a more reliable reference source than using a single gene C_t value.

The descriptive statistics indicate that *18S rRNA* has the least amount of variance and the highest correlation with the BestKeeper index and would be the most suitable choice for a reference gene (Appendix C.1 and Appendix C.2). The standard deviation is still high (1.3), as the BestKeeper software suggests rejecting any reference gene with a higher than one standard deviation. However, the BestKeeper software relies on the equal loading of RNA/cDNA quantity, and it is possible that the variance observed is due to unequal loading rather than expression instability.

Since the C_t values in most cases are lower for 16-32 cell and blastocyst samples, this could indicate a higher amount of starting material loaded (Appendix C.3). As the ratio of the target gene and reference gene should remain consistent with variable concentrations of starting materials, I have chosen to accept the slightly high standard deviation of the *18S* C_t values and use this gene as my reference.

4.3.2 Optimisation of post-implantation RNA analysis

RNA was supplied by Dr L.M. Cree from 150 PGCs collected by FACS at various stages of post-implantation embryogenesis (7.5, 8.5, 9.5 and 11.5 d.p.c.).

Post-implantation sample quantification and quality control

The RNA was not quantifiable via standard spectrophotometry (using NanoDrop 2000 UV-Vis Spectrophotometer) or by analysis by the Agilent 2100 Bioanalyzer RNA 6000 Nano kit, with the lower sensitivity rating of 5 ng.

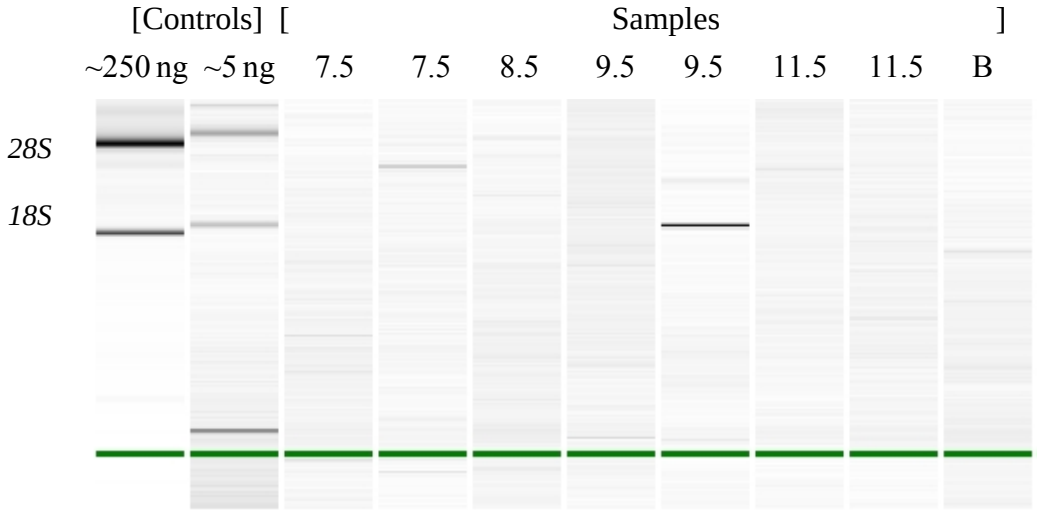

Figure 4.4 Agilent 2100 Bioanalyzer Nano Gel Image. Gel image produced from the Agilent 2100 Bioanalyzer software showing the quality of control and sample RNA.

As the RNA was at low concentration, cDNA was generated using the One-Direct System (NuGEN) which is capable of amplifying cDNA from as little as 10 pg of RNA.

However, qPCR results from the TLDA cards showed much lower signal intensity for all genes in the post-implantation samples. The average C_t value for *18S rRNA* in pre-implantation blastocyst samples was 18.43, but for post-implantation samples was 36.5. A ΔC_t of 18.06 is equivalent to ~275,000 fold less signal in post-implantation samples.

The other reference genes, such as *B2m* and *Gapdh* also failed to amplify successfully (Figure 4.5).

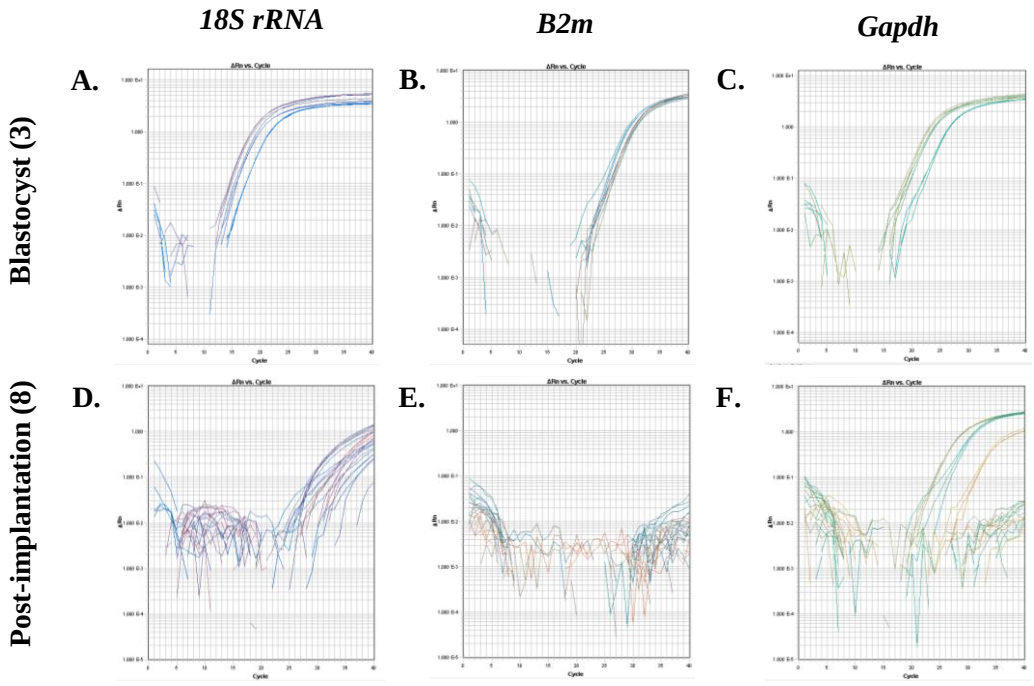

Figure 4.5 TLDA trace comparisons for selected reference genes. The pre-implantation samples from blastocysts (3) show successful amplification of (A) *18S rRNA*, (B) *B2m* and (C) *Gapdh* reference genes. However, samples extracted from post-implantation PGCs (7.5, 8.5, 9.5 and 11.5 d.p.c. in duplicate) show (D) poor amplification for *18S rRNA*, (E) no amplification for *B2m* and (F) variable amplification success for *Gapdh* reference genes.

RNA amplification

RNA amplification allows generation of microgram amounts of anti-sense/amplified RNA (aRNA) from low amounts of input total RNA. Lang and colleagues (2009) tested three methods of RNA amplification: Modified T7 amplification, the Arcturus® RiboAmp® HS RNA Amplification Kit and the Balanced PCR method. They found the RiboAmp® HS kit gave the most reliable amplification from sub-nanogram amounts of total RNA.

Table 4.3 Signal comparison before and after RNA amplification. The table shows the Ct value for *Actb* (at a threshold of 500 RFU) of control and post-implantation samples before and after amplification, indicating where applicable the improvement.

Sample	Before Amp.	After Amp.	Improvement	Fold Change
Control	29.79	20.95	8.84	451.50
7.5	No Signal	No Signal	-	-
8.5	31.28	26.28	5.00	31.73
8.5B	N/A	23.60	-	-
9.5	N/A	24.66	-	-
11.5	N/A	No Signal	-	-

Samples amplified with RiboAmp kit were found to be incompatible with the NuGen WT-Ovation and One-direct kits, which successfully increased the signal of an unamplified pre-implantation sample by ~380 fold (Table 4.4).

Table 4.4 Comparison between WT-Ovation and Superscript III cDNA synthesis kits. The table shows that aRNA does not produce cDNA with the NuGen WT-Ovation system but does with Superscript III. However, unamplified samples (Blasto) show much higher signal for *Actb* with the WT-Ovation system compared to Superscript III.

Sample	WT-Ovation	Superscript III	Difference	Fold Change
Blasto.	21.49	30.08	8.59	379.82
8.5A	No Signal	27.53	-	-
8.5B	No Signal	25.62	-	-
9.5	No Signal	23.15	-	-

This would indicate more signal is lost by not being able to generate cDNA with the NuGen kit than has been gained by amplifying the RNA.

Post-implantation TLDA results after RNA amplification

Post-implantation samples that have undergone RNA amplification were also loaded into TLDA cards and analysed. Although there was an improvement in *18S rRNA* signal with the RNA amplification method, the signal for mRNA transcripts was lower or unreliable (across technical replicates). The signal for the pre-implantation blastocyst sample was also dramatically lower for both *18S rRNA* and mRNA transcripts. This would suggest that the WT-Ovation® RNA One-Direct Systems (NuGEN) can amplify the signal of mRNA transcripts more efficiently than the Arcturus® RiboAmp® HS PLUS RNA Amplification Kit.

Table 4.5 Comparison of post-implantation TLDA results. The table shows the TLDA results obtained using either the WT-Ovation® RNA One-Direct Systems (NuGEN) for cDNA synthesis or Arcturus® RiboAmp® HS PLUS RNA Amplification Kit. Both methods produce unreliable signal from post-implantation samples.

	NuGEN cDNA synthesis				RNA amplification			
	8.5A	8.5B	9.5A	Blasto	8.5A	8.5B	9.5A	Blasto
18S	34.35	35.96	34.26	18.47	26.84	29.47	25.15	26.78
B2M				26.80				
Bax		21.16	36.46	26.49	28.66	32.60	27.55	
Dnm1l		29.29		27.73				36.27
Fis1				31.26	33.23	28.22		
Gapdh	32.58	25.35	27.57	23.42		33.71	26.44	31.31
Hif1a				30.03				
Hist2h2				28.65				
Lrpprc				24.97			30.35	34.14
Mfn1			31.51	23.84				33.84
Mfn2								
Nrf1				26.75				35.61
Opa1	35.20			27.08				37.08
Pdx1			30.62					
Peo1	27.15							
Phb2			26.73	27.53			34.32	34.75
Polg								
Polg2								
Polrmt								
Pop5		35.30		26.31			33.68	
Pparg								
Ppargc1a								
Ppargc1b				33.13				36.42
Pprc1		29.02		27.80			34.17	34.14
Rnaseh1								
Sirt5								
Sod2	23.23		34.8	27.09				34.39
Sp1			23.28	27.46				
Tfam	36.03			33.28				35.92
Tfb1m				28.99				36.39
Tfb2m								
Txn1				29.46				

4.3.3 RNA extraction from somatic cells collected by FACS

The previously extracted post-implantation samples are at unacceptably low RNA concentration, with no way of identifying the quality of the samples. For potential further studies, it is important to identify the number of cells required for successful gene expression analysis of RNA from samples gathered using FACS.

As fluorescently marked PGCs are extremely limited, I have chosen to analyse a reference gene in RNA extracted from somatic cells acquired through FACS. The Arcturus® PicoPure® RNA Isolation Kit (Life Technologies) has been shown to successfully recover high-quality RNA from fewer than 10 cultured cells. Since there

are approximately 50 PGCs at early post-implantation stages, cells from separate FACS sessions may need to be pooled. After lysis, the samples in the extraction buffer can be stored at -80 °C before being pooled and extracted on one column at a later date. To test the efficiency of this method, five aliquots of 50 cells were pooled to a total of 250 cells. A range of cells from 10 to 1000 were collected into the RNA extraction buffer from the Arcturus® Picopure® kit (Figure 4.6).

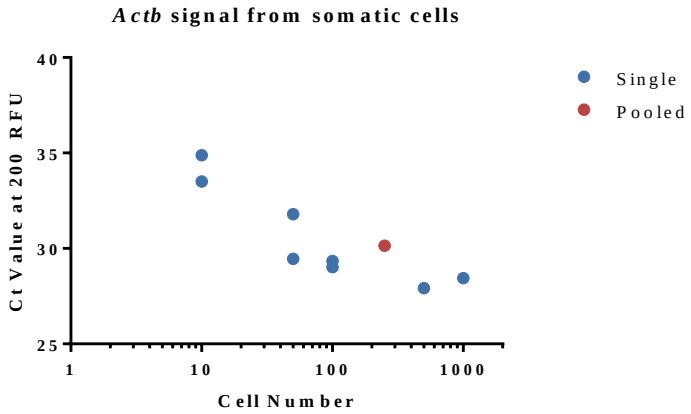

Figure 4.6 *Actb* signal in somatic mouse cells. The C_t values at 200 RFU for RNA extracted from somatic cells collected using FACS. The signal gets stronger with increasing number of cells up to 500 and 1000, which have similar signal. The duplicate RNA extracted from 10 and 50 cells show some variance. RNA from approximately 250 pooled cells shows similar signal to that of 50 and 100 individual cells.

Using the same cDNA synthesis and qPCR technique (with a threshold of 200 RFU), successfully analysed pre-implantation blastocyst samples had a C_t of 28.11. The biological duplicates for 100 cells had an average C_t value of 29.18, a much stronger signal than any previously analysed post-implantation samples extracted from Trizol® Reagent using the PureLink® RNA Mini Kit. However, when pooling aliquots of 50 cells, 250 cells had lower signal than 100 cells (30.15), suggesting a greater number of cells may be required if 100 cells cannot be collected from one FACS session. Since the previously collected samples were 150 pooled PGCs, this suggests either PGCs contain considerably less RNA than a mixed population of somatic cells, or the previously used RNA extraction technique was not optimal for use with limited input tissue.

Unfortunately, the fecundity of the mice became reduced and severely limited the availability of GFP-*Stella* expressing PGCs, making further analysis of post-implantation samples at this stage impossible. However, the success of extraction using the Arcturus® PicoPure® RNA Isolation Kit indicates that combining this technique with

the WT-Ovation® RNA Amplification and One-Direct Systems (NuGEN) for cDNA synthesis would generate sufficient material for analysis using the TLDA cards in future studies.

4.4 Results and Discussion

4.4.1 Pre-implantation TLDA results

RNA was supplied by Dr L.M. Cree from pooled pre-implantation embryos at the 2-cell, 4-cell, 6-8-cell, 16-32-cell and blastocyst stages of development.

Replication genes

The expression of the replication genes *Peo1*, *Polg*, *Polg2* and *Rnaseh1* were measured during pre-implantation . *Peo1*, the mitochondrial helicase, is most highly expressed at the 2-cell stage, with very low expression throughout the rest of pre-implantation development (Figure 4.7A). *Polg* is detected at low levels at both the 2-cell and blastocyst stage, and at higher levels in 16-32-cell stage, but only in one replicate (Figure 4.7B). *Polg2* was only detected in one blastocyst replicate (Figure 4.7C). *Rnaseh1* is detected in only one sample at the 2-cell stage, but detected at higher and more consistent levels throughout the remainder of pre-implantation development (Figure 4.7D). No differences were statistically significant (unpaired t test).

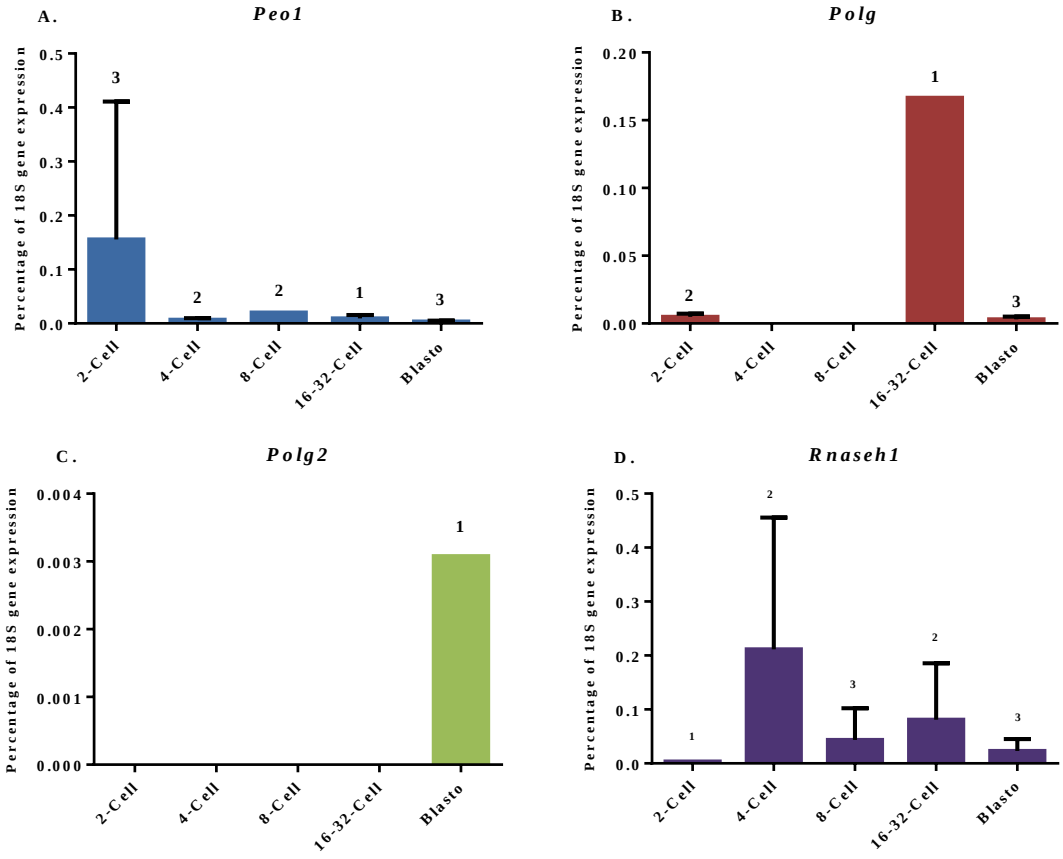

Figure 4.7 The expression of mitochondrial replication genes relative to *18S*. The bar charts represent the gene expression of mitochondrial replication genes (A) *Peo1*, (B) *Polg*, (C) *Polg2* and (D) *Rnaseh1* as a percentage of *18S* gene expression. The error bars are representative of the standard deviation between biological replicates. As the signal was not present in all samples for all genes, the number above each bar represents the number of biological replicates contributing to the mean (maximum 3).

The higher levels of expression of *Peo1* and *Polg* at the 2-cell stage of development could indicate increased rate of replication. This would correlate with the increased rate of mtDNA turnover discovered at this stage by McConnell and Petrie (2004). The low frequency of detection for *Polg2* is likely to be due to the low level of expression of this gene (0.003% of *18S* expression). Thundathil and colleagues (2005) reported an increase in the expression of replication genes as pre-implantation development progresses, it is plausible that the increased loading concentration of RNA at the 16-32 cell and blastocyst stages, suggested by previous analysis of reference gene expression, could account for *Polg* and *Polg2* only being detectable at these later stages. The higher, and more consistent levels of *Rnaseh1* are explained by the majority of the protein being

localised to the nucleus, and only approximately 10% associated with mitochondrial function (Figure 4.7D) (Suzuki *et al.*, 2010).

Mitochondrial transcription genes

The expression of the mitochondrial transcription genes *Tfam*, *Tfb2m*, *Polrmt*, *Nrf1*, *Lrpprc* and *Sp1* were measured during pre-implantation development.

Tfam and *Tfb2m* both show increased expression from the 8-cell stage onwards, though are not always detected in all replicates (Figure 4.7A-B). *Polrmt* has increased expression in all three replicates at the 8-cell stage, but dropped dramatically in the 16-32-cell and blastocyst stages (Figure 4.8C). *Nrf1* is expressed higher in the 2- and 4-cell stages, compared to the later stages of development (Figure 4.8D). *Lrpprc* also shows higher expression from the 8-cell stage onwards (Figure 4.8E). Although increased at the 8-cell stage, similarly to *Polrmt*, the levels reduce again at the 16-32-cell stage and blastocyst stage (Figure 4.8F). None of the gene expression changes were statistically significant (unpaired t-test).

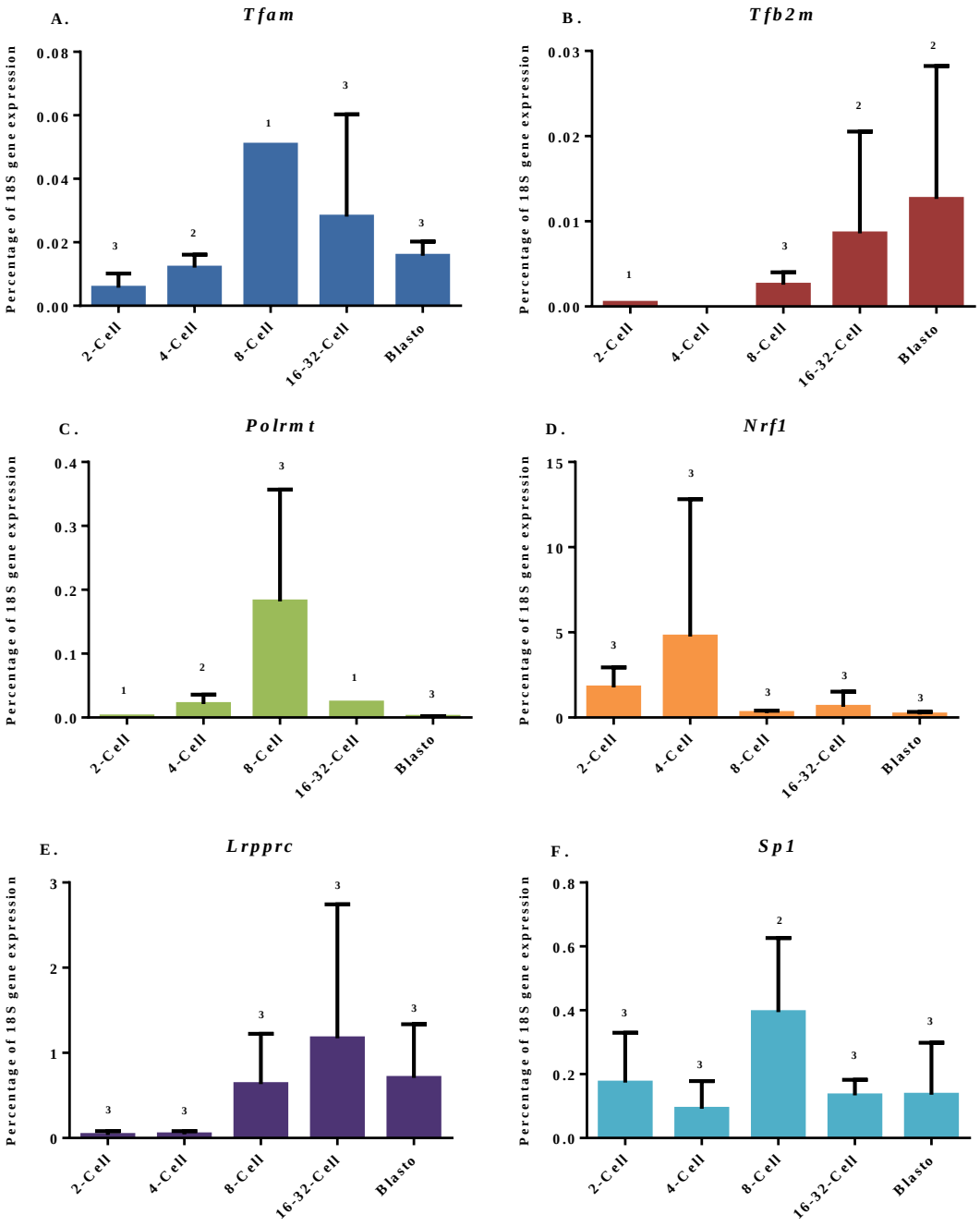

Figure 4.8 The expression of mitochondrial transcription genes relative to *18S*. The bar charts represent the gene expression of mitochondrial transcription genes (A) *Tfam*, (B) *Tfb2m*, (C) *Polrmt*, (D) *Nrf1*, (E) *Lrpprc* and (F) *Sp1* as a percentage of *18S* gene expression. The error bars are representative of the standard deviation between biological replicates. As the signal was not present in all samples for all genes, the number above each bar represents the number of biological replicates contributing to the mean (maximum 3).

Thundathil and colleagues (2005) measured steadily increasing expression of mitochondrial genes from the 8-cell stage onwards during pre-implantation

development. *Tfam* and *Tfb2m* both show increased expression from this stage onwards, indicating they are good markers for mitochondrial transcription. LRPPRC has been shown to not directly interact with POLRMT as a transcription factor. It modifies mitochondrial gene expression post-transcriptionally through increasing mRNA stability, modulating transcript polyadenylation and coordination of mitochondrial translation (Harmel *et al.*, 2013). *Lrpprc* also shows higher expression from the 8-cell stage onwards, suggesting expression of this gene is tightly linked to mitochondrial transcription rate.

Mitochondrial dynamics genes

The expression of the mitochondrial dynamics genes *Dnm1l*, *Fis1*, *Mfn1* and *Mfn2* were measured in pre-implantation samples.

The expression levels of *Dnm1l*, *Fis1*, and *Mfn1* do not change significantly over the course of pre-implantation development (Figure 4.9A-C). *Mfn2* is expressed at the highest levels from the 6-8 cell stage onwards (Figure 4.9D), and is significantly different between the 8- cell stage (0.08 %; SD±0.003 %) and the blastocyst stage (0.02 %; SD±0.002 %; $p < 0.01$ unpaired t test), though only detected in two of the replicates.

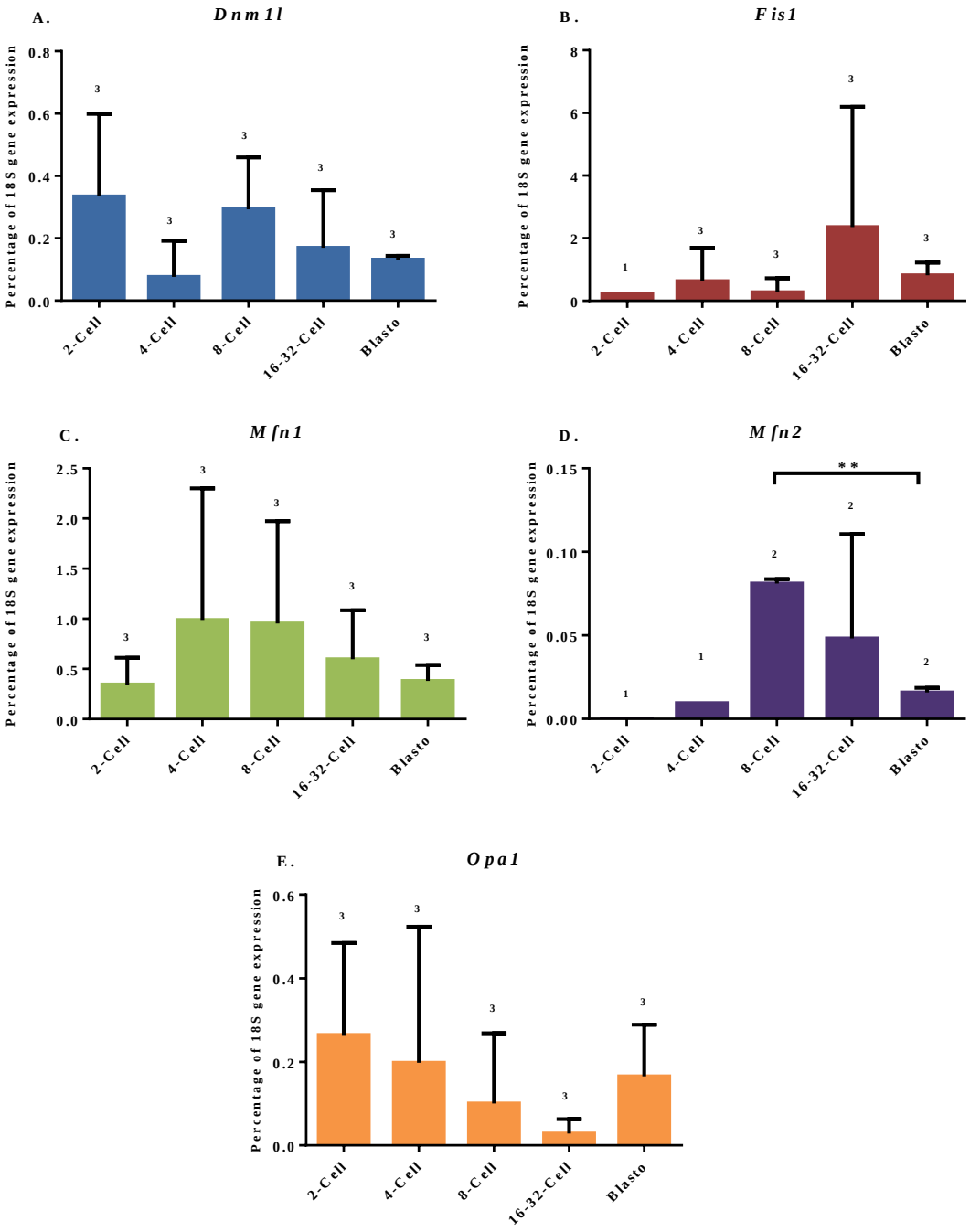

Figure 4.9 The expression of mitochondrial dynamics genes relative to *18S*. The bar charts represent the gene expression of mitochondrial dynamics genes (A) *Dnm1l* (B) *Fis1* (C) *Mfn1* (D) *Mfn2* and (E) *Opa1* as a percentage of *18S* gene expression. The error bars are representative of the standard deviation between biological replicates. As the signal was not present in all samples for all genes, the number above each bar represents the number of biological replicates contributing to the mean (maximum 3). ** $p < 0.01$ unpaired t test.

Continuous mitochondrial fission and fusion allows the exchange of replication factors between mitochondrial compartments. Impairing mitochondrial dynamics through knockdown of fission proteins, DNM1L and FIS1, or knockout of fusion proteins MFN1, MFN2 and OPA1 has been shown to cause mtDNA depletion in cultured cells and skeletal muscle respectively (Chen *et al.*, 2010, Malena *et al.*, 2009). *Mfn2* is expressed at the highest levels from the 6-8 cell stage onwards, similar to *Tfam* and *Tfb2m*, suggesting it could contribute to an increase in mitochondrial transcription rate.

Mitochondrial biogenesis genes

The expression of the mitochondrial biogenesis genes, *Ppargc1b*, *Ppargc1a*, *Ppargc1b* and *Pprc1* was measured throughout pre-implantation development.

Ppargc1a (encoding PGC1α) was not detectable at any stage during pre-implantation. *Pparg* is expressed in just one replicate at the 2-cell and 16-32-cell stages, but reliably detected at low levels in blastocysts (Figure 4.10A). *Ppargc1b* (encoding PGC1β) is expressed at high levels in all three replicates at the blastocyst stage and in one replicate at 16-32-cell stage (Figure 4.10B). *Pprc1* is expressed consistently throughout pre-implantation development (Figure 4.10C). No expression changes were statistically significant (unpaired t test).

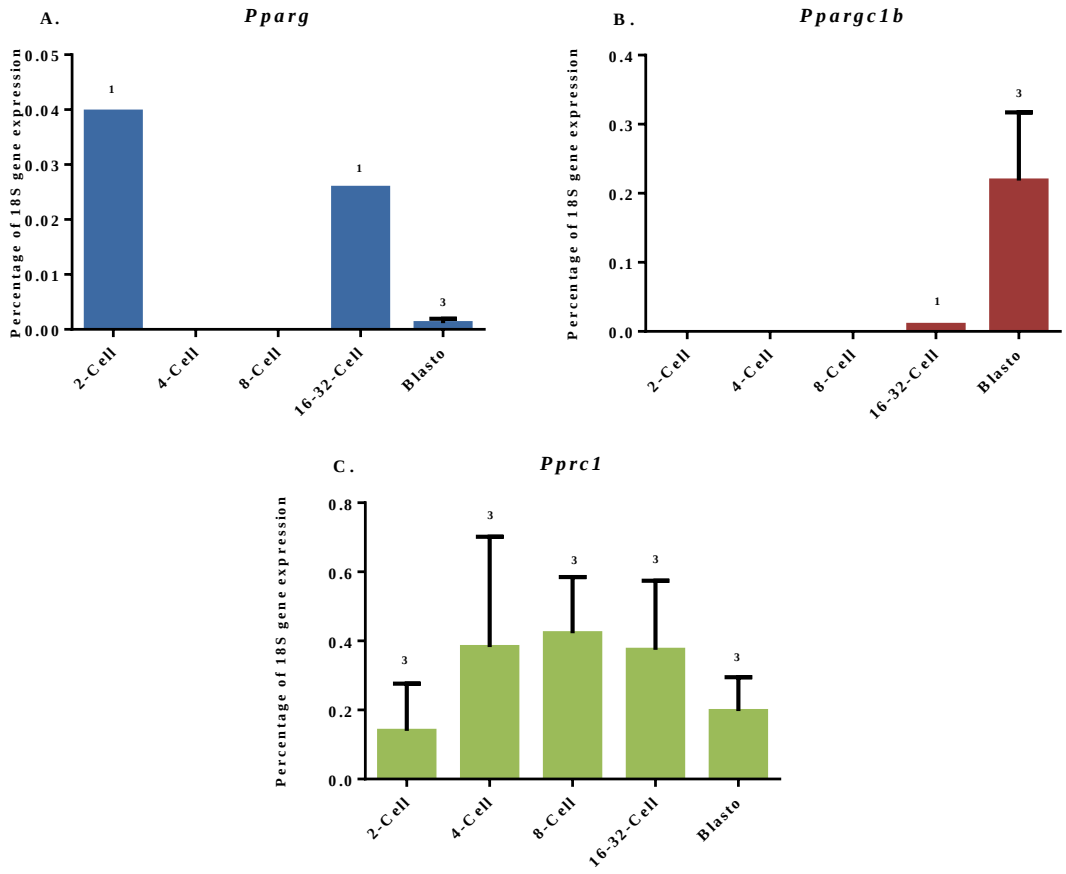

Figure 4.10 The expression of mitochondrial biogenesis genes relative to *18S*. The bar charts represent the gene expression of mitochondrial biogenesis genes (A) *Pparg*, (B) *Ppargc1b* and (C) *Pprc1* as a percentage of *18S* gene expression. The error bars are representative of the standard deviation between biological replicates. The number above each bar represents the number of biological replicates contributing to the value (maximum 3).

Many of the molecular pathways which influence mitochondrial biogenesis do so through induction or activation of PGC1α (see Section 1.4.6). However, *Ppargc1a* (encoding PGC1α) was not detectable at any stage during pre-implantation. The expression of *Pparg* and *Ppargc1b* was most reliable in blastocysts, suggesting an increase in mitochondrial biogenesis at the later stage of pre-implantation development. PGC1β has similar transcriptional responses to PGC1α, and may be the main regulator of mitochondrial biogenesis in blastocysts. *Pprc1* has recently shown to be critical to early mouse development, with homozygous knockout mice failing to implant correctly in the uterine wall (He *et al.*, 2012), but is not regulated during these stages.

Mitochondrial stress and apoptosis genes

The expression of genes involved in mitochondrial stress response (*Sod2* and *Hif1a*) and in apoptosis (*Bax*) were measured during pre-implantation.

There was a slight increase in *Sod2* expression as development progresses (Figure 4.11A). Hif1a expression is increased at both the 2-cell stage and at the blastocyst stage (Figure 4.11B). *Bax* expression was significantly lower at the 2-cell stage compared to the blastocyst stage ($p < 0.05$ unpaired t test) (Figure 4.11C).

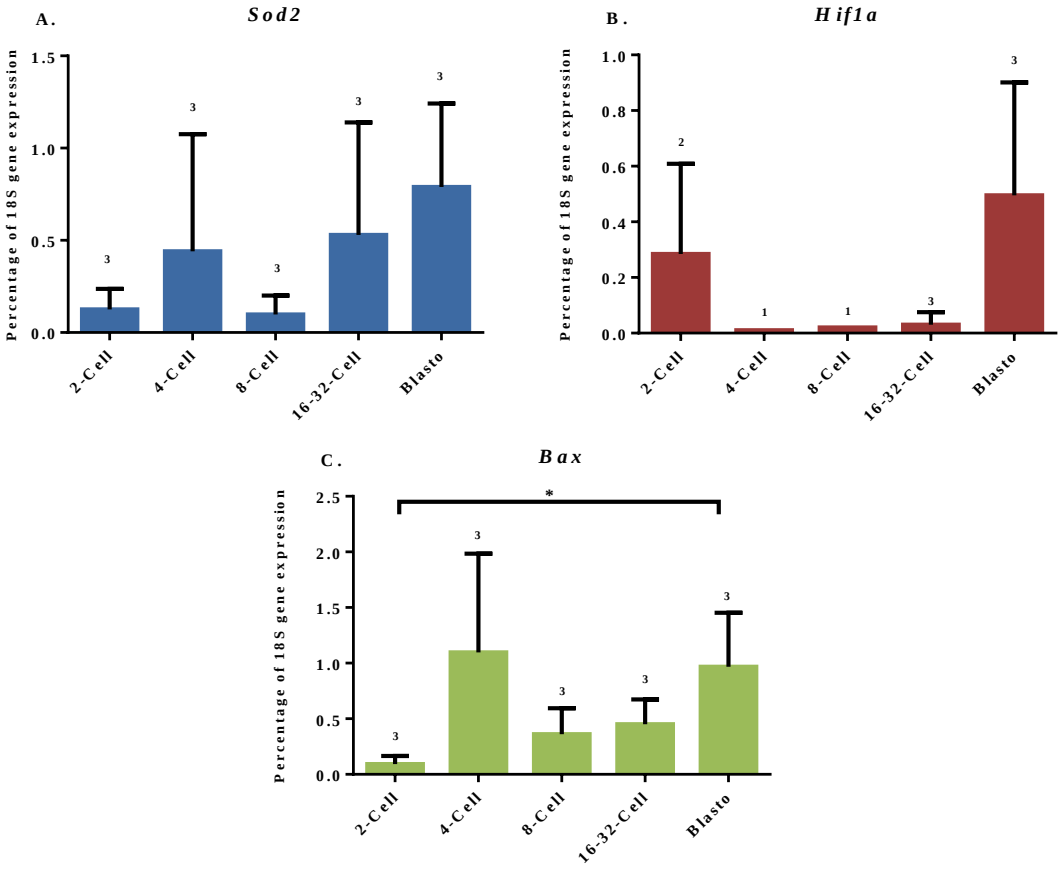

Figure 4.11 The expression of mitochondrial stress and apoptosis genes relative to *18S*. The bar charts represent the gene expression of mitochondrial stress and apoptosis genes (A) *Sod2*, (B) *Hif1a* and (C) *Bax* as a percentage of gene expression. The error bars are representative of the standard deviation between biological replicates. The number above each bar represents the number of biological replicates contributing to the value (maximum 3). * $p < 0.05$ unpaired t test.

In some tissues, it was reported that manganese superoxide dismustase (MnSod; encoded by *Sod2*) correlates with mtDNA copy number, to maintain low levels of oxidative stress markers (Aiken *et al.*, 2008). Although mtDNA copy number remains stable in the total embryo during pre-implantation development, the slight increase in

Sod2 expression as development progresses, which potentially correlates with the increase in transcription and biogenesis. Increased mitochondrial ROS production can lead to activation of hypoxia-inducible factor 1-α (encoded by *Hif1a*) inducing downstream transcriptional responses to compensate for physiological stress such as hypoxia (Guzy and Schumacker, 2006). *Hif1a* expression was increased at the stages when replication rate and mitochondrial biogenesis were highest.

Apoptosis has been found to be repressed in 2-cell embryos, through increased anti-apoptotic proteins (Bcl) and reduced pro-apoptotic proteins (Bax), which prevent mitochondrial depolarisation (Hansen and Fear, 2011). Although transcript levels of *Bax* were not found to be affected by stage in bovine embryos, there was a detectable reduction observed in murine 2-cell embryos. There has been little speculation on why apoptosis is repressed at the 2-cell stage, but it is possibly linked to the increased mtDNA replication observed at the 2-cell stage.

Overview of pre-implantation results

Biological variability can be introduced through the uncertain timing of fertilisation and the staging of embryos, which have to be determined by eye. By pooling 15 embryos in batches, it is possible the average time since fertilisation in each biological replicate is different. The main technical limitation of the study was low amounts of starting material, with lower expressed genes unable to be detected or at the limit of detection (LOD) where expression isn't reliable. In some cases one of the technical replicates was also undetectable, most likely due to the nature of loading the TLDA cards by centrifugation into nano-sized reaction chambers.

4.4.2 Analysis of published microarray data

The mtDNA bottleneck has been shown to have occurred by 13.5 d.p.c. (Freyer *et al.*, 2012). Our analysis attempted to study mitochondrial gene expression from PGCs as early as possible, using GFP-Stella mice (7.5 d.p.c.) to identify the stage at which mtDNA replication and biogenesis is at the highest levels. We hypothesised this would indicate the point where the PGCs began recovering from their lowest mtDNA copy number (the critical stage of the mtDNA bottleneck).

To identify new genes, specifically expressed in female and male germ cells, Sabour and colleagues (2011) isolated PGCs at 8.5 to 18.5 d.p.c. from OG2/CD1 (△PE-GFP)

mice. Their data is publically available online, allowing for analysis of our genes of interest during post-implantation. Unfortunately, they were only able to perform microarray analysis from 11.5 d.p.c. onwards, after the predicted stages, 8.5-9.5 d.p.c., when mtDNA copy number in PGCs has been discovered to increase (Cree *et al.*, 2008, Wai *et al.*, 2008).

The expression patterns of the mtDNA replication genes *Peo1*, *Polg*, *Polg2* and *Rnaseh1* are variable during post-implantation (Appendix D.1). Expression levels of *Polg* and *Polg2* would suggest a slightly higher replication rate up to and including 13.5 d.p.c., before decreasing for a few days, fitting with the prediction that mtDNA replication rate has already increased. The expression of mitochondrial transcription genes, in particular *Tfb2m*, *Polrmt* and *Nrf1* (Appendix D.2), would suggest the transcription rate increases from approximately 14.5 d.p.c., after when we know the mtDNA bottleneck has already been formed. The genes regulating mitochondrial dynamics steadily increase throughout post-implantation development, peaking between 14.5 and 16.5 d.p.c., before decreasing again (Appendix D.3). However, *Pparg* expression increases from 11.5 d.p.c., peaking at 14.5 d.p.c. before decreasing again, in a similar pattern to both *Polg* and *Polg2*, suggesting it could be linked to the increased mitochondrial biogenesis required to repopulate the dividing population of PGCs (Appendix D.4A). *Ppargc1a* and *Ppargc1b* are detected at low levels throughout post-implantation development, without a clear pattern of expression (Appendix D.4B-C).

4.5 Concluding remarks

Despite the limitations of the study there is evidence that during pre-implantation development, the mtDNA replication and transcription rate correlates to that suggested in previous research (McConnell and Petrie, 2004, Piko and Taylor, 1987, Thundathil *et al.*, 2005). *Lrpprc* has only recently been implicated in post-transcriptional regulation of mitochondrial expression, and this study has shown it also increases during cleavage of the pre-implantation embryo. Although *Mfn2* also shows a similar expression pattern to the components of the transcription machinery, none of the other genes regulating fission or fusion follow a particular expression pattern. This means there is no clear evidence that mitochondrial dynamics regulates mitochondrial copy number during pre-implantation development.

Chapter 5. Identification of Factors Affecting mtDNA Copy Number Regulation

Table of Contents

5.1 Introduction

The availability of sufficient material for large gene expression analysis has limited our study of regulation of mtDNA content. Cellular models offer an alternative to primary tissue for studying basic cell biology and biochemistry. Cell culture conditions are simple to manipulate, allowing investigation of different physiological conditions or drug treatments.

5.1.1 Regulation of mtDNA content

The majority of research investigating regulation of mtDNA content relies on hypothesis-driven selection of a gene of interest. Expression of various POLG-fusion proteins confirmed the mitochondrial localisation of POLG protein, established the necessity of the 3'-5'-exonuclease in preventing accumulation of mutations and showed that although *POLG* mutations cause mtDNA depletion, increased activity of *POLG* does not elevate mtDNA content (Spelbrink *et al.*, 2000). Overexpression and knockout of *TFAM* in mice demonstrated that TFAM protein levels correlate directly with mtDNA content, but that increased mtDNA content does not necessarily increase mitochondrial gene expression or biogenesis (Ekstrand *et al.*, 2004). Overexpression of the mitochondrial helicase *Twinkle* (encoded by *C10orf2*) in transgenic mice caused 3-fold upregulation of mtDNA content in some tissues, and siRNA knockdown of *Twinkle* in cultured 143B human osteosarcoma cells immediately reduced mtDNA copy number (Tyynismaa *et al.*, 2004).

However, changes in mtDNA content upon overexpression, knockout or knockdown of a gene does not necessarily mean that the expression of that gene is altered in physiological relevant situations where mtDNA copy number is regulated. We want to identify which genes are regulated in order to control mtDNA content, and to potentially screen for new factors influencing mtDNA copy number. To do this, we need to generate a model whereby mtDNA replication rate is increased, independent of manipulating gene expression. Altering the expression of these genes during embryogenesis may influence how the mtDNA bottleneck skews inheritance of mtDNA mutations.

5.1.2 The mtDNA repopulation assay

The mtDNA repopulation assay uses ethidium bromide (EtBr), a dsDNA-intercalating drug, to reversibly inhibit mitochondrial transcription and replication, depleting cultured cells of mtDNA (King and Attardi, 1989). Upon drug removal, mtDNA replication can resume, allowing cells to recover their mtDNA levels.

The mtDNA repopulation assay has been used to show how primary sequence and molecule size can affect the mtDNA replication rate (Diaz *et al.*, 2002, Moraes *et al.*, 1999). It can also be used as a tool for investigating whether pathogenic, nuclear mutations in mtDNA maintenance genes affect the rate of mtDNA replication (Stewart *et al.*, 2011).

Upon depletion of mtDNA, protein levels of the mitochondrial transcription machinery, TFAM and POLRMT, also become dramatically reduced (Seidel-Rogol and Shadel, 2002). Importantly, they found that after removal of EtBr, mitochondrial transcription occurs prior to recovery of mtDNA and transcription machinery levels. Resumption of high transcription rates is clearly critical to increasing mtDNA replication rates, as the fastest replication rate occurs when accumulation of TFAM and POLRMT is most dramatic. Depletion and repopulation in four cell lines (143B, D16.10.40, and HP4) was found not to significantly alter the expression of *POLG*, *TFAM*, *POLRMT* and *SSBP* transcripts, when analysed by northern blot (Moraes *et al.*, 1999). However, only the final time point after 15 days of depletion and then after 15 days of repopulation were studied, and therefore initial responses to changes in EtBr concentration may have been overlooked.

Myoblasts are primitive muscle cells, which fuse together to generate multi-nucleated myotubes, which will eventually develop into striated muscle fibres. Myoblasts are derived from muscle biopsies, making this cell-type one of the most physiologically relevant to mitochondrial disorders. In previous research from our group, it was found that myoblasts failed to thrive after 10 days of treatment with 50 ng/ mL EtBr (Stewart, 2008). Therefore, depletion of mtDNA in myoblasts will need to be optimised before the full assay can be completed.

Treatment of human immunodeficiency virus (HIV)-infected patients with nucleoside reverse transcriptase inhibitors (NRTIs) induces many phenotypes similar to those observed in mitochondrial disease. As nucleoside analogues, they not only block viral

reverse transcriptase, but also endogenous DNA polymerases, such as mitochondrial polymerase γ (Martin *et al.*, 1994). Myoblasts have proved sensitive to mtDNA depletion by some NRTIs, particularly Didanosine (2',3'-dideoxyinosine; ddI) and Zalcitabine (2'-3'-dideoxycytidine, ddC) (Birkus *et al.*, 2002) and provide an alternative to EtBr. However, even at low concentrations, NRTIs can negatively affect cellular proliferation over long treatment courses (Benbrik *et al.*, 1997). An optimal concentration which both effectively depletes mtDNA without preventing cellular proliferation must be found.

5.1.3 Research aims

We will use the mtDNA repopulation assay to model the reduction and subsequent increase in mtDNA copy number observed during embryogenesis, forming the mtDNA bottleneck (Cree *et al.*, 2008, Wai *et al.*, 2008). We will assess gene expression throughout the depletion/repopulation phase, identifying which genes are regulated to induce an increase in mtDNA copy number. With regular sampling, we will be able to identify a more accurate timing of the gene expression changes which occur.

If the repopulation assay proves a suitable model for studying mtDNA replication, we will then perform a non-hypothesis-driven analysis of gene expression to identify new regulatory factors, and explore how manipulation of these genes can affect the segregation of mutant mtDNA molecules.

5.2 Materials and Methods

5.2.1 Myoblast and fibroblast primary cell lines

The information for myoblast and fibroblast primary cell lines are found in Table 5.1.

Table 5.1 Cell line information. The identifier, gender and age of patients used to generate myoblasts and fibroblasts.

I.D	Cell type	Identifier	Gender	Age
Control 1	Myoblast	C018	Male	22
Control 2	Myoblast	C049	Male	21
Control 3	Myoblast	C010	Male	42
MERRF	Myoblast	M028	Male	12
Control	Fibroblast	F010	-	Embryonic

5.2.2 Depletion of mtDNA in myoblasts and fibroblasts

The drugs chosen to deplete mtDNA were EtBr (Sigma-Aldrich) and ddC (Sigma-Aldrich). Several concentrations were chosen to identify the conditions able to produce maximum depletion with minimal toxicity. EtBr concentrations used were 10 ng/ mL and 25 ng/ mL, and ddC concentrations were 0.2 µg/ mL, 0.6 µg/ mL and 1 µg/ mL.

5.2.3 Galactose (glucose-free) media treatment

Galactose medium for fibroblast culture was created by the addition of 5 mM D-(+)-galactose (Sigma-Aldrich), 10% dialysed FBS (Gibco), 500 units/ mL Penicillin/Streptomycin (Gibco) and 50 µg/ mL uridine (Sigma-Aldrich) to glucose-free DMEM (Gibco).

5.2.4 qPCR for quantification of mtDNA copy number per cell

Relative mtDNA copy number per cell was calculated using the ΔCt technique, using a mitochondrial gene fragment (*MT-ND1*) and a nuclear gene fragment (*B2M*).

Generation of templates for the mtDNA copy number assay

DNA templates for real-time qPCR standards were created using standard 25 µL Immolase reaction (Section 2.2.2).

Table 5.2 Primers to create templates for copy number real-time standards. Primer sequences to generate large DNA fragments which are purified by gel extraction, quantified and which serve as templates for standard curves analysed by qPCR.

Gene	Genome	Primer Sequence	Fragment Size (bp)
ND1	Mitochondrial	F-TGTAAAACGACGGCCAGTCAGCCGCTATTAAAGGTTCG R-CAGGAAACAGCTATGACCAGAGTGCGTCATATGTTGTTC	1040
B2M	Nuclear	F-CGCAATCTCCAGTGACAGAA R-GCAGAATAGGCTGCTGTTCC	1092

PCR products were electrophoresed (Section 2.2.3) and the product bands were excised. The DNA was extracted using the standard QIAquick Gel Extraction Kit (QIAGEN) protocol.

The concentration of the extracted DNA is determined using a NanoDrop 2000 UV-Vis Spectrophotometer. The copy number/ µL can be determined by calculating the molecular weight of each DNA fragment and using the concentration to estimate the DNA content of the purified samples.

$$Mw = fragment\ size\ (bp) \times 2\ (dsDNA) \times 330\ (Av.Mw\ of\ 1\ base)$$

$$Moles/_{\mu L} = \frac{Conc.\ (g/\mu L)}{Mw}$$

$$Copy\ number/_{\mu L} = Moles/\mu L \times 6.03 \times 10^{23}\ (Molecules/Mole)$$

qPCR reaction

A standard 25 µL qPCR reaction mix (Section 2.12.1) was used with the following primers in Table 5.3.

Table 5.3 Primers to amplify DNA from *MT-ND1* and *B2M* templates. Primer sequences to generate mitochondrial and nuclear fragments for use in qPCR to quantify mtDNA copy number.

Gene	Fragment	Primer Sequence	Fragment Size (bp)
ND1	Mitochondrial	F-ACGCCATAAAACTCTTCACCAAAG R-GGGTTCATAGTAGAAGAGCGATGG	111
B2M	Nuclear	F-CACTGAAAAAGATGAGTATGCC R-AACATTCCCTGACAATCCC	231

5.2.5 Real-time PCR for assessing gene expression

RNA was extracted using the RNeasy® Mini Kit (QIAGEN) (Section 2.9.2). cDNA was generated using the standard Superscript III reaction (Section 2.11). A standard 25 µL qPCR reaction mix (Section 2.12.1) was used with the following primers in Table 5.4.

Table 5.4 qPCR primers for assessing gene expression. Primer sequences for use with cDNA templates for gene expression analysis by qPCR, listing the related function and fragment sizes.

Gene	Related Function	Primer Sequence	Fragment Size (bp)
ACTB	Reference gene	F-GATGCAGAAGGAGATCACTGC R-ACATCTGCTGGAAGGTGGAC	131
GAPDH	Reference gene	F-CTGACTTCAACAGCGACACC R-ATGAGGTCCACCACCCTGT	133
B2M	Reference gene	F-CACCCCCACTGAAAAAGATG R-TTCAAACCTCCATGATGCTG	112
TFAM	Transcription	F-GCTCCCCCTTCAGTTTTGTGT R-TTTTGCATCTGGGTTCTGAGCT	140
POLG	Replication	F-AGAGTTTATGACCAGCCGTGTGA R-CAAACTCTTCAAACAGCCACTTCA	101
POLG2	Replication	F-CAATGTGTCTAAATTACATGGCCGAG R-CGGTCTAGGTCCCCATTTACAGA	81
NRF1	Transcription	F-TTGCTTCGGAAACTTCGAGCC R-GTACTTACGCACCACATTCTCC	146
OPA1	Fusion	F-GTTCAACTGGCGGAAGACC R-TGCAGAGCTGATTATGAGTACGA	117
PEO1	Replication	F-ATATGATCACTGGGCTGACC R-AACTGCAGGTTGTCGATGAT	150
FIS1	Fission	F-AGGAGGAACAGCGGGATTAC R-AGTTCCTTGGCCTGGTTGTT	130
POLRMT	Transcription	F-ACTTCATCCACTCGCTGGAC R-ACCTGGTTCATGACGGAGAC	133
PPARG	Biogenesis	F-TTGAATGTCGTGTCTGTGGAG R-GGATCCGACAGTTAAGATCACA	138
SOD2	ROS	F-GGGTTGGCTTGGTTTCAATA R-GTAGTAAGCGTGCTCCCACA	130
COII (mt)	Mitochondrial respiratory subunit	F-CCATCCCTACGCATCCTTTA R-GCCGTAGTCGGTGTACTCGT	108
COX4I1	Nuclear respiratory subunit	F-CTAGTTGGCAAGCGAGCAAT R-ACGCCGATCCATATAAGCTG	102
PGC1a	Biogenesis	F-TCTGGAACTGCAGGCCTAACT R-CCTTTCTTGGTGGAGTTATTGC	179

Gene Expression analysis

Fold change was generated using the equation developed for the Relative Expression Software Tool (REST©), which accounts for the individual efficiency of each primer pair (Pfaffl *et al.*, 2002).

$$Fold\ change = \frac{1 + E(Tar)^{\Delta Ct\ (Tar)}}{1 + E(Ref)^{\Delta Ct\ (Ref)}}$$

E = Efficiency as a ratio of 1 Ref = Reference Gene Tar = Target Gene

BestKeeper analysis

To assess the stability of selected reference genes, samples were chosen from a range of treatments and time points. The concentration of each sample was measured using the NanoDrop 2000 UV-Vis Spectrophotometer. The same amount of RNA (400 ng) was converted into cDNA using Superscript III® (Section 2.11). Each sample was analysed by qPCR for *ACTB*, *GAPDH*, and *B2M*. The stability of C_t values across samples was assessed using the BestKeeper software (Pfaffl *et al.*, 2004).

5.2.6 Immunohistochemistry of myotubes

Myoblasts were differentiated into myotubes following the protocol in Section 2.7.6. Differentiation was assessed using antibodies for Slow Myosin Heavy Chain (ab11083; Abcam, Cambridge, UK).

5.2.7 SDS-PAGE and western blotting

SDS-PAGE and western blotting were completed using the standard protocol in Section 2.14. All mitochondrial subunits were analysed with β-Actin on a 14% acrylamide gel. POLG protein was analysed with β-Actin on an 8% acrylamide gel. Antibodies for western blotting are listed in Table 5.5.

Table 5.5 Antibodies used for western blotting. The table below lists the antibodies used for determining mitochondrial protein expression, indicating the species in which the antibody was raised (Ms, mouse; Rb, rabbit; Sw, Swine) and the clonality (mAb, monoclonal; pAb polyclonal), the size of the target protein, the concentration (Conc.) of the antibody used when probing the blot and the distributor information.

Type	Antigen	Species	Size (kDa)	Conc. used (µg/mL)	Distrib.	Code
1°	Anti-β-Actin (Loading Control)	Ms mAb	42	0.1	Sigma	A1978
1°	VDAC1 / Porin (Mito Mass)	Ms mAb	39	0.1	Abcam	ab14734
1°	SDHA (CII Nuclear)	Ms mAb	70	0.2	Abcam	ab14715
1°	COX4 (CIV Nuclear)	Ms mAb	20	1	Abcam	ab110261
1°	Cytochrome C oxidase subunit II (CIV Mitochondrial)	Ms mAb	26	1	Abcam	ab110258
1°	DNA Polymerase gamma	Rb pAb	130	2	Abcam	ab97661
2°	Anti-Mouse (Ms)	Rb pAb	-	0.5	DAKO	P0260
2°	Anti-Rabbit (Rb)	Sw pAb	-	1.5	DAKO	P0399

5.3 Assay Development

Before the expression of mitochondrially-related genes can be studied, the optimum cell culture conditions must be established. This includes the drug and concentration to use, treatment and recovery times and viability of the cells.

5.3.1 Determination of drug concentrations

Using data from previous publications (Birkus *et al.*, 2002, Saitoh *et al.*, 2008, Stewart *et al.*, 2011), a range of concentrations to test was established. For EtBr, these were 10 ng/mL and 25 ng/mL. For ddC, these were 0.2 µg/mL, 0.6 µg/mL and 1 µg/mL. Two control myoblast cell lines were either cultured in standard media or treated for 11 days and then allowed to recover in standard media for a further nine days. Cells were harvested at each passage, and the mtDNA copy number calculated using relative qPCR technique, comparing the signal of an mtDNA amplicon to a nuclear amplicon (Figure 5.1).

Myoblasts treated with either 10 or 25 ng/mL had 5-15% mtDNA copy number after 11 days of treatment. In both control cell lines, treatment with the lower concentration of EtBr allowed an earlier onset of recovery (Control 1-Day 18, 10 ng/mL EtBr 13.8 % (SD±3.2 %) , 25 ng/mL EtBr 7.2 % (SD±0.1 %); Control 2-Day 21, 10 ng/mL EtBr 13.1 % (SD±2.4 %), 25 ng/mL EtBr 7.2 % (SD±1.3 %). Culturing myoblasts with 1 µg/mL ddC depletes mtDNA levels as rapidly as either EtBr concentration (Control 1-Day 12, 11.7 % (SD±1.1 %); Control 2-Day 12, 6.5 % (SD±0.1 %). Cells began

recovering their mtDNA levels at the same rate, or more rapidly after depletion with 1 µg/mL ddC than those depleted with 10 ng/mL EtBr (Control 1-Day 18, 16.0 % (SD±0.2 %); Control 2-Day 18, 16.8 % (SD±4.5 %). The lower concentrations of ddC failed to regularly deplete mtDNA levels to the same extent (Control 1-Day 12, 0.2 µg/mL ddC 61.6 % (SD±2.9 %), 0.6 µg/mL ddC 20.9 % (SD±0.02 %); Control 2, 0.2 µg/mL ddC 31.6 % (SD±0.63 %), 0.6 µg/mL ddC 14.2 % (SD±0.4 %)).

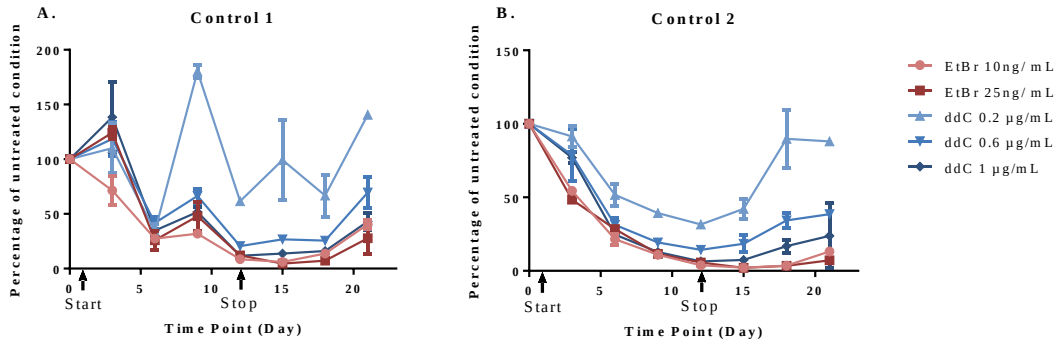

Figure 5.1 MtDNA depletion and repopulation curve using different drugs with a range of concentrations. The mtDNA depletion and repopulation rates in two control cell lines caused by treatment with EtBr or ddC at varying concentrations. Each mtDNA copy number is presented as a percentage of the untreated condition. Error bars represent standard deviation of biological duplicates.

As the depletion rate is the same for both concentrations of EtBr and 1 µg/mL ddC, there may be a plateau effect whereby increasing concentrations of the inhibiting drugs cannot deplete cells in culture any faster. Since the mechanism of the drugs is to block replication of new mtDNA molecules, rather than destroy existing mtDNA, this could represent the natural turnover rate of mtDNA, and implies that mtDNA replication has been completely blocked by these treatments. As the lower concentrations of ddC had slower depletion rates, this suggests mtDNA replication is only partially blocked. Since 1 µg/mL ddC depletes mtDNA at the maximal rate whilst allowing more rapid recovery from treatment, this is the optimal condition taken forward for further study.

Throughout the experiment the mtDNA copy number in the untreated condition was steadily increased. This means, by the end of the repopulation phase, the mtDNA copy number was higher than the starting copy number, but still only a fraction of the untreated condition. This is a concern, since through the depletion/repopulation there

needs to be a state in which replication rate is increased in treated cells compared to the untreated condition.

5.3.2 Stability of mtDNA copy number

The stability of the copy number in untreated cells is crucial to establishing a detectable gene expression difference in repopulating cells. The increased copy number could also be a stress response to inadequate tissue culture conditions, which would compromise the integrity of the results. To establish whether increasing copy number is a regular, repeatable occurrence, one control (Control 2) and one MERRF myoblast cell line were cultured for 18 days without drug treatments from two independent aliquots of frozen, stored cells (e.g. Control-A and Control-B; MERRF-A and MERRF-B). Cells were passage four at Day 0 and were passage 10 by Day 18. At the beginning of cell culture, both cell lines had similar mtDNA copy number (Control 387 (SD±64); MERRF 352 (SD±32.8). At the point of greatest increase, control myoblasts reached 334 % (SD±61 %) of their original mtDNA copy number and MERRF myoblasts reach 235 % (SD±19 %).

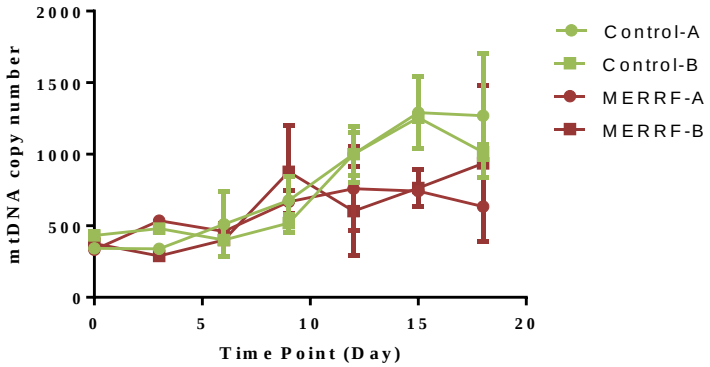

Figure 5.2 mtDNA copy number in untreated cultured myoblasts. mtDNA copy number measurements in one control and one MERRF myoblast line cultured without drug treatment for 18 days. Increased mtDNA copy number is observed in both control and MERRF myoblasts. Error bars represent standard deviation of biological duplicates.

Independent aliquots of the same cell line increased in mtDNA copy number to a similar extent. This suggests that whatever influences the rise in mtDNA copy number may affect cell lines differently or could relate to the condition of particular cells, rather than being an artefact of the tissue culture process.

5.3.3 Modulating FBS concentration and passage confluency

To investigate the possible causes for the increase in mtDNA copy number during myoblasts culture, modulation of growth conditions was applied to the control and MERRF cell lines. Firstly, the cells might have been reaching confluency and ceasing to divide, which could lead to an accumulation of mtDNA in cells. To avoid this, cells were passaged every two days instead of 3, but reseeding with the same number of cells to avoid becoming too sparse and impairing growth. Secondly, increasing concentration of FBS to 15% may provide a richer growth medium for the cells to grown in (Figure 5.3). The best combination of conditions was for both cell lines to be passaged every three days with 15 % FBS. The second best condition was cells to be passaged every two days with 15 % FBS with both passage frequencies in 10 % FBS having the greatest increase in mtDNA copy number.

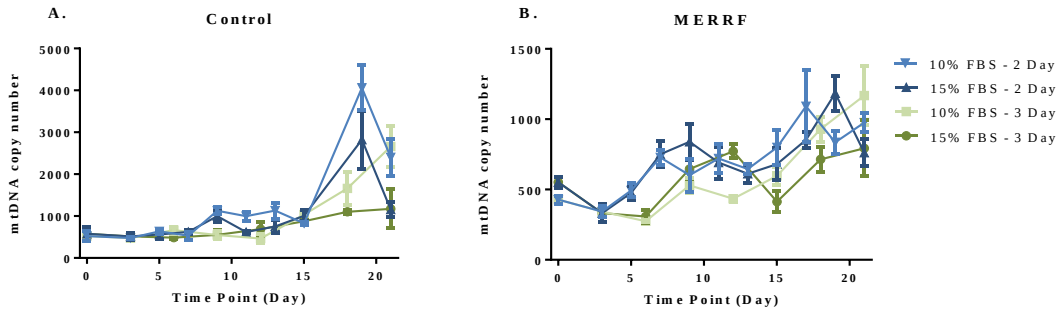

Figure 5.3 mtDNA copy number in untreated myoblasts using variable conditions. The mtDNA copy number trends in (A) a Control and (B) a MERRF myoblast cell line passaged either every two days (blue lines) or 3 days (green lines) and either cultured using 10% (light) or 15% (dark) FBS. The greater the number of passages, the more pronounced the increase in mtDNA copy number is; however, 15% FBS improves the stability of mtDNA copy number in myoblasts. Error bars represent standard deviation of biological duplicates.

Passaging cells every two days only led to a more pronounced increase in mtDNA copy number, suggesting that the increase could be a stress response related to passaging the cells. In both cell lines, 15% FBS gave the lowest rate of increase, with the best-case scenario being passaging every three days and 15% FBS supplementation. Even so, the effect of increased FBS concentration was minimal, and an increase in mtDNA copy number was still observed.

The trend in data observed by passage number (during the experiment) rather than by the day point was much more similar between cell lines passaged every two days or three days when accounting only for the first eight passages (Figure 5.4). The lowest slope observed was cells passaged every two days in 15 % FBS and the highest slope was cells passaged every three days in 10 % FBS.

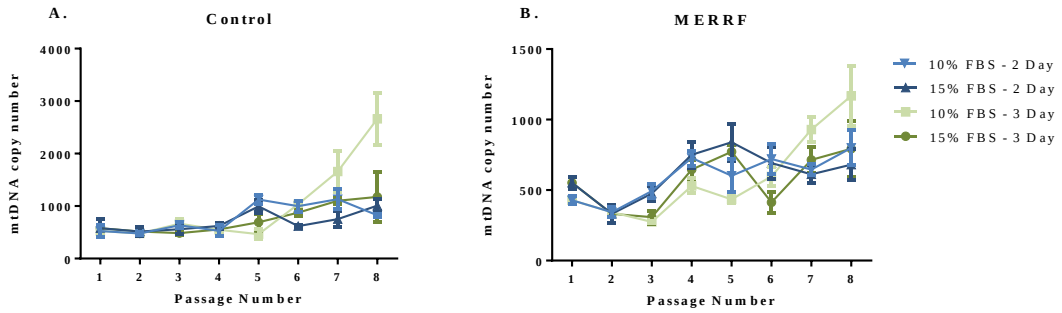

Figure 5.4 Copy number in myoblasts normalised for passage number. The copy number trends in (A) a Control and (B) a MERRF myoblast cell line passaged either every two days (blue lines) or three days (green lines) and either cultured using 10% (light) or 15% (dark) FBS. When ordered by passage number, the difference in mtDNA copy number between cell lines passaged every two or three days is reduced. Error bars represent standard deviation of biological duplicates.

The cell lines which have the lowest rate of mtDNA copy number increase have changed to cells passaged every two days with 15% FBS, reflecting not only the benefit of higher FBS concentration, but also that each passage has a greater effect than simply length of time in culture. It is probable that length of time in culture does have some effect, as the first eight passages of the cell lines passaged every two days only represents the first 15 days of culture, as opposed to the entire 21 days of culture for the cell lines passaged every three days. The worst-case scenario is now being passaged every three days in 10% FBS, suggesting that general time in culture does contribute to the increase in mtDNA copy number, but not as severely as passaging cell lines.

The passage of mitotic cells in culture for a long period of time is unavoidable. Although the culture of post-mitotic cells such as myotubes (differentiated from myoblasts) for a long enough period of time is possible (Ferrer-Martinez *et al.*, 2006), it would rely on sampling non-passaged replicates at each time point rather than a fraction of the cells during subculture. This means there is no guarantee that cells sampled at a later date were behaving in a similar way to those sampled at earlier time points, and thus increases the likelihood of misleading results.

5.3.4 Assessing differentiation in myoblasts

Primary myoblast cultures have the potential to differentiate into myotubes if the serum levels are reduced, or the cells remain fully confluent for a long period of time (Capers, 1960). To exclude the possibility of unintentional differentiation of the myoblasts during culture, the cells were probed for Myosin Heavy Chain Slow (MYHC–Slow). MYHC-Slow is specifically expressed in type I myotubes and not myoblasts (Figure 5.5).

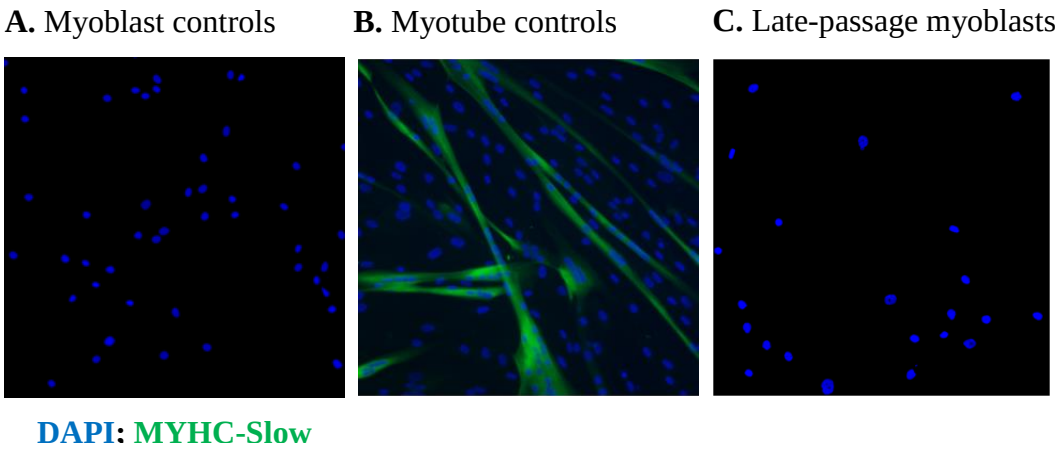

Figure 5.5 Immunocytochemistry assessing differentiation of myoblasts. (A) Control myoblasts show no staining for MYH-Slow (Green) and individual single nucleated cells (Blue). (B) Myoblasts differentiated into myotubes showing staining for MYH-Slow in Type I myotubes and show long multi-nucleated fibres. (C) Myoblasts at day 18 are observed as individual nucleated cells with no MYH-Slow staining, suggesting that they are not differentiating into myotubes.

Myoblasts at the end of experimentation (Day 18) are still observed as individual nuclei (DAPI stained) with no MYHC-Slow staining, suggesting they have not differentiated into myotubes, though further markers are required to determine whether myoblasts are in the early stages of differentiation.

5.4 Results and Discussion

5.4.1 Gene expression during depletion/repopulation in myoblasts

With the optimum concentrations for EtBr and ddC established, and the modulation of FBS concentration increased to 15% to reduce mtDNA copy number increase in untreated cells, the expression of genes with known importance to mtDNA replication was measured. Control and MERRF myoblasts were depleted for six days with 25 ng/ mL EtBr or 1 µg/ mL ddC, and allowed to repopulate for 12 days afterwards (total

of 18 days). Cells were subcultured every third day and samples collected for DNA and RNA extraction. First, copy number measurements were made to select for the optimum depletion/repopulation curve (Figure 5.6). Control myoblasts treated with 25 ng/ mL failed to repopulate by Day 18 (6.12 %; SD±1 %). Myoblasts treated with 1 µg/ mL ddC began repopulation at Day 15 (Control, 48.4 % (SD±12.8 %); MERRF, 99.8 % (SD±8.55 %)).

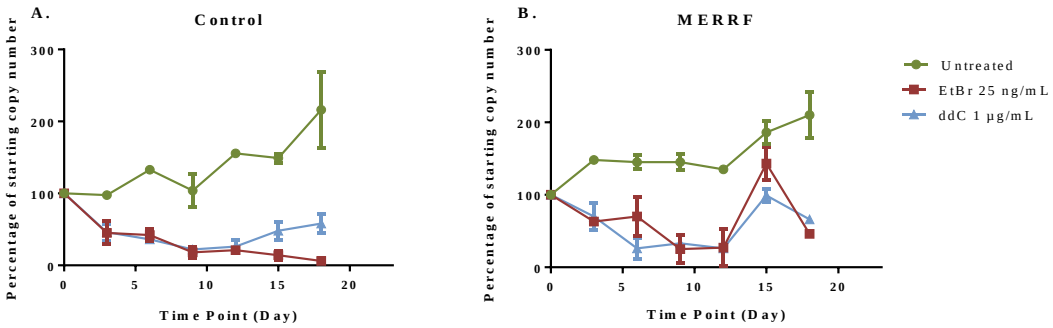

Figure 5.6 Depletion and repopulation of mtDNA in control and MERRF myoblasts. mtDNA copy number as a percentage of starting value on Day 0, in (A) control and (B) MERRF myoblasts. Cells were either untreated (green), treated with EtBr (red) or treated with ddC (blue) until day six. The drugs are removed at day six, allowing mtDNA to repopulate for a further 12 days. Error bars represent standard deviation of biological triplicates.

The control cell line failed to repopulate with EtBr treatment, but both cell lines repopulated to varying degrees with ddC treatment. Therefore, cell lines depleted only with ddC were chosen to study gene expression patterns.

The fold change in ddC-treated compared to untreated cell lines was calculated using the ΔΔCt technique, comparing the expression of a target gene (e.g. *TFAM*) to a reference gene (e.g. *ACTB*), and then comparing this ratio in a target sample (e.g. treated) to a control sample (e.g. untreated). A fold change of one represents no difference in gene expression between the two compared samples (shown at day 0 as there was only one sample, with no treated condition) (Figure 5.7).

TFAM gene expression levels show a reduction correlating with mtDNA copy number during at the lowest point of depletion (Control-Day 9, 0.79 (SD±0.06); MERRF-Day 9, 0.56 (SD±0.06)) and a subsequent increase in expression after repopulation (Control-Day 18, 1.62 (SD±0.11); MERRF-Day 18, 1.42 (SD±0.02), $p < 0.05$ unpaired t test). There was a decline in *POLG* expression in control myoblasts only (Control-Day 6,

0.46 (SD± 0.43); MERRF-Day 6, 1.31 (SD±0.31) and after repopulation, *POLG* gene expression is no different from the untreated condition (Control-Day 18, 0.99 (SD±0.33); MERRF-Day 18, 0.94 (SD±0.1). *POLG2* also shows slight reduction in expression after depletion (Control-Day 6, 0.61 (SD±0.2); MERRF-Day 6, 0.78 (SD±0.05) with recovery to normal or higher levels (Control-Day 18, 2.04 (SD±0.00), $p < 0.005$ unpaired t test; MERRF 1.23 (SD±0.1). *NRF1* levels do not appear to correlate with depletion and repopulation.

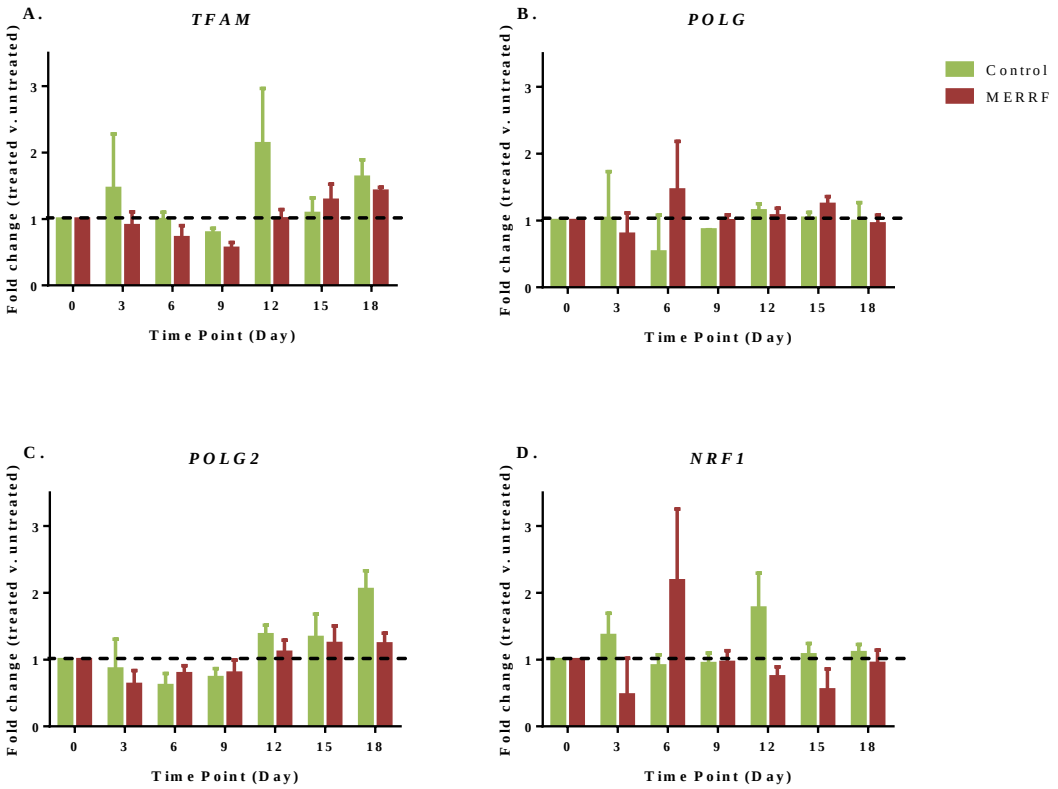

Figure 5.7 Gene expression in myoblast cell lines normalised against untreated. The gene expression of (A) *TFAM*, (B) *POLG*, (C) *POLG2* and (D) *NRF1* using *ACTB* as a reference gene in control and MERRF myoblast cell lines. Fold change calculated between treated (1 µg/mL ddC) and untreated cells at each time point. Error bars are based on the standard deviation of fold changes calculated when treated biological triplicates are normalised against the mean untreated Ct values. * $p < 0.005$ unpaired t test.

When comparing treated to untreated cell lines at each time point, there seems to be a slight, non-significant reduction in gene expression of *TFAM*, *POLG* and *POLG2* between Day 0 and Day 6-9 with a steady increase either back to normal (*POLG*) or slightly higher levels (*TFAM* and *POLG2*). *NRF1* has an unstable gene expression profile which does not seem to correlate well between cell lines or conditions.

The highest fold change observed is below 2.5 fold, which is not a high enough difference to be valuable if performing whole transcriptome profiling, and especially not when hoping to identify novel genes involved with mtDNA replication regulation which may have more subtle expression changes to genes such as *POLG* and *TFAM*.

5.4.2 Gene expression during mtDNA depletion/repopulation in fibroblasts with and without galactose

Cells in standard culture media containing glucose can rely on glycolysis for the majority of their energy demands. This means there is little pressure on cells to repopulate their mtDNA after depletion when in glucose media. To make cells reliant on mitochondria, it is possible to culture them on a glucose-free media supplemented with galactose. To utilise galactose for glycolysis, it must first be converted into a component of glycolysis, glucose-6-phosphate (G6P), in a 4-step process. Although the net yield of ATP per galactose molecule is the same as for glucose (+2ATP), the flux rate at which G6P can be produced from galactose is much slower than for glucose (Demir and Aksan Kurnaz, 2006, Pritchard and Kell, 2002). The slow production of ATP through glycolysis when metabolising purely galactose is not sufficient to supply the energy demands of the cell, meaning a higher reliance on ATP production through oxidative phosphorylation in the mitochondria. This phenomenon allows the use of galactose-only media as a test of mitochondrial dysfunction in patient cell lines (Robinson *et al.*, 1992).

Reliance on oxidative phosphorylation may be a way to drive mtDNA replication in repopulating cells and observe a more extreme transcriptional response to depletion. In this model, fibroblasts were cultured for six days with 1µg/mL ddC in high-glucose media; upon removal of ddC some cells were placed in galactose media whilst others returned to standard glucose media (Figure 5.8).

Fibroblasts were depleted of mtDNA to below 10 % by Day 9 (Glucose, 5 % (SD±1.34 %); Galactose, 7 % (SD±0.53 %)). Repopulation rate is initially similar in glucose and galactose conditions (Glucose-Day 12, 53.46 % (SD±14.33); Galactose-Day 12 48.21 % (SD±13.96 %)). By Day 15, however, fibroblasts in the galactose condition have a dramatically increased mtDNA copy number compared to those in glucose (Control-Day 15, 86.68 % (SD±9.62); MERRF-Day 15, 410.09 % (SD±36.50 %).

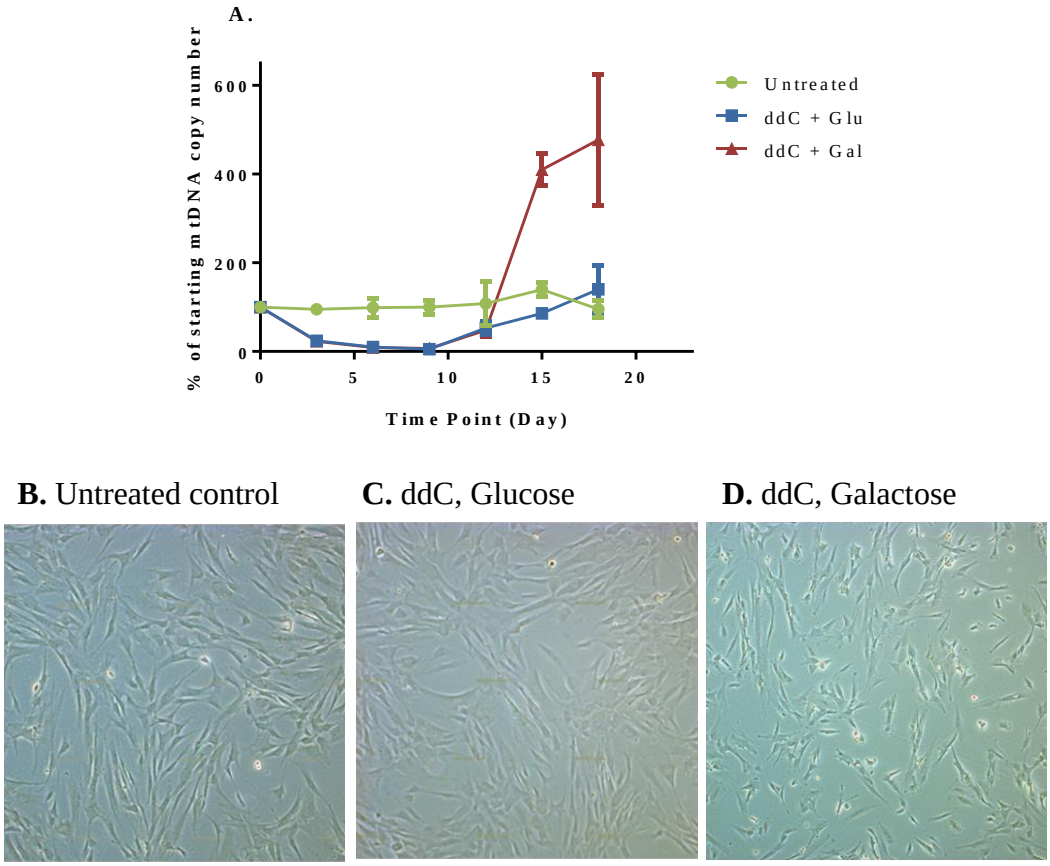

Figure 5.8 Fibroblast mtDNA repopulation with and without galactose. Fibroblasts were depleted for six days with 1 µg/mL ddC and allowed to repopulate in either standard glucose media or 5 mM galactose media. (A) Copy number is significantly higher in fibroblasts cultured with galactose. Brightfield microscopy images taken on Day 9 showing (B) untreated and (C) 1 µg/mL ddC treated fibroblasts having no significant morphological differences, but (D) fibroblasts cultured in galactose for three days after depletion showing growth defects.

There was early evidence of culture in galactose after depletion having a negative effect on cellular growth and morphology (Figure 5.8D). Without cells dividing, it is difficult to gauge the replication rate since mtDNA can accumulate without compensation for mtDNA copy number halving upon division. The dramatic reduction in cell number towards the end of the experiment also meant a reduction in DNA recovered for use in the qPCR assays to determine mtDNA copy number. The signal for the nuclear gene (*B2M*) was close to the limit of sensitivity of the assay, which could account for the apparent dramatic increase in mtDNA copy number and larger standard deviation in galactose treated fibroblasts on Day 18.

The gene expression of *TFAM*, *POLG*, *POLG2* and *NRF1* were also measured relative to *ACTB* in both glucose and galactose culturing conditions (Figure 5.9). There is

significant difference of *POLG* expression at Day 3 and *NRF1* expression at Day 6; however at this stage of the experiment the two samples were in the same media conditions. There was a significant difference between glucose and galactose condition in the gene expression of *TFAM* at Day 9 (Glucose, 1.34 (SD±0.30); Galactose, 2.11 (SD±0.37) and Day 18 (Glucose, 0.78 (SD±0.24); Galactose, 1.68 (SD±0.38). There is also significant difference of POLG expression at Day 9 (Glucose, 1.17 (SD±0.17); Galactose 1.65 (SD±0.23)), Day 12 (Glucose, 1.04 (SD±0.31); Galactose, 2.44 (SD±0.7)) and Day 18 (Glucose, 0.88 (SD±0.15); Galactose, 2.92 (SD±0.79)). POLG2 expression is significantly different between media conditions at Day 12 (Glucose, 1.59 (SD±0.22); Galactose 4.09 (SD±1.0) and Day 15 (Glucose, 2.04 (SD±0.33); Galactose 4.00 (SD±1.08). *NRF1* expression is significantly different between media conditions at Day 9 only, and then reduces in expression in the galactose condition whilst increasing in the glucose condition (Glucose, 0.38 (SD±0.2); Galactose, 2.07 (SD±0.21).

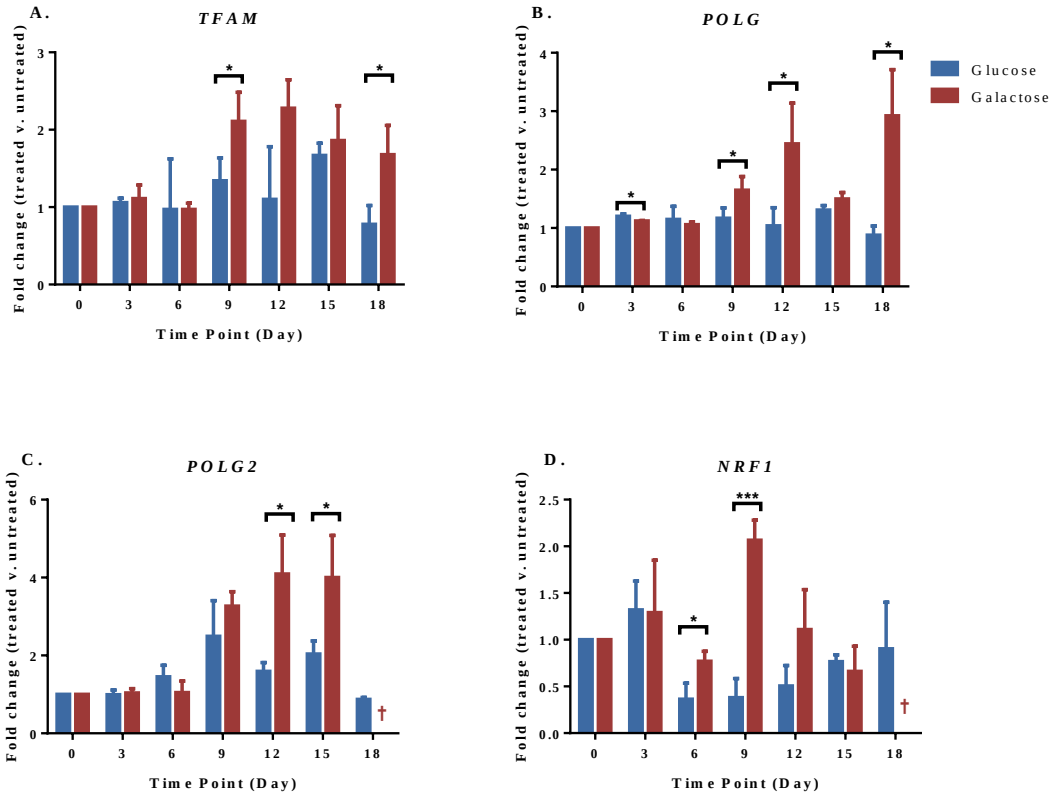

Figure 5.9 Gene expression in control fibroblasts. The gene expression of (A) *TFAM*, (B) *POLG*, (C) *POLG2* and (D) *NRF1* using *ACTB* as a reference gene. Fold change calculated between treated (1µg/mL ddC) and untreated cells at each time point. Error bars are based on the standard deviation of fold changes calculated when treated biological triplicates are normalised against the average of untreated biological triplicates. † Signal for *POLG2* and *NRF1* was below the sensitivity range of the assay on Day 18. * $p < 0.05$, ** $p < 0.01$, *** <0.001 unpaired t test.

All genes show significantly increased expression induced by culturing with galactose instead of glucose at one or more time points after repopulation resumes. However, with the growth of cells compromised, it is not a valid model to study gene expression as any changes observed may be due to cellular stress rather than simply increased replication rate.

5.4.3 Culture in variable concentrations of galactose-based media

Fibroblasts were depleted for six days with 1 µg/mL ddC. Between Day 6 and 9, fibroblasts were subjected to different percentages of galactose/glucose ranging from between 0% (glucose only) and 100% (galactose only) in 25% increments. Daily, between Day 9 and 12, the galactose concentration was increased, and glucose concentration reduced, by 25% (Figure 5.10A). The mtDNA copy number was

measured at each passage and the cell number determined by haemocytometer (Figure 5.10B-C).

At Day 15, only the 75 % galactose condition shows a significantly higher mtDNA copy number than the glucose control condition (Glucose, 121.9 % (SD±16.9 %); 75 % > Galactose, 203.0 % (SD±22.1 %); $p < 0.01$ unpaired t test). Cells grown for three days in galactose directly after drug removal showed a decreased cell number (52.5 % (SD±22.9 %)). Between Days 9 and 12, any cells exposed to pure glucose also showed a decrease in cell number (25% > Gal, 35.76 (SD±16.9 %); 50 % > Gal, 65.5 % (SD±21.5 %); 75 % > Gal, 47.7 % (SD±10.3 %)).

A.

Treatment	Condition	Day 6	9	10	11	12	15
Untreated	Untreated (0%)						
1ug/mL ddC	Glu-Control (0%)						
	0%					0	3
	25%				0	1	4
	50%			0	1	2	5
	75%		0	1	2	3	6
	Gal-Control (100%)	0	3	4	5	6	9

*Days in galactose

Key	Glucose (mM)	Galactose (mM)
0%	25	0
25%	18.75	1.25
50%	12.5	2.5
75%	6.25	3.75
100%	0	5

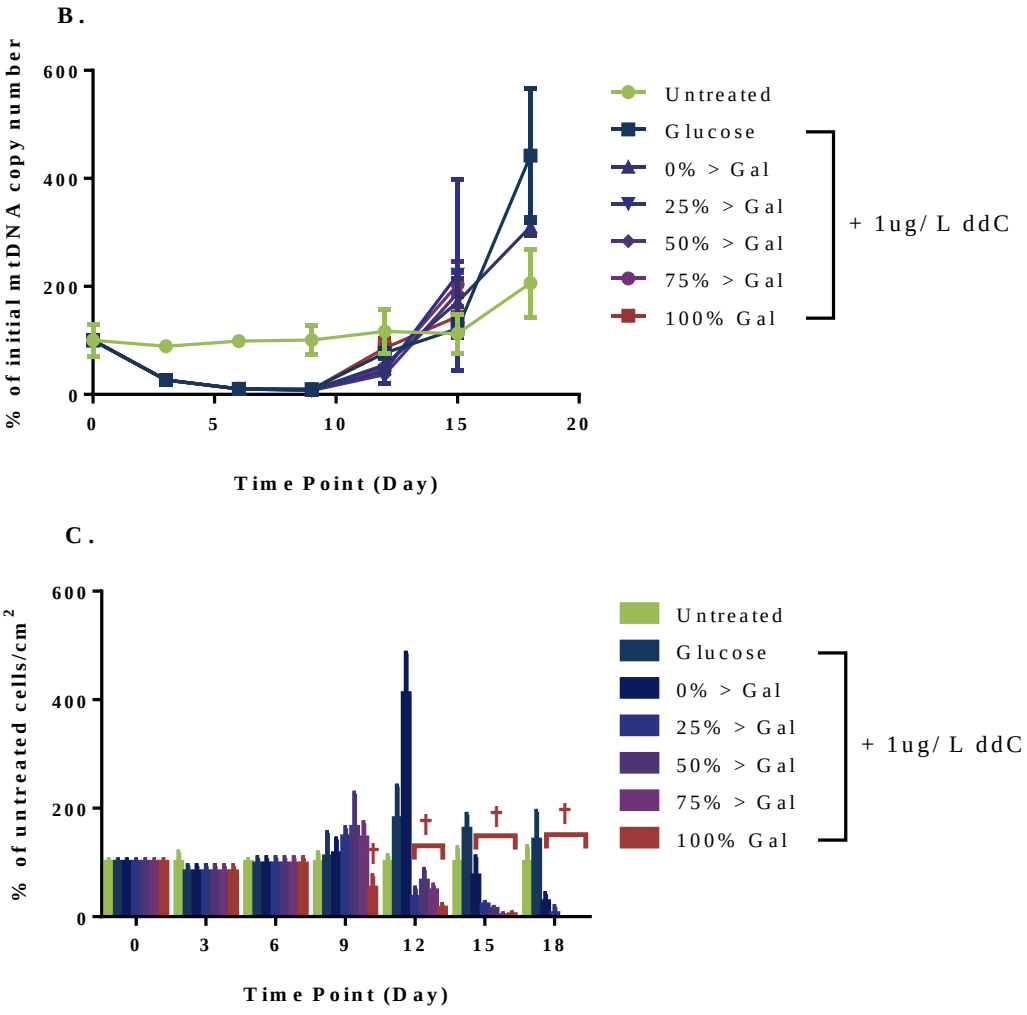

Figure 5.10 Fibroblast depletion and repopulation with galactose. Fibroblasts were depleted for 6 days with 1µg/mL ddC. From Day 6 fibroblasts were exposed to variable ratios of glucose and galactose. A) Demonstration of when the glucose: galactose ratio changes. B) mtDNA copy number measurements shows no difference in repopulation rates between cell lines. C) Cell counts normalised to untreated showing depleted cells are not viable in 100% galactose. † Denotes cells in galactose for at least one day.

Fibroblasts depleted of mtDNA have reduced proliferation rates in galactose media as they cannot generate sufficient energy for cell division through limited glycolysis. However, by Day 15 mtDNA copy number in all depleted lines have recovered beyond that observed in the untreated condition, yet fibroblasts moved to pure galactose media at this point still fail to thrive.

Although there was no difference in mtDNA repopulation rate, the gene expression of the four replication/transcription genes was assayed to determine whether the variable galactose concentration has induced any gene expression changes (Figure 5.11). Although there are many statistically significant differences between time points for *TFAM*, *POLG2* and *NRF1*, the only significant difference between media conditions was for *NRF1* expression on day 12 (Glucose, 1.16 (SD±0.1); 0 > 75% Gal, 1.48 (SD±0.02), $p < 0.05$ unpaired t test).

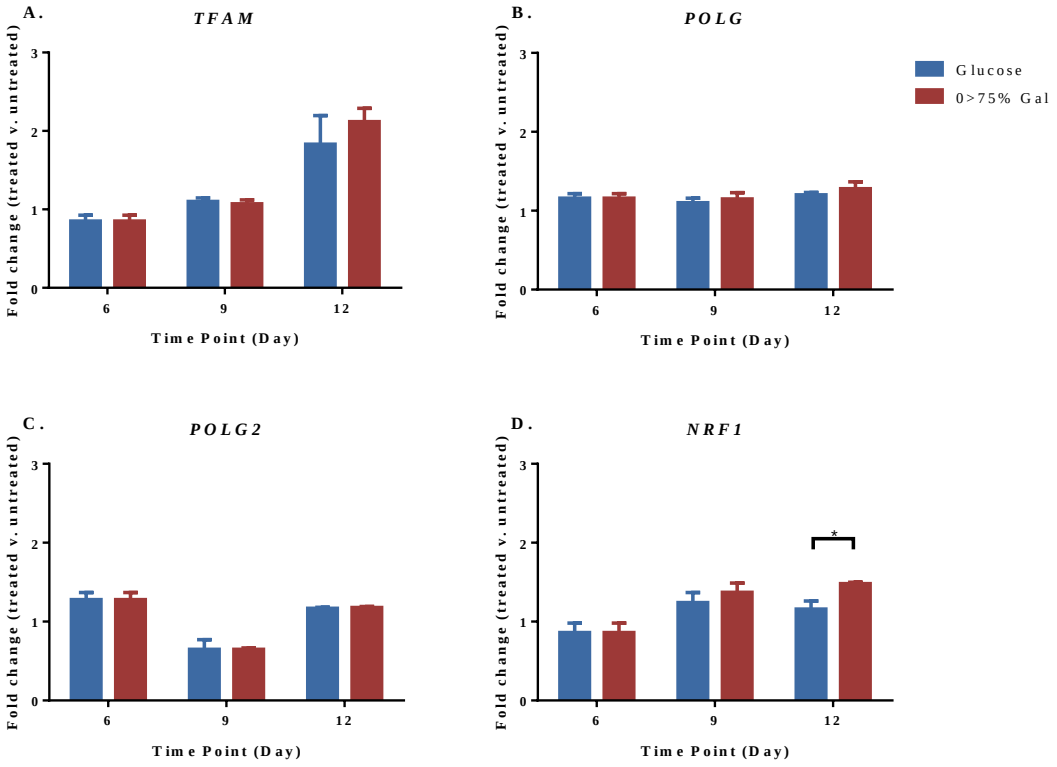

Figure 5.11 Gene expression under variable galactose concentrations. The gene expression of A) *TFAM*, B) *POLG*, C) *POLG2* and D) *NRF1* using *ACTB* as a reference gene. Mean fold changes calculated between treated biological triplicates (1µg/mL ddC) and the mean of untreated triplicates at each time point. Error bars represent the SD. * $p < 0.05$ unpaired t test.

NRF1 expression is not significantly affected by media conditions at Day 9 and the difference observed at Day 12 represents a fold change difference of just 0.32 fold. It is clear that although fibroblasts can proliferate in up to 75% galactose, there is little difference in either the mtDNA copy number repopulation rate or associated gene expression.

5.4.4 Mitochondrial protein levels during depletion/repopulation

In the previous experiment, mtDNA copy number was repopulated to between 35-85% by Day 12 in variable concentrations of galactose. By Day 15, all conditions had recovered to above that of the untreated condition, yet the fibroblasts could not proliferate in pure galactose media.

For the respiratory chain to be functional, the mitochondrial-encoded proteins must be translated and incorporated into the respiratory complexes. It may be that although mtDNA has fully repopulated, the mitochondrial-encoded protein levels have not returned to sufficient levels to restore adequate mitochondrial function.

To investigate when translation of mitochondrial-encoded proteins recommences, protein lysates from untreated and treated (1µg/mL ddC) fibroblasts were analysed by SDS-PAGE and western blotting. Membranes were probed with antibodies against a reference protein (β-Actin), a mitochondrial outer membrane protein unrelated to respiration (Porin/VDAC), a subunit from the entirely nuclear-encoded Complex II (SDHA) and Complex IV subunits. COXII is a Complex IV subunit encoded on the mtDNA, whereas CIV SIV is nuclear encoded (Figure 5.12).

SDHA is one of four nuclear subunits comprising Complex II. Although expression of SDHA is significantly lower in ddC-treated fibroblasts at Day 12 (Untreated, 0.21 (SD±0.02); ddC, 0.12 (SD±0.01), $p < 0.05$ unpaired t test), it is detectable at all stages after depletion. However, COXII, which is mitochondrially encoded, is not detectable in ddC-treated fibroblasts until Day 15 (Untreated, 0.08 (SD±0.03); ddC, 0.05 (SD±0.03), ns). Despite the lack of mitochondrial complexes, the nuclear subunit of complex IV, SIV, is expressed at consistent levels at both Day 9 and Day 12. Porin/VDAC shows increased expression in ddC-treated fibroblasts from Day 12 (Untreated, 0.06 (SD±0.03); ddC, 0.28 (SD±0.07); ns) and is at over 10-fold expression by Day 15 (Untreated, 0.04 (SD±0.01); ddC, 0.49 (SD±0.01); $p < 0.001$ unpaired t test).

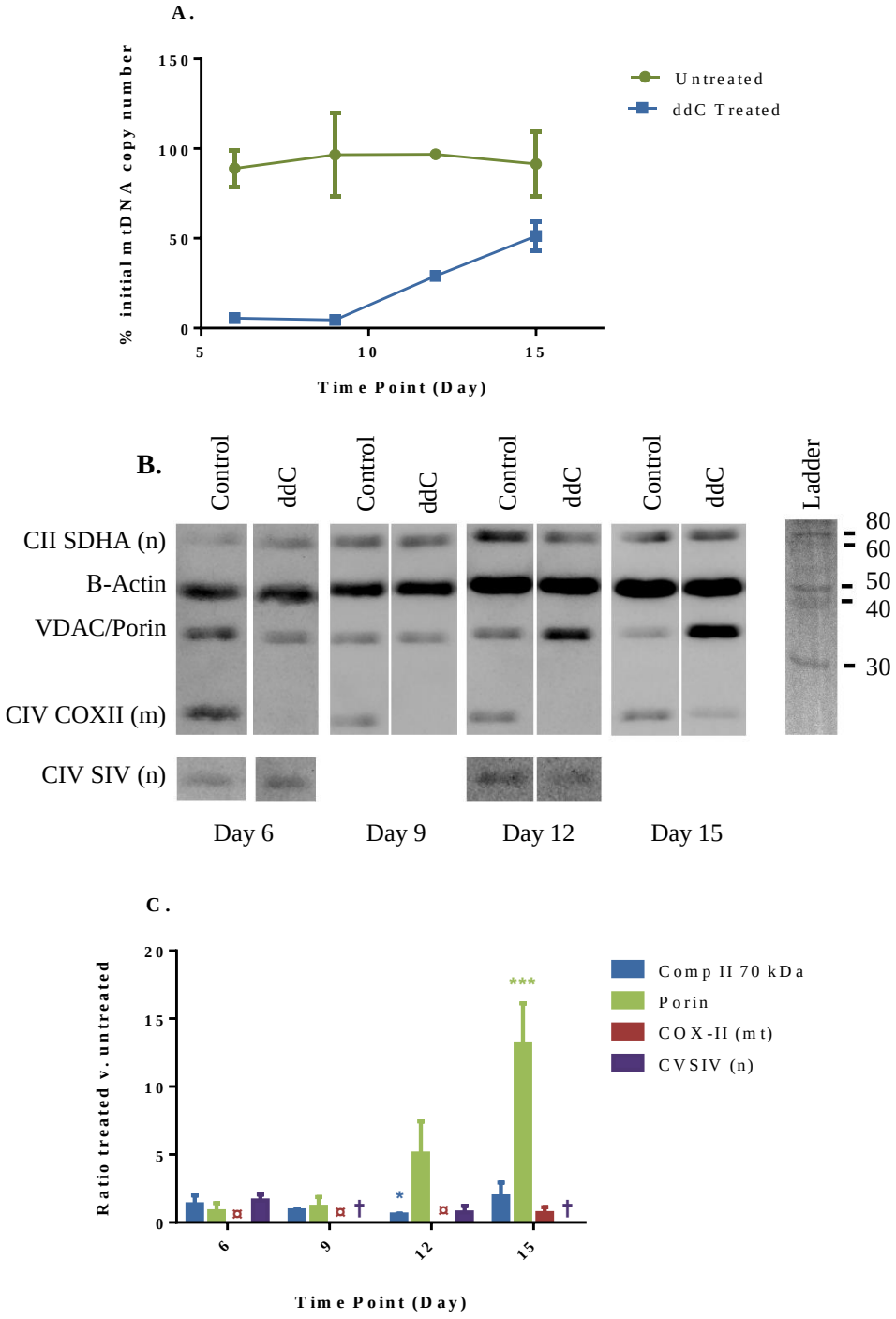

Figure 5.12 Protein expression during repopulation. A) mtDNA copy number during repopulation. B) Western blot images comparing protein expression in untreated fibroblasts compared to ddC-treated fibroblasts, showing lack of expression of mitochondrial COXII after mtDNA depletion and an increase in mitochondrial biogenesis (indicated by VDAC/Porin) as the cell repopulates. C) Densitometry quantification of the expression levels of Complex II SDHA (CII), VDAC/Porin and Complex IV subunit II (COXII) relative to β-Actin during repopulation, from biological duplicates. ¤ COXII not detectable in Days 6-12. † CIVSIV was not analysed at Day 9 or Day 15. * $p < 0.05$, *** $p < 0.001$ unpaired t test.

Depletion of mtDNA prevents translation of mitochondrial-encoded proteins. However, this does not affect the expression of nuclear-encoded proteins, even those from complexes with mitochondrial-encoded subunits, such as Complex IV.

The increased expression of Porin/ VDAC from Day 12 suggests there might be general upregulation of mitochondrial biogenesis to compensate for reduced respiration capacity cause by mtDNA depletion.

Polymerase gamma protein levels

To determine whether the increase in mtDNA copy number could be regulated at the protein level rather than the mRNA level, the expression of polymerase gamma protein was assessed between Day 6 and Day 15.

POLG protein is reduced between Day 6 and Day 12 (ddC-Day 6, 0.64 (SD±0.2), ns; ddC-Day 9, 0.49 (SD±0.13), ns; ddC-Day 12, 0.42 (SD±0.12), $p < 0.005$ unpaired t test) but begins to recover by Day 15 (ddC, 0.82 (SD±0.08)).

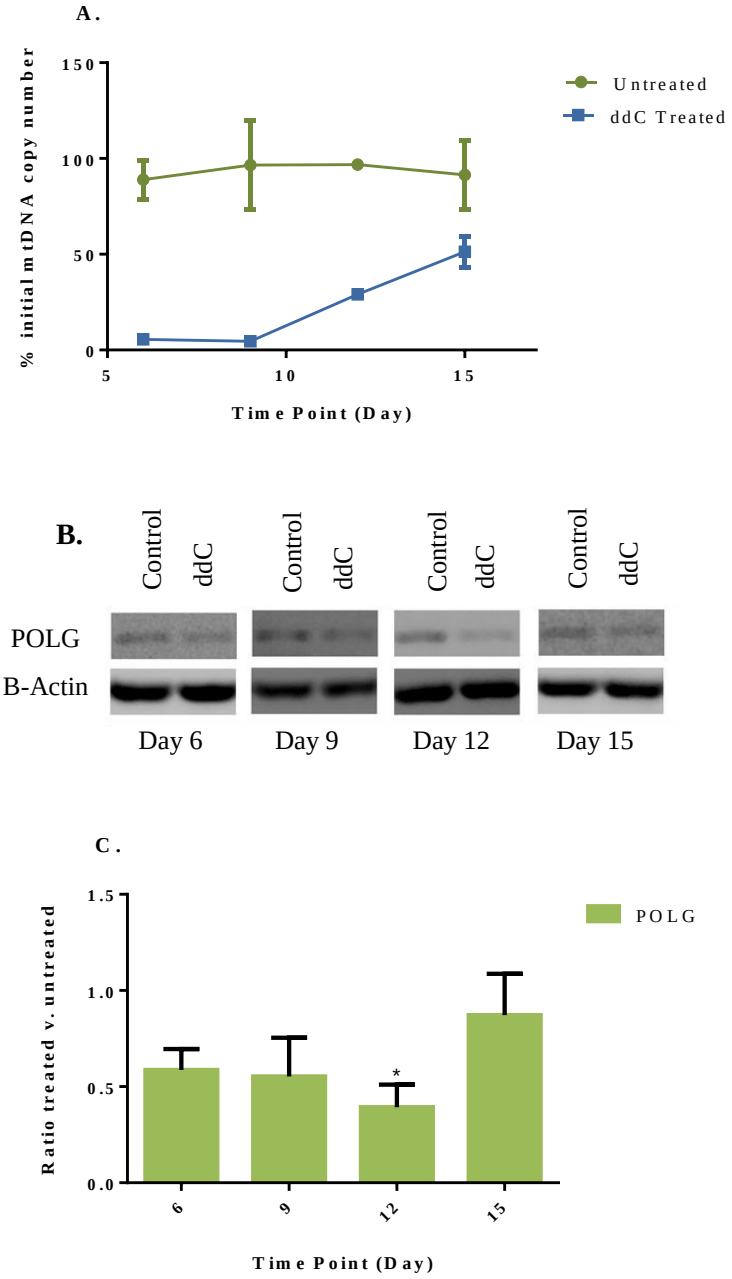

Figure 5.13 Analysis of Polymerase Gamma protein levels. A) mtDNA copy number during repopulation. B) Western blot images comparing protein expression in untreated fibroblasts to compared to ddC-treated fibroblasts, showing decreased expression of mitochondrial polymerase gamma after mtDNA depletion until recovery at Day 15. C) Densitometry quantification of the expression levels of polymerase gamma relative to β-Actin during repopulation, from biological duplicates. * $p < 0.05$ unpaired t test.

Previous analysis of polymerase gamma in 143B (TK-) ρ^0 cells, containing no mtDNA, indicate no decrease in either protein or mRNA levels from that observed in the parental (ρ^+) cell lines (Davis *et al.*, 1996). However, after just six days in ddC the Polg protein levels are ~60% of that in untreated cells, dropping to ~40% before recovering. mtDNA depletion has previously been shown to cause reduction in TFAM protein levels

(Larsson *et al.*, 1994). It is possible that reduction of mtDNA and TFAM protein compromises nucleoid structure, causing the decrease in other components of nucloids, such as POLG.

5.4.5 Investigation of alternative functions at intermediate time points

Previously, gene expression was only sampled at 3-day intervals, upon passaging the fibroblasts. It is possible that some important gene expression signals are being overlooked between these time points. The only genes analysed have functions related to mitochondrial transcription and replication, but there are many other biological functions which contribute to regulation of mtDNA copy number. To address these potential problems, fibroblasts will be sampled daily after removal of ddC, and the range of genes analysed will be expanded to include a other possible functions that are critical to regulation of mtDNA replication, such as mitochondrial dynamics or biogenesis.

To ensure the most appropriate reference gene is being used, the stability of expression of various 'housekeeping' genes were analysed by the BestKeeper software, using samples under variable conditions (Appendix E.1). Although *ACTB* is considered acceptable, *GAPDH* shows lower deviation between samples and will be used as a reference gene instead.

Fibroblasts were treated with 1 µg/ mL ddC for six days, as in previous experiments. To allow for sampling fibroblasts every day without passaging, at each three-day interval 1/3 of a t75 was sampled for DNA/RNA extraction, whilst the remaining fibroblasts seeded one t75 and three t25s. The day after passaging, two t25s were sampled for extraction, and the second day after, one t25 was sampled.

Treated fibroblasts at Day 9 have lower mtDNA copy number than at Day 6 (Day 6, 5.51 % (SD±0.62 %); Day 9, 4.53 % (SD±0.85 %)), though the lowest point of depletion is actually Day 8 (3.64 % (SD±1.09 %)), meaning recovery has already begun at Day 9. mtDNA copy number peaks at Day 13 (72.93 % (SD±8.14 %), before decreasing in both the untreated and treated conditions.

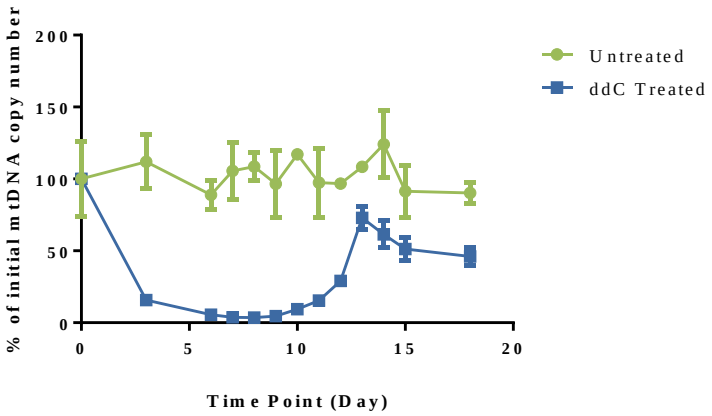

Figure 5.14 Measuring mtDNA depletion and repopulation in fibroblasts each day. Fibroblasts were depleted with 1µg/mL ddC for six days and allowed to repopulate for a following 12 days in standard glucose media. Cells were passaged every three days but samples collected each day to make mtDNA copy number measurements.

Investigating intermediate time points reveals that mtDNA replication has resumed by Day 9. Without the intermediate time points, it would be possible for the resumption of mtDNA replication to have occurred at any stage from Day 8 to Day 12, making interpretation of results difficult. It has also revealed a peak in mtDNA copy number after Day 12, which has decreased again by Day 15.

Gene expression was analysed during the optimal stages of repopulation, between Day 6 and Day 13. Fold change was calculated using the $\Delta\Delta C_t$ method, normalising treated biological triplicates against the average for untreated samples. Statistical significance was calculated between the treated samples, and the untreated samples normalised against the average.

There was no statistically significant difference at any time point for *TFAM*, *POLG*, *POLG2* or *NRF1* (Figure 5.15).

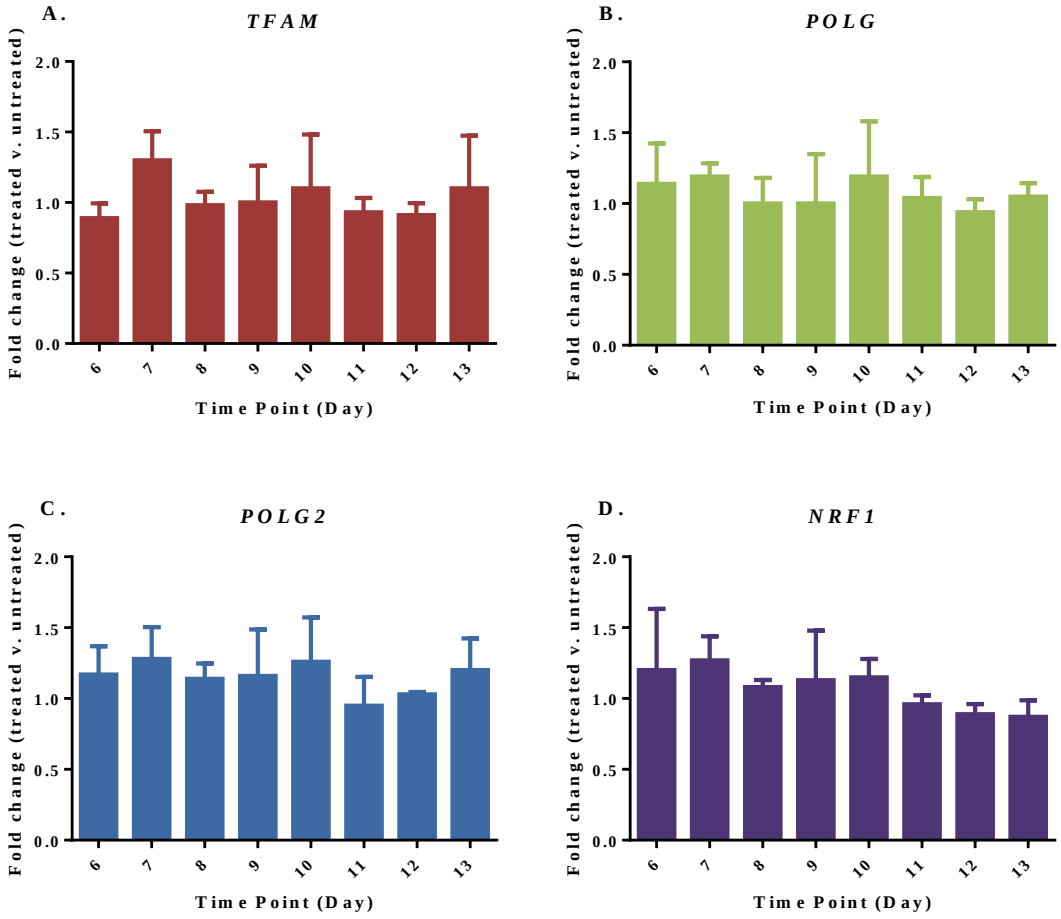

Figure 5.15 Gene expression in fibroblasts during mtDNA repopulation. The fold change of (A) *TFAM*, (B) *POLG*, (C) *POLG2* and (D) *NRF1* relative to *GAPDH* reveals no change in gene expression in intermediate points of mtDNA repopulation. Error bars based on standard deviation when the fold change is calculated from treated biological triplicates against the average of untreated controls.

The gene expression of mitochondrial subunits for Complex IV was also measured. There is a statistically significant decrease in transcription of mitochondrial-encoded MT-COII from Day 7. Similarly to mtDNA, the lowest level of *MT-COII* transcript was at Day 8 (Untreated,1.02 (SD±0.26); ddC, 0.15 (SD±0.004)) (Figure 5.16A). Expression of *COX4I1*, a nuclear subunit of Complex IV, in treated fibroblasts is only significantly higher than that of untreated fibroblasts at Day 10 (Untreated, 1.00 (SD±0.02); ddC, 1.22 (SD±0.12)) (Figure 5.16B).

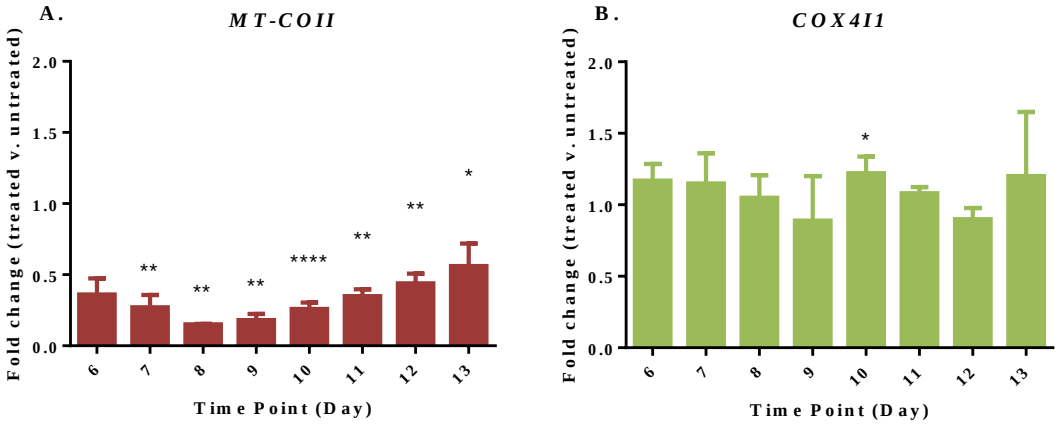

Figure 5.16 Gene expression of Complex IV subunits during mtDNA repopulation. Shows how depletion of mtDNA causes a (A) reduction in gene expression relative to *GAPDH* of the mitochondrially encoded subunit *MT-COII* until Day 8 which begins to recover by Day 9. (B) Nuclear encoded subunit *COX4I1* transcript levels show no depletion by Day 6 and remain stable throughout repopulation. * $p < 0.05$, ** $p < 0.01$, **** $p < 0.0001$ unpaired t test.

The depletion and repopulation of *MT-COII* transcript follows the same pattern as for mtDNA, though does not deplete to the same extent. This suggests that either more transcripts are being generated from each mtDNA molecule in depleted fibroblasts, or mitochondrial transcripts are long-lived and depletion lags behind that of mtDNA.

Further genes were analysed to assess the contribution of replication (*PEO1*/*Twinkle*), transcription (*POLRMT*), fission and fusion (*OPA1*, *FIS1*), mitochondrial biogenesis (*PPARG*) and reactive oxygen species (*SOD2*) to regulation of mtDNA copy number. There were no statistically significant differences between untreated and treated cells from Day 6 to Day 12 for any genes (Figure 5.17).

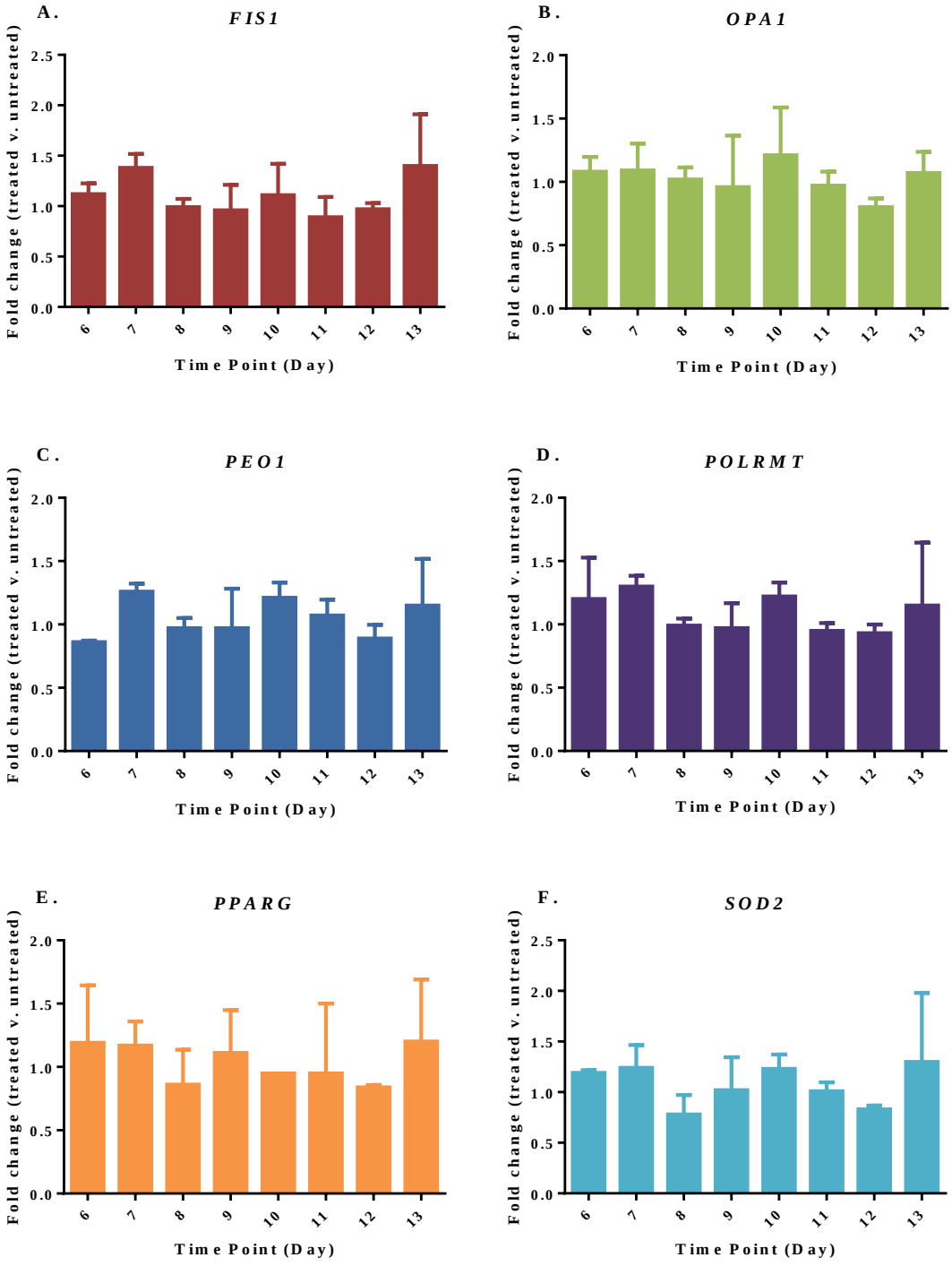

Figure 5.17 Gene expression of additional genes during repopulation. Expression of (A) *FIS1* (fission), (B) *OPA1* (fusion), (C) PEO1 (replication), (D) POLRMT (transcription), (E) *PPARG* (biogenesis) and (F) *SOD2* (oxidative stress) show no response to mtDNA depletion by Day 6 and remain stable throughout repopulation.

Kao and colleagues (2012) investigated the effect of six weeks treatment with EtBr and chloramphenicol (inhibitor of mitochondrial protein synthesis) on mitochondrial biogenesis. After six weeks of EtBr treatment, the expression of *TFAM*, *NRF1* and *POLG* was decreased (*TFAM*, 0.42-fold; *NRF1*, 0.19-fold; *POLG*, 0.10-fold). After two weeks without EtBr, *TFAM* and *NRF1* expression had increased beyond that of untreated cells (*TFAM*, 5.09-fold; *NRF1*, 2.92-fold) and *POLG* expression had returned to normal (1.15-fold) (Kao *et al.*, 2012). Some mild depletion and recovery of gene expression has been observed over the course of experimentation with six days ddC treatment. Even though mtDNA copy number was depleted to <10%, longer exposure to the ddC may be needed to induce more dramatic compensatory mechanisms.

5.5 Concluding remarks

The instability of mtDNA copy number in myoblasts or fibroblasts during long periods of culture suggests there are other factors, such as cellular stress, contributing to regulation of mtDNA replication or content. Although there have been significant changes in gene expression induced by depletion of mtDNA with ddC, the results are not always regularly repeatable and do not provide large changes in gene expression.

Fibroblasts cannot be forced to rely on mitochondrial function through culture in galactose medium after depletion of mtDNA. Recovery of normal levels of mitochondrial-encoded proteins is too slow to allow proliferation of fibroblasts in medium without glucose.

Chapter 6. Gene Expression Analysis in MERRF Muscle Fibres

Table of Contents

6.1 Introduction

6.1.1 Gene expression analysis in mitochondrial disease

The analysis of mitochondrial gene expression profiles was first done by northern blot and revealed dramatic transcript level rises, including increased amounts of unprocessed transcripts, in the tissues of patients with mitochondrial syndromes such as Kearns-Sayre Syndrome (KSS), Myoclonic Epilepsy with Ragged-Red Fibre (MERRF) and Mitochondrial Encephalomyopathy, Lactic acidosis, and Stroke-like episodes (MELAS) (Heddi *et al.*, 1993, Heddi *et al.*, 1994). This includes, but is not restricted to, both mitochondrial- and nuclear-encoded OXPHOS subunits, with altered expression of ancillary genes such as adenine nucleotide transporter 1 (*ANT1*) and E1α subunit of pyruvate dehydrogenase (*E1αPDH*) (Heddi *et al.*, 1999).

The advent of microarray technology has allowed analysis of thousands of gene transcripts in parallel, without the requirement for preselecting target genes. This provides a powerful tool for the analysis of mitochondrial disease. However, particular care must be taken during experimental design and data analysis, as misleading gene expression alterations can be induced easily. Sources of experimental variability have been shown to be minor, if the correct quality control measures are in place, but large variability can be caused by tissue heterogeneity, sample limitations and inter-individual variation (Bakay *et al.*, 2002). For example, agonal duration and brain pH has been shown to influence expression of mitochondrial genes in control post-mortem brain samples analysed by microarray (Vawter *et al.*, 2006). Also, generation of transmitochondrial cytoplasmic hybrid (cybrid) cell lines by depletion and repopulation, a commonly used assay for studying mtDNA mutations in a common nuclear background (King and Attardi, 1989), has been shown to induce over 1,500 significant expression changes compared to non-manipulated cell counterparts (Danielson *et al.*, 2005).

Regardless of such concerns, microarrays have consistently noted the general downregulation of transcription in mitochondrial disease, since it is a heavily energy-dependent process, and implicated several biochemical processes as causes or effects in the pathogenesis of mitochondrial disease.

As previously discussed, ROS levels are increased in the tissues of patients with mitochondrial disease (Piccolo *et al.*, 1991, Smits *et al.*, 2010a). This leads to an

increased expression of antioxidant enzymes, such as manganese-superoxide dismutase (Mn-SOD), in the attempt to alleviate the ROS burden in mitochondrial disease patient tissues (Rusanen *et al.*, 2000, Wani *et al.*, 2008). However, catalase (CAT) and gluatathione peroxidise (G-Px) levels are not always upregulated alongside Mn-SOD, which can result in an accumulation of H_2O_2, as it is produced faster than it can be detoxified (Kunishige *et al.*, 2003, Lu *et al.*, 2003).

Oxidative stress has been shown to have a regulatory effect on cytoskeletal remodelling. Upregulation of oxidative stress markers and matrix metalloproteinases (MMPs) with concomitant downregulation of cytoskeleton proteins in the fibroblasts of MERRF (m.8344A>G) patients, causes disruption to the dynamics of mitochondrial networks (Ma *et al.*, 2005).

Increased ROS production and levels of misfolded or damaged proteins caused by mtDNA deletions has been shown to have a inhibitory effect on the ubiquitin-proteasome system. This has a negative impact on the amino acid salvage pathway, causing a global drop in amino acid levels within cells, and triggers autophagy through the mTOR pathway (Alemi *et al.*, 2007, Kadowaki and Kanazawa, 2003).

Comparison of transcription levels in various cell types from patients with different mitochondrial disease identified shared responses to mitochondrial deficiency are upregulation of the unfolded protein response (UPR) and cell cycle pathway, with a secondary effect of inhibition of vesicular secretion and protein synthesis. The UPR is related to endoplasmic reticulum (ER) disruption, resulting in protein folding and processing errors. Perturbation of the ER through mitochondrial dysfunction was confirmed by the use of rotenone as a mitochondrial inhibitor, which also caused upregulation of the UPR regulators ATF4 and CHOP (Cortopassi *et al.*, 2006).

Gene expression profiling has been completed in the skeletal muscle of a number mitochondrial encephalomyopathy (MEM) patients, including those with MELAS or Progressive, External Opthalmoplegia (PEO) caused by the m.3243A>G point mutation, or PEO caused by macrodeletions (Crimi *et al.*, 2005). Their results indicate that shared biochemical processes upregulated in all MEM patients include fatty acid metabolism and the urea cycle. ARG2 is localised to the mitochondria, and converts arginine to ornithine and is essential for amino acid metabolism. Reduction of arginine levels

because of ARG2 overexpression triggers apoptosis through conversion of nitric oxide (NO) to peroxynitrite, a metabolite toxic to mitochondria (Wiesinger, 2001).

Other predominant biological processes dysregulated in skeletal muscle of MEM patients, identified by Crimi and colleagues (2005) includes cell cycle regulation, genetic information processing, protein biosynthesis, metabolism, development and signal transduction.

6.1.2 Ragged-red fibres (RRFs)

RRFs visualised in skeletal muscle sections are a classic hallmark of mitochondrial disease and often used as an aid to diagnosis (Taylor *et al.*, 2004). However, although common to some diseases such as MERRF and MELAS, they are rarely observed in others such as LHON and NARP (Bourgeois and Tarnopolsky, 2004). They are also observed in normal aged muscle tissue (Cao *et al.*, 2001), other diseases such as inclusion body myositis (Horvath *et al.*, 1998) and can be induced by use of anti-retroviral drugs, such as zidovudine, which clonally expand pre-existing age-related mutations (Dalakas *et al.*, 1990, Payne *et al.*, 2011).

Single-fibre analysis indicates that RRFs demonstrate higher heteroplasmy levels compared to the 'normal' fibres from the same patient. The threshold level for fibres to become ragged-red is dependent on the mutation, the individual and even varies between fibres within some patients, showing overlap of the heteroplasmy levels in 'normal' and 'ragged-red' fibres. However, the threshold for a fibre to become ragged-red is generally considered to be >80% (Campos *et al.*, 2001, Nishigaki *et al.*, 2003, Ozawa *et al.*, 1998)

Research from Durham and colleagues (2006) indicates that with some mutations, but not m.3243A>G, maintenance of an absolute value of wild-type mtDNA molecules, as opposed to a heteroplasmy threshold, is crucial for retaining cytochrome c oxidase (COX)-activity in individual fibres. They also demonstrated highly variable mtDNA copy numbers in fibres of different sizes; together, this data could account for how there is variability in threshold levels for conversion to RRFs (Durham *et al.*, 2006).

COX-positive and -negative RRFs

RRFs can be either COX-positive or COX-negative. RRFs observed in MERRF patients are usually COX-negative; however, muscle samples of patients with different

mitochondrial diseases, such as MELAS, often show both COX-positive and COX-negative RRFs (Bourgeois and Tarnopolsky, 2004, Nishigaki *et al.*, 2003, Petruzzella *et al.*, 1994).

When Petruzella and colleagues (1999) investigated single-fibre analysis of m.3243A>G heteroplasmy levels in MELAS and PEO, they noticed that in both cases RRFs had much higher heteroplasmy levels compared to 'normal' fibres, and that COX-negative fibres had a slightly higher heteroplasmy than COX-positive fibres. MELAS (m.3243A>G) has a generally higher proportion of mutant mtDNA compared to PEO (m.3243A>G) in total; however, the homogeneous distribution of heteroplasmy levels means that in MELAS fewer fibres exceed the critical threshold of mutant levels to produce COX-negativity in fibres. In PEO, the distribution of mutant mtDNA is more heterogeneous, meaning, despite a lower overall mutation level, more fibres cross the threshold and lose COX activity (Petruzzella *et al.*, 1994).

The effect of fibre type on RRF and COX activity

The population of fibres in muscle tissue is diverse and can be generally categorised into three groups. Type I fibres are heavily reliant on oxidative phosphorylation and are slow twitch (tonic), providing sustainable but moderate strength. Type IIx fibres are reliant almost entirely on glycolysis and are fast twitch (clonic), providing rapid, high strength action but only for short durations before experiencing fatigue. Type IIa are an intermediate between type I and type IIx fibres, relying on both glycolysis and oxidative phosphorylation with moderately fast action but higher sustainability. Each fibre type expresses predominantly one myosin heavy chain isoform; myosin-7 (slow I); myosin-2 (fast IIa); and myosin-1 (fast IIx), with some overlapping expression evident in a subset of fibres (Scott et al., 2001).

Categorising fibres in MELAS patients as either type I or type II, as well as whether they are ragged-red or not, allowed Tokunaga and colleagues (1994) to show a higher percentage of type I fibres to be ragged-red than observed in type II fibres. It was also apparent that type I RRFs are generally COX-positive whereas type II RRFs are generally COX-negative. Interestingly, the difference in heteroplasmy level between type I and II ragged-red fibres was not statistically significant. Despite higher hybridisation signal for mtDNA in RRF compared to normal fibres, there was again no significant difference between RRF of different fibre types (Tokunaga *et al.*, 1994).

RRF specific expression changes

In situ hybridisation for mRNA and immunohistochemistry have been used to analyse the expression of particular genes and proteins specifically in RRFs. Myoglobin (Mb), involved in transport and storage of oxygen, was shown to have both mRNA transcript and protein upregulation in the RRF of mitochondrial disease patient biopsies (Kunishige *et al.*, 1996). As Mb has been shown to increase production of hydroxyl radicals, this was later shown to correspond to upregulation of ROS response proteins such as Mn-SOD, CAT and G-Px (Kunishige *et al.*, 2003). Similar immunohistochemical analysis has shown RRF specific upregulation of heat-shock 60 kDa protein 1 (HSP-60) and ubiquitin (UB), involved in regulation of protein folding and degradation (Sparaco *et al.*, 1993), and also neurotrophin-4 (NT-4), a signalling molecule predicted to be involved with skeletal muscle innervation (Walker and Schon, 1998) (Figure 6.1).

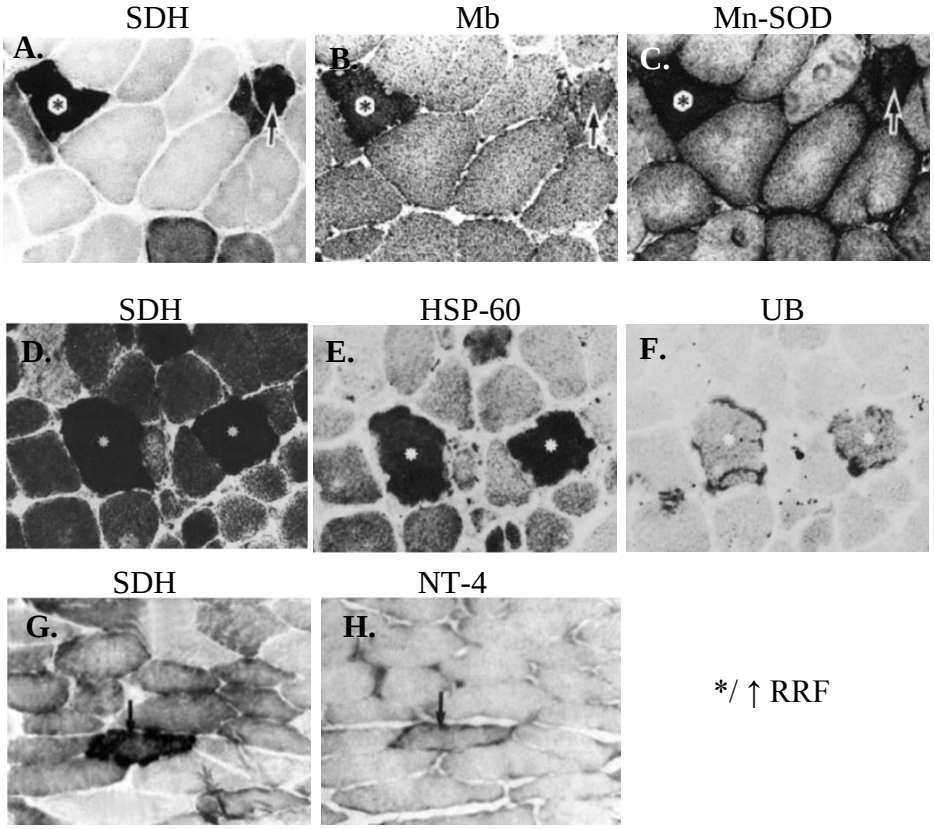

Figure 6.1 Immunohistochemical analysis of ROS response proteins in RRFs. Muscle biopsy sections from (A-C) a CPEO patient (Adapted from Kunishige *et al.*, 2003), (D-F) a KSS patient (Adpated from Sparaco *et al.*, 1993) and (G-H) a PEO patient (Adapted from Walker and Schon, 1998). (A, D, G) RRF identified by SDH staining, showing RRF specific upregulation of (B) myoglobin (Mb), (C) manganese-superoxide dismutase (Mn-SOD), (E) heat-shock protein 60 (HSP-60), (F) ubiquitin (UB) and (H) neurotrophin-4 (NT-4).

Figure 6.1 shows the dramatic upregulation of a set number of proteins in RRFs investigated with immunohistochemistry, comparable to *in situ* hybridisation to analyse mRNA levels. Unfortunately, analysis using these techniques requires predetermination of targets of interest and only semi-quantitative analysis of results. Microarray analysis allows investigation of a broad spectrum of genes; however, the use of tissue homogenates often does not reflect the gene expression in specific cell populations of interest (Betsuyaku *et al.*, 2001, Fink *et al.*, 2002). If attempting to elucidate the mechanism for RRF formation and identify novel related genes, it is important the signal is not diluted by gene expression from the unaffected fibres, typically representing the majority of fibres in a biopsy.

6.1.3 Identification of RRF and fibre types

Common histochemical stains used in the diagnosis of mitochondrial disease are combined COX-SDH and modified Gomori trichome staining. RRF acquired their name from their appearance with modified Gomori trichrome staining, where mitochondria in the subsarcolemma sequester the red stain and give a ragged-red appearance to fibres with increased mitochondrial mass. RRFs are also easily identifiable using singular SDH histochemistry (Figure 6.2).

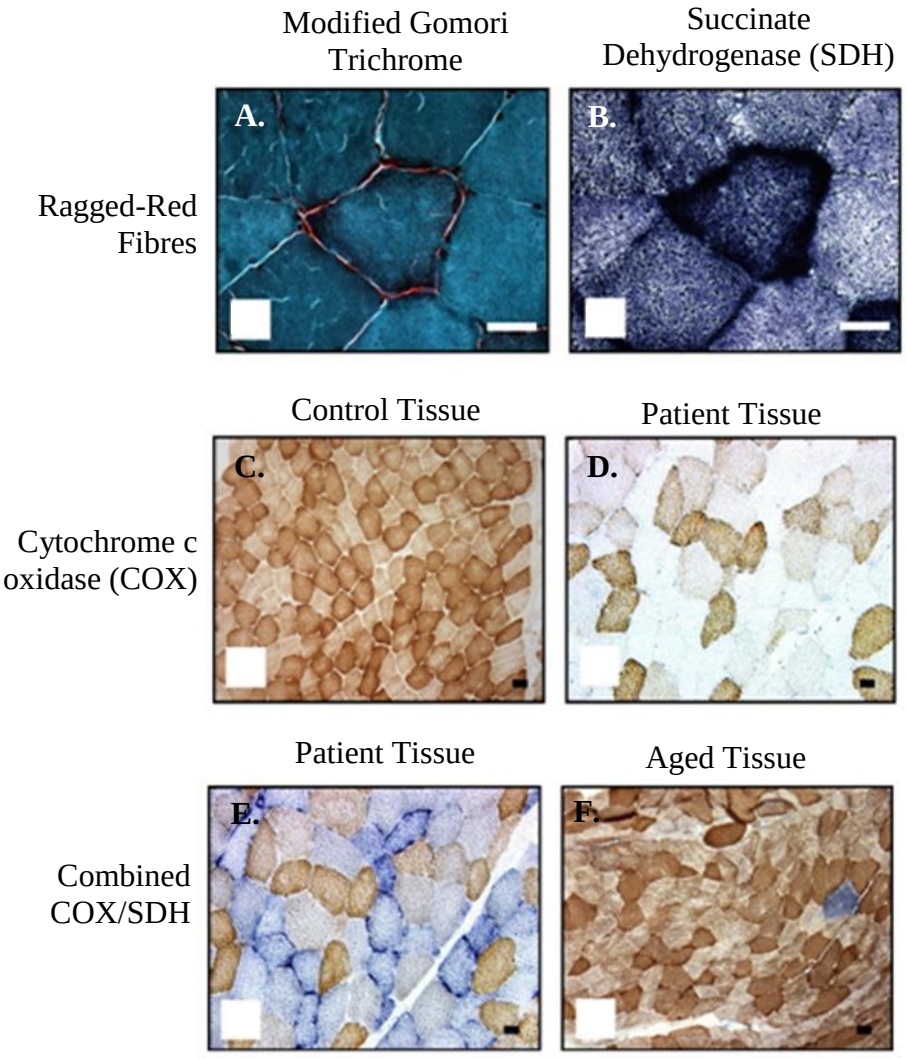

Figure 6.2 Histochemical stains of muscle sections in mitochondrial disease. Routine stains include (A) Gomori trichrome stain and (B) SDH stain identifying ragged-red fibres in muscle sections. (C) Normal COX staining in control muscle showing type I fibres with higher activity than type II fibres. (D) COX staining of patient muscle with mitochondrial disease showing many COX-negative fibres with no colouration, (E) highlighted by the use of sequential COX-SDH staining as COX-negative fibres retain SDH activity. (F) A single COX negative fibre as a result of ageing (Adapted from Taylor *et al.*, 2004). Scale bars = 30 µm.

Identification of fibre types using myosin-ATPase staining relies on pH sensitivity rather than the ATP hydrolysis rates (Brooke and Kaiser, 1970). The standard ATPase stain at ~9.4 pH shows type I fibres as light and type II fibres as dark, though manipulation of pH treatment can result in alternative staining patterns for further resolution of fibre typing (Figure 6.3).

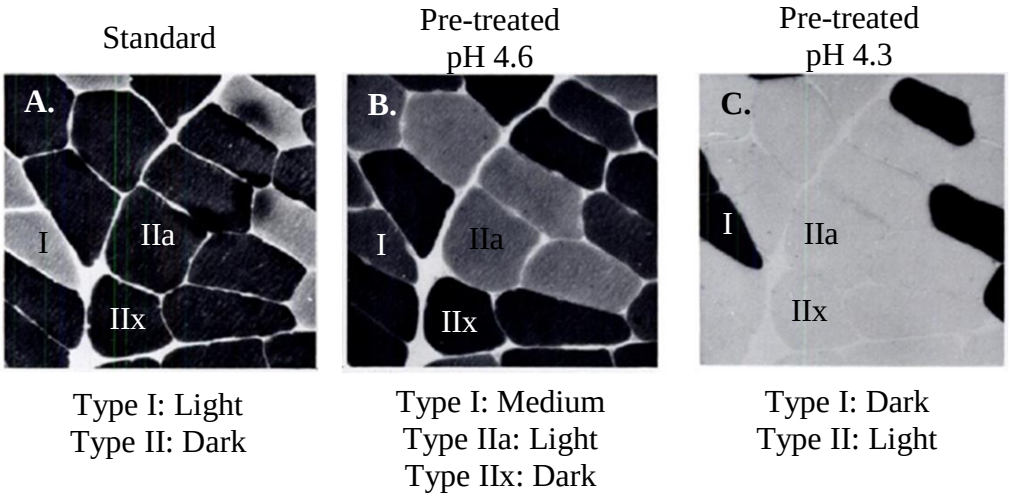

Figure 6.3 Myosin-ATPase staining for fibre typing. Myosin-ATPase staining at (A) standard alkali pH identifies all type II fibres by dark staining, whereas pretreatment with acid at (B) pH 4.6 distinguishes all three fibre types as IIa (light), I (medium) and IIx (dark) but (C) pH 4.3 identifies type I fibres by dark staining (Adapted from Brooke and Kaiser, 1970)

Immunohistochemistry

Although not regularly used in diagnostic investigation, it is possible to identify RRFs in muscle sections using immunohistochemistry. RRFs are characterised by having accumulation of mitochondria in the subsarcolemma of fibres and using antibodies targeted to mitochondrial proteins. This can show RRFs with more intense staining than surrounding fibres for some mitochondrial proteins. However, the heterogeneous nature of mitochondrial disease means mitochondrial protein expression can be variable between disease, patients and even fibres within the same patient (De Paepe *et al.*, 2009) (Figure 6.4).

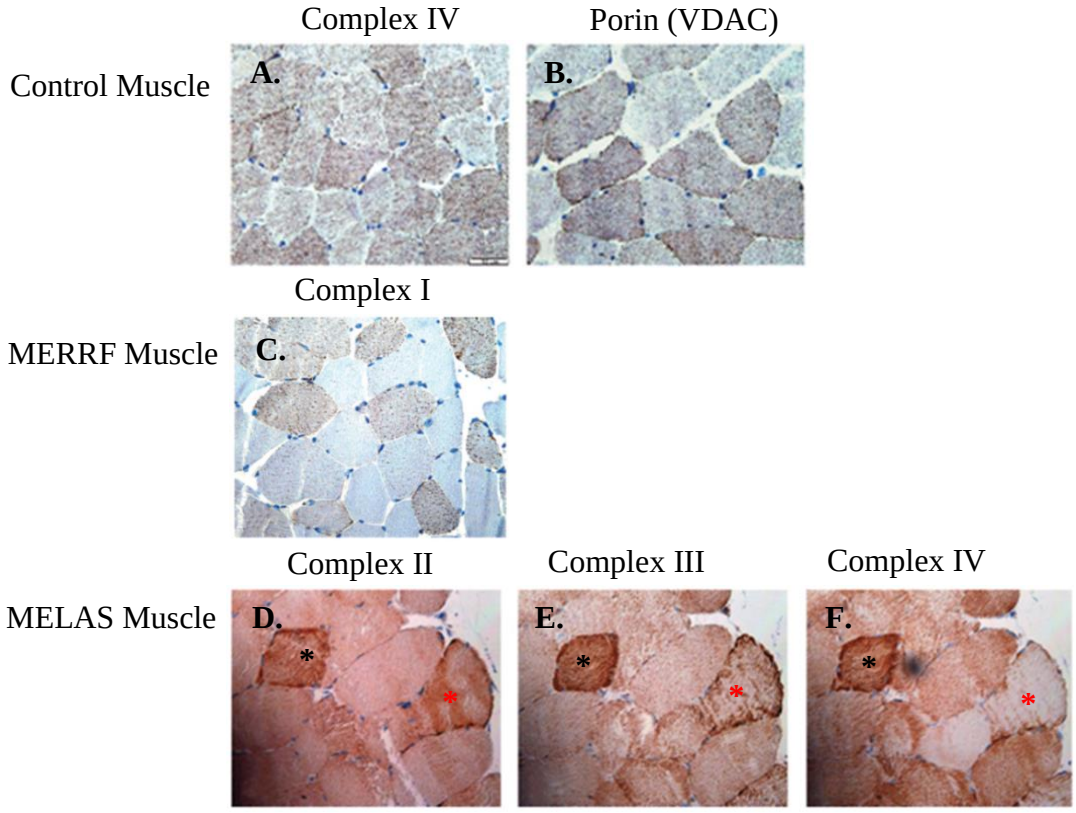

Figure 6.4 Immunohistochemical analysis of mitochondrial proteins. (A-B) Antibody staining of mitochondrial proteins in control muscle sections shows heterogenous intensity due to variation in mitochondrial mass between fibre types. (C) Heterogenous distribution of Complex I subunits in MERRF muscle sections. (D-F) Complex IV –positive and –negative RRF identified using mitochondrial subunit targeted antibodies (Adapted from De Paepe *et al.*, 2009).

Type I fibres have higher mitochondrial activity than both type IIa and particularly type IIx fibres, which are predominantly glycolytic. This explains heterogeneous staining pattern for mitochondrial proteins, even in control tissue (Figure 6.4 (A-B)). This can be exacerbated in mitochondrial diseases where expression of mitochondrial proteins becomes even more irregular (Figure 6.4 (C-F)).

Immunohistochemistry allows the use of multiple antibodies on one section when using fluorescently tagged antibodies, which is particularly useful when fibre typing muscle sections (Figure 6.5).

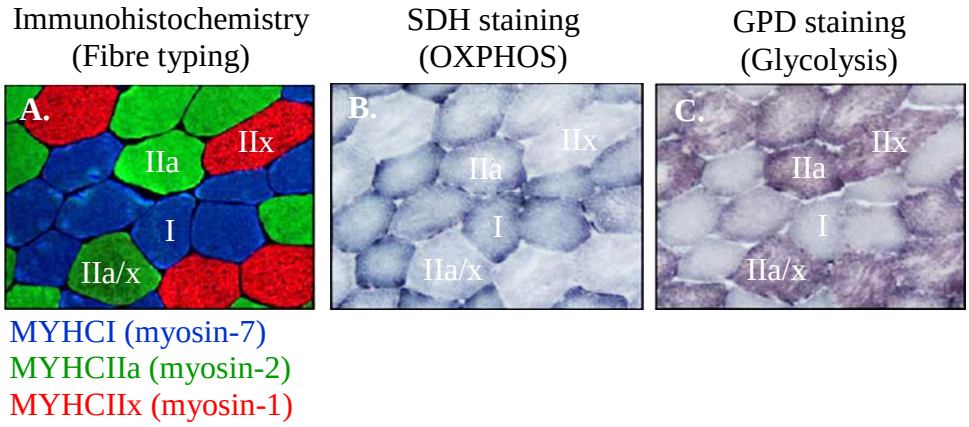

Figure 6.5 Immunohistochemical fibre typing and enzyme activities. Serial sections of human skeletal muscle. (A) using immunolabelling of different myosin isoforms to demonstrate fibre types (type I, myosin-7, blue; type IIa+a/x, myosin-2, green; type IIx, myosin-1, red). (B) SDH staining demonstrating high oxidative phosphorylation (OXPHOS) capacity in type I fibres, moderate in type IIa fibres and low in IIa/x and IIx fibres. (C) α-glycerophosphate dehydrogenase (GDP) staining demonstrating high capacity for glycolysis in all type II fibres, but lower in type I fibres (Adapted from Bloemberg and Quadrilatero, 2012).

This allows the possibility of fibre typing and identification of RRFs within one section, avoiding the use of serial sections. The heteroplasmy distribution can change along the longitudinal length of muscle fibres, meaning the nature of fibres from serial sections may vary when many sections spanning a large region need to be used (Durham *et al.*, 2006, Elson *et al.*, 2002).

6.1.4 RNA integrity

As short, single-stranded molecules, RNA is prone to degradation. RNA quality has been shown to have a dramatic impact on the qPCR measurement of gene expression, affecting both the signal intensity and the variability of RNA samples, with a minor effect on qPCR efficiency, giving a less reliable measurement of gene expression (Fleige *et al.*, 2006, Vermeulen *et al.*, 2011).

To ensure the quality of gene expression data, Bustin and colleague (2009) determined a structured set of guidelines to govern the standards of qPCR experiments, the 'Minimum Information for Publication of Quantitative Real-Time PCR Experiments' (MIQE) (Bustin *et al.*, 2009). The MIQE guidelines implore authors to provide adequate details on experimental design, sample description and RNA quality control and make sure all are of satisfactory compliance with requirements to produce accurate, reproducible gene expression data.

The gold standard for RNA integrity determination was achieved by measuring the ratio between the *28S* and *18S* rRNA bands on an agarose gel, which should be approximately 2:1 ratio, with degraded RNA having a lower ratio as the larger, 28S rRNA fragment degrades more rapidly. A ratio of 1.8 was considered to indicate high quality RNA suitable for downstream analysis. However, calculation of the *28S/18S* ratio is subjective to human interpretation and can give misleading results (Copois *et al.*, 2007).

In recent years, the RNA integrity has been most regularly analysed using microfluidic capillary electrophoresis chips such as the BioRad Experion System or Agilent 2100 Bioanalyzer. These systems generate information on RNA quantity and quality, providing not only the *28S/18S* ratio but generating a RNA Integrity Number (RIN), based on the *28S/18S* peak sizes and the appearance of short fragments in the 'fast' region (Schroeder *et al.*, 2006).

Microfluidic capillary electrophoresis specifically measures the integrity of rRNA genes, which are abundant enough to visualise. However, mRNAs are the target molecule of interest in most gene expression studies, and rRNA integrity might poorly reflect the state of mRNA transcripts. mRNA is known to degrade usually from the 5' direction, leading to development of a qPCR based technique comparing the relative levels of each end of an mRNA transcript. Both the RIN score and 3':5' assay have been shown to correlate well with RNA integrity (Auer *et al.*, 2003, Copois *et al.*, 2007, Nolan *et al.*, 2006a)

The final aspect of RNA quality is the purity of the sample, in relation to contaminants which may act as PCR inhibitors. These contaminants could be reagents from extraction or copurified components from the biological sample (Rossen *et al.*, 1992). Nucleic acid purity is typically measured using UV spectrophotometric analysis of absorbance at different wavelengths, with nucleic acids absorbing specifically at 260 nm, but possible contaminants absorbing at 230 or 280 nm. The effect of PCR inhibitors are most pronounced with absolute quantification from qPCR data, but may also affect relative quantification if the assays used are variably affected. The presence of PCR inhibitors in samples can be tested by use of the SPUD assay, whereby a fragment of DNA with no homology to sample being tested is amplified in the presence of either water or the

sample. No product must amplify from the nucleic acids in the sample, but presence of an inhibitor will affect the amplification of the other product (Nolan *et al.*, 2006b).

Technical obstacles to overcome

Formalin fixation and paraffin embedding is known to cause degradation and chemical modification of RNA transcripts (Goldsworthy *et al.*, 1999, Masuda *et al.*, 1999). Alternative solutions involve extraction from freshly frozen tissue samples (Guo and Catchpoole, 2003) using alcohol-based fixatives such as 70% ethanol or modified methacarn (8:1 ratio of methanol and acetic acid), which have been found to successfully preserve the morphology of tissue sections but also cause the least degradation to RNA within tissues (Cox *et al.*, 2006).

Recovery of intact RNA from immunolabelled or stained tissues is more difficult than for DNA or proteins, as immersion in aqueous solutions, for even short periods of time, makes RNA vulnerable to degradation by endogenous RNases (Tangrea *et al.*, 2011).

6.1.5 Research aims

To dissect the specific expression differences between ragged-red and normal fibres of an individual. Optimise a technique to identify the fibre type and location of RRFs within patient muscle sections and dissect them for RNA extraction and gene expression analysis. Crucial to the experiment is the preservation of RNA quality and maintenance of a stable gene expression profile once fibres have been dissected.

6.2 Materials and Methods

6.2.1 Sample information

The age and gender information for the control and patient tissue used in this study are found in Table 6.1.

Table 6.1 Muscle sample information. Two control and two MERRF patient muscle tissue was used in this study. The final samples for microarray analysis were age- and gender-matched.

Type	Purpose	Sample I.D	Gender	Age
Control	Assay Development	MCTB-0017	Male	52
Control	Microarray	MTCB-064	Male	61
MERRF	Assay Development	PFC-PM1947	Male	61
MERRF	Microarray	M0086-11	Male	58

6.2.2 Tissue processing and quality control

Muscle blocks were transported at all times in liquid nitrogen or on dry ice and must not thaw between cryosectioning. The cryostat was cleaned with 100% ethanol prior to cryosectioning and a new blade was used between samples to avoid contamination. For each sample, a muscle section was taken directly after cryosectioning to assess the starting quality of RNA in each muscle block. A RIN score >8 was required in freshly cut tissue.

Sections required for RNA extraction were stored at -80°C in individual 50 mL Falcon tubes to create an air and water tight seal and avoid cross contamination of sections.

6.2.3 Immunohistochemistry

Immunohistochemistry was used to determine the fibre type and the mitochondrial localisation in muscle sections. The antibodies used in these experiments are listed in Table 6.2.

Table 6.2 Antibodies used for immunohistochemistry. The table below lists the antibodies used for determining fibre type and mitochondrial localisation, indicating the species in which the antibody was raised (Ms, mouse; Rb, rabbit; Dk, Donkey, Gt, Goat) and the clonality (mAB, monoclonal; pAb, polyclonal), the concentration (Conc.) or dilution of the antibody used and the distributor information.

Type	Description	Antigen	Species	Conc. used (µg/ mL)	Distributor	Code
1°	Fibre Typing	Slow Myosin Heavy Chain	Ms mAb	1:5000*	Abcam	ab11083
1°	Mitochondria	Cytochome c	Rb pAb	0.1	Abcam	ab90529
1°	Mitochondrial mass	VDAC1 / Porin	Ms mAb	0.1	Abcam	ab14734
1°	Mitochondrial marker	MTC02	Ms mAb	0.5	Abcam	ab3298
2°	Alexa Fluor(R) 488 Conjugate	Anti-mouse (Ms)	Gt pAb	1	Invitrogen	A11001
2°	Alexa Fluor(R) 488 Conjugate	Anti-rabbit (Rb)	Dk pAb	1	Invitrogen	A21206

*Dilution factor given as antibody is in acites fluid.

High salt buffer immunolabelling

The addition of 2M NaCl to DEPC PBS has been shown to significantly increase RNA integrity from immunolabelled tissue sections through inhibition of endogenous RNases (Brown and Smith, 2009). All solutions were used ice-cold and the procedure carried out at 4 °C; all H_2O in solutions was pre-treated with DEPC (see Section 2.9.1). Fresh frozen sections were rinsed in PBS and immediately fixed in 70% ethanol, rinsed in PBS, and moved to 2 M NaCl PBS buffer (salt buffer). Sections were incubated for 2 h in primary antibody, then were washed for 2 x 5 min in salt buffer and incubated with secondary antibodies for 2 h. All antibodies were diluted in salt buffer at the concentrations specified in Table 6.2. The sections were then washed first in salt buffer, then in PBS to remove the salt and dehydrated in 70% and 100% ethanol for 3 min each. The sections were then air dried at ambient room temperature for 5 min and were then ready for laser microdissection.

Zenon® immunolabelling

Zenon® labelling technology noncovalently labels primary antibodies with fluorophores to eliminate the need for secondary antibody incubation. Zenon® fragments are specifically designed to target and bind to the Fc portion of the primary antibody only. As primary antibodies are pre-labelled separately, antibodies raised in the same species can be used together.

Using the Zenon® Tricolor Mouse IgG1 Labeling Kit #2 (for Blue, Green and Red Fluorescence Imaging), the Slow Myosin Heavy Chain antibody for fibre-typing was labelled with Alexa Fluor® 594 and the mitochondrial marker (MTC02) was labelled with Alexa Fluor® 488. Firstly, approximately 1 µg of primary antibody was diluted to 10 µL in PBS. As the Slow Myosin Heavy Chain is in ascites fluid, a dilution of 1:10 was used as an estimate and found to give efficient labelling. The dilution was incubated with 5 µL of the appropriate Zenon® mouse IgG labelling reagent for 5 minutes. Zenon® blocking reagent (at a ratio of 1:4) was used to quench any unbound labelled IgGs. Once the conjugate solution is blocked, it steadily loses potency as the fluorophore fragments unbind primary antibodies and become sequestered by the blocking proteins. Therefore, labelled but unblocked antibodies were stored at 4°C with the addition of 2 mM sodium azide and blocked in batches when required. Blocked antibodies were used within 30 minutes to prevent loss of signal. Conjugated Slow

Myosin Heavy Chain was used at a dilution of 1:1000, and conjugated mitochondrial marker (MTC02) was used at a dilution of 1:250.

6.2.4 Laser microdissection

The stage and slide mounts were cleaned with Ambion RNaseZap® to destroy any surface RNases. Excess extraction buffer (15 µL) was loaded into the cap of a 0.5 mL tube to account for evaporation during dissection. Each section was processed within one hour to prevent collection of seriously degraded material.

6.2.5 RNA extraction and cDNA synthesis

RNA was extracted using Arcturus® Picopure® RNA Isolation Kit (Life Technologies). Some muscle sections were collected directly into 0.5 mL tubes after cryosectioning. Sections were kept on dry ice, stored at -80°C or processed immediately. 10 µL 'Extraction Buffer (XB)' was added to sections in the tube and incubated at 42 °C for 30 min to lyse cells. The lysate was stored at -80 °C or immediately processed further.

When muscle sections were sampled from microscope slides, 20 µL 'Extraction Buffer (XB)' was pipetted directly onto the section, allowed to incubate for 15 s, agitated with the pipette tip and then moved to a 0.5 mL tube. The tubes were incubated at 42 °C for 30 min to lyse cells and the lysate stored at -80 °C or immediately processed further.

Cells were dissected directly into the extraction buffer and were lysed at 42 °C for 30 min. If more cells were required, the lysate was stored at -80 °C, otherwise they were processed immediately.

The rest of the protocol is followed as in Section 2.9.3, eluting the RNA in between 10-20 µL 'Elution Buffer (EB)'.

In control experiments, cDNA was synthesised using Superscript® III Reverse Transcriptase as described in Section 2.11.

6.2.6 Real-time qPCR

qPCR was performed as described in Section 2.12. 3' primers were designed across the last exon boundary and the 5' primers were designed around the first. High GC content in the 5' of *ACTB* prevented design of a suitable primer. Primers used in control experiments are presented in Table 6.3.

The average Ct value of control samples was used as the calibrator when doing ΔΔCt analysis. Each other control sample is also normalised against the average and provides a standard deviation for the control group.

Table 6.3 Primer information for real-time qPCR analysis of RNA quality. Primer sequences, positions and fragment sizes for use in control experiments to analyse the gene expression profile and transcript integrity of human reference genes.

Gene	Primer Sequence	Exon Junction (No. exons)	Dist. from 5'/ total bp	Size (bp)
ACTB-3'	F-GATGCAGAAGGAGATCACTGC R-ACATCTGCTGGAAGGTGGAC	5-6 (6)	1019/1812	131
GAPDH-3'	F-CTGACTTCAACAGCGACACC R-ATGAGGTCCACCACCCTGT	8-9 (9)	952/1310	133
B2M-3'	F-CACCCCCACTGAAAAAGATG R-TTCAAACCTCCATGATGCTG	2-3 (3)	329/987	112
GAPDH-5'	F-CTCTGCTCCTCCTGTTCGAC R-ACGACCAAATCCGTTGACTC	1-3 (9)	29/1310	112
B2M-5'	F-GGCATTCCTGAAGCTGACA R-TCTCTGCTGGATGACGTGAG	1-2 (3)	27/987	142

6.2.7 Microarray gene expression analysis

Microarray analysis was outsourced to AROS Applied Biotechnology AS (Skejby, Denmark).

The NuGEN Ovation Pico WTA System V2 (NuGEN Technologies, Inc; San Carlos, USA) was used to generate cDNA the microarray gene expression study. It is a whole transcriptome amplification system for preparing cDNA from as little as 500 picograms total RNA.

The GeneChip Human Genome U133 Plus 2.0 Array (Affymetrix) is the most comprehensive whole human genome expression array, with probes covering over 47,000 transcripts. Analysis was performed using the Affymetrix® Expression Console™ Software using the MAS5 algorithm, using the Affymetrix Micro Array Suite 5.0 (MAS 5.0) algorithm to identify differentially expressed genes.

Filtering process

Probes which were not detected at > 50 signal and present (P) in at least one sample were removed from the analysis. The fold change between each sample pair was calculated and each probe was binned into 1 of 6 categories. A cut-off threshold of 3-

fold up- or downregulation was established. Where the probes in normal and ragged-red fibres from the MERRF patient are similarly dysregulated compared to in the control, these were considered MERRF-specific. If probes in RRFs are dysregulated compared to those in normal fibres from the MERRF patient and control, these were considered RRF-specific. In instances where dysregulation is more prounounced in RRFs more than in normal fibres from the MERRF patient, these probes are considered 'exacerbated in RRF'. An overview of this filtering process can be found in Figure 6.6.

Bioinformatic analysis of regulated processes and pathways

Functional annotation and clustering was performed using The Database for Annotation, Visualization and Integrated Discovery (DAVID) v6.7 (Dennis *et al.*, 2003). Gene lists were always compared to the *Homo Sapien* background.

Functionally enriched pathways were processed and adapted from KEGG: Kyoto Encyclopedia of Genes and Genomes (Kanehisa and Goto, 2000).

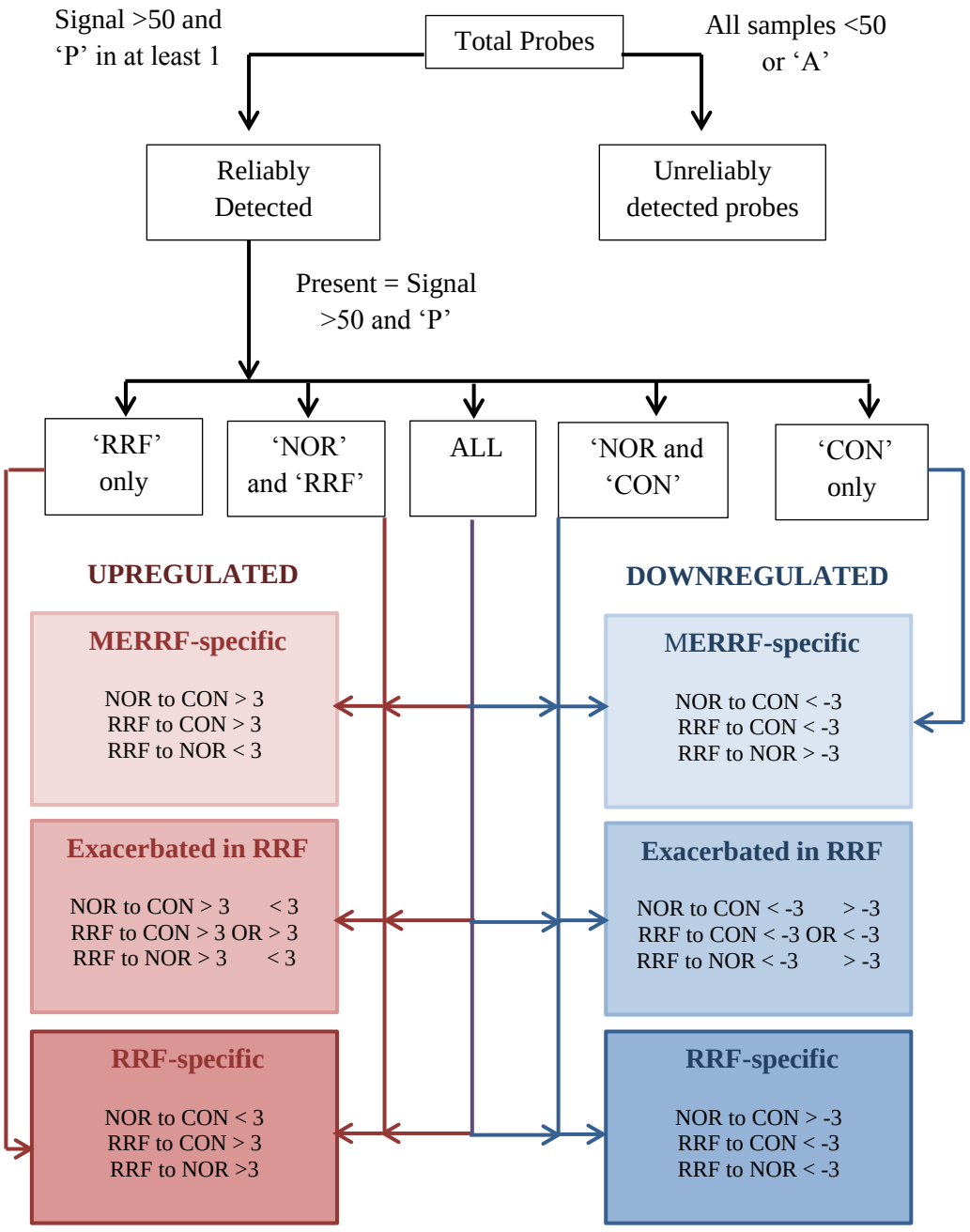

Figure 6.6 Filtering process for differentially expressed genes. Probes which were not detected at > 50 signal and present (P) in at least one sample were removed from the analysis. The fold change between each sample pair was calculated was allowed categorisation of probes first as up- or down-regulated and second, as 'MERRF-specific', 'exacerbated in RRF' or 'RRF-specific'.

6.3 Assay Development

The stages of developing a technique to study gene expression specifically in RRFs involved optimisation of a laser microdissection technique and a method to identify both fibre type and RRFs with RNA from dissected fibres maintained at high quality.

6.3.1 Analysis of RNA quality and quantity from laser microdissected cells

The difficulty with obtaining RNA from laser-assisted microdissected tissues is the processing time at room temperature needed to collect a sufficient amount of material for analysis. When RNA from 1-100 laser microdissected cells was analysed on the Agilent Bioanalyzer, there was no detectable signal to analyse the RNA quality (data not shown). To pool more cells for RNA analysis means longer times dissecting cells from tissue, which could compromise the RNA integrity, or pooling cell lysates or RNA post-dissection.

Ethanol Precipitation of RNA

Ethanol precipitation allows concentration of DNA or RNA samples without using heat or vacuum centrifugation. Ethanol precipitation was carried out following the protocol in Section 2.9.4. Samples were precipitated from 20 and 50 µL to 10 µL, and the RNA concentration and purity measured on the NanoDrop 2000 UV-Vis Spectrophotometer (Table 6.4).

Table 6.4 RNA purity and concentration before and after ethanol precipitation. Assessing the RNA purity and yield after ethanol precipitation to concentrate a sample. Values are given for volumes used, concentrations and absorbance ratios.

Before Precipitation				After Precipitation				
Vol. (µL)	Conc. (ng/ µL)	260/280 Ratio	260/230 Ratio	Vol. (µL)	Conc. (ng/ µL)	260/280 Ratio	260/230 Ratio	%
20	86.4	2.05	0.64	10	161.6	1.72	2.27	93.5%
50	86	2.07	0.66	10	410.5	1.86	2.32	95.5%

The yield calculated indicates that ethanol precipitation with high concentration samples from small and large volumes is an efficient way to concentrate RNA samples. The absorbance ratios also suggested the process removed some contaminants absorbing at 230nm (such as phenol, carbohydrates and EDTA), but has introduced some that absorb at 280nm (likely to be residual ethanol which can affect the absorbance at 280nm when measuring RNA in water). However, despite using ice-cold solutions and centrifugation

at 4 °C, it is possible that the process of ethanol precipitation could compromise the RNA integrity of the samples. The Agilent Bioanalyzer was used to investigate the effect of ethanol precipitation on rRNA integrity, and found that precipitation does not adversely affect the RNA integrity (Figure 6.7). Samples after precipitation were diluted to bring the RNA concentration within the limits of the machine specifications.

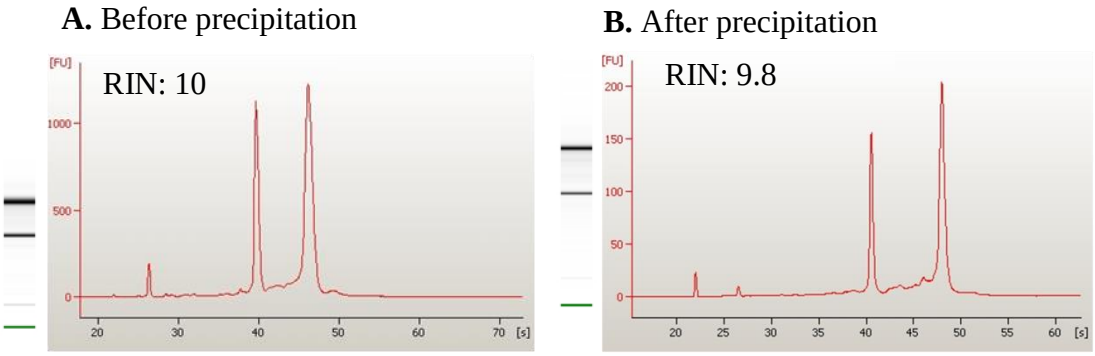

Figure 6.7 Quality of RNA after ethanol precipitation. RNA analysed on the Agilent Bioanalyzer shows the integrity of the rRNA transcripts are maintained at high levels (A) before and (B) after ethanol precipitation.

With ethanol precipitation providing a viable method of pooling RNA from many laser microdissection sessions, unstained control sections were prepared at room temperature with dehydration in 70% and 100% ethanol for 3 min each. Individual fibres were dissected with 100-200 cells from each section into dry 0.5 mL caps and RNA extracted individually. The ethanol precipitation protocol was then applied to a pool of the five RNA extractions and finally eluted in 10 µL of buffer. RNA was also collected from the remaining sections after laser microdissection, and the RNA from both analysed on the Agilent Bioanalyzer (Figure 6.8).

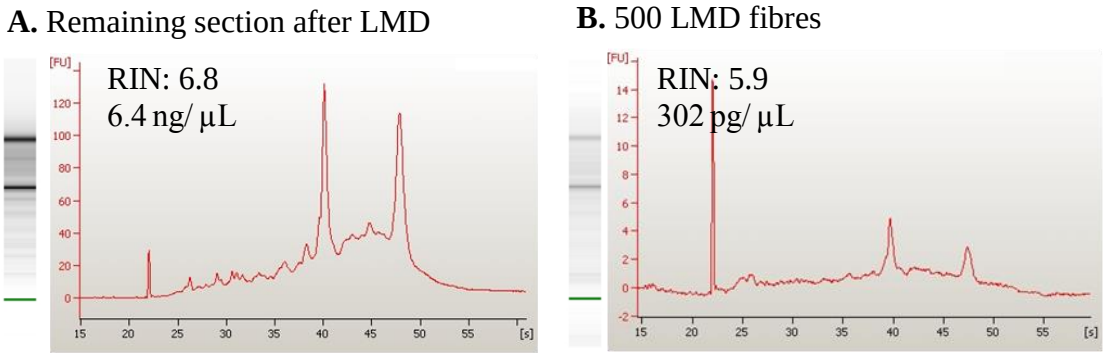

Figure 6.8 RNA quality after laser microdissection. Electropherogram and 'reproduced' gel images analysed by the Agilent Bioanalyzer of (A) RNA from sections post-laser microdissections and (B) RNA from 500 pooled laser microdissected fibres.

Despite evidence of some degradation and the inaccuracies associated with measuring quality and quantity of such low amounts of RNA from dissected fibres, it was apparent that a reasonable amount of RNA can be obtained from 500 fibres. Improvement in techniques to preserve RNA quality should also impact in the amount of RNA extracted.

The protocol was improved by dehydration in ice-cold ethanol solutions with the procedure carried out at 4 °C. Processing time for laser microdissection was restricted to 1 h after dehydration, and cells were dissected directly into 15 µL lysis buffer.

6.3.2 Analysis of RNA quality and quantity from stained tissue

A method for identifying RRFs and fibre types whilst preserving RNA is essential to obtaining high quality material from specific cell populations. RNA was analysed from whole sections stained with SDH or modified Gomori trichrome used to identify ragged-fibres (Figure 6.9).

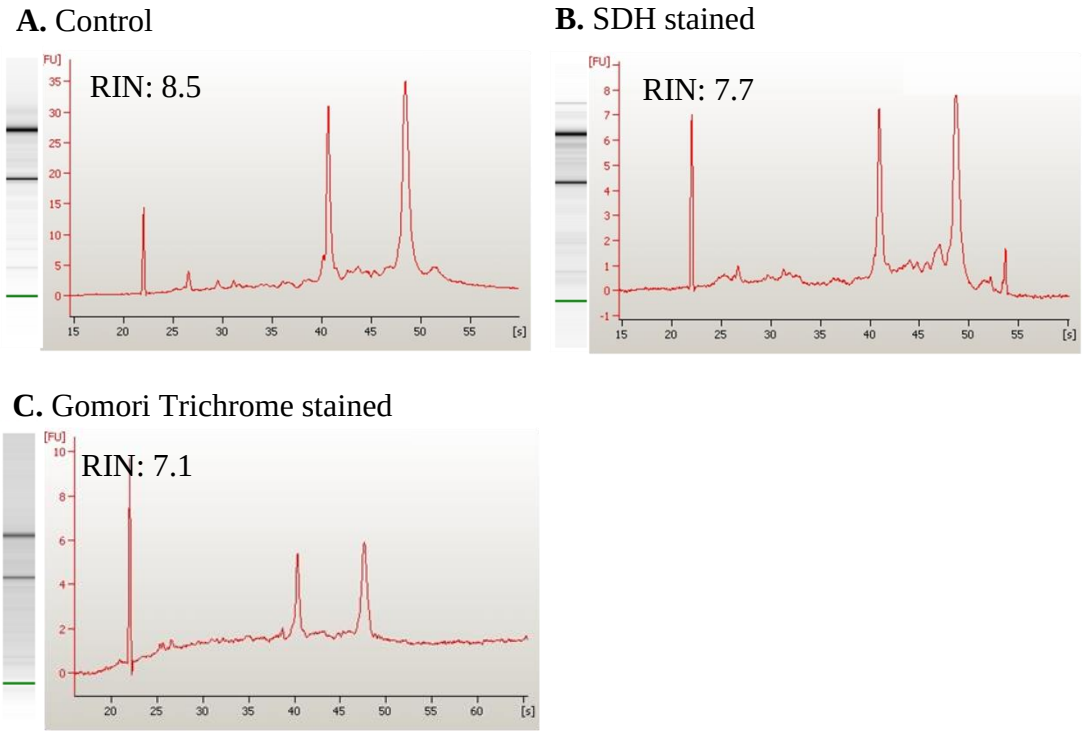

Figure 6.9 Quality of RNA extracted from unstained and stained muscle sections. Quality of RNA from (A) unstained muscle section is very high with a 8.5 RIN (B) RNA from SDH stained muscle sections shows only slight degradation, but lower concentration compared to unstained sections (C) RNA from Gomori trichrome stain muscle sections shows slightly higher degradation and a lower concentration compared to unstained sections.

Despite the RNA integrity seeming to remain high with SDH and even Gomori trichrome staining, the concentration of the sample was severely compromised by the presence of the stains (Table 6.5).

Table 6.5 RNA quality and quantity statistics from muscle sections. After electrophoresis and analysis on the Agilent 2100 Bioanalyzer the measured concentration and RIN number indicates that the histochemical stains have reduced the RNA quantity extracted but only slightly affected the quality of the RNA.

Sample	RNA Area:	RNA Concentration (pg/ µl):	rRNA Ratio [28s / 18s]:	RNA Integrity Number (RIN):
Control Section	227.46	1000.86	1.46	8.5
SDH	78.97	347.50	1.35	7.7
Gomori Trichrome	89.11	354.54	1.24	7.1

Studying the integrity of rRNA is only one technique to analyse the quality of RNA. It is also important to ensure manipulation of the samples is not affecting the relative

expression profiles of mRNA transcripts. This can be done using the ΔΔCt technique which normalises one gene against another to account for loading control, and then compares the relative expression of those genes to a control sample (in this case, unstained tissue). A fold change of 1 indicates the same expression profile in control and stained samples (Figure 6.10).

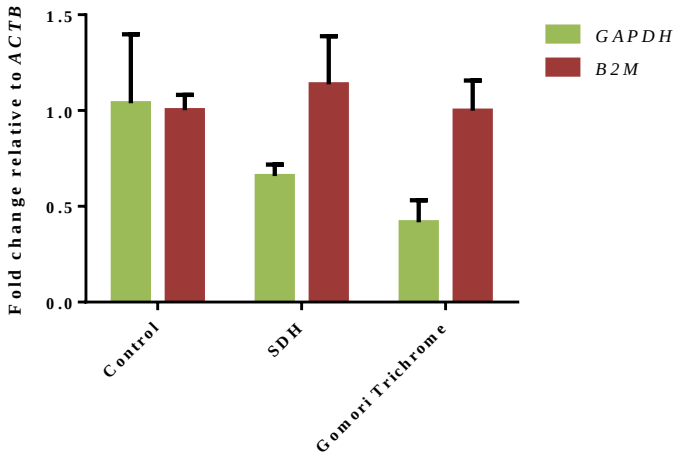

Figure 6.10 Stability of reference gene mRNAs in unstained and stained muscle sections. Fold change of expression of reference genes in SDH and Gomori trichrome stained muscles sections relative to unstained tissue. Error bars derived from the standard deviations.

Although *B2M* when normalised against *ACTB* remains satisfactorily close to a fold-change of 1, the decreased level of *GAPDH* compared to *ACTB* suggests a drop in signal for *GAPDH* in both SDH and Gomori trichrome stained sections.

6.3.3 Optimisation of immunohistochemistry techniques

The poor quality and quantity of RNA obtained from stained sections is likely due to the duration the section is exposed to aqueous solutions. Once sections are incubated in aqueous solutions, the endogenous RNases become activated and rapidly degrade RNA. This is also a challenge when looking to immunolabelling as a solution for rapid protocols for identifying RRF and fibre types. Even in the presence of an RNase inhibitor in PBS for only a 2 min incubation, there is some evidence of RNA degradation (Grimm *et al.*, 2004).

Firstly, it is essential to identify the most appropriate antibodies for identification of RRF and fibre types. The homology between myosin (MYH) genes makes selecting an antibody for fibre typing difficult. Since there are different subtypes of type II fibres,

antibodies for identifying fast-twitch fibres would need to recognise protein products from MYH1 and MYH2 (type II predominant) but not MYH7 (type I predominant). Anti-Slow Skeletal Myosin Heavy chain antibody (ab11083) is a monoclonal antibody which specifically reacts with adult human skeletal slow myosin in type I fibres, and is known to not react with fast-type myosin in type II fibres.

The expression of mitochondrial subunit proteins is known to have a fibre-type dependent, heterogeneous staining patterning, also highly variable in disease tissue (Figure 6.4). Three antibodies were chosen as candidates for identifying ragged-red fibres without showing fibre type specific intensity: Cytochrome c, the electron carrier between Complex III and IV of the electron transport chain; VDAC (Porin), an outer mitochondrial membrane channel; and a 'mitochondrial marker' antibody generated using semi purified protein preparation (MTC02).

Live fluorescent imaging on a microdissector can be less sensitive than conventional microscopy, and it is important that RRF are easily identifiable using both technologies. Muscle sections (12 µm) from control and MERRF patients on PEN-membrane slides were immunolabelled with these antibodies, targeted by an Alexa Fluor® 488 conjugated secondary antibody, and visualised on the Leica AS LMD (Leica Microsystems) using the FITC filter (Figure 6.11).

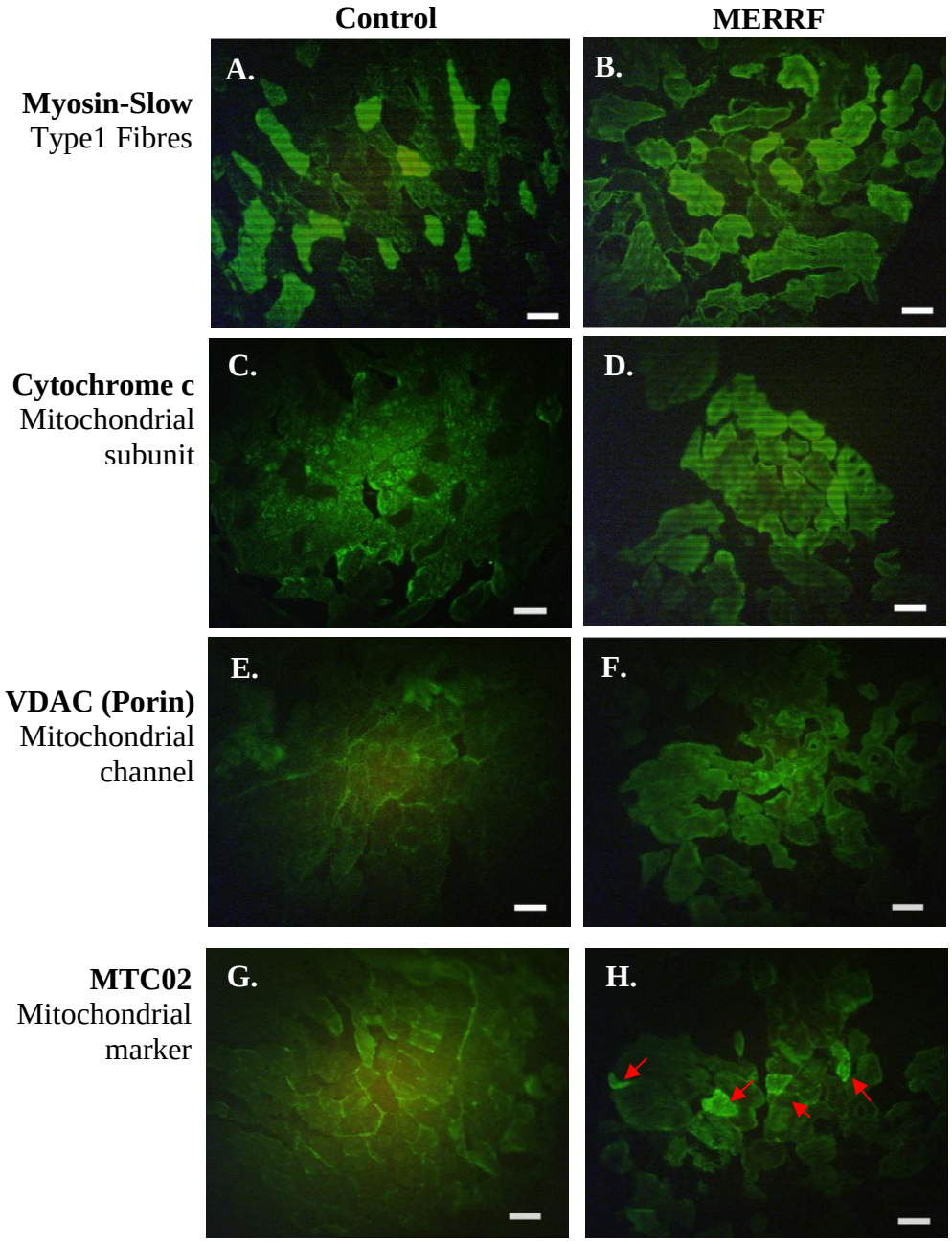

Figure 6.11 Laser microdissector imaging of fluorescence immunohistochemistry in muscle sections. (A, C, E, G, I) Control muscle sections and (B, D, F, H, J) MERRF muscle sections stained on PEN-membrane slides for (A, B) mysosin-slow, (C,D) cytochrome c, (E,F) VDAC (Porin), (G,H) Mitochondrial marker (MTC02). Red arrows indicate RRF. Scale bar = 100 µm.

Myosin-Slow shows clear staining of a subset of fibres, easily discerning type I from type II fibres. Cytochrome c shows mosaic staining in control tissues, though many more fibres than either type I or type II alone. This implies the intensely-staining cells are a combination of both oxidative type I and IIA fibres. The negatively-staining fibres are likely type IIx/d glycolytic reliant fibres. Both VDAC and 'mitochondrial marker'

antibodies showed similar staining patterns; however the intensity of 'mitochondrial marker' staining is higher and the increased signal aids in clear identification of individual cells with much higher mitochondrial mass (RRFs).

Control and MERRF muscle tissue sections on glass slides were co-stained for nuclei (DAPI) with MYH-slow or 'mitochondrial marker' (MTC02). Imaging of control and MERRF tissue was completed on an AxioImager (Zeiss) using an ApoTome (Figure 6.12).

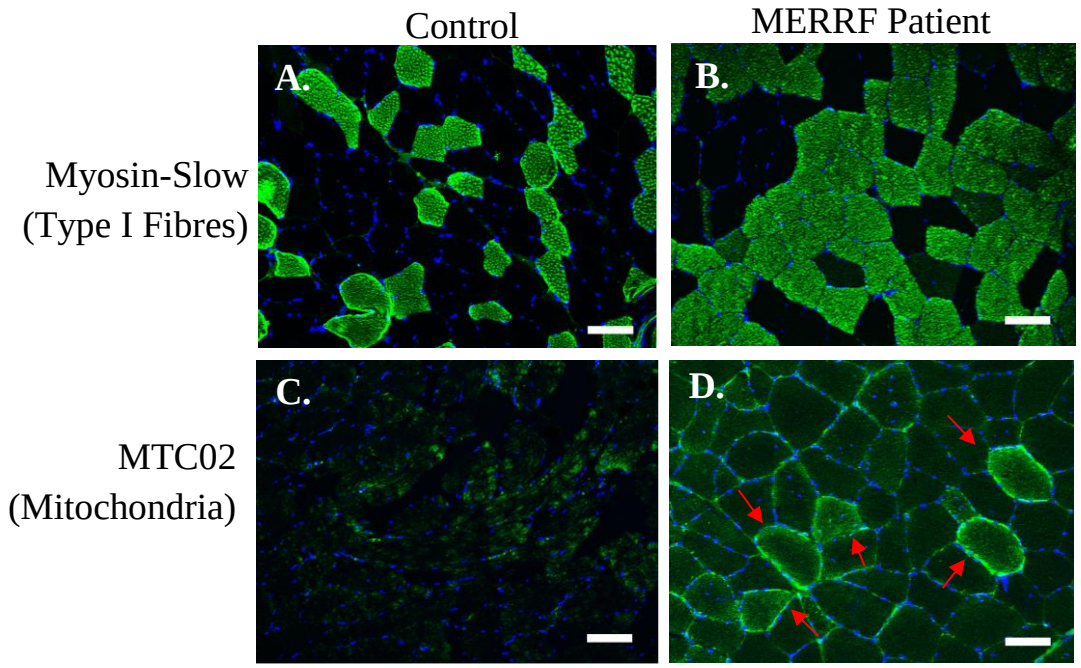

Figure 6.12 Fluorescent imaging in muscle sections. Immunolabelling in (A, C) control tissue and (B, D) MERRF tissue for (A-B) Myosin-slow and (C-D) 'mitochondrial marker' and counter stained for nuclei (DAPI; blue). Red arrows indicate potential RRFs.

In Figure 6.12A-B it is noticeable that there is a higher percentage of type I than type II fibres in MERRF patient muscle than in the control. Fibre type abnormalities are common to mitochondrial disorders, usually resulting in type I fibre predominance (T1FP), but sometimes in type II fibre predominance (T2FP), and often include variations in size and fibre atrophy (Enns *et al.*, 2005, Makino *et al.*, 2000). The pathogenesis of T1FP is postulated to be a compensatory mechanism to increase the energy capacity of the muscle by having a higher percentage of purely oxidative fibres (Koo *et al.*, 1993).

There are clearly fibres with higher intensity of mitochondrial marker (MTC02) which are suspected to be RRF (indicated by red arrows in Figure 6.12B). It is important to establish that the fibres identified by immunohistochemistry are the same as would be conventionally considered as RRF, as identified by modified Gomori trichrome or SDH histochemistry. This is evident when using both visualisation techniques on serial sections of MERRF patient muscle (Figure 6.13).

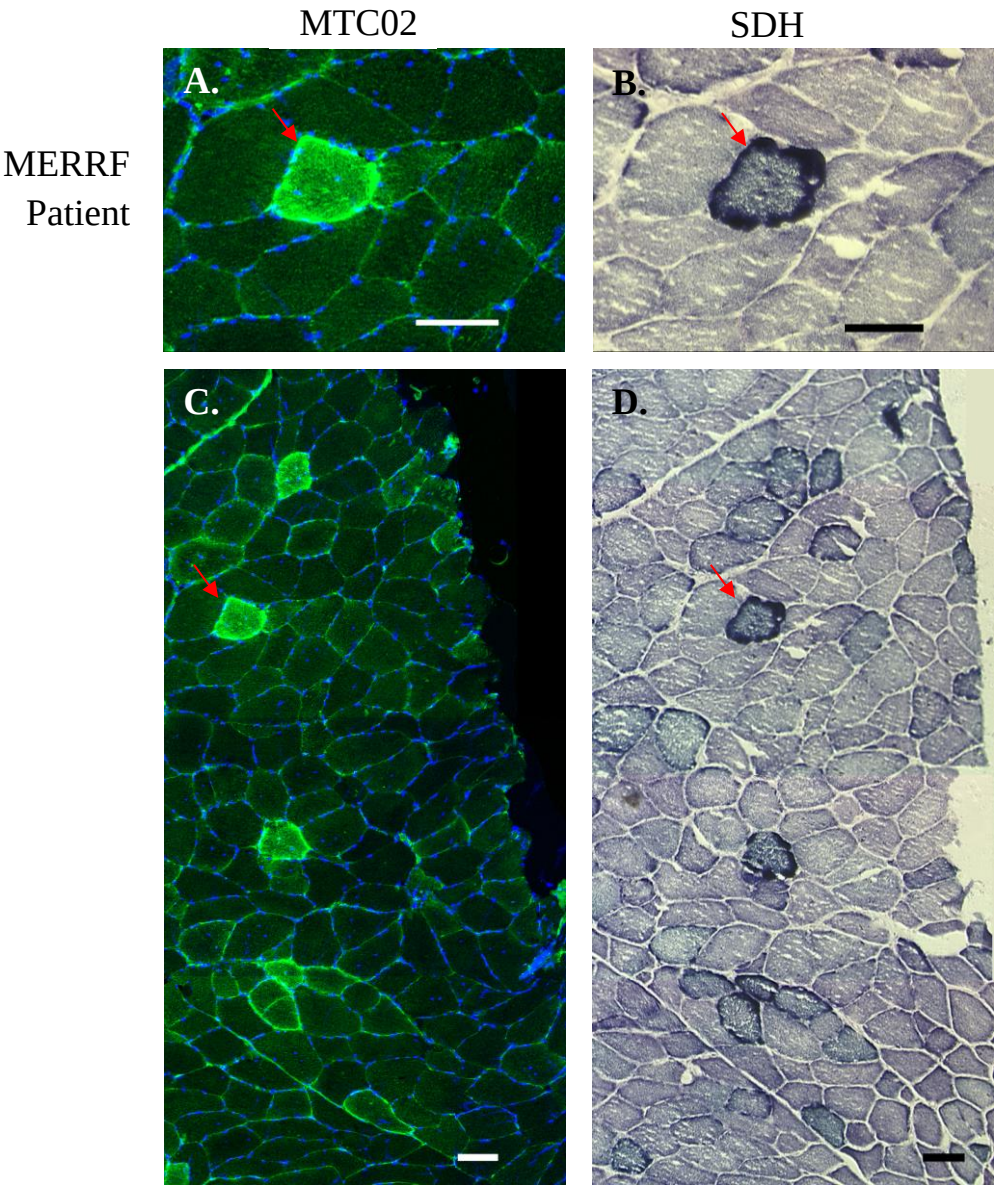

Figure 6.13 Confirmation of immunhistochemical identification of RRFs. (A,C) Immunohistochemistry using mitochondrial marker antibody (MTC02; green), co-stained for nuclei (DAPI; blue) and a serial section (B,D) with SDH histochemistry. (A,B) An individual RRF identified specifically by both immuno- and SDH histochemistry and (C,D) a large portion of section showing similar intensity patterns for MTC02 and SDH staining. Red arrows indicate the same fibre. Scale bar = 100µm.

Despite subtle differences in staining intensity, explained by the heterogeneous nature of fibres along their longitudinal profile (Durham *et al.*, 2007), the pattern for 'mitochondrial accumulation' visualised by SDH and immunohistochemistry is comparable not only for individual fibres but across large areas of sections, as shown in Figure 6.13-C,D .

Preservation of RNA during immunohistochemistry

Standard immunohistochemistry requires long antibody incubations in aqueous buffers, typically not compatible with preservation of RNA quality. One method developed for RNA preservation during immunolabelling uses the addition of salt (NaCl) into the buffers used for washes and antibody incubations. RNA quality was investigated using electrophoresis and rRNA integrity analysis, maintenance of stable gene expression profiles, and 5' to 3' signal assays and concluded 2 M NaCl included in buffers gave almost identical preservation to the commonly used RNase inhibitor RNAlater® from Ambion (which was found to be incompatible with immunolabelling) and better than inclusion of RNaseOUT® from Invitrogen (Brown and Smith, 2009).

Another method of improving RNA preservation is to use much shorter antibody incubation times with fluorescently labelled primary antibodies, using direct labelling kits such as Zenon® IgG Labelling Kits (Molecular Probes, Invitrogen).

Serial sections were either sampled freshly from sections, after 3 min dehydration in 70% and 100% ice-cold ethanol, after 5 h incubation in DEPC water, after immunolabelling in high-salt buffer, after using the standard Zenon® protocol but with standard secondary antibodies rather than fluorescently-tagged primary antibodies or using a modified version of the Zenon® protocol including 95 °C pretreatment of blocking buffer and only a 20 min antibody incubation period at 4 °C. RNA was extracted and analysed on the Agilent Bioanalyzer (Figure 6.14).

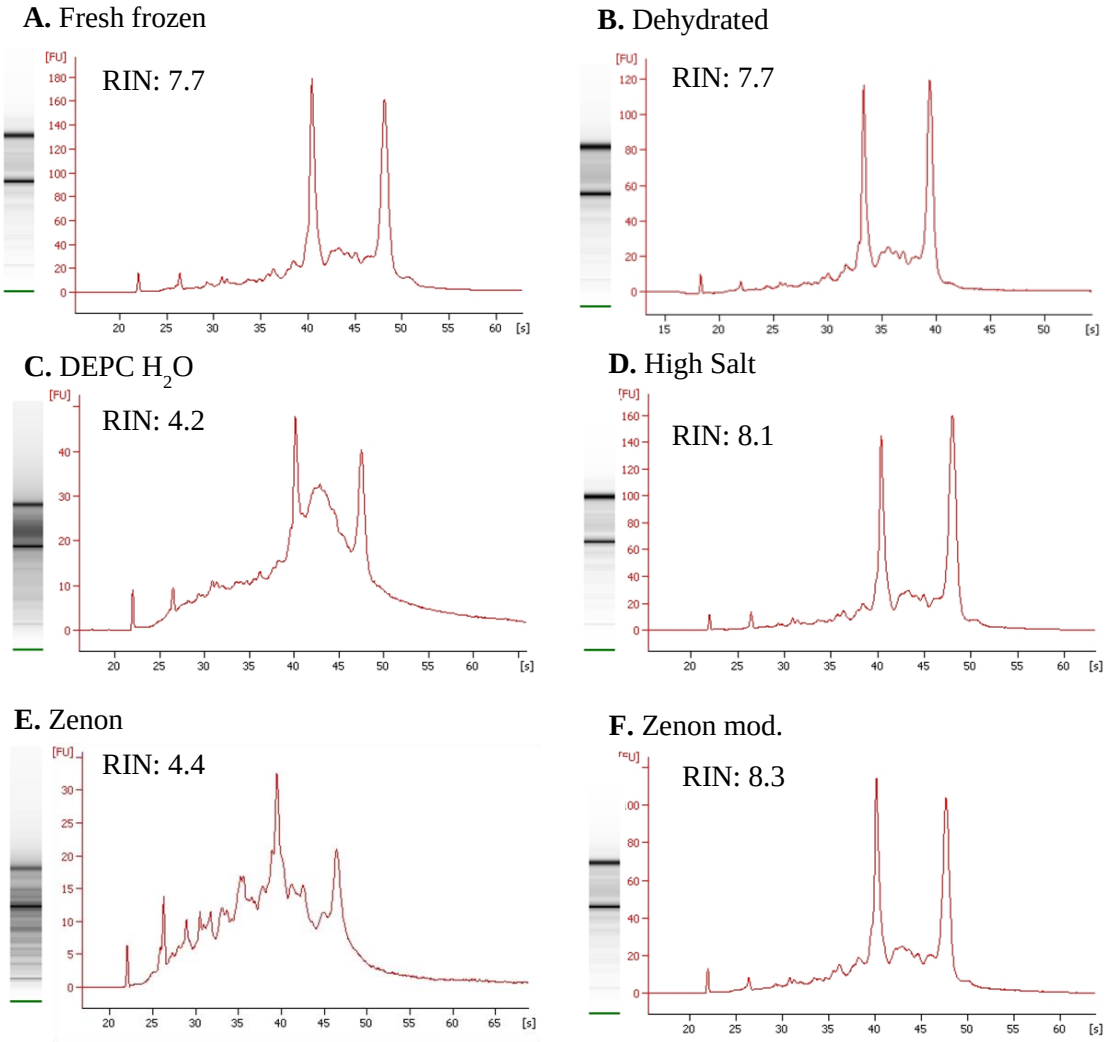

Figure 6.14 RNA integrity in immunolabelled sections. Control muscle sections were (A) sampled immediately after thawing, (B) after only dehydration, (C) after long incubation in just DEPC water, (D) after immunolabelling in high-salt buffer (High Salt), using the standard Zenon® protocol (Zenon) or using a modified version of the Zenon® protocol (Zenon mod.). Electropherograms and RIN scores indicate high preservation of RNA when using either the High-Salt or Modified Zenon® protocol.

The reference gene expression profile and 3'-5' assay was performed on RNA extracted from immunolabelled sections (Figure 6.15).

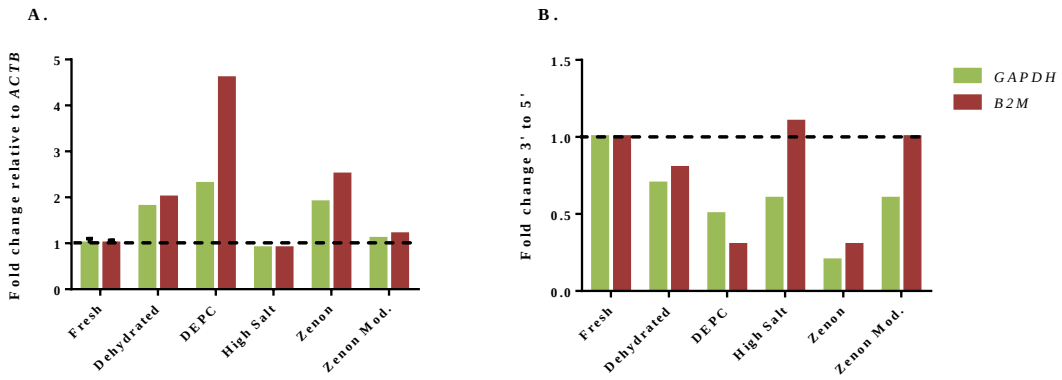

Figure 6.15 mRNA profile integrity during immunhistochemistry. (A) The relative gene expression of the reference genes *ACTB*, *GAPDH* and *B2M* were measured in RNA (cDNA) extracted from muscle sections treated with different immunolabelling conditions. The ΔCt for combinations of these reference genes were normalised against a control sample from fresh, untreated tissue to obtain fold changes (ΔΔCt). (B) 5' to 3' assay for *B2M* and *GAPDH* comparing the relative fold change of each end of the mRNA transcript. Fold change ~1 (dashed line) indicates no difference in gene expression profile from the control sample.

The 3'-5' assay reveals loss of *GAPDH* 5' sequence, even when only dehydrating the samples in ethanol, without immunolabelling. Both the high-salt buffer and modified Zenon® protocol offer a good solution to preservation of RNA during immunohistochemistry compared to using standard aqueous solutions such as DEPC water or PBS.

6.3.4 Analysis of RNA quality and quantity for immunolabelled and LMD fibres

Immunohistochemistry with high-salt buffer was tested on control muscle with only MYH-Slow antibody staining for type I fibres. The staining pattern and intensity of fluorescent signal was comparable to that of tissue stained using the standard technique, and type I fibres were easily identified and dissected (Figure 6.16).

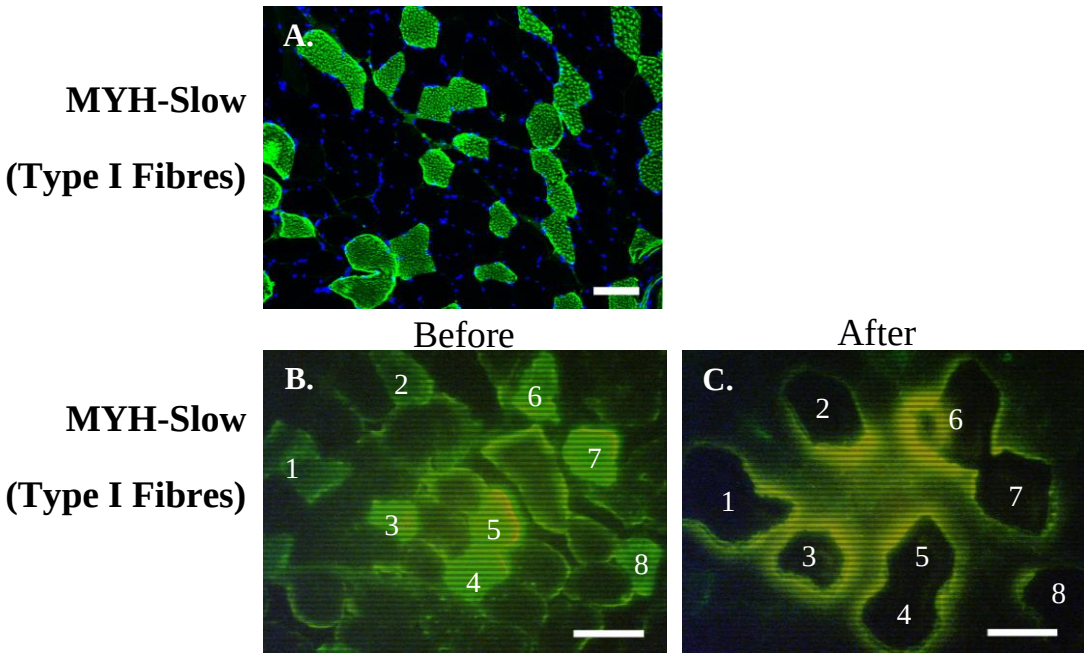

Figure 6.16 Laser microdissection of type I muscle fibres. Control muscle sections were labelled with MYH-Slow in high-salt buffer. (A) Mounted on glass slides and counterstained with DAPI for nuclei imaging. (B-C) Mounted on PEN-membrane slides and visualised (B) before and (C) after laser microdissection of Type I immunofluorescent fibres (numbered 1-8). Scale bar = 100µm.

Sections were processed within a maximum of a 1 h period from ethanol fixation. 125 fibres were pooled into each cap containing extraction buffer. After incubation at 42 °C lysates may be stored safely at -80 °C, which is crucial for the ability to pool samples from separate LMD sessions. Fibres were pooled either before application to the extraction column or were pooled via ethanol precipitation after extraction. The RNA was reverse transcribed to cDNA, and the gene expression profiles of three reference genes analysed by qPCR and the fold changes calculated (Figure 6.17A). Amplicons from the 5' and 3' of *GAPDH* and *B2M* were compared to assess RNA quality (Figure 6.17B).

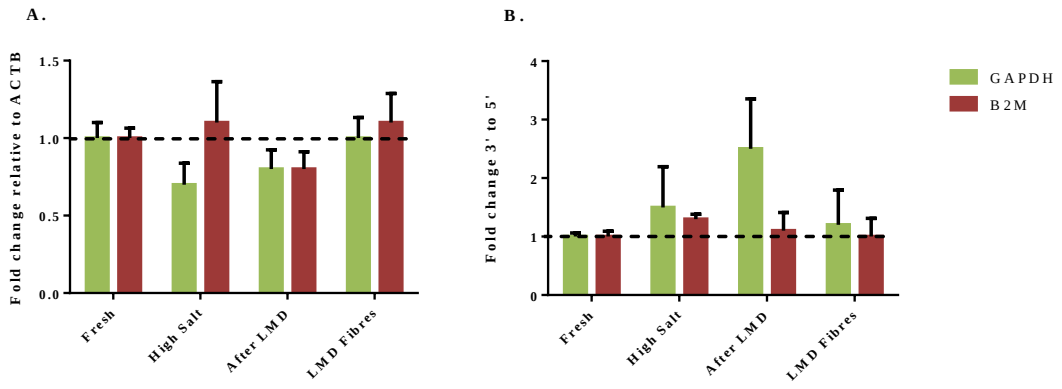

Figure 6.17 mRNA transcript profile and integrity during laser microdissection. (A) The expression of the reference genes *GAPDH* and *B2M* relative to *ACTB* were measured from muscle sections before and after laser microdissection (LMD). (B) Amplicons from the 5' and 3' region of both *GAPDH* and *B2M* were compared to assay for RNA quality. The ΔCt for these reference genes were normalised against a control sample from fresh, untreated tissue to obtain fold changes (ΔΔCt). A fold change of 1 (dashed line) indicates no difference in gene expression profile from the control sample.

Comparison of expression in laser microdissected tissue compared to muscle homogenates might not be appropriate for *GAPDH* as different fibre types have variable amounts *GAPDH* protein and only Type I fibres were dissected (Galpin *et al.*, 2012).

Zenon® Molecular Probes

Zenon® Mouse IgG Labelling Kits allow direct labelling of primary antibodies with fluorophores to allow one-step immunolabelling of target proteins and the use of multiple antibodies raised in the same species. Since both the MYH-Slow and MTC02 antibodies are raised in mice, this kit enabled us to target both proteins on the same section without having to find suitable alternative primary antibodies from a different species, and allows for a shorter incubation time which can aid preservation of the RNA in the muscle samples.

The fluorophores are bound to a Fab fragment which is directed against the Fc portion of antibodies from a particular species. They are not covalently bound, and consequently the protocol for immunohistochemistry with the Zenon® labelling kit recommends fixation with PFA after antibody incubation to prevent dissociation of the fluorophore from antibody. As direct labelling can sometimes have reduced fluorescent intensity the protocol also recommends incubation with a detergent such as triton X-100 to increase the permeability of the section. The protocol developed for maintaining

RNA integrity during immunohistochemistry relies on the use of a high salt buffer and shorter incubation times, so it is important to establish whether the PFA fixation and triton X-100 treatment is necessary and also whether the fluorophore and antibody remain bound when used in a high-salt buffer instead of standard PBS (Figure 6.18).

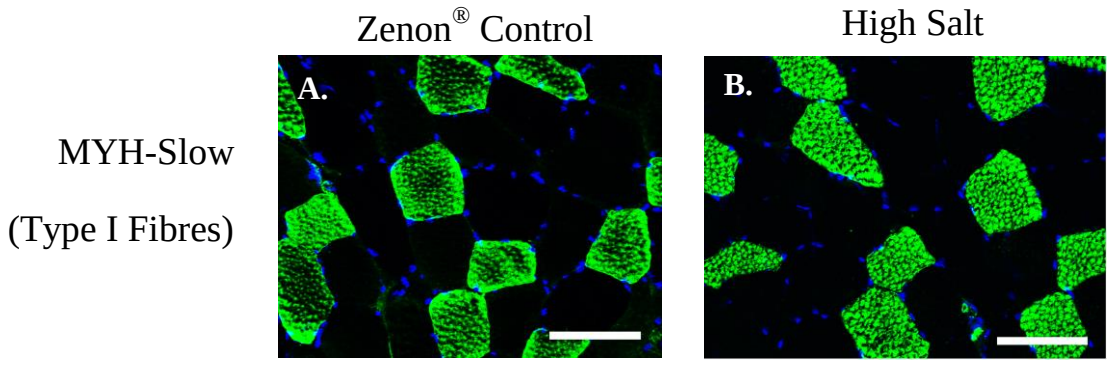

Figure 6.18 Immunohistochemistry using Zenon® labelling kits. A comparison of immunohistochemistry for MYH-slow using (A) the standard Zenon® fluorphore conjugated antibody labelling with tritonX-100 and PFA fixation and (B) labelling without tritonX-100 permeabilisation and PFA fixation and using a high-salt buffer. Scale bar = 100µm.

Immunohistochemistry with high-salt buffer is compatible with the Zenon® labelling kits. The staining from standard immunolabelling with secondary antibodies shows similar patterns to that using the Zenon® labelling kit protocol and there is no reduction in fluorescent signal when not using triton X-100 or PFA fixation and with the use of high-salt buffer instead of standard PBS.

The multiplex assay is capable of identification of type I and type II RRFs in the muscle tissue of patients with MERRF (Figure 6.19).

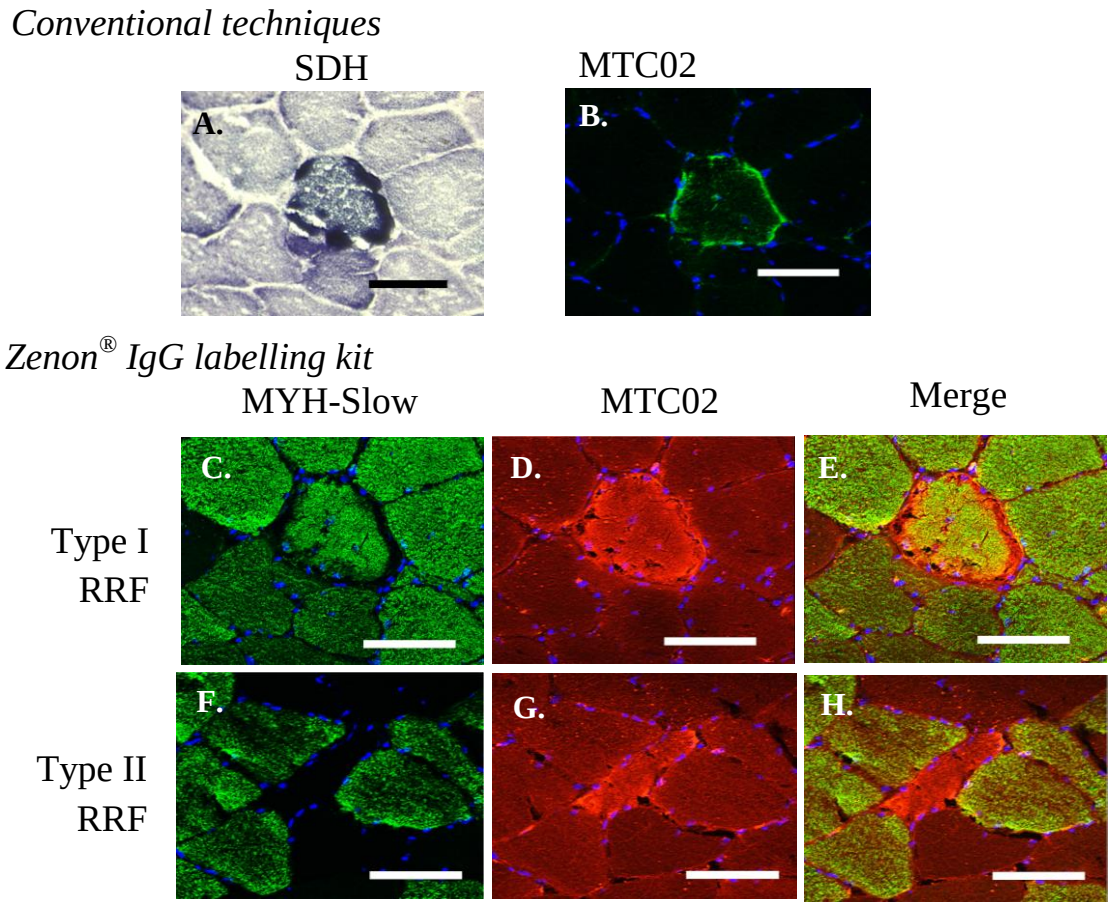

Figure 6.19 Fibre type and RRF identification using Zenon® IgG labelling kits. RRFs were identified by standard techniques such as (A) SDH histochemistry and (B) conventional immunohistochemistry using mitochondrial marker antibodies (MTC02). Zenon® IgG labelling technology was used for multiplex immunohistochemistry of (C,F) MHC-Slow (Green) and (D,G) MTC02 (Red). Merged images demonstrate the appearance of type I RRF (E) and type II RRF (H). (A-E) Images of the same fibre in serial sections identified using (A) SDH, (B) conventional labelling or (D) using Zenon® technology. Scale bar = 100µm.

All successfully optimised components of the staining procedure were combined for the final protocol. An overview of the final protocol process can be found in Figure 6.20.

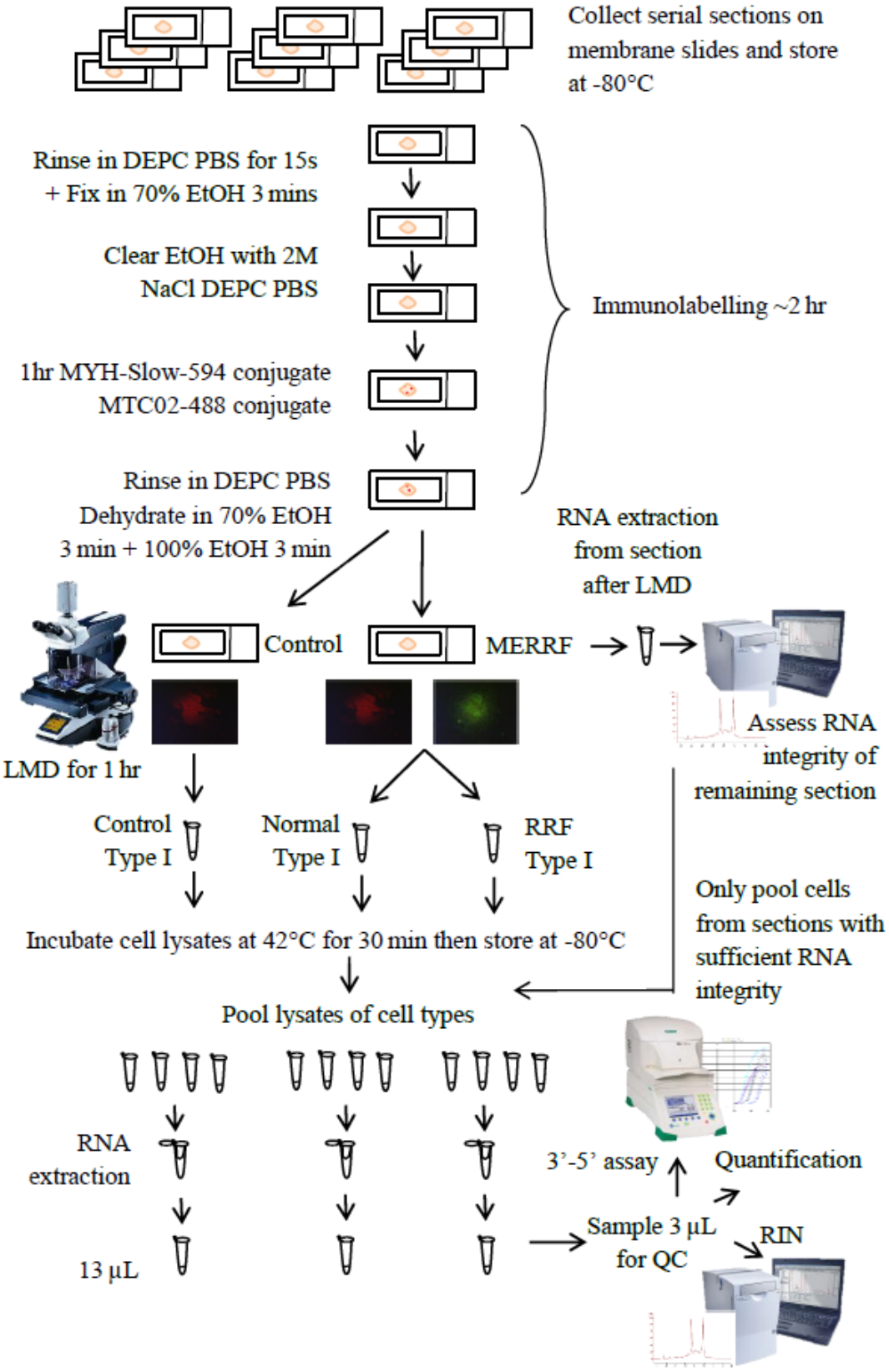

Figure 6.20 An overview of the final experimental procedure. The optimised procedure for preparation, staining and dissection of muscle fibres and the extraction and quality control of RNA from the dissected tissue.

6.4 Results and Discussion

6.4.1 Preparation of final samples

The tissue samples were collected from the muscle biopsy of a 58 year old male diagnosed with MERRF and an age-matched control male who donated muscle whilst undergoing knee surgery.

Muscle sections for both participants were dual-stained for MYH-Slow and MTC02 to simultaneously identify type I fibres and RRF (patient only) (Figure 6.21). Type I, normal fibres were dissected from the control (CON) and MERRF patient (NOR). Type I, RRFs were dissected from the MERRF patient (RRF).

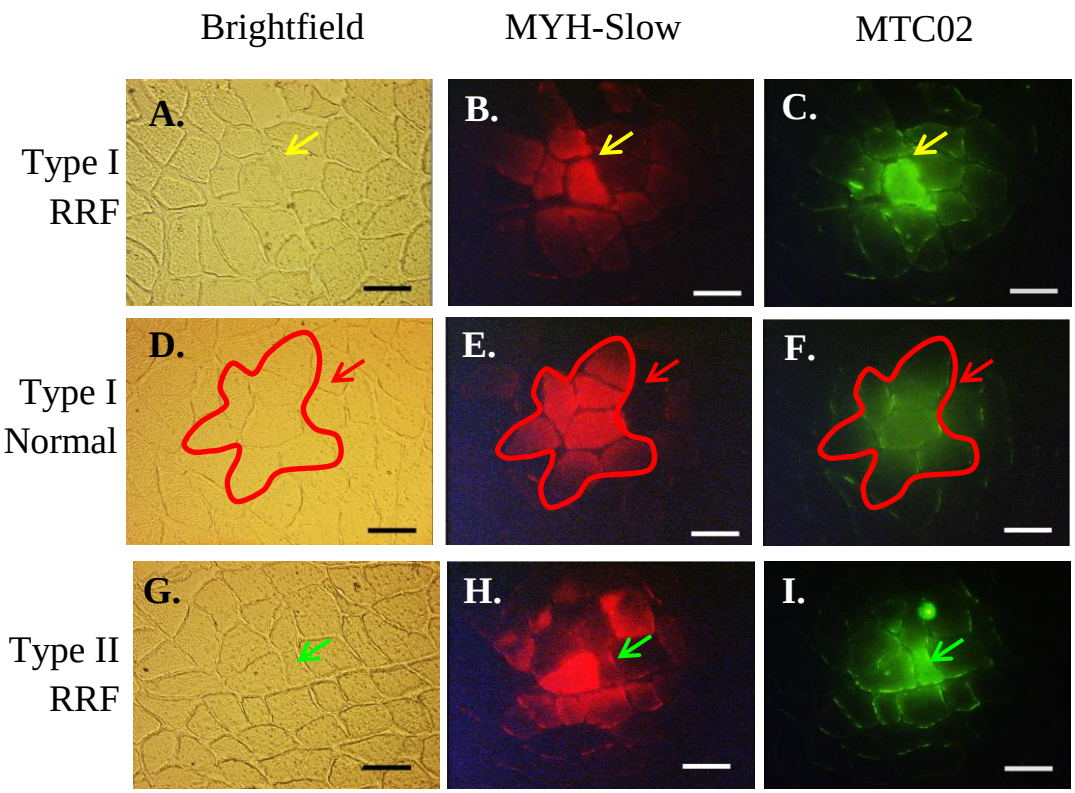

Figure 6.21 Isolating cell populations using laser microdissection. Muscle sections are visualised on x20 magnification with brightfield (A, D, G), a rhoadmine (red) filter set for MYH-Slow (B, E, H) and a FITC (green) filter set for MTC02. (A-C) Type I RRF stain strongly for both MYH-Slow and MTC02, (D-F) normal Type I fibres only stain strongly for MYH-Slow but not MTC02. (G-I) Any RRF which do not stain for MYH-Slow are Type II fibres and are not included in the study.

Each slide was processed within an hour, continuing with fresh sections until ~ 500 fibres of each type were been dissected. After quality control assessment, cell lysates were pooled and the RNA extracted.

RNA quality of final samples

The expression of the three reference genes (*GAPDH*, *B2M* and *ACTB*) were assessed in the samples from sections remaining after laser-microdissection and in the dissected fibres. The gene expression does not change by more than 2-fold for either gene in any of the microdissected samples (Figure 6.22A). The 5' to 3' assay indicates ~50% reduction in 5' signal in samples from the MERRF patient(RRF and NOR) (Figure 6.22B).

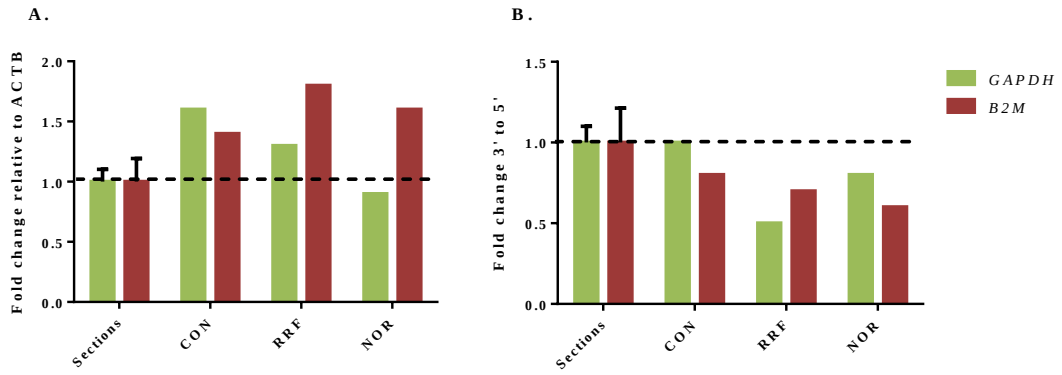

Figure 6.22 mRNA transcript profile and integrity of final samples for microarray analysis. (A) The expression of the reference genes *GAPDH* and *B2M* relative to *ACTB* were measured from control and MERRF muscle sections before dissection and all laser-microdissected samples (B) Amplicons from the 5' and 3' region of both *GAPDH* and *B2M* were compared to assay for RNA quality. The ΔCt for these reference genes were normalised against a sample from fresh, untreated tissue to obtain fold changes (ΔΔCt). A fold change of 1 (dashed line) indicates no difference in gene expression profile from the control sample.

The RNA concentration of the final samples could not be accurately determined by conventional methods, but was estimated as ~ 1 ng/ µL using the gene expression of the reference genes (Appendix F.).

6.4.2 Microarray results

Quality assessment

The RNA samples, and following cDNA samples were spiked with bacterial gene sequences to assess labelling and hybridisation efficiency. All genes were detected as

present at the correct ratios, indicating efficient microarray preparation for all samples (Appendix G.1). The raw probe cell intensity from CEL files and expression signal was calculated using Affymetrix® Expression Console™. The probe cell intensity values are similar for each sample indicating a similar quantity of cDNA hybridised onto each microarray. After application of the MAS5 algorithm, the expression signal is normalised and the mean is the same for all samples (Appendix G.2). The RawQ, scaling factor (SF), background (BG), noise and percentage present calls (%P) values were calculated by the Affymetrix® Expression Console™ and are similar across all samples, suggesting preparation and quality of samples are consistent.

The expression values for the three reference genes, *GAPDH*, *B2M* and *ACTB* were normalised against that of the control (CON). Although there is a decrease of *GAPDH* (0.6) and *B2M* (0.8) in RRF, the ACTB level in RRF and all genes in NOR remained stable (1.0). The 5' to 3' ratio of GAPDH should ideally be above 0.8 (1.25 3'/5'); however, some of the final samples from the microarray fall below this range (CON, 0.80; RRF, 0.71; NOR, 0.77) (Appendix G.4).

Although the integrity of the RNA could be improved, the samples are similar enough to be comparable, allowing for analysis of gene expression between these samples.

Gene dysregulation

Genes were filtered following procedure set out in Figure 6.6 (Section 6.2.7), assigning dysregulated genes into three groups for up- and downregulation, based on a cut-off threshold of 3-fold. Where genes in RRF were up- or downregulated compared to normal fibres from both the MERRF and control individuals, these genes were considered 'RRF-specific'. If genes were up- or downregulated in both fibre types from the MERRF patient compared to the control, these genes were considered 'MERRF-specific'. Genes were considered 'exacerbated in RRF' where some dysregulation observed in MERRF normal fibres was dysregulated to a greater extent in RRFs.

A total of 12,512 genes were detected (present; P) in at least one of the samples. Of these, 1188 (9.5 %) have mitochondrial-related functions (based on gene ontology (Ashburner *et al.*, 2000)). A total of 1770 (13.3 %) were classified as MERRF-specific, 957 genes (7.3 %) were classified as exacerbated in RRF and 1636 genes (12.4 %) were classified as RRF-specific (Table 6.6).

The proportions of mitochondrial genes dysregulated in the sample groups are similar to the proportion in overall detected genes; though the highest increase is observed in those genes exacerbated in RRF (11.6 % compared to 9.5 % in total).

Table 6.6 Statistics for gene dysregulation from microarray analysis. The total number of genes and the proportion of those that have mitochondrial-related function are given for all detected genes, and those that are dysregulated within RRFs or MERRF patient tissue.

Group		Total	RRF-Specific	Exacerbated in RRF	MERRF-Specific
Detected genes	Total	12512			
	Mitochondrial	1188			
	Mito % of Total	9.5 %			
Total dysregulated genes	Upregulated		880	430	616
	Downregulated		756	527	1154
	Total dysregulated		1636	957	1770
	% of Total		12.4 %	7.3 %	13.4 %
Mitochondrial genes	Upregulated		79	61	63
	Downregulated		61	50	67
	Total mitochondrial		140	111	130
	% of Dysregulated		8.6 %	11.6 %	7.3 %

There are more genes up- than downregulated specifically in RRF, but the opposite is true for genes ‘exacerbated in RRF’ and ‘MERRF-specific’ genes. Of the genes detected on this array, a similar number are dysregulated between the MERRF samples compared to the control samples, and the normal fibres of both individuals compared to RRF. This is more than was previously expected as both MERRF samples were extracted from the same sections of muscle, with the only difference being noticeable increase in mitochondrial biogenesis.

The proportion of genes with mitochondrial-related function does not change depending on the classification. This is unexpected, considering the increased mitochondrial biogenesis observed in RRFs; however, it is plausible that some mitochondrial processes are downregulated as others are upregulated.

Comparison to previous skeletal muscle microarray analysis

Gene expression profiling was performed from the skeletal muscle homogenates of patients with either MELAS or PEO caused by the m.3243A>G point mutation, or PEO caused by macrodeletions (Crimi *et al.*, 2005). The genes found to be commonly dysregulated between these groups of patients were compared to the microarray results from laser-microdissected MERRF fibres (Table 6.7). Two genes were commonly regulated across all disease types (not specific to RRFs), these were *CDKN1A* and *MAOA*. A further four genes had similar dysregulation to one or two of the other disease groups. A total of six genes were dysregulated in the opposite direction to those observed in other patient groups, though disagreement was common between all groups within the study.

Table 6.7 Gene dysregulation common to mitochondrial encephalomyopathies. The genes reported to be commonly dysregulated in either MELAS or PEO caused by m.3243A>G or the common deletion (ΔmtDNA) (Crimi *et al.*, 2005) were compared to the microarray analysis results from laser-microdissected MERRF muscle fibres.

	Each gene between disease types	MELAS m.3243A>G	PEO m.3243A>G	PEO ΔmtDNA	MERRF m.8344A>G
In agreement	1	10	6	9	3
	2	5	5	6	1
	3	2	2	2	2
	Total agreements	26	22	27	11
In disagreement	1	2	6	9	5
	2		3		1
	3	-	-	-	-
	Total disagreements	2	12	9	7

A higher degree of correlation in gene dysregulation would be expected in the patient groups studied by Crimi and colleagues (2005). Firstly, the samples are all tissue homogenates rather than laser-microdissected type I fibres; secondly, each group either shares the same genetic cause of disease (m.3243A>G) or same clinical phenotype (PEO).

An additional study compared the muscle tissue of patients and carriers with m.3243A>G to controls and found dysregulation in genes related to the immune response, protein transport, programmed cell death (van Eijsden *et al.*, 2008). Of note, 4 of the 9 genes found dysregulated in relation to protein transport (*ARHGEF2, RPL23*,

RRBP1 and *TRAM2*) are also dysregulated specifically in RRF, or are exacerbated in RRF in this study.

Enriched biological processes

The genes which are classified as either 'RRF-specific', 'exacerbated in RRFs' or 'MERRF-specific' can be grouped by whether they are up- or downregulated in MERRF tissues and subjected to functional annotation clustering by the Database for Annotation, Visualization and Integrated Discovery (DAVID) v6.7 software (Dennis *et al.*, 2003). This software assigns biological processes to known genes based on their ontology, and compares the proportion of genes for each process in the target list to a background (e.g. human expressed genes) and then groups them into functionally-related clusters.

To assess the biological processes dysregulated in MERRF tissue, genes exacerbated in RRF and specific to MERRF are combined to generate enriched biological processes for the up- and downregulated gene sets (Table 6.8). Each cluster is assigned an enrichment score (E), and each biological process within the cluster has an associated Bonferroni-corrected p-value, to determine significance with multiple comparisons.

The highest enrichment in upregulated genes was negative regulation of transcription (E=5.35; corrected p-value < 0.001 for most significant included process). Three of the top 10 enriched biological processes which are upregulated remain significant after Bonferroni correction.

The highest enrichment in downregulated genes was in phosphorylation-related processes (E=4.7; corrected p-value < 0.01). Six of the top 10 enriched biological processes which are downregulated remain significant after Bonferroni correction.

Table 6.8 Enriched biological processes in MERRF patient tissues. Functional annotation clustering generates enriched biological processes and groups them by related function. Exacerbated in RRF and MERRF-specific categories have been pooled by up- or downregulation for an overall impression of dysfunction in MERRF. Enrichment score (E) represents the whole cluster, the total processes are the number of individual biological processes included in the cluster, and p-values given are for only the most significant process within the cluster, before and after Bonferroni correction. * $p < 0.05$, ** $p < 0.01$, *** $p < 0.001$, **** $p < 0.0001$ Fisher Exact.

	Cluster	Description	Enrchment Score (E)	Total processes	p-value / corrected	
Upregulated	1	Negative regulation of cellular macromolecule biosynthetic process / transcription	5.35	12	****	***
	2	Positive regulation of cellular macromolecule biosynthetic process / transcription	3.89	16	****	**
	3	Apoptosis	2.96	4	***	n.s.
	4	Regulation of gene-specific transcription	2.55	6	****	*
	5	Proteolysis / macromolecule catabolic process	2.26	9	***	n.s.
	6	Chromatin organisation	2.07	3	***	n.s.
	7	Stem-cell maintenance	2.03	3	***	n.s.
	8	Intracellular receptor-mediated signalling pathway / steroid hormone signalling	1.91	3	**	n.s.
	9	RNA splicing / mRNA processing	1.63	7	**	n.s.
	10	Blood vessel/vasculature development	1.44	4	**	n.s.
Downregulated	1	Phosphorylation / Phosphate metabolism	4.7	4	****	**
	2	Skeletal muscle development	3.12	7	****	*
	3	Cellular response to stress/DNA repair	2.96	4	****	*
	4	Blood vessel/vasculature development	2.92	4	***	*
	5	Intracellular transport/ cellular protein localisation	2.8	7	****	**
	6	Regulation of transcription, DNA-dependent	2.66	4	***	*
	7	Positive regulation of cellular macromolecule biosynthetic process / transcription	2.46	12	**	n.s.
	8	Regulation of translation	2.22	3	**	n.s.
	9	Transcription, DNA-dependent	2.07	3	**	n.s.
	10	Peptidyl-threonine/serine phosphorylation	2.06	4	***	n.s.

Biological processes related to regulation of transcription are enriched in in both up- and downregulated genes in MERRF patient tissue. Clusters of positive and negative

regulation of transcription were both upregulated, in addition to regulation of gene-specific transcription, chromatin organisation and mRNA processing. However, only positive regulation of transcription and DNA-dependent transcripton were enriched in downregulated genes. Therefore, although certain transcriptional pathways may be upregulated, overall there is a decrease in transcriptional activity in MERRF tissue compared to that of an age-matched control individual, evidenced by higher numbers of downregulated MERRF-specific genes (Table 6.7). Since transcription is an energy-demanding process, a decrease in transcription is an expected result of lowered energy production in the muscle of MERRF patients.

Vasculature development is also enriched in both up- and downregulated genes. Vasculopathy is a common occurrence in mitochondrial disorders, as blood vessels have increased protein nitration causing a reduction in flow-mediated vasodilatation in mitochondrial diseases (Vattemi *et al.*, 2011).

Phosphorylation-related biological processes are downregulated, specifically peptidyl-threonine/serine phosphorylation which might relate to the upregulation of genes in intracellular receptor-mediated signalling pathways.

The biological processes dysregulated in MERRF patient tissue as a whole can be compared to those dysregulated specifically in RRFs. The genes classified as ‘exacerbated in RRF’ and ‘RRF-specific’ were pooled and subjected to the same functional annotation clustering (Table 6.9).

The most enriched cluster of biological processes observed in upregulated genes was negative regulation of transcription (E=3.45), though this did not remain statistically significant after Bonferonni correction. Only one cluster included a statistically significant biological process included after Bonferroni correction, which was regulation of intracellular protein localisation (E=3.41, p-value <0.05).

Overall, enrichment of biological process clusters was much stronger in downregulated genes. The most enriched cluster of biological processes was mRNA splicing and processing (E=5.79; corrected p-value < 0.0001). All of the top 10 clusters contain statistically significant biological processes.

Table 6.9 Enriched biological processes in RRFs. Functional annotation clustering generates enriched biological processes and groups them by related function. RRF-specific and exacerbated in RRF categories have been pooled by up- or downregulation for an overall impression of dysfunction in RRF. Enrichment score (E) represents the whole cluster, the total processes are the number of individual biological processes included in the cluster, and p-values given are for only the most significant process within the cluster, before and after Bonferroni correction. * $p < 0.05$, ** $p < 0.01$, *** $p < 0.001$, **** $p < 0.0001$ Fisher Exact.

	Cluster	Description	Enrchment Score	Total processes	p-value / corrected	
Upregulated	1	Negative regulation of cellular macromolecule biosynthetic process / transcription	3.45	12	****	n.s.
	2	Intracellular protein localisation	3.41	8	****	*
	3	Cytoskeletal organisation/ protein binding	2.73	4	***	n.s.
	4	Intracellular receptor-mediated signalling pathway / steroid hormone signalling	2.31	3	***	n.s.
	5	Regulation of transcription, DNA-dependent	2.15	4	**	n.s.
	6	Positive regulation of cellular macromolecule biosynthetic process / transcription	1.96	12	***	n.s.
	7	Phosphorylation	1.87	4	**	n.s.
	8	Chromatin silencing / epigenetic negative regulation of gene expression	1.82	6	***	n.s.
	9	Cellular response to stress/ DNA repair	1.73	4	**	n.s.
	10	mRNA splicing/processing	1.66	4	**	n.s.
Downregulated	1	mRNA splicing/processing	5.79	7	****	****
	2	Intracellular protein localisation	5.36	15	****	****
	3	Positive regulation of cellular macromolecule biosynthetic process / transcription	3.96	16	****	***
	4	Transcription, DNA-dependent	3.94	3	****	*
	5	Proteolysis / macromolecule catabolic process	3.62	9	****	**
	6	Chromatin organisation	3.36	3	***	*
	7	Phosphorylation	2.97	4	***	*
	8	mRNA localisation	2.94	8	***	*
	9	Post-transcriptional regulation of gene expression / translation	2.82	3	****	**
	10	Negative regulation of cellular macromolecule biosynthetic process / transcription	2.76	11	***	*

Many of the biological processes enriched in dysregulated genes specific to MERRF tissue were also dysregulated in RRFs. There was increased focus of regulation of

transcription, with upregulation of chromatin-silencing and epigenetic negative regulation of gene expression further corroborating decreased transcription observed in disease tissue. mRNA splicing processes were somewhat enriched in upregulated genes, but highly enriched in downregulated genes, along with chromatin organisation and DNA-dependent transcription.

The controlled intracellular trafficking of macromolecules was also dysregulated in RRFs, with upregulation of cytoskeletal organisation and intracellular protein localisation. Biological processes for intracellular protein and mRNA localisation are also observed significantly enriched in downregulated genes.

Enriched pathways and processes

Using the same grouping system, functional annotation of each gene with the related KEGG pathways (Kanehisa and Goto, 2000) allowed identification of biochemical pathways which are dysregulated in both MERRF tissue in general and specifically in RRFs. The 15 most enriched pathways upregulated in MERRF and specifically in RRFs are listed in Table 6.10 (excluding disease pathways). The majority of listed pathways are signalling pathways, which are enriched in genes dysregulated in both MERRF and specifically in RRFs. There are three pathways only enriched in genes dysregulated in RRFs: the spliceosome (corrected p-value <0.01); ubiquitin-mediated proteolysis (corrected p-value <0.05); and the citric acid (TCA) cycle (corrected p-value <0.05).

Table 6.10 Enriched pathways. KEGG pathways found to be enriched by functional annotation analysis. RRF-specific and exacerbated in RRF categories have been pooled by up- or downregulation for an overall impression of dysfunction in RRF. Each pathway is ranked and the number of gene contributing to enrichment given. p-values given are for each pathway, before and after Bonferoni correction. * $p < 0.05$, ** $p < 0.01$, *** $p < 0.001$, **** $p < 0.0001$ Fisher Exact.

	RRF-specific				MERRF-specific			
Term	Rank	Count	P-Value / corrected		Rank	Count	P-Value / Corrected	
Wnt signalling pathway	1	41	****	***	5	35	***	*
Spliceosome	2	32	****	**	-	-	-	-
Insulin signalling pathway	3	33	***	**	2	40	****	****
Focal adhesion	4	43	***	*	6	43	***	*
ErbB signalling pathway	5	23	***	*	4	25	***	**
Neurotrophin signalling pathway	6	29	***	*	1	38	****	****
Ubiquitin-mediated proteolysis	7	31	***	*	-	-	-	-
mTOR signalling pathway	8	16	**	*	3	22	****	****
Apoptosis	9	22	**	*	13	21	**	n.s.
MAPK signalling pathway	10	50	**	*	19	48	*	n.s.
Citrate cycle (TCA cycle)	11	11	**	*	-	-	-	-
Adherens junction	12	19	**	n.s.	10	20	**	*
Adipocytokine signalling pathway	13	17	**	n.s.	8	19	**	*
Regulation of actin cytoskeleton	14	40	**	n.s.	15	41	*	n.s.
VEGF signalling pathway	15	17	*	n.s.	12	19	**	n.s.
Aldosterone-regulated sodium reabsorption	-	-	-	-	7	14	**	*
GnRH signalling pathway	-	-	-	-	9	24	**	*
TGF-beta signalling pathway	32	17	n.s.	n.s.	23	19	*	n.s.
RNA degradation	16	14	*	n.s.	11	16	**	n.s.
Toll-like receptor signalling pathway	34	19	n.s.	n.s.	14	23	**	n.s.

When analysed on KEGG, the enriched pathways dysregulated in MERRF tissue form a complex, inter-connected network of signalling pathways, ultimately leading to the regulation of cytoskeletal remodelling and focal adhesions, ubiquitin-mediated proteolysis, apoptosis and regulation of autophagy (Appendix H.1).

The spliceosome is the most significant pathway dysregulated specifically in RRFs. The spliceosome is typically comprised of five small nuclear ribonucleoproteins (snRNPs) and several spliceosome-associated proteins (SAPs) and is responsible for correct assembly of intronic sequence from the transcribed pre-mRNA. A total of 32 spliceosome components or regulatory genes are dysregulated (18 downregulated and 13 upregulated) specifically in RRFs. Spliceosome dysfunction has not been previously

reported in mitochondrial diseases and suggests the importance of expanding gene expression studies to include differential transcript expression.

Dysregulated genes in these pathways can be seen on the adapted KEGG pathways in Appendix H.

Regulation of mitochondrial biogenesis

To gain insight into the regulation of mitochondrial biogenesis in RRFs, the expression changes for known regulators of mitochondrial biogenesis were collated from the microarray analysis (Table 6.11).

Many gene expression changes are somewhat validated by two probe sets, or by two genes within the same protein complex showing similar dysregulation. Although gene expression changes have been classified as 'MERRF-specific', 'Exacerbated in RRF' or 'RRF-specific' there is often an overlap when close to the threshold of ± three fold-change.

MERRF-specific changes include upregulation of *FOXO1* and *FOXO3* transcription factors and downregulation of the adenylate cyclase genes *ADCY1*, *ADCY5* and *ADCY9*.

A significant finding is the RRF-specific upregulation of *PPARGC1A*, encoding PGC1α, the core regulator of mitochondrial biogenesis (7.68-fold compared to normal fibres from the same patient, and 16.31-fold compared to the age-matched control). In addition, *NRF1* is only upregulated in RRF compared to control (3.79).

All three isoforms of the retinoid X receptor (*RXRA*, *RXRB* and *RXRG*) are downregulated either specifically in ragged-red fibres or not present in either sample from MERRF.

Table 6.11 Gene expression changes in mitochondrial biogenesis genes. The expression changes of known regulators of mitochondrial biogenesis from literature have been collated. Gene expression changes ≤ -3 or ≥ 3 are shown.

Descriptive	Gene Symbol	Definition	Present	NOR to CON	RRF to CON	RRF to NOR
AMPK Transcriptional stimulator	*PRKAA2*	Exac. in RRF	All		-4.13	
	PRKAB2	RRF Specific	All		-3.52	-3.53
	PRKAG3	MERRF Specific	All	-6.96	-4.63	
CAMKs Transcriptional stimulator	*CAMK2A*	MERRF Specific	All	-4.11	-4.03	
	CAMK2B	Exac. in RRF	All		-3.66	
		Exac. in RRF	All		-5.01	
	CAMK2D	RRF Specific	All		3.01	8.85
		MERRF Specific	All	3.91	4.05	
	CAMK2G	Exac. in RRF	NOR/ CON		-3.34	
			All		-3.92	
Cn (Calcineurin) Transcriptional stimulator	*PPP3CA*	RRF Specific	All			-3.98
					-4.54	-3.81
	PPP3CB	Exac. In RRF	All		-3.07	
	PPP3CC	Exac. In RRF	All		3.13	
		MERRF Specific	All	4.36	3.96	
Adenylate cyclase Transcriptional stimulator	*ADCY9*	MERRF Specific	CON	-3.29	-3.29	
	ADCY5	MERRF Specific	CON	-3.31	-3.31	
	ADCY1	MERRF Specific	All	-6.40	-6.42	
cAMP-dependent protein kinase	*PRKACB*	RRF Specific	NOR/ CON		-3.27	-11.01
		Exac. in RRF	RRF/ NOR		3.54	
MAPK Transcriptional stimulator	*MAPK1*	RRF Specific	NOR/ CON		-12.85	-6.82
					-3.79	-7.08
		Exac. in RRF	All		-4.80	
	MAPK8	MERRF Specific	NOR/ CON	-3.02	-3.82	
	MAPK12	MERRF Specific	NOR/ CON	-5.42	-8.44	
RXR Transcription Factor	*RXRA*	RRF Specific	All		-3.57	-9.91
		RRF Specific	NOR/ CON		-21.51	-36.63

Descriptive	Gene Symbol	Definition	Present	NOR to CON	RRF to CON	RRF to NOR
	RXRB	RRF Specific	All		-3.45	-5.00
	RXRG	MERRF Specific	CON	-25.34	-25.34	
MEF2 Transcription Factor	*MEF2A*	RRF Specific	NOR/ CON		-4.37	-11.04
c/EBP Transcription Factor	*CEBPD*	MERRF Specific	All	5.26	3.93	
				14.39	9.51	
	CEBPG	RRF Specific	All		-5.09	-4.37
FOXO Transcription Factor	*FOXO1*	MERRF Specific	All	21.21	12.74	
				7.09	5.15	
				12.67	3.53	
	FOXO3	MERRF Specific	All	9.93	5.28	
				5.69	3.19	
	FOXO6	MERRF Specific	CON	-11.72	-11.72	
MyoD Transcription Factor	*MYOD1*	MERRF Specific	CON	-3.21	-3.21	
E2A Transcription Factor	*TCF3*	RRF Specific	RRF/ NOR		3.59	8.88
AKT Transcription/ Post-translational Repressor	*AKT2*	RRF Specific	NOR/ CON		-3.63	-3.86
		Exac. in RRF	All		-3.58	
	AKT3	Exac. in RRF	NOR/ CON		-3.70	
		MERRF Specific	All	-3.90	-3.63	
GCN5 Post-translational Repressor	*KAT2A*	RRF Specific	All			-4.08
MYBBP1A Post-translational Repressor	*MYBBP1A*	MERRF Specific	NOR/ CON	-4.68	-6.56	
PRMT1 Post-translational activator	*PRMT1*	Exac. in RRF	All		-3.19	

Descriptive	Gene Symbol	Definition	Present	NOR to CON	RRF to CON	RRF to NOR
GSK-3β Post-translational activator	*GSK3B*	Exac. in RRF	All		-3.27	
PGC-1α Core regulator	*PPARGC1A*	RRF Specific	RRF/ NOR		16.31	7.68
PPARδ Transcriptional response initiator	*PPARD*	Exac. in RRF	NOR/ CON	-3.70	-19.27	-5.21
PPARα Transcriptional response initiator	*PPARA*	RRF Specific	All		4.60	6.21
		Exac. in RRF	NOR/ CON		-4.17	
		MERRF Specific	All	4.34	4.97	
				8.13	3.60	
ERRγ Transcriptional response initiator	*ESRRG*	MERRF Specific	RRF/ NOR	8.02		
			CON	-3.05	-3.05	
NRF2 Transcriptional response initiator	*GABPB1*	MERRF Specific	CON	-3.32	-3.32	
NRF1 Transcriptional response initiator	*NRF1*	Exac. in RRF	All		3.79	
YY1 Transcriptional response initiator	*YY1*	Exac. in RRF	All		-4.24	
	YY1AP1	RRF Specific	All		-3.33	-4.23

The increased expression of *PPARGC1A* (PGC1α) and *NRF1* in RRFs is unsurprising considering the massive mitochondrial proliferation observed in these fibres.

RXR proteins, downregulated specifically in RRFs, form heterodimers with PPARγ and bind peroxisome proliferator response elements (PPREs) with PGC1α functioning as a transcriptional coactivator (Delerive *et al.*, 2002). The transcriptional responses induced by RXR/PPARγ binding include lipid metabolism, insulin sensitisation and

inflammatory response. One action of RXR/PPARγ is inhibition of NF-κB and mitogen-activated protein (MAP) kinase cascades (Desreumaux *et al.*, 2001, Dubuquoy *et al.*, 2002). RXR is already proving a potential therapeutic target for the treatment of inflammatory disease, cancer and even metabolic conditions such as diabetes and obesity (Perez *et al.*, 2012).

6.5 Concluding Remarks

The study of gene expression in mitochondrial diseases has previously been restricted to cell culture models or tissue homogenates. By optimising a multiplex assay for the simultaneous identification of fibre type and "ragged-red" status, whilst maintaining high-quality RNA, it has been possible to analyse the gene expression differences between normal and 'ragged-red' fibres from the same individual.

Several previous reports of gene expression changes and dysregulated biochemical processes in mitochondrial diseases, and in particular MERRF, have been corroborated by microarray analysis of laser-microdissected tissue. In addition, three pathways have been identified as being enriched in genes specifically dysregulated in RRFs, including components of the spliceosome machinery. No previous reports of wide-spread spliceosomal dysfunction in mitochondrial diseases have been reported and present an interesting potential direction for future study.

The retinoid X receptor (RXR) family of proteins are downregulated specifically in RRFs. As these have proved potential therapeutic targets other diseases, further study of this family of proteins in mitochondrial disease is warranted.

Chapter 7. General Discussion

7.1 Overview

The research described in this thesis was undertaken to further understand how mtDNA replication and mitochondrial biogenesis are regulated and investigate the importance of these biological processes to human health.

The aim was to address the following questions:

1. How does the mtDNA bottleneck influence the inheritance of pathogenic mutations?
2. How are mtDNA replication and biogenesis regulated throughout formation of the mtDNA bottleneck in mice?
3. Can the mtDNA bottleneck be modelled in a cell culture system to assess gene expression critical to regulation of the mtDNA replication?
4. Can disease tissue, where mitochondrial biogenesis is observed (such as RRFs in muscle tissue), be used to study how mtDNA replication is regulated in a biologically relevant situation?

7.2 Investigating Inheritance of Pathogenic mtDNA Mutations

The studies of mtDNA heteroplasmy transmission have often included only one particular mutation or are limited to a small number of pedigrees (Howell *et al.*, 1994, Wong *et al.*, 2002). Analysis of heteroplasmy in 82 single primary oocytes from a woman carrying m.3243A>G suggested a random genetic drift mechanism of inheritance (Brown *et al.*, 2001). A similar study for m.8993T>G reported skewed segregation; however, only seven oocytes from this patient were assayed (Blok *et al.*, 1997).

Meta-analysis of the published data in the past has suggested that pathogenic mtDNA mutations may behave differently (Chinnery *et al.*, 2000b), but the techniques used to assay heteroplasmy levels can vary greatly, potentially causing bias between studies. Many early studies relied on counting the proportion of mutant and control sequences in bacterial clones, giving only a rough estimation of true mtDNA heteroplasmy, with recent techniques having greater accuracy and sensitivity.

This study was undertaken to: firstly, determine the most accurate, appropriate method for measuring the heteroplasmy levels of numerous mtDNA mutations; secondly, assay

the heteroplasmy level of numerous mutations in a large number of mother-child pairs to determine whether inheritance patterns are truly different for some mutations; thirdly, to compare these results to that of published studies to determine whether the results from meta-analysis can be validated experimentally.

Pyrosequencing out-performed fluorescent-based RFLP and has the advantage of being applicable to any mutation, not requiring the addition or removal of a specific restriction site. Heteroplasmy level measurements were made for three mutations, m.3243A>G, m.8344A>G and m.8993T>G and were used to calculate the O-M values. Frequency distributions for these mutations corroborated previously published data suggesting a random genetic drift model of inheritance for the tRNA mutations, m.3243A>G and m.8344A>G but skewed segregation for m.8993T>G. In addition, the mutations m.11778G>A and m.3460G>A also showed a positive increase in heteroplasmy level between generations. The reliability of the m.3460G>A finding is called into question because of the apparent decrease of heteroplasmy level observed in blood with age, similar to that of m.3243A>G (Kaplanova *et al.*, 2004). Why some mutations are selected against in blood precursor cells has still not been established. If severity of mutation alone was the cause, m.3460G>A should not be selected against, as it has low penetrance and is frequently observed as homoplasmic in individuals (Black *et al.*, 1996).

Samples from non-mitotic tissues, such as muscle, would have been more suitable for this study; however, muscle biopsies are often only sampled for proband cases, with DNA samples from family members only available from peripheral tissues such as blood, saliva or urine.

Further confounding factors still remain which give caution to interpretation of such data. It is unavoidable that the only pedigrees in any study have been brought to the attention of clinical services by a proband case, and even upon exclusion of the proband could still introduce bias. There was variable tolerance for high mutation load observed for different mutations, with a reduced frequency of cases with >80 % heteroplasmy level for m.3243A>G and m.8344A>G; however, the other mutations m.8993T>G, m.11778G>A and m.3460G>A are commonly homoplasmic. Many individuals in m.8344A>G and m.8993T>G pedigrees are homoplasmic for wild-type molecules, suggesting either complete loss of the mutation in these individuals or *de novo* mutation

upon another branch of the pedigree. Fixation to wild-type homoplasmy from a heteroplasmic individual is evident at relatively high proportions in m.8344A>G pedigrees (17.3 %) but low in m.8993T>G pedigrees (3.4 %), suggesting a higher proportion of pedigrees containing *de novo* occurrence of the m.8993T>G mutation.

Determining whether selection is occurring for particular mutations is of critical importance when genetic counselling is given to women known to carry pathogenic mtDNA molecules. If mtDNA mutations undergo positive selection with tendency to increase mutation load with subsequent generations, there would be greater probability of earlier onset of a more severe phenotype. In contrast, a tendency to decrease mutation load by negative selection might simply lead to the loss of the mutation without the child presenting any clinical phenotype. Mutation-specific advice is of particular importance with pre-implantation genetic diagnosis (PGD) becoming a common service offered to women with known mtDNA mutations and the potential future prospect of pronuclear transfer to prevent transmission of mitochondrial disease (Craven *et al.*, 2010).

7.3 Gene Expression during Murine Embryogenesis

The existence of a mtDNA bottleneck, responsible for the shifts in heteroplasmy observed between generations has been long-established (Hauswirth and Laipis, 1982, Laipis *et al.*, 1988, Olivo *et al.*, 1983). Since then, many studies have attempted to elucidate the mechanism and timing of the mtDNA bottleneck (Cao *et al.*, 2007, Cree *et al.*, 2008, Jenuth *et al.*, 1996, Wai *et al.*, 2008). Due to differences in techniques for identifying PGCs and subsequently isolating them from somatic tissue, several mechanisms for the mtDNA bottleneck have been proposed and there is a clear need for validation with an independent technique.

Recently, Freyer and colleagues (2012) assayed the heteroplasmy levels of a pathogenic mtDNA mutation in PGCs at 13.5 d.p.c. during mouse embryonic development. They observed substantial variance between PGCs already established by 13.5 d.p.c., supporting a prenatal mtDNA bottleneck.

Critical to formation of the mtDNA bottleneck is the regulation of mtDNA replication. Since establishing that the mtDNA bottleneck occurs before 13.5 d.p.c. it has become more essential to study mtDNA replication in PGCs before this point.

This study sought to investigate the expression of genes critical to regulation of mtDNA replication during embryonic development in mice. A panel of 32 appropriate genes was established and their expression studied during five stages of pre-implantation development. This corroborated previous research into the turnover and replication rate of mtDNA during pre-implantation (McConnell and Petrie, 2004), and identified *Lrpprc* as having a similar gene expression profile to other transcription genes. Further study is required to determine the significance of this finding. Technical limitations prevented assessing expression in PGCs during post-implantation. Assessing the expression of key replication genes during pre-implantation development alone cannot bring any further insight into mtDNA replication in PGCs during formation of the mtDNA bottleneck. The number of PGCs per embryo at the early stages of development is exponentially lower than at later stages. Whilst microarray analysis is feasible from gender-specific embryos at 12.5 d.p.c. onwards, it remains challenging to obtain sufficient material from any earlier time-points (Sabour *et al.*, 2011). A technique is required for pooling PGCs from many female embryos, often spaced days to weeks apart, while maintaining high-quality RNA and without compromising the integrity of the results.

Preliminary assessment of new RNA extraction techniques with somatic cells, obtained through FACS, suggests that sufficient material could be obtained from 100-250 cells extracted from either a single embryo or pooled from many. Utilising *Prdm* as a PGC-specific reporter in addition to *Dppa3* (Stella) would allow identification of PGCs from as early as 6.5 d.p.c. (Ohinata *et al.*, 2008).

If mtDNA replication can be assessed during formation of the mtDNA bottleneck, it would be possible to assess whether manipulation of the involved genes could affect how mtDNA mutations are inherited. The availability of mice with stable, heteroplasmic, pathogenic mtDNA mutations make this a feasible possibility for the near-future.

7.4 Identification of Factors Affecting mtDNA Copy Number Regulation

The majority of research investigating regulation of mtDNA content has relied upon hypothesis-driven selection of a gene of interest, which is subsequently knocked-down, knocked-out or overexpressed (Ekstrand *et al.*, 2004, Spelbrink *et al.*, 2000, Tyynismaa *et al.*, 2004). However, changes in mtDNA content upon gene manipulation are not necessarily relevant to biological situations where mtDNA replication is regulated.

The mtDNA repopulation assay was successfully employed by this research group to demonstrate reduced mtDNA replication capacity in the fibroblasts of patients with mutations in *POLG* (Stewart *et al.*, 2011). This study sought to adapt this assay to model the reduction and subsequent increase in mtDNA copy number observed during formation of the mtDNA bottleneck, and identify which genes are regulated in order to modify mtDNA content.

The mtDNA repopulation assay was adapted for use with myoblasts using ddC as a depletion agent. Although myoblasts survived the duration of the experiment and were successfully depleted and repopulated, the mtDNA copy number in untreated myoblasts increased as cells were passaged. Since the gene expression of *TFAM*, *POLG*, *POLG2* and *NRF1* was not considerably dysregulated during depletion/repopulation, reliance on oxidative phosphorylation was induced by culture in glucose-free galactose media.

mtDNA-depleted fibroblasts failed to thrive in pure galactose media, and media containing both glucose and galactose failed to induce substantial gene expression changes. No other analysed genes from other biological processes were dysregulated; therefore the mtDNA repopulation assay is not a suitable model to study gene expression changes responsible for regulation of mtDNA replication.

It is possible that the increase in mtDNA content in fibroblasts after removal of the drug is instead due to lower turnover rate, rather than increased replication rate. The lack of any substantial gene expression changes during mtDNA repopulation contradicts the concept that increased expression of replication genes such as *POLG*, *TFAM*, *NRF1* and *C10orf2* (*Twinkle/PEO1*) is essential for an increase in mtDNA content.

Contrary to previous reports (Davis *et al.*, 1996), the expression of POLG protein was decreased during depletion and later recovered as fibroblasts repopulated their mtDNA. This suggests that perhaps more than just TFAM and POLRMT are downregulated (Seidel-Rogol and Shadel, 2002) and the stability of more components of the nucleoid complexes are also affected by the absence of mtDNA.

The levels of mtDNA-encoded proteins recover much slower than that of mtDNA or mitochondrial transcripts. Since nucleoids and translational machinery form a linked series of protein complexes, it is possible that perturbation of nucleoids also disrupts correct assembly or function of the mitochondrial translation machinery.

7.5 Gene Expression Analysis in MERRF Muscle Fibres

RRFs commonly appear in the muscle biopsies from patients with mitochondrial disease, defined by the massive upregulation of mitochondria in the subsarcolemmal region between fibres. This study sought to determine the plausibility of studying the gene expression changes induced by the mitochondrial biogenesis upregulated specifically in these fibres, alongside any other RRF-specific biological pathways.

Previously, the study of RRF-specific gene or protein expression has been under taken in a hypothesis-driven manner by *in situ* hybridisation or immunohistochemistry for a pre-selected target of interest (Kunishige *et al.*, 2003, Sparaco *et al.*, 1993). Large-scale gene expression analyses to study mitochondrial diseases, such as MERRF, have either relied on tissue homogenates or cell culture models (Crimi *et al.*, 2005, Ma *et al.*, 2005). Although useful, cell culture models are not as biologically relevant as primary tissue, and homogenates often introduce variability through tissue heterogeneity and inter-individual changes.

Type I (oxidative) fibre predominance, a common compensatory mechanism for patients with mitochondrial diseases, was observed in the muscle of the MERRF patient used for this study (Enns *et al.*, 2005). This finding highlights the need for fibre-specific gene expression analysis. Many gene expression differences observed between the homogenates of this patient and a healthy control would relate to fibre type composition, and not necessarily due to biochemical differences in the fibres.

A multiplex assay for the simultaneous identification of fibre type and “ragged-red” status, whilst maintaining high-quality RNA, was successfully established. This is of critical importance, as utilising pre-stained serial sections can be time-consuming and unreliable. In addition to the technical difficulty of locating specific fibres from serial sections, the biochemical properties of muscle fibres have been shown to alter longitudinally (Durham *et al.*, 2007). Therefore, even upon correct identification of the fibres from serial sections, there is no guarantee of the same biochemical property in the unstained tissue.

Importantly, our study analyses differences not only between a MERRF patient and an age-matched control, but also between the normal and ‘ragged-red’ fibres of an individual patient. This not only allows a unique study of this pathological

phenomenon, but also eliminates variation introduced by tissue heterogeneity and comparisons between different individuals.

Crimi and colleagues (2005) performed microarray analysis on skeletal muscle homogenates of 12 patients with either MELAS (m.3243A>G), PEO (m.3243A>G) or PEO (deletions). Four of the gene expression changes identified in two or more of these patient groups were validated in our microarray study of MERRF dissected fibres (m.8344A>G).

As this study was a pilot to test the plausibility of the technique, the greatest limitation was the comparison of just one patient (both ragged-red and normal fibres) to one control. The microarray analysis would be strengthened by inclusion of further mitochondrial disease patients; however, sourcing an appropriate patient with high numbers of RRFs and sufficient available material prevented extension of the project.

Due to this limitation, individual probe data is not reliable until validated by q-PCR, *in situ* hybridisation or immunohistochemistry. However, utilising gene ontology terms assigned to each gene allows clustering of dysregulated targets by enriched biological processes or pathways. Many of the enriched biological processes and pathways either up- or downregulated in MERRF tissue as a whole have been reported as altered in previous studies (Alemi *et al.*, 2007, Crimi *et al.*, 2005, Kadowaki and Kanazawa, 2003, Ma *et al.*, 2005).

Ubiquitin-mediated proteolysis and the spliceosome were found dysregulated specifically in RRF and not MERRF tissue in general. Ubiquitin-mediated proteolysis has been observed as being dysregulated in mitochondrial patients with mtDNA deletions (Alemi *et al.*, 2007), and importantly ubiquitin has already been observed as being specifically upregulated in RRFs visualised by immunohistochemistry (Sparaco *et al.*, 1993). However, there are currently no reports of specific spliceosome downregulation in mitochondrial disease patients.

Future development of these results would require assembling a suitable cohort of patients to allow more reliable microarray analysis. Since the spliceosome is strongly dysregulated, specifically in RRFs, a more suitable technique for RNA analysis would be an Exon Array or RNASeq to also identify splicing variants. Further analysis of the downregulation RXR receptors specifically in RRFs is warranted as, as they are promising therapeutic targets for metabolic conditions, such as diabetes and obesity.

7.6 Concluding remarks

This thesis has explored the complex regulation of mtDNA replication and mitochondrial biogenesis and its implications to mitochondrial disease. Attempting to accurately model situations of increased mtDNA replication and biogenesis has proved challenging, highlighting the importance of studying the regulation of these processes in biologically relevant tissues.

Chapter 8. Appendices

Table of Contents

Appendix E. Repopulation

Appendix F. Quality control microarray RNA samples.

Appendix G. Quality control of microarray data

Appendix H. Regulated pathways

Appendix A. Column statistics for measured mtDNA heteroplasmy frequency histograms.

This appendix contains the descriptive statistics, normality test results and t-test results for m.3243A>G, m.8344A>G and m.8893T>G heteroplasmy results measured by pyrosequencing.

Appendix A.1 Descriptive statistics for measured transmissions. Descriptive statistics for O-M variance distributions include: median and mean, minimum (min) and maximum (max) values, interquartile ranges (25 %, 75 %), standard deviation (Std. Dev) and standard error of the mean (SEM).

Mutation	Descriptive Statistics								
	n	Min.	25%	Median	75%	Max.	Mean	Std. Dev.	SEM
m.3243A>G	60	-84.3	-13.73	5.65	26.65	79.2	5.77	31.34	4.05
m.8344A>G	19	-57	-23.7	-4.70	20	55.3	-3.15	26.64	6.11
m.8993T>G	12	-50.3	2.69	48.83	72.33	89.33	33.03	46.87	13.53

Appendix A.2 Normality statistics for measured transmissions. Each distribution was subjected to the D'Agostino-Pearson omnibus normality test and the skewness and kurtosis calculated.

Mutation	D'Agostino & Pearson omnibus normality test				Skewness	Kurtosis
	K2	p-value	Passed?	Significant?		
m.3243A>G	1.695	0.4286	Yes	ns	-0.31	0.39
m.8344A>G	0.2964	0.8623	Yes	ns	0.18	0.18
m.8993T>G	1.896	0.3875	Yes	ns	-0.86	-0.31

Appendix A.3 One-sample t-test results for measured transmissions. Each distribution was subjected to a one-sample t-test against a theoretical mean of 0 and an alpha of 0.005. The discrepancy, 95 % confidence interval (CI) and p-value are given.

Mutation	One-sample t test					
	Mean	Discrepancy	95% CI of discrepancy	t, df	p-value	Significant?
m.3243A>G	5.767	-5.767	-2.33 to 13.86	t=1.425 df=59	0.16	No
m.8344A>G	-3.147	3.147	-15.99 to 9.69	t=0.5150 df=18	0.61	No
m.8993T>G	33.03	-33.03	3.25 to 62.81	t=2.441 df=11	0.03	Yes

Appendix A.4 Descriptive statistics for m.3243A>G with potential sources of bias removed. Descriptive statistics for O-M variance distributions include: median and mean, minimum (min) and maximum (max) values, interquartile ranges (25 %, 75 %), standard deviation (Std. Dev) and standard error of the mean (SEM).

Sample	Descriptive Statistics								
	n	Min.	25%	Median	75%	Max.	Mean	Std. Dev.	SEM
m.3243A>G Total	60	-84.30	-13.73	5.65	26.65	79.20	5.77	31.34	4.05
Without Probands	15	-36.30	-10.20	16.60	45.80	79.20	16.71	31.95	8.25
Excluding MHet Bias	36	-46.79	-12.87	2.63	20.01	34.72	1.99	20.80	3.47
<15 % Het	29	-52.4	-15.25	5.1	23.05	50.7	3.85	25.47	4.73

Appendix A.5 Normality statistics for m.3243A>G with potential sources of bias removed. Each distribution was subjected to the D'Agostino-Pearson omnibus normality test and the skewness and kurtosis calculated.

Sample	D'Agostino & Pearson omnibus normality test				Skewness	Kurtosis
	K2	p-value	Normal?	Significant?		
m.3243A>G Total	1.70	0.43	Yes	ns	-0.31	0.39
Without Probands	0.3235	0.8507	Yes	ns	0.26	-0.50
Excluding MHet Bias	1.514	0.4691	Yes	ns	-0.36	-0.58
<15 % Het	0.9386	0.6255	Yes	ns	-0.39	-0.36

Appendix A.6 One-sample t-test results for m.3243A>G with potential sources of bias removed. Each distribution was subjected to a one-sample t-test against a theoretical mean of 0 and an alpha of 0.005. The discrepancy, 95 % confidence interval (CI) and p-value are given.

Sample	One sample t test					
	Mean	Discrepancy	95% CI of discrepancy	t, df	p-value	Significant?
m.3243A>G Total	5.77	-5.77	-2.33 to 13.86	t=1.425 df=59	0.16	ns
Excl. Probands	16.71	-16.71	-15.99 to 9.69	t=2.026 df=14	0.06	ns
Excl. Bias	1.99	-1.99	3.25 to 62.81	t=0.5727 df=35	0.57	ns
Excl. <15 % Het	3.852	-3.852	-5.83 to 13.54	t=0w8144 df=28	0.42	ns

Appendix B. Meta analysis

This appendix contains the sources of published studies used to collate data for the meta analysis and the descriptive statistics, normality test results and t-test results for the 5 mutations: m.3243A>G; m.8344A>G; m.8993T>G; m.11778G>A and m.3460G>A.

Appendix B.1 Publications contributing heteroplasmy values for meta analysis. Heteroplasmy values were collated for m.3243A>G; m.8344A>G; m.8993T>G; m.11778G>A and m.3460G>A. The number of pedigrees and total O-M transmissions contributed by each publication have been given.

Mutation	Pedigrees	Transmissions	Reference
	3	8	Ciafaloni *et al.* (1992)
	2	8	Martinuzzi *et al.* (1992)
	1	5	Huang *et al.* (1994)
	1	4	Liou *et al.* (1994)
	6	15	Hammans *et al.* (1995)
	3	8	Iwanishi *et al.* (1995)
	1	2	Rusanen *et al.* (1995)
	1	1	Fabrizi *et al.* (1996)
	1	3	Huang *et al.* (1996)
	2	8	Jansen *et al.* (1997)
	1	2	Vilarinho *et al.* (1997)
m.3243A>G	1	1	Wilichowski *et al.* (1998)
	3	12	Olsson *et al.* (1998)
	2	2	Onishi *et al.* (1998)
	1	2	Chinnery *et al.* (1999)
	1	8	Dubeau *et al.* (2000)
	1	1	Hotta *et al.* (2001)
	1	2	Ko *et al.* (2001)
	1	5	Lien *et al.* (2001)
	1	2	Morovvati *et al.* (2002)
	1	3	Cervin *et al.* (2004)
	1	1	Chou *et al.* (2004)
	1	1	Lu *et al.* (2002)
	2	28	Larsson *et al.* (1992)
	3	7	Hammans *et al.* (1993)
	2	4	Hammans *et al.* (1995)
	1	7	Piccolo *et al.* (1993)
m.8344A>G	2	4	Silvestri *et al.* (1993)
	1	8	Campos *et al.* (1994)
	1	6	Seibel *et al.* (1994)
	1	5	Traff *et al.* (1995)
	1	2	Howell *et al.* (1996)

Mutation	Pedigrees	Transmissions	Reference
m.8993T>G	1	3	Gamez *et al.* (1998)
	1	22	Munoz-Malaga *et al.* (2000)
	1	9	Wong *et al.* (2002)
	1	7	van de Glind *et al.* (2007)
	1	3	Holt *et al.* (1990)
	1	1	Sakuta *et al.* (1992)
	1	2	Puddu *et al.* (1993)
	1	4	Shoffner *et al.* (1992)
	1	5	Tatuch *et al.* (1992)
	1	2	Ciafaloni *et al.* (1993)
	4	6	Santorelli *et al.* (1993)
	1	5	Fryer *et al.* (1994)
	1	1	Lodi *et al.* (1994)
	1	1	Pastores *et al.* (1994)
	1	6	Degoul *et al.* (1995)
	1	3	Houstek *et al.* (1995)
	1	8	Makela-Bengs *et al.* (1995)
	1	2	Tulinius *et al.* (1995)
	1	3	Bartley *et al.* (1996)
	1	3	Mak *et al.* (1996)
	1	4	Ferlin *et al.* (1997)
	4	9	Uziel *et al.* (1997)
	4	16	White *et al.* (1999b)
	1	2	Porto *et al.* (2001)
	1	2	Wong *et al.* (2002)
	1	3	Enns *et al.* (2006)
	1	3	Steffann *et al.* (2007)
	2	5	Mkaouar-Rebai *et al.* (2009)
m.11778G>A	1	3	Holt *et al.* (1989)
	1	5	Sweeney *et al.* (1992)
	4	16	Zhu *et al.* (1992)
	1	15	Howell *et al.* (1994)
	3	6	Harding *et al.* (1995)
	3	7	Carelli *et al.* (1997)
	2	8	Juvonen *et al.* (1997)
	1	10	Tanaka *et al.* (1998)
	1	7	Simon *et al.* (1999)
	1	5	Chuenkongkaew *et al.* (2005)
	3	30	Phasukkijwatana *et al.* (2006)
m.3460G>A	1	4	Howell *et al.* (1991)
	1	5	Howell *et al.* (1992b)
	1	3	Sweeney *et al.* (1992)
	2	8	Harding *et al.* (1995)

Mutation	Pedigrees	Transmissions	Reference
	1	23	Black *et al.* (1996)
	1	7	Ghosh *et al.* (1996)
	2	5	Carelli *et al.* (1997)
	1	11	Kaplanova *et al.* (2004)
	1	7	Volod'ko *et al.* (2006)

Appendix B.2 Descriptive statistics for five mutations from published data. Descriptive statistics for O-M variance distributions include: median and mean, minimum (min) and maximum (max) values, interquartile ranges (25 %, 75 %), standard deviation (Std. Dev) and standard error of the mean (SEM).

Sample	Descriptive Statistics								
	n	Min.	25%	Median	75%	Max.	Mean	Std. Dev.	SEM
m.3243A>G	111	-59.52	-12.08	0	18.53	80.07	3.32	27.01	2.56
m.8344A>G	96	-84	-18.5	-2.5	10	63	-4.96	26.72	2.73
m.8993T>G	118	-54	10	32	53.25	100	32.67	33.07	3.04
m.11778G>A	118	-54	-2	10.26	36	82	15.4	27	2.49
m.3460G>A	74	-40	-3.21	17.5	51.25	91.8	22.02	32.13	3.735

Appendix B.3 Normality statistics for five mutations from published data. Each distribution was subjected to the D'Agostino-Pearson omnibus normality test and the skewness and kurtosis calculated.

Sample	D'Agostino & Pearson omnibus normality test					
	K2	p-value	Normal?	Significant?	Skewness	Kurtosis
m.3243A>G	5.06	0.0797	Yes	ns	0.4696	0.4005
m.8344A>G	3.712	0.1563	Yes	ns	-0.245	0.8995
m.8993T>G	1.592	0.4512	Yes	ns	-0.2182	0.2781
m.11778G>A	1.521	0.4673	Yes	ns	0.2563	-0.2179
m.3460G>A	8.55	0.0139	No	*	0.3268	-0.9184

Appendix B.4 One-sample t-test results for five mutations from published data. Each distribution was subjected to a one-sample t-test against a theoretical mean of 0 and an alpha of 0.005. The discrepancy, 95 % confidence interval (CI) and p-value are given.

Sample	One sample t test					
	Mean	Discrepancy	t, df	p-value	Significant?	Mean
m.3243A>G	3.32	-3.32	-1.762 to 8.407	t=1.296 df=110	0.1977	No
m.8344A>G	-4.96	4.961	-10.38 to 0.4612	t=1.819 df=95	0.072	No
m.8993T>G	32.67	-32.67	26.64 to 38.70	t=10.73 df=117	< 0.0001	Yes
m.11778G>A	15.4	-15.4	10.48 to 20.33	t=6.196 df=117	< 0.0001	Yes
m.3460G>A	22.02	-22.02	14.57 to 29.47	t=5.896 df=73	< 0.0001	Yes

Appendix C. Mouse gene expression BestKeeper analysis.

Appendix C.1 Descriptive statics for 'reference gene' C_t values. BestKeeper software calculates the geometric and arithmetic mean, the minimum and maximum C_t values, standard deviation and the coefficient of variance (CV) for all the 'reference genes'.

Statistic	*18S rRNA*	*B2m*	*Gapdh*	*Hist2a*
n	15	14	15	12
geo Mean [Ct]	19.638	30.832	26.092	30.327
ar Mean [Ct]	19.705	30.955	26.287	30.534
min [Ct]	16.655	27.477	20.814	24.837
max [Ct]	22.354	36.547	31.413	35.297
std dev [± Ct]	**1.301**	**2.353**	**2.749**	**2.984**
CV [% C]	6.600	7.602	10.457	9.772

Appendix C.2 Pearson correlation coefficient calculations. First, the BestKeeper software generates coefficients of correlation between all reference genes; those with high correlation are used to generate a BestKeeper Index value, which is in turn compared to each gene.

BestKeeper vs.	*18S rRNA*	*B2m*	*Gapdh*	*Hist2a*
coeff. of corr. [r]	0.866	0.736	0.845	0.865
p-value	0.001	0.003	0.001	0.001

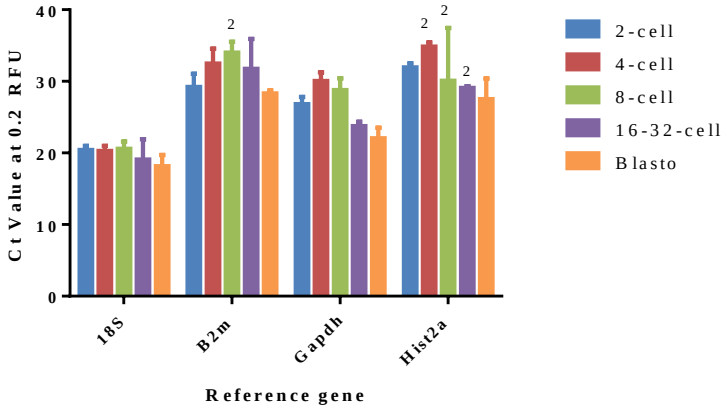

Appendix C.3 Average Ct values for reference genes. The bar chart shows the average C_t values for all reference genes for the different pre-implantation samples. *18S* has much higher expression than the other reference genes and is also more stable. The Ct values for 16-32-cell and Blastocyst (Blasto) are generally lower than the 2-cell, 4-cell and 8-cell samples.

Appendix D. Mouse microarray expression profiles

Microarray data from Sabour and colleagues (2011) was analysed using GEO2R through the NCBI's Gene Expression Omnibus (Edgar *et al.*, 2002). Duplicate RNA samples were extracted from PGCs between 11.5 and 18.5 d.p.c. PGCs at 11.5 d.p.c. were not gender typed; however all other stages selected for analysis are collected from female embryos only.

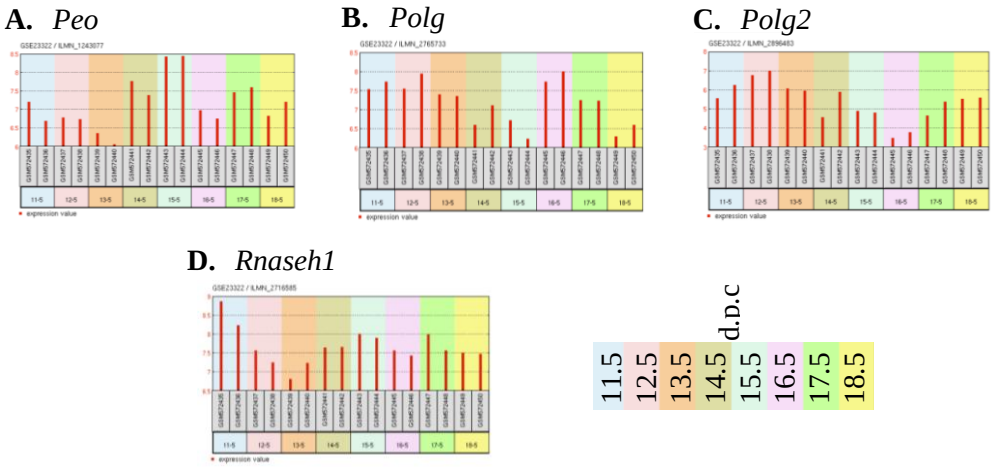

Appendix D.1 Microarray analysis of mitochondrial replication genes. The bar charts represent the raw gene expression signal of mitochondrial replication genes (A) *Peo1*, (B) *Polg*, (C) *Polg2* and (D) *Rnaseh1* taken from published microarray data during post-implantation embryonic development.

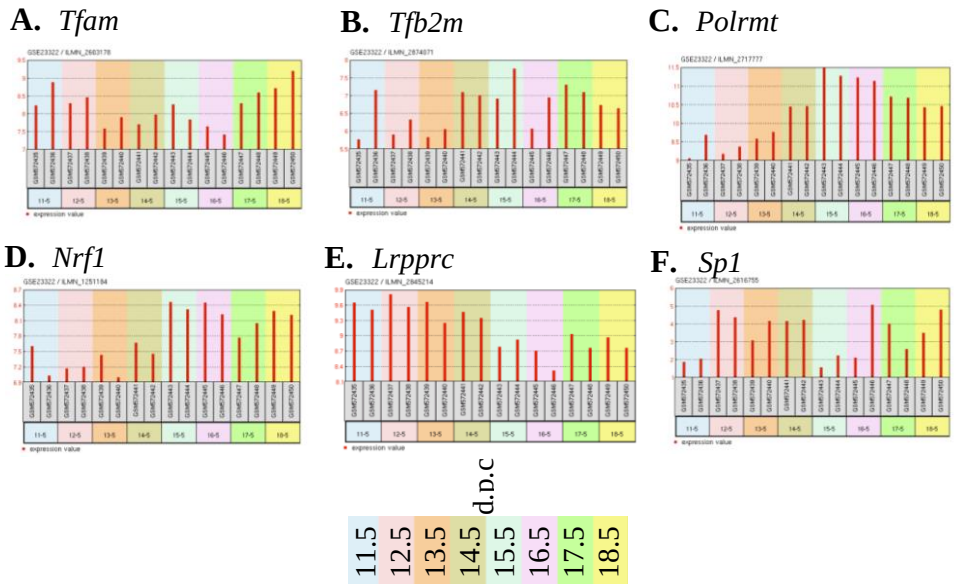

Appendix D.2 Microarray analysis of mitochondrial transcription genes. The bar charts represent the raw gene expression signal of mitochondrial transcription genes (A) *Tfam*, (B) *Tfb2m*, (C) *Polrmt*, (D) *Nrf1*, (E) *Lrpprc* and (F) *Sp1* taken from published microarray data during post-implantation embryonic development.

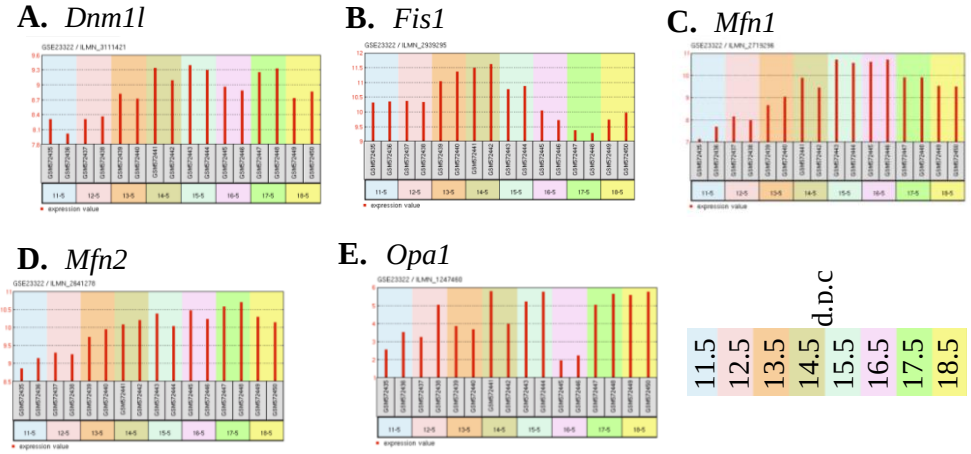

Appendix D.3 Microarray analysis of mitochondrial dynamics genes. The bar charts represent the raw gene expression signal of mitochondrial transcription genes (A) *Dmn1l*, (B) *Fis1*, (C) *Mfn1*, (D) *Mfn2* and (E) O*pa1* taken from published microarray data during post-implantation embryonic development.

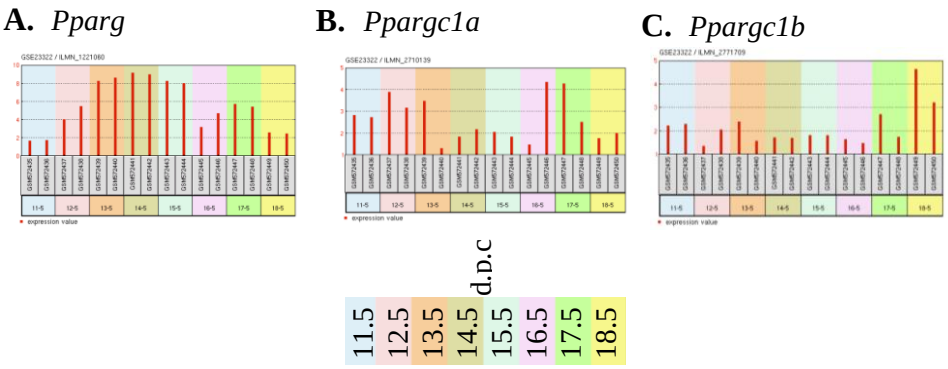

Appendix D.4 Microarray analysis of mitochondrial biogenesis genes. The bar charts represent the raw gene expression signal of mitochondrial transcription genes (A) *Pparg*, (B) *Ppargc1a* and (C) *Ppargc1b* taken from published microarray data during post-implantation embryonic development.

Appendix E. Repopulation

This appendix contains the BestKeeper analysis, performed on RNA samples for a variety of different conditions to establish the most stable housekeeping gene.

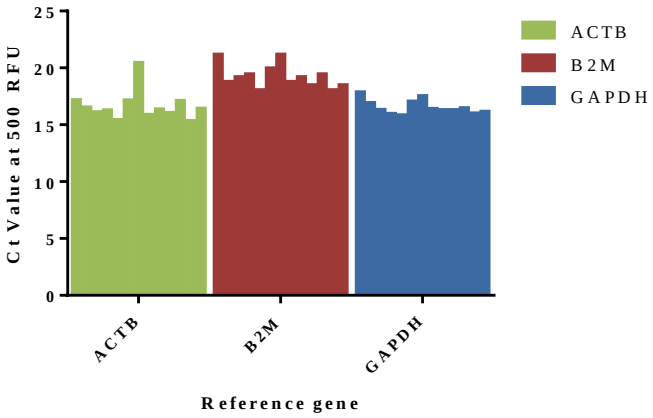

Appendix E.1 The stability of Ct values for 'reference genes' across variable biological conditions. The bar chart shows the average Ct values for all reference genes for fibroblast under different experimental conditions.

Appendix E.2 Descriptive statics for 'reference gene' Ct values and Pearson correlation coefficients. BestKeeper software calculates the geometric and arthithmetic mean, the minimum and maximum Ct values, standard deviation and the coefficient of variance (CV) for all the 'reference genes'. BestKeeper software generates coefficients of correlation between all reference genes, those with high correlation are used to generate a BestKeeper Index value, which is in turn compared to each gene.

Statistic	*ACTB*	*B2M*	*GAPDH*
n	14	14	14
geo Mean [Ct]	16.22	18.96	16.41
ar Mean [Ct]	16.23	18.98	16.42
min [Ct]	15.32	18.04	15.83
max [Ct]	17.16	21.15	17.84
std dev [± Ct]	0.47	0.63	0.37
CV [% Ct]	2.9	3.31	2.23
coeff. of corr. [r]	0.921	0.957	0.909
p-value	0.001	0.001	0.001

Appendix F. Quality control microarray RNA samples.

This appendix contains the standard curves generated for quantification of RNA concentration from dilute samples, and the calculations made for the final microarray samples.

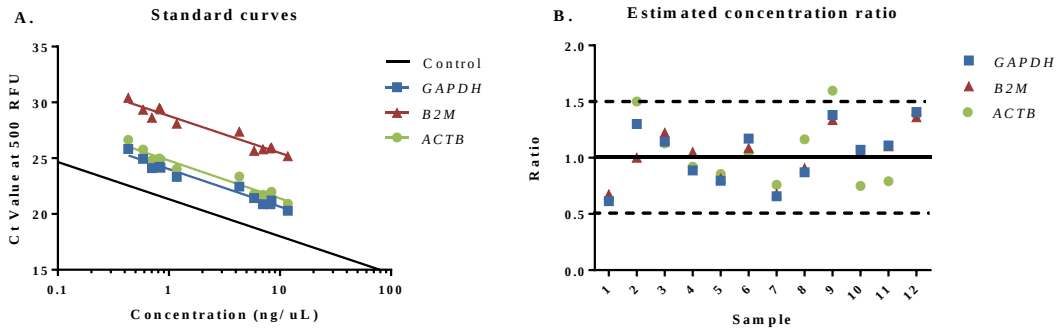

Appendix F.1 Generation of standard curves from Ct values for estimation of RNA concentration. (A) Standard curves are generated for the reference genes *GAPDH*, *B2M* and *ACTB* using RNA samples where concentration has also be assessed by Agilent Bioanalyzer. (B) Using the standard curve equations for each gene, the concentration for each sample was calculated and compared to the measured concentration. Each sample falls within a 50% range of the measured concentration.

Appendix F.2 Quantification of final sample concentration. The Ct values measured in the final samples for *GAPDH, B2M, ACTB* are used to estimate the concentration of RNA from the previously calculated standard curves.

Sample	Concentration (pg/µL)						
	GAPDH	*B2M*	*ACTB*	Min	Max	Average	StdDev
CON	1094.5	791.2	511.2	253.6	1636.0	799.0	291.7
RRF	969.9	1412.8	782.1	365.5	2068.2	1054.9	323.8
NOR	511.1	938.7	592.2	226.8	1361.6	680.6	227.1

Appendix G. Quality control of microarray data.

This appendix contains details of quality control measures to ensure preparation of the microarray was sufficient and gene expression signals were reliable.

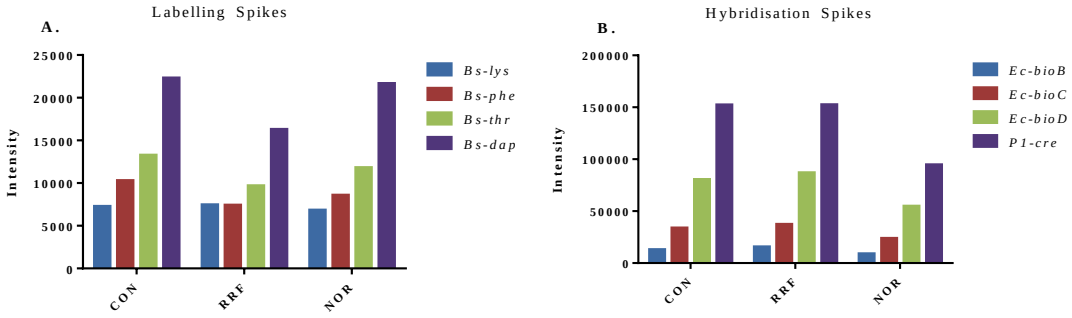

Appendix G.1 Microarray labelling and hybdrisation efficiency. (A) RNA samples were spiked with unlabelled *B.subtilis* genes *lys*, *phe*, *thr* and *dap* at increasing concentrations to assess labelling efficiency. (B) cDNA samples were spiked with prelabelled *E.coli* genes *bioB, bioC, bioD* and *Cre* at increasing concentrations to assess hybridisation efficiency. Labelling and hybridisation was successful in all samples.

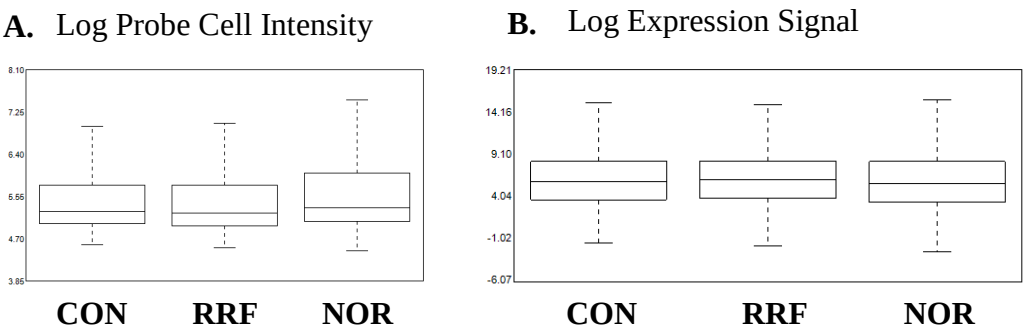

Appendix G.2 Signal intensity from microarray. Box-plots calculated by the Affymetrix® Expression Console™. The (A) raw probe cell intensity from CEL files and (B) MAS5 calculated expression signal was similar for all samples.

Appendix G.3 Statistics for microarray samples. RawQ, scaling factor (SF), background (BG), noise and percentage present calls (%P) values calculated by the Affymetrix® Expression Console™ are similar across all samples for microarray analysis.

	RawQ	TGT	SF	BG Avg	BG Std	Noise Avg	Noise Std	%P
CON	0.62	500.00	21.85	27.13	0.20	0.60	0.05	32.85
RRF	0.58	500.00	24.53	25.64	0.14	0.55	0.04	32.01
NOR	0.62	500.00	15.53	26.35	0.11	0.67	0.03	33.48

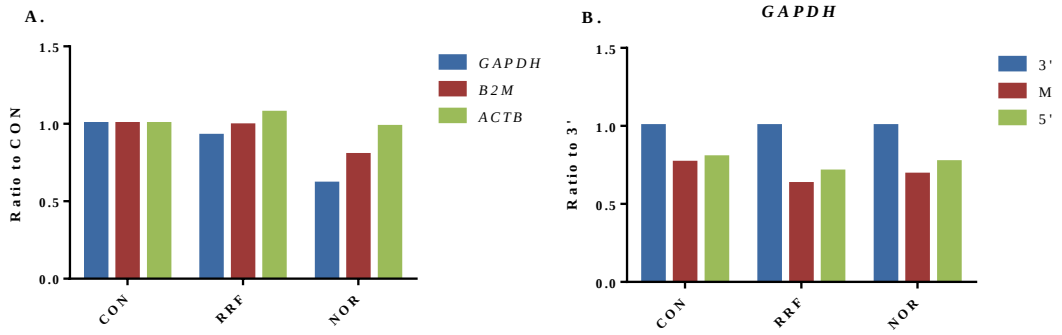

Appendix G.4 Reference gene profile integrity from microarray analysis. (A) The gene expression profile of *GAPDH*, *B2M* and *ACTB* relative to that in CON. RRF has lower *GAPDH* expression than CON or NOR. (B) 5' to 3' ratio for GAPDH in CON, RRF and NOR shows a similar amount of loss of 5' signal for all samples.

Appendix H. Regulated pathways

This appendix contains pathway information modified from the KEGG database (Kanehisa and Goto, 2000).

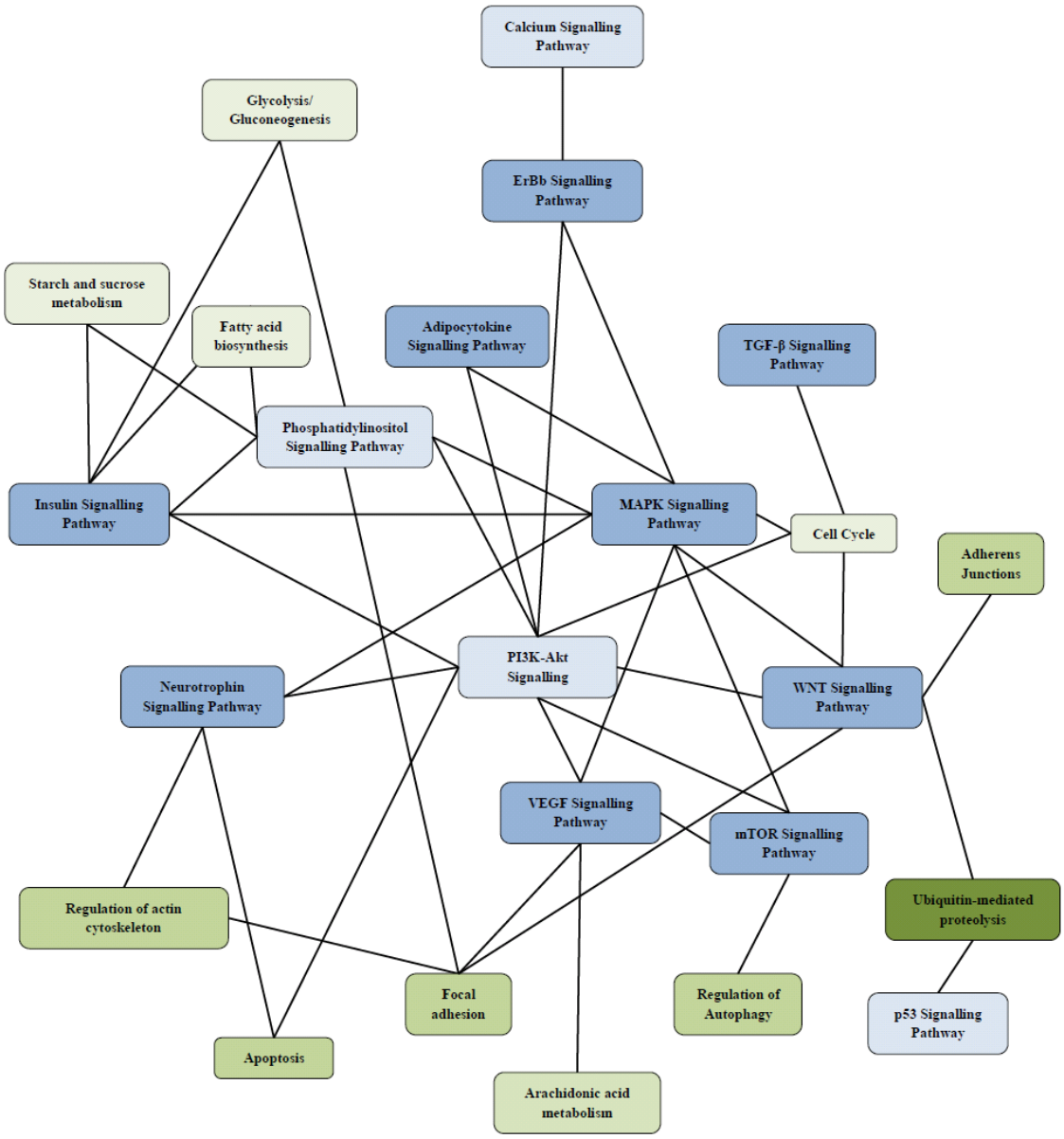

Appendix H.1 An overview of inter-connected enriched biological pathways in MERRF patient tissue. Signalling pathways are labelled blue and functional pathways are labelled green. Pathways not enriched are labelled in light colours, those enriched in all MERRF tissue are labelled in medium colours. The only pathway enriched specifically in RRF, ubiquitin-mediated proteolysis is labelled in dark green.

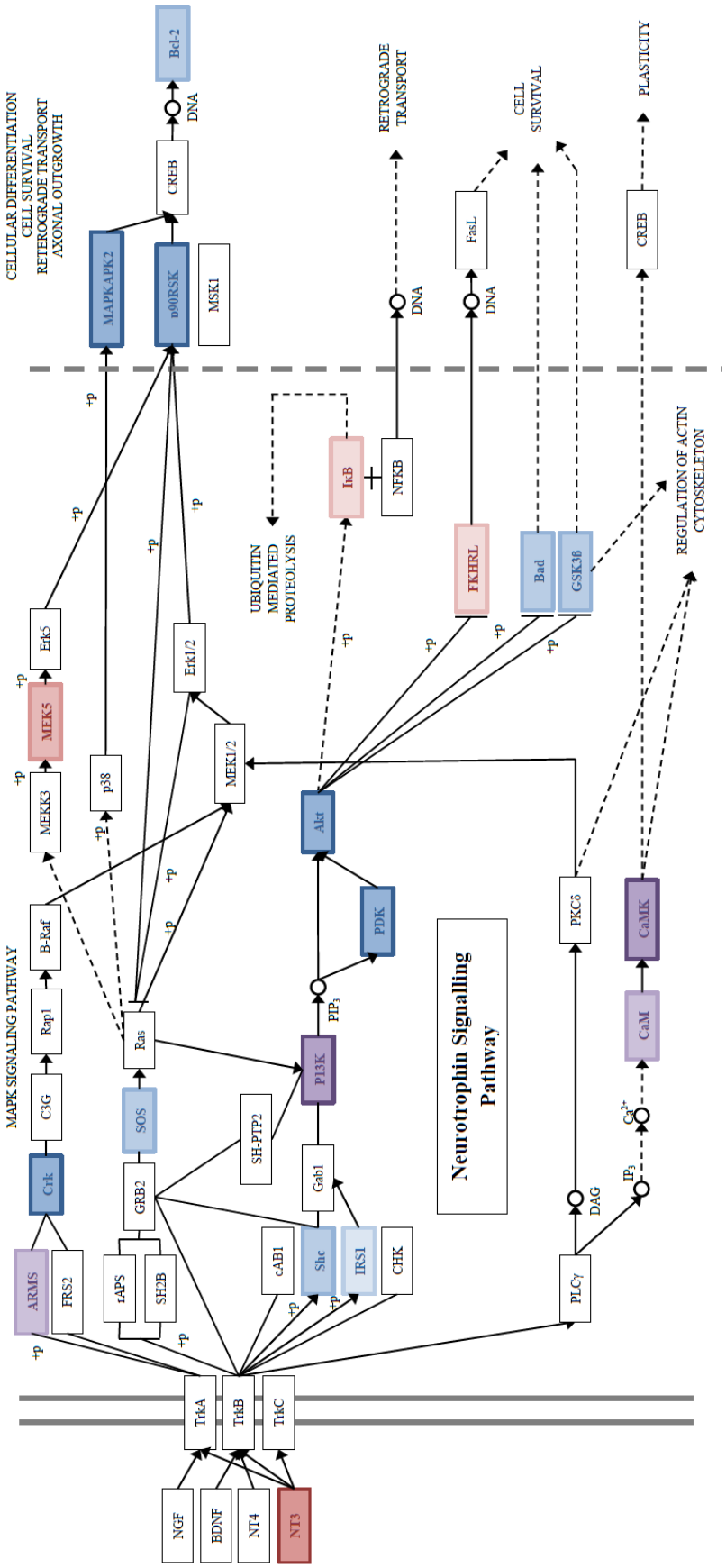

Appendix H.2 Neutrotrophin Signalling Pathway. Pathway maps are adapted from KEGG. Red annotations indicate upregulated genes, blue annotations indicate downregulated genes. If there are both up and downregulated genes within each term, the annotation is purple. Light colours indicate MERRF-specificity, medium colours indicate 'exacerbated in RRF' and dark colours indicate RRF-specificity.

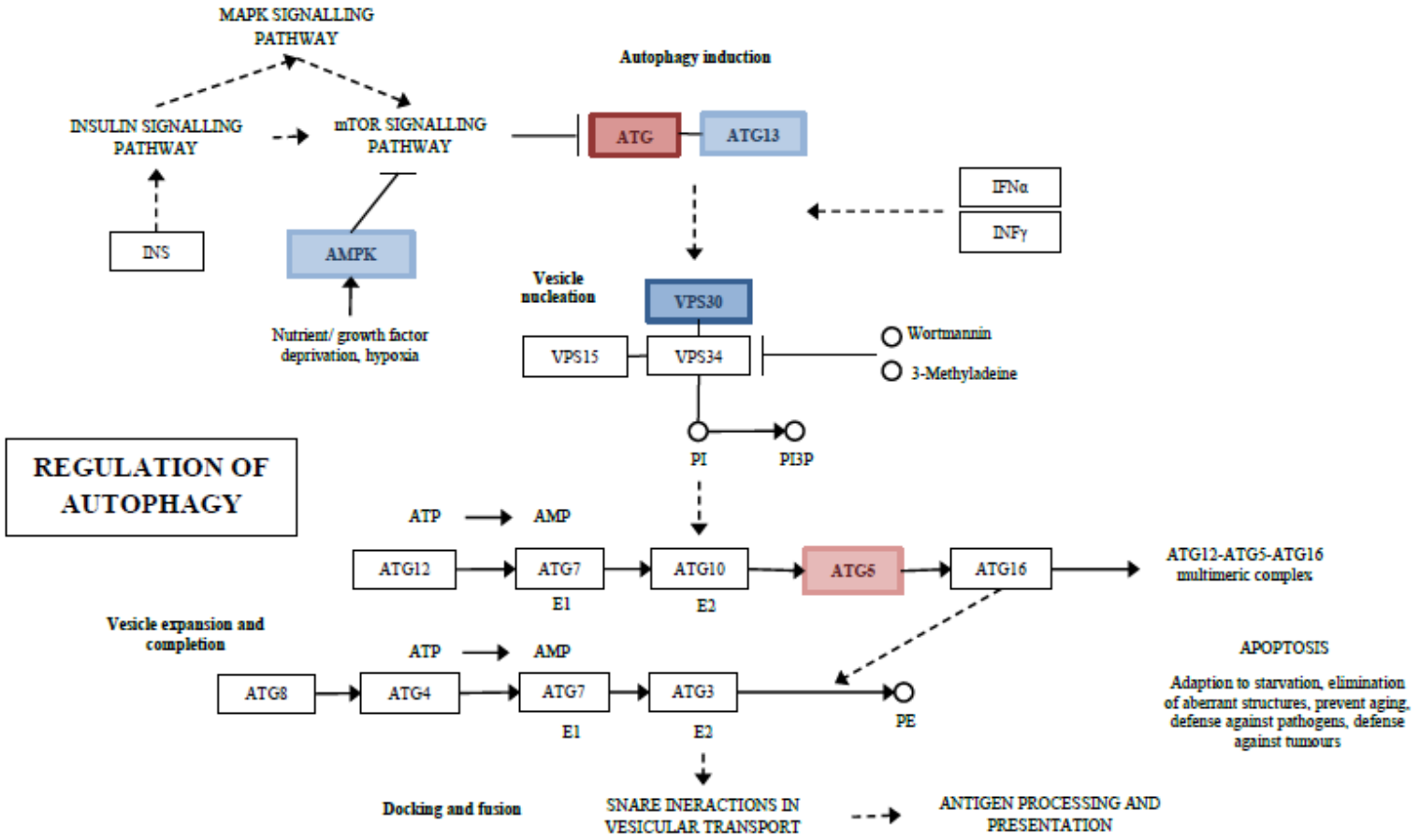

Appendix H.3 Regulation of Autophagy. Pathway maps are adapted from KEGG. Red annotations indicate upregulated genes, blue annotations indicate downregulated genes. If there are both up and downregulated genes within each term, the annotation is purple. Light colours indicate MERRF-specificity, medium colours indicate 'exacerbated in RRF' and dark colours indicate RRF-specificity.

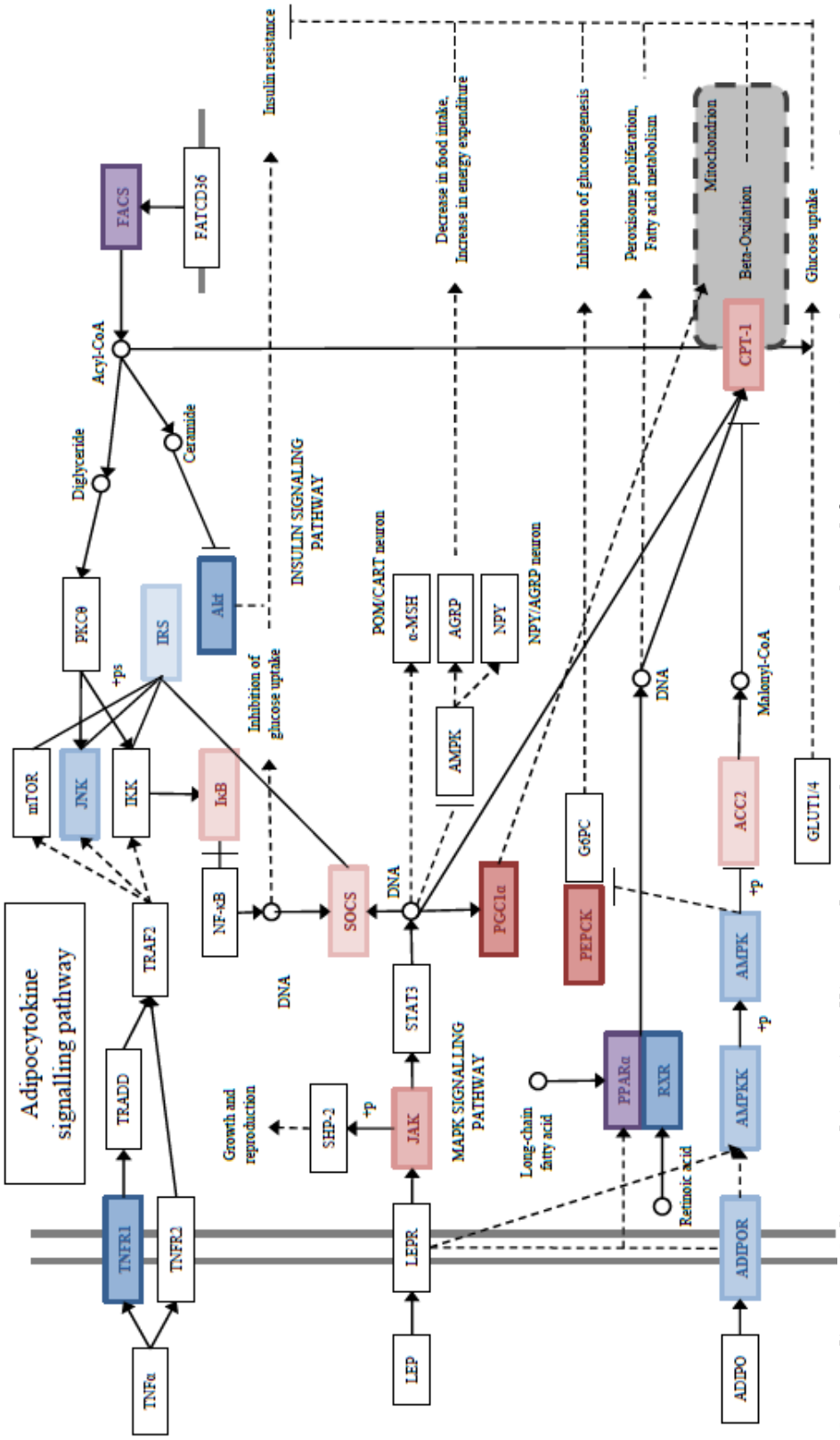

Appendix H.4 Adipocytokine signalling pathway. Pathway maps are adapted from KEGG. Red annotations indicate upregulated genes, blue annotations indicate downregulated genes. If there are both up and downregulated genes within each term, the annotation is purple. Light colours indicate MERRF-specificity, medium colours indicate 'exacerbated in RRF' and dark colours indicate RRF-specificity.

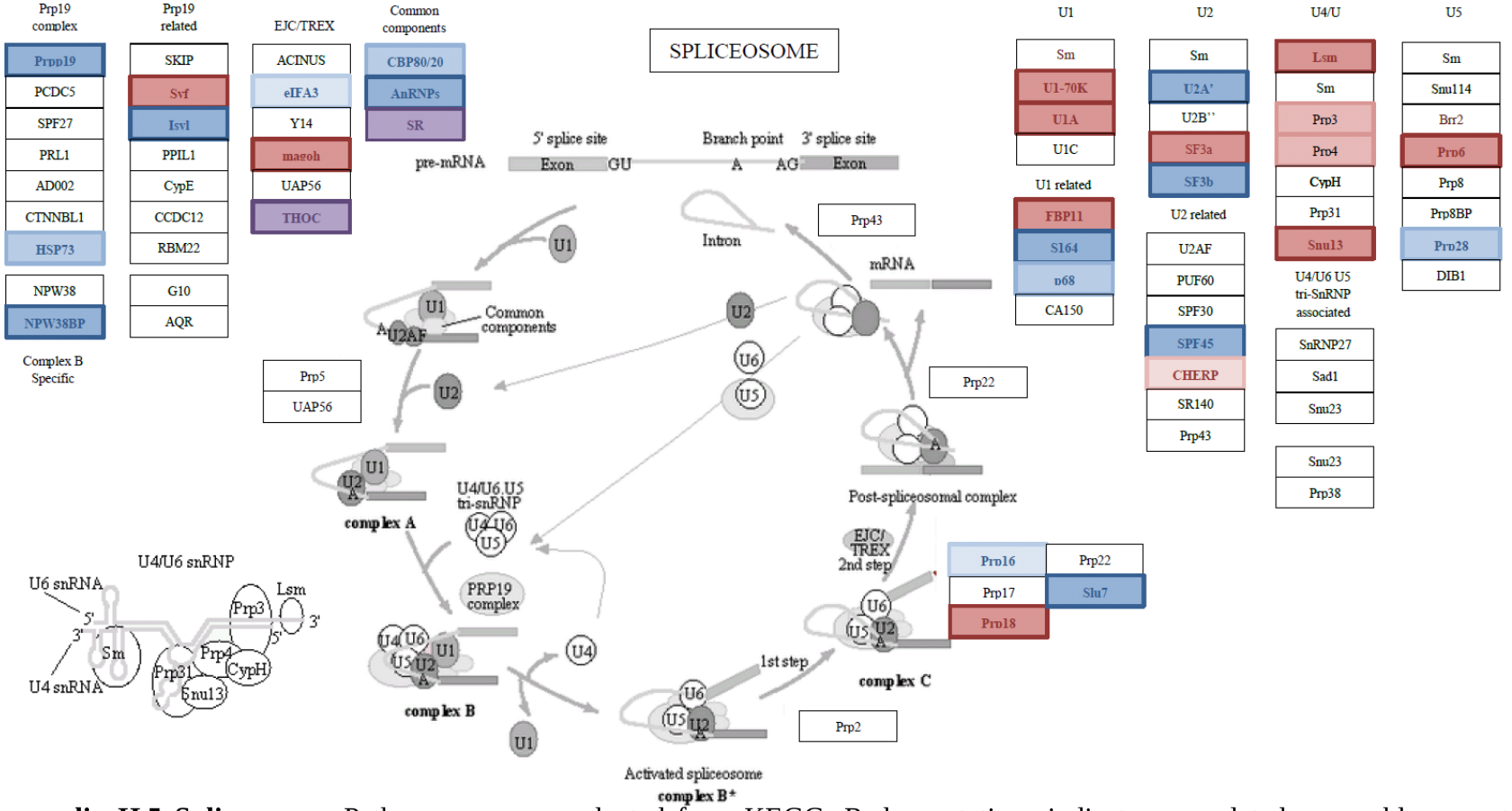

Appendix H.5 Spliceosome. Pathway maps are adapted from KEGG. Red annotations indicate upregulated genes, blue annotations indicate downregulated genes. If there are both up and downregulated genes within each term, the annotation is purple. Light colours indicate MERRF-specificity, medium colours indicate 'exacerbated in RRF' and dark colours indicate RRF-specificity.

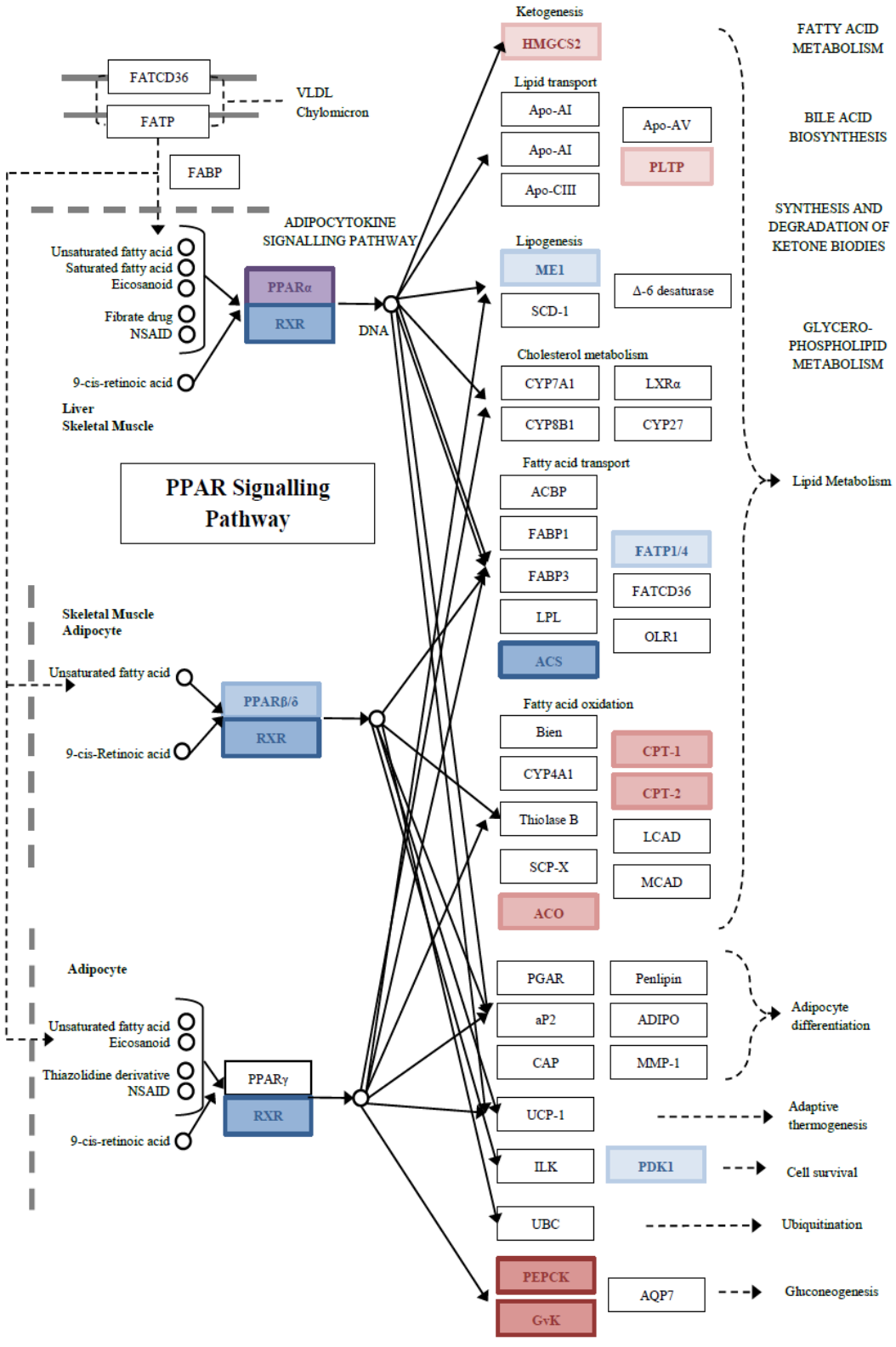

Appendix H.6 PPAR Signalling Pathway. Pathway maps are adapted from KEGG. Red annotations indicate upregulated genes, blue annotations indicate downregulated genes. If there are both up and downregulated genes within each term, the annotation is purple. Light colours indicate MERRF-specificity, medium colours indicate 'exacerbated in RRF' and dark colours indicate RRF-specificity.

Chapter 9. Bibliography

Aamann, M. D., Sorensen, M. M., Hvitby, C., Berquist, B. R., Muftuoglu, M., Tian, J., De Souza-Pinto, N. C., Scheibye-Knudsen, M., Wilson, D. M., 3rd, Stevnsner, T.Bohr, V. A. 2010. Cockayne syndrome group B protein promotes mitochondrial DNA stability by supporting the DNA repair association with the mitochondrial membrane. *FASEB J,* 24**,** 2334-46.

Abe, Y., Shodai, T., Muto, T., Mihara, K., Torii, H., Nishikawa, S., Endo, T.Kohda, D. 2000. Structural basis of presequence recognition by the mitochondrial protein import receptor Tom20. *Cell,* 100**,** 551-60.

Aguilera, P., Barry, T.Tovar, J. 2008. Entamoeba histolytica mitosomes: organelles in search of a function. *Exp Parasitol,* 118**,** 10-6.

Ahmed, S., Passos, J. F., Birket, M. J., Beckmann, T., Brings, S., Peters, H., Birch-Machin, M. A., Von Zglinicki, T.Saretzki, G. 2008. Telomerase does not counteract telomere shortening but protects mitochondrial function under oxidative stress. *J Cell Sci,* 121**,** 1046-53.

Aiken, C. E., Cindrova-Davies, T.Johnson, M. H. 2008. Variations in mouse mitochondrial DNA copy number from fertilization to birth are associated with oxidative stress. *Reprod Biomed Online,* 17**,** 806-13.

Akimoto, T., Li, P.Yan, Z. 2008. Functional interaction of regulatory factors with the Pgc-1alpha promoter in response to exercise by in vivo imaging. *Am J Physiol Cell Physiol,* 295**,** C288-92.

Akimoto, T., Pohnert, S. C., Li, P., Zhang, M., Gumbs, C., Rosenberg, P. B., Williams, R. S.Yan, Z. 2005. Exercise stimulates Pgc-1alpha transcription in skeletal muscle through activation of the p38 MAPK pathway. *J Biol Chem,* 280**,** 19587-93.

Alam, T. I., Kanki, T., Muta, T., Ukaji, K., Abe, Y., Nakayama, H., Takio, K., Hamasaki, N.Kang, D. 2003. Human mitochondrial DNA is packaged with TFAM. *Nucleic Acids Res,* 31**,** 1640-5.

Alemi, M., Prigione, A., Wong, A., Schoenfeld, R., Dimauro, S., Hirano, M., Taroni, F.Cortopassi, G. 2007. Mitochondrial DNA deletions inhibit proteasomal activity and stimulate an autophagic transcript. *Free Radic Biol Med,* 42**,** 32-43.

Allen, J. F. 1993. Control of gene expression by redox potential and the requirement for chloroplast and mitochondrial genomes. *J Theor Biol,* 165**,** 609-31.

Amati-Bonneau, P., Valentino, M. L., Reynier, P., Gallardo, M. E., Bornstein, B., Boissiere, A., Campos, Y., Rivera, H., De La Aleja, J. G., Carroccia, R., Iommarini, L., Labauge, P., Figarella-Branger, D., Marcorelles, P., Furby, A.,

Beauvais, K., Letournel, F., Liguori, R., La Morgia, C., Montagna, P., Liguori, M., Zanna, C., Rugolo, M., Cossarizza, A., Wissinger, B., Verny, C., Schwarzenbacher, R., Martin, M. A., Arenas, J., Ayuso, C., Garesse, R., Lenaers, G., Bonneau, D.Carelli, V. 2008. OPA1 mutations induce mitochondrial DNA instability and optic atrophy 'plus' phenotypes. *Brain,* 131**,** 338-51.

Anderson, S., Bankier, A. T., Barrell, B. G., De Bruijn, M. H., Coulson, A. R., Drouin, J., Eperon, I. C., Nierlich, D. P., Roe, B. A., Sanger, F., Schreier, P. H., Smith, A. J., Staden, R.Young, I. G. 1981. Sequence and organization of the human mitochondrial genome. *Nature,* 290**,** 457-65.

Andersson, S. G.Kurland, C. G. 1998. Reductive evolution of resident genomes. *Trends Microbiol,* 6**,** 263-8.

Andersson, U.Scarpulla, R. C. 2001. Pgc-1-related coactivator, a novel, serum-inducible coactivator of nuclear respiratory factor 1-dependent transcription in mammalian cells. *Mol Cell Biol,* 21**,** 3738-49.

Andreu, A. L., Hanna, M. G., Reichmann, H., Bruno, C., Penn, A. S., Tanji, K., Pallotti, F., Iwata, S., Bonilla, E., Lach, B., Morgan-Hughes, J.Dimauro, S. 1999. Exercise intolerance due to mutations in the cytochrome b gene of mitochondrial DNA. *N Engl J Med,* 341**,** 1037-44.

Andrews, R. M., Kubacka, I., Chinnery, P. F., Lightowlers, R. N., Turnbull, D. M.Howell, N. 1999. Reanalysis and revision of the Cambridge reference sequence for human mitochondrial DNA. *Nat Genet,* 23**,** 147.

Aphasizheva, I., Maslov, D., Wang, X., Huang, L.Aphasizhev, R. 2011. Pentatricopeptide repeat proteins stimulate mRNA adenylation/uridylation to activate mitochondrial translation in trypanosomes. *Mol Cell,* 42**,** 106-17.

Ashburner, M., Ball, C. A., Blake, J. A., Botstein, D., Butler, H., Cherry, J. M., Davis, A. P., Dolinski, K., Dwight, S. S., Eppig, J. T., Harris, M. A., Hill, D. P., Issel-Tarver, L., Kasarskis, A., Lewis, S., Matese, J. C., Richardson, J. E., Ringwald, M., Rubin, G. M.Sherlock, G. 2000. Gene ontology: tool for the unification of biology. The Gene Ontology Consortium. *Nat Genet,* 25**,** 25-9.

Asin-Cayuela, J., Schwend, T., Farge, G.Gustafsson, C. M. 2005. The human mitochondrial transcription termination factor (mTERF) is fully active in vitro in the non-phosphorylated form. *J Biol Chem,* 280**,** 25499-505.

Astuti, D., Latif, F., Dallol, A., Dahia, P. L., Douglas, F., George, E., Skoldberg, F., Husebye, E. S., Eng, C.Maher, E. R. 2001. Gene mutations in the succinate dehydrogenase subunit SDHB cause susceptibility to familial pheochromocytoma and to familial paraganglioma. *Am J Hum Genet,* 69**,** 49-54.

Auer, H., Lyianarachchi, S., Newsom, D., Klisovic, M. I., Marcucci, G.Kornacker, K. 2003. Chipping away at the chip bias: RNA degradation in microarray analysis. *Nat Genet,* 35**,** 292-3.

Baar, K., Song, Z., Semenkovich, C. F., Jones, T. E., Han, D. H., Nolte, L. A., Ojuka, E. O., Chen, M.Holloszy, J. O. 2003. Skeletal muscle overexpression of nuclear respiratory factor 1 increases glucose transport capacity. *FASEB J,* 17**,** 1666-73.

Babcock, G. T.Wikstrom, M. 1992. Oxygen activation and the conservation of energy in cell respiration. *Nature,* 356**,** 301-9.

Bach, D., Naon, D., Pich, S., Soriano, F. X., Vega, N., Rieusset, J., Laville, M., Guillet, C., Boirie, Y., Wallberg-Henriksson, H., Manco, M., Calvani, M., Castagneto, M., Palacin, M., Mingrone, G., Zierath, J. R., Vidal, H.Zorzano, A. 2005. Expression of Mfn2, the Charcot-Marie-Tooth neuropathy type 2A gene, in human skeletal muscle: effects of type 2 diabetes, obesity, weight loss, and the regulatory role of tumor necrosis factor alpha and interleukin-6. *Diabetes,* 54**,** 2685-93.

Bach, D., Pich, S., Soriano, F. X., Vega, N., Baumgartner, B., Oriola, J., Daugaard, J. R., Lloberas, J., Camps, M., Zierath, J. R., Rabasa-Lhoret, R., Wallberg-Henriksson, H., Laville, M., Palacin, M., Vidal, H., Rivera, F., Brand, M.Zorzano, A. 2003. Mitofusin-2 determines mitochondrial network architecture and mitochondrial metabolism. A novel regulatory mechanism altered in obesity. *J Biol Chem,* 278**,** 17190-7.

Bakay, M., Chen, Y. W., Borup, R., Zhao, P., Nagaraju, K.Hoffman, E. P. 2002. Sources of variability and effect of experimental approach on expression profiling data interpretation. *BMC Bioinformatics,* 3**,** 4.

Balaban, R. S., Nemoto, S.Finkel, T. 2005. Mitochondria, oxidants, and aging. *Cell,* 120**,** 483-95.

Baldauf, S. L., Palmer, J. D.Doolittle, W. F. 1996. The root of the universal tree and the origin of eukaryotes based on elongation factor phylogeny. *Proc Natl Acad Sci U S A,* 93**,** 7749-54.

Barrell, B. G., Anderson, S., Bankier, A. T., De Bruijn, M. H., Chen, E., Coulson, A. R., Drouin, J., Eperon, I. C., Nierlich, D. P., Roe, B. A., Sanger, F., Schreier, P. H., Smith, A. J., Staden, R.Young, I. G. 1980. Different pattern of codon recognition by mammalian mitochondrial tRNAs. *Proc Natl Acad Sci U S A,* 77**,** 3164-6.

Barritt, J. A., Brenner, C. A., Cohen, J.Matt, D. W. 1999. Mitochondrial DNA rearrangements in human oocytes and embryos. *Mol Hum Reprod,* 5**,** 927-33.

Bartley, J., Senadheera, D., Park, P., Brar, H., D, A.Wong, L. 1996. Prenatal diagnosis of T8993G mitochondrial DNA point mutation in amniocytes by heteroplasmy detection. *Am J Hum Genet,* 59.

Bastin, J., Aubey, F., Rotig, A., Munnich, A.Djouadi, F. 2008. Activation of peroxisome proliferator-activated receptor pathway stimulates the mitochondrial respiratory chain and can correct deficiencies in patients' cells lacking its components. *J Clin Endocrinol Metab,* 93**,** 1433-41.

Baysal, B. E., Ferrell, R. E., Willett-Brozick, J. E., Lawrence, E. C., Myssiorek, D., Bosch, A., Van Der Mey, A., Taschner, P. E., Rubinstein, W. S., Myers, E. N., Richard, C. W., 3rd, Cornelisse, C. J., Devilee, P.Devlin, B. 2000. Mutations in SDHD, a mitochondrial complex II gene, in hereditary paraganglioma. *Science,* 287**,** 848-51.

Benard, G., Bellance, N., James, D., Parrone, P., Fernandez, H., Letellier, T.Rossignol, R. 2007. Mitochondrial bioenergetics and structural network organization. *J Cell Sci,* 120**,** 838-48.

Benbrik, E., Chariot, P., Bonavaud, S., Ammi-Said, M., Frisdal, E., Rey, C., Gherardi, R.Barlovatz-Meimon, G. 1997. Cellular and mitochondrial toxicity of zidovudine (AZT), didanosine (ddI) and zalcitabine (ddC) on cultured human muscle cells. *J Neurol Sci,* 149**,** 19-25.

Benit, P., Beugnot, R., Chretien, D., Giurgea, I., De Lonlay-Debeney, P., Issartel, J. P., Corral-Debrinski, M., Kerscher, S., Rustin, P., Rotig, A.Munnich, A. 2003. Mutant NDUFV2 subunit of mitochondrial complex I causes early onset hypertrophic cardiomyopathy and encephalopathy. *Hum Mutat,* 21**,** 582-6.

Benton, C. R., Wright, D. C.Bonen, A. 2008. PGC-1alpha-mediated regulation of gene expression and metabolism: implications for nutrition and exercise prescriptions. *Appl Physiol Nutr Metab,* 33**,** 843-62.

Bereiter-Hahn, J.Voth, M. 1994. Dynamics of mitochondria in living cells: shape changes, dislocations, fusion, and fission of mitochondria. *Microsc Res Tech,* 27**,** 198-219.

Berg, O. G.Kurland, C. G. 2000. Why mitochondrial genes are most often found in nuclei. *Mol Biol Evol,* 17**,** 951-61.

Bergstrom, C. T.Pritchard, J. 1998. Germline bottlenecks and the evolutionary maintenance of mitochondrial genomes. *Genetics,* 149**,** 2135-46.

Berquist, B. R., Canugovi, C., Sykora, P., Wilson, D. M., 3rdBohr, V. A. 2012. Human Cockayne syndrome B protein reciprocally communicates with mitochondrial proteins and promotes transcriptional elongation. *Nucleic Acids Res*.

Bertram, G., Innes, S., Minella, O., Richardson, J.Stansfield, I. 2001. Endless possibilities: translation termination and stop codon recognition. *Microbiology,* 147**,** 255-69.

Betsuyaku, T., Griffin, G. L., Watson, M. A.Senior, R. M. 2001. Laser capture microdissection and real-time reverse transcriptase/ polymerase chain reaction of bronchiolar epithelium after bleomycin. *Am J Respir Cell Mol Biol,* 25**,** 278-84.

Birkus, G., Hitchcock, M. J.Cihlar, T. 2002. Assessment of mitochondrial toxicity in human cells treated with tenofovir: comparison with other nucleoside reverse transcriptase inhibitors. *Antimicrob Agents Chemother,* 46**,** 716-23.

Black, G. C., Morten, K., Laborde, A.Poulton, J. 1996. Leber's hereditary optic neuropathy: heteroplasmy is likely to be significant in the expression of LHON in families with the 3460 ND1 mutation. *Br J Ophthalmol,* 80**,** 915-7.

Bloemberg, D.Quadrilatero, J. 2012. Rapid determination of myosin heavy chain expression in rat, mouse, and human skeletal muscle using multicolor immunofluorescence analysis. *PLoS One,* 7**,** e35273.

Blok, R. B., Gook, D. A., Thorburn, D. R.Dahl, H. H. 1997. Skewed segregation of the mtDNA nt 8993 (T-->G) mutation in human oocytes. *Am J Hum Genet,* 60**,** 1495-501.

Bogenhagen, D.Clayton, D. A. 1977. Mouse L cell mitochondrial DNA molecules are selected randomly for replication throughout the cell cycle. *Cell,* 11**,** 719-27.

Bogenhagen, D. F. 2012. Mitochondrial DNA nucleoid structure. *Biochim Biophys Acta,* 1819**,** 914-20.

Bogenhagen, D. F., Rousseau, D.Burke, S. 2008. The layered structure of human mitochondrial DNA nucleoids. *J Biol Chem,* 283**,** 3665-75.

Bonawitz, N. D., Clayton, D. A.Shadel, G. S. 2006. Initiation and beyond: multiple functions of the human mitochondrial transcription machinery. *Mol Cell,* 24**,** 813-25.

Bonnefoy, N., Fiumera, H. L., Dujardin, G.Fox, T. D. 2009. Roles of Oxa1-related inner-membrane translocases in assembly of respiratory chain complexes. *Biochim Biophys Acta,* 1793**,** 60-70.

Boore, J. L. 1999. Animal mitochondrial genomes. *Nucleic Acids Res,* 27**,** 1767-80.

Bourdon, A., Minai, L., Serre, V., Jais, J. P., Sarzi, E., Aubert, S., Chretien, D., De Lonlay, P., Paquis-Flucklinger, V., Arakawa, H., Nakamura, Y., Munnich, A.Rotig, A. 2007. Mutation of RRM2B, encoding p53-controlled ribonucleotide reductase (p53R2), causes severe mitochondrial DNA depletion. *Nat Genet,* 39**,** 776-80.

Bourgeois, J. M.Tarnopolsky, M. A. 2004. Pathology of skeletal muscle in mitochondrial disorders. *Mitochondrion,* 4**,** 441-52.

Bourgeron, T., Rustin, P., Chretien, D., Birch-Machin, M., Bourgeois, M., Viegas-Pequignot, E., Munnich, A.Rotig, A. 1995. Mutation of a nuclear succinate dehydrogenase gene results in mitochondrial respiratory chain deficiency. *Nat Genet,* 11**,** 144-9.

Bowmaker, M., Yang, M. Y., Yasukawa, T., Reyes, A., Jacobs, H. T., Huberman, J. A.Holt, I. J. 2003. Mammalian mitochondrial DNA replicates bidirectionally from an initiation zone. *J Biol Chem,* 278**,** 50961-9.

Brandt, U. 2006. Energy converting NADH:quinone oxidoreductase (complex I). *Annu Rev Biochem,* 75**,** 69-92.

Braun, H. P.Schmitz, U. K. 1997. The mitochondrial processing peptidase. *Int J Biochem Cell Biol,* 29**,** 1043-5.

Brierley, E. J., Johnson, M. A., Lightowlers, R. N., James, O. F.Turnbull, D. M. 1998. Role of mitochondrial DNA mutations in human aging: implications for the central nervous system and muscle. *Ann Neurol,* 43**,** 217-23.

Brooke, M. H.Kaiser, K. K. 1970. Three "myosin adenosine triphosphatase" systems: the nature of their pH lability and sulfhydryl dependence. *J Histochem Cytochem,* 18**,** 670-2.

Brown, A. L.Smith, D. W. 2009. Improved RNA preservation for immunolabeling and laser microdissection. *RNA,* 15**,** 2364-74.

Brown, D. T., Samuels, D. C., Michael, E. M., Turnbull, D. M.Chinnery, P. F. 2001. Random genetic drift determines the level of mutant mtDNA in human primary oocytes. *Am J Hum Genet,* 68**,** 533-6.

Brown, M. D., Torroni, A., Reckord, C. L.Wallace, D. C. 1995. Phylogenetic analysis of Leber's hereditary optic neuropathy mitochondrial DNA's indicates multiple independent occurrences of the common mutations. *Hum Mutat,* 6**,** 311-25.

Brown, T. A., Tkachuk, A. N., Shtengel, G., Kopek, B. G., Bogenhagen, D. F., Hess, H. F.Clayton, D. A. 2011. Superresolution fluorescence imaging of mitochondrial nucleoids reveals their spatial range, limits, and membrane interaction. *Mol Cell Biol,* 31**,** 4994-5010.

Brown, W. M., George, M., Jr.Wilson, A. C. 1979. Rapid evolution of animal mitochondrial DNA. *Proc Natl Acad Sci U S A,* 76**,** 1967-71.

Bustin, S. A., Benes, V., Garson, J. A., Hellemans, J., Huggett, J., Kubista, M., Mueller, R., Nolan, T., Pfaffl, M. W., Shipley, G. L., Vandesompele, J.Wittwer, C. T. 2009. The MIQE guidelines: minimum information for publication of quantitative real-time PCR experiments. *Clin Chem,* 55**,** 611-22.

Bykhovskaya, Y., Casas, K., Mengesha, E., Inbal, A.Fischel-Ghodsian, N. 2004a. Missense mutation in pseudouridine synthase 1 (PUS1) causes mitochondrial myopathy and sideroblastic anemia (MLASA). *Am J Hum Genet,* 74**,** 1303-8.

Bykhovskaya, Y., Mengesha, E., Wang, D., Yang, H., Estivill, X., Shohat, M.Fischel-Ghodsian, N. 2004b. Human mitochondrial transcription factor B1 as a modifier gene for hearing loss associated with the mitochondrial A1555G mutation. *Mol Genet Metab,* 82**,** 27-32.

Calvo, J. A., Daniels, T. G., Wang, X., Paul, A., Lin, J., Spiegelman, B. M., Stevenson, S. C.Rangwala, S. M. 2008. Muscle-specific expression of PPARgamma coactivator-1alpha improves exercise performance and increases peak oxygen uptake. *J Appl Physiol,* 104**,** 1304-12.

Camara, Y., Asin-Cayuela, J., Park, C. B., Metodiev, M. D., Shi, Y., Ruzzenente, B., Kukat, C., Habermann, B., Wibom, R., Hultenby, K., Franz, T., Erdjument-Bromage, H., Tempst, P., Hallberg, B. M., Gustafsson, C. M.Larsson, N. G. 2011. MTERF4 regulates translation by targeting the methyltransferase NSUN4 to the mammalian mitochondrial ribosome. *Cell Metab,* 13**,** 527-39.

Campos, Y., Bautista, J., Gutierrez-Rivas, E., Chinchon, D., Cabello, A., Segura, D.Arenas, J. 1995. Clinical heterogeneity in two pedigrees with the 3243 bp tRNA(Leu(UUR)) mutation of mitochondrial DNA. *Acta Neurol Scand,* 91**,** 62-5.

Campos, Y., Esteban, J., Cabello, A.Arenas, J. 1994. Genetic analysis of one family with myoclonic epilepsy and ragged-red fibers (MERRF). *Muscle Nerve,* 17**,** 1229-31.

Campos, Y., Gamez, J., Garcia, A., Andreu, A. L., Rubio, J. C., Martin, M. A., Del Hoyo, P., Navarro, C., Cervera, C., Garesse, R.Arenas, J. 2001. A new mtDNA mutation in the tRNA(Leu(UUR)) gene associated with ocular myopathy. *Neuromuscul Disord,* 11**,** 477-80.

Canto, C., Chibalin, A. V., Barnes, B. R., Glund, S., Suarez, E., Ryder, J. W., Palacin, M., Zierath, J. R., Zorzano, A.Guma, A. 2006. Neuregulins mediate calcium-induced glucose transport during muscle contraction. *J Biol Chem,* 281**,** 21690-7.

Cao, L., Shitara, H., Horii, T., Nagao, Y., Imai, H., Abe, K., Hara, T., Hayashi, J.Yonekawa, H. 2007. The mitochondrial bottleneck occurs without reduction of mtDNA content in female mouse germ cells. *Nat Genet,* 39**,** 386-90.

Cao, W., Daniel, K. W., Robidoux, J., Puigserver, P., Medvedev, A. V., Bai, X., Floering, L. M., Spiegelman, B. M.Collins, S. 2004. p38 mitogen-activated protein kinase is the central regulator of cyclic AMP-dependent transcription of the brown fat uncoupling protein 1 gene. *Mol Cell Biol,* 24**,** 3057-67.

Cao, Z., Wanagat, J., Mckiernan, S. H.Aiken, J. M. 2001. Mitochondrial DNA deletion mutations are concomitant with ragged red regions of individual, aged muscle fibers: analysis by laser-capture microdissection. *Nucleic Acids Res,* 29**,** 4502-8.

Capers, C. R. 1960. Multinucleation of skeletal muscle in vitro. *J Biophys Biochem Cytol,* 7**,** 559-66.

Cardenas, C., Miller, R. A., Smith, I., Bui, T., Molgo, J., Muller, M., Vais, H., Cheung, K. H., Yang, J., Parker, I., Thompson, C. B., Birnbaum, M. J., Hallows, K. R.Foskett, J. K. 2010. Essential regulation of cell bioenergetics by constitutive InsP3 receptor Ca2+ transfer to mitochondria. *Cell,* 142**,** 270-83.

Carelli, V., Ghelli, A., Ratta, M., Bacchilega, E., Sangiorgi, S., Mancini, R., Leuzzi, V., Cortelli, P., Montagna, P., Lugaresi, E.Degli Esposti, M. 1997. Leber's hereditary optic neuropathy: biochemical effect of 11778/ND4 and 3460/ND1 mutations and correlation with the mitochondrial genotype. *Neurology,* 48**,** 1623-32.

Carroll, J., Fearnley, I. M., Shannon, R. J., Hirst, J.Walker, J. E. 2003. Analysis of the subunit composition of complex I from bovine heart mitochondria. *Mol Cell Proteomics,* 2**,** 117-26.

Casari, G., De Fusco, M., Ciarmatori, S., Zeviani, M., Mora, M., Fernandez, P., De Michele, G., Filla, A., Cocozza, S., Marconi, R., Durr, A., Fontaine, B.Ballabio, A. 1998. Spastic paraplegia and OXPHOS impairment caused by mutations in paraplegin, a nuclear-encoded mitochondrial metalloprotease. *Cell,* 93**,** 973-83.

Cerritelli, S. M., Frolova, E. G., Feng, C., Grinberg, A., Love, P. E.Crouch, R. J. 2003. Failure to produce mitochondrial DNA results in embryonic lethality in Rnaseh1 null mice. *Mol Cell,* 11**,** 807-15.

Cervin, C., Liljestrom, B., Tuomi, T., Heikkinen, S., Tapanainen, J. S., Groop, L.Cilio, C. M. 2004. Cosegregation of MIDD and MODY in a pedigree: functional and clinical consequences. *Diabetes,* 53**,** 1894-9.

Chagnon, P., Gee, M., Filion, M., Robitaille, Y., Belouchi, M.Gauvreau, D. 1999. Phylogenetic analysis of the mitochondrial genome indicates significant differences between patients with Alzheimer disease and controls in a French-Canadian founder population. *Am J Med Genet,* 85**,** 20-30.

Chami, M., Prandini, A., Campanella, M., Pinton, P., Szabadkai, G., Reed, J. C.Rizzuto, R. 2004. Bcl-2 and Bax exert opposing effects on Ca2+ signaling, which do not depend on their putative pore-forming region. *J Biol Chem,* 279**,** 54581-9.

Chan, C. C., Liu, V. W., Lau, E. Y., Yeung, W. S., Ng, E. H.Ho, P. C. 2005. Mitochondrial DNA content and 4977 bp deletion in unfertilized oocytes. *Mol Hum Reprod,* 11**,** 843-6.

Chang, D. D.Clayton, D. A. 1985. Priming of human mitochondrial DNA replication occurs at the light-strand promoter. *Proc Natl Acad Sci U S A,* 82**,** 351-5.

Chen, H., Chomyn, A.Chan, D. C. 2005. Disruption of fusion results in mitochondrial heterogeneity and dysfunction. *J Biol Chem,* 280**,** 26185-92.

Chen, H., Vermulst, M., Wang, Y. E., Chomyn, A., Prolla, T. A., Mccaffery, J. M.Chan, D. C. 2010. Mitochondrial fusion is required for mtDNA stability in skeletal muscle and tolerance of mtDNA mutations. *Cell,* 141**,** 280-9.

Chen, X., Prosser, R., Simonetti, S., Sadlock, J., Jagiello, G.Schon, E. A. 1995. Rearranged mitochondrial genomes are present in human oocytes. *Am J Hum Genet,* 57**,** 239-47.

Chinnery, P. F., Dimauro, S., Shanske, S., Schon, E. A., Zeviani, M., Mariotti, C., Carrara, F., Lombes, A., Laforet, P., Ogier, H., Jaksch, M., Lochmuller, H., Horvath, R., Deschauer, M., Thorburn, D. R., Bindoff, L. A., Poulton, J., Taylor, R. W., Matthews, J. N.Turnbull, D. M. 2004. Risk of developing a mitochondrial DNA deletion disorder. *Lancet,* 364**,** 592-6.

Chinnery, P. F., Howell, N., Lightowlers, R. N.Turnbull, D. M. 1997. Molecular pathology of MELAS and MERRF. The relationship between mutation load and clinical phenotypes. *Brain,* 120 (Pt 10)**,** 1713-21.

Chinnery, P. F., Howell, N., Lightowlers, R. N.Turnbull, D. M. 1998. MELAS and MERRF. The relationship between maternal mutation load and the frequency of clinically affected offspring. *Brain,* 121 (Pt 10)**,** 1889-94.

Chinnery, P. F., Johnson, M. A., Wardell, T. M., Singh-Kler, R., Hayes, C., Brown, D. T., Taylor, R. W., Bindoff, L. A.Turnbull, D. M. 2000a. The epidemiology of pathogenic mitochondrial DNA mutations. *Ann Neurol,* 48**,** 188-93.

Chinnery, P. F., Thorburn, D. R., Samuels, D. C., White, S. L., Dahl, H. M., Turnbull, D. M., Lightowlers, R. N.Howell, N. 2000b. The inheritance of mitochondrial DNA heteroplasmy: random drift, selection or both? *Trends Genet,* 16**,** 500-5.

Chinnery, P. F., Zwijnenburg, P. J., Walker, M., Howell, N., Taylor, R. W., Lightowlers, R. N., Bindoff, L.Turnbull, D. M. 1999. Nonrandom tissue distribution of mutant mtDNA. *Am J Med Genet,* 85**,** 498-501.

Chou, Y. J., Ou, C. Y., Hsu, T. Y., Liou, C. W., Lee, C. F., Tso, D. J.Wei, Y. H. 2004. Prenatal diagnosis of a fetus harboring an intermediate load of the A3243G mtDNA mutation in a maternal carrier diagnosed with MELAS syndrome. *Prenat Diagn,* 24**,** 367-70.

Chowdhury, S. K., Gemin, A.Singh, G. 2005. High activity of mitochondrial glycerophosphate dehydrogenase and glycerophosphate-dependent ROS production in prostate cancer cell lines. *Biochem Biophys Res Commun,* 333**,** 1139-45.

Christian, B. E.Spremulli, L. L. 2009. Evidence for an active role of IF3mt in the initiation of translation in mammalian mitochondria. *Biochemistry,* 48**,** 3269-78.

Christian, M., White, R.Parker, M. G. 2006. Metabolic regulation by the nuclear receptor corepressor RIP140. *Trends Endocrinol Metab,* 17**,** 243-50.

Chuenkongkaew, W. L., Suphavilai, R., Vaeusorn, L., Phasukkijwatana, N., Lertrit, P.Suktitipat, B. 2005. Proportion of 11778 mutant mitochondrial DNA and clinical expression in a thai population with leber hereditary optic neuropathy. *J Neuroophthalmol,* 25**,** 173-5.

Ciafaloni, E., Ricci, E., Servidei, S., Shanske, S., Silvestri, G., Manfredi, G., Schon, E. A.Dimauro, S. 1991. Widespread tissue distribution of a tRNALeu(UUR) mutation in the mitochondrial DNA of a patient with MELAS syndrome. *Neurology,* 41**,** 1663-4.

Ciafaloni, E., Ricci, E., Shanske, S., Moraes, C. T., Silvestri, G., Hirano, M., Simonetti, S., Angelini, C., Donati, M. A., Garcia, C.Et Al. 1992. MELAS: clinical features, biochemistry, and molecular genetics. *Ann Neurol,* 31**,** 391-8.

Ciafaloni, E., Santorelli, F. M., Shanske, S., Deonna, T., Roulet, E., Janzer, C., Pescia, G.Dimauro, S. 1993. Maternally inherited Leigh syndrome. *J Pediatr,* 122**,** 419-22.

Clark, C. G.Roger, A. J. 1995. Direct evidence for secondary loss of mitochondria in Entamoeba histolytica. *Proc Natl Acad Sci U S A,* 92**,** 6518-21.

Claros, M. G., Perea, J., Shu, Y., Samatey, F. A., Popot, J. L.Jacq, C. 1995. Limitations to in vivo import of hydrophobic proteins into yeast mitochondria. The case of a cytoplasmically synthesized apocytochrome b. *Eur J Biochem,* 228**,** 762-71.

Cockburn, K.Rossant, J. 2010. Making the blastocyst: lessons from the mouse. *J Clin Invest,* 120**,** 995-1003.

Conrad, C. C., Choi, J., Malakowsky, C. A., Talent, J. M., Dai, R., Marshall, P.Gracy, R. W. 2001. Identification of protein carbonyls after two-dimensional electrophoresis. *Proteomics,* 1**,** 829-34.

Copeland, W. C. 2008. Inherited mitochondrial diseases of DNA replication. *Annu Rev Med,* 59**,** 131-46.

Copois, V., Bibeau, F., Bascoul-Mollevi, C., Salvetat, N., Chalbos, P., Bareil, C., Candeil, L., Fraslon, C., Conseiller, E., Granci, V., Maziere, P., Kramar, A., Ychou, M., Pau, B., Martineau, P., Molina, F.Del Rio, M. 2007. Impact of RNA degradation on gene expression profiles: assessment of different methods to reliably determine RNA quality. *J Biotechnol,* 127**,** 549-59.

Corral-Debrinski, M., Shoffner, J. M., Lott, M. T.Wallace, D. C. 1992. Association of mitochondrial DNA damage with aging and coronary atherosclerotic heart disease. *Mutat Res,* 275**,** 169-80.

Cortopassi, G., Danielson, S., Alemi, M., Zhan, S. S., Tong, W., Carelli, V., Martinuzzi, A., Marzuki, S., Majamaa, K.Wong, A. 2006. Mitochondrial disease activates transcripts of the unfolded protein response and cell cycle and inhibits vesicular secretion and oligodendrocyte-specific transcripts. *Mitochondrion,* 6**,** 161-75.

Cortopassi, G. A., Shibata, D., Soong, N. W.Arnheim, N. 1992. A pattern of accumulation of a somatic deletion of mitochondrial DNA in aging human tissues. *Proc Natl Acad Sci U S A,* 89**,** 7370-4.

Cotney, J., Mckay, S. E.Shadel, G. S. 2009. Elucidation of separate, but collaborative functions of the rRNA methyltransferase-related human mitochondrial transcription factors B1 and B2 in mitochondrial biogenesis reveals new insight into maternally inherited deafness. *Hum Mol Genet,* 18**,** 2670-82.

Cotney, J., Wang, Z.Shadel, G. S. 2007. Relative abundance of the human mitochondrial transcription system and distinct roles for h-mtTFB1 and h-mtTFB2 in mitochondrial biogenesis and gene expression. *Nucleic Acids Res,* 35**,** 4042-54.

Cox, C. J., Foster, P. G., Hirt, R. P., Harris, S. R.Embley, T. M. 2008. The archaebacterial origin of eukaryotes. *Proc Natl Acad Sci U S A,* 105**,** 20356-61.

Cox, M. L., Schray, C. L., Luster, C. N., Stewart, Z. S., Korytko, P. J., Kn, M. K., Paulauskis, J. D.Dunstan, R. W. 2006. Assessment of fixatives, fixation, and tissue processing on morphology and RNA integrity. *Exp Mol Pathol,* 80**,** 183-91.

Crane, F. L.Beinert, H. 1956. On the mechanism of dehydrogenation of fatty acyl derivatives of coenzyme A. II. The electron-transferring flavoprotein. *J Biol Chem,* 218**,** 717-31.

Craven, L., Tuppen, H. A., Greggains, G. D., Harbottle, S. J., Murphy, J. L., Cree, L. M., Murdoch, A. P., Chinnery, P. F., Taylor, R. W., Lightowlers, R. N., Herbert, M.Turnbull, D. M. 2010. Pronuclear transfer in human embryos to prevent transmission of mitochondrial DNA disease. *Nature,* 465**,** 82-5.

Cree, L. M., Samuels, D. C., De Sousa Lopes, S. C., Rajasimha, H. K., Wonnapinij, P., Mann, J. R., Dahl, H. H.Chinnery, P. F. 2008. A reduction of mitochondrial DNA molecules during embryogenesis explains the rapid segregation of genotypes. *Nat Genet,* 40**,** 249-54.

Crimi, M., Bordoni, A., Menozzi, G., Riva, L., Fortunato, F., Galbiati, S., Del Bo, R., Pozzoli, U., Bresolin, N.Comi, G. P. 2005. Skeletal muscle gene expression profiling in mitochondrial disorders. *FASEB J,* 19**,** 866-8.

Crofts, A. R. 2004. The cytochrome bc1 complex: function in the context of structure. *Annu Rev Physiol,* 66**,** 689-733.

Cruciat, C. M., Brunner, S., Baumann, F., Neupert, W.Stuart, R. A. 2000. The cytochrome bc1 and cytochrome c oxidase complexes associate to form a single supracomplex in yeast mitochondria. *J Biol Chem,* 275**,** 18093-8.

Cunningham, J. T., Rodgers, J. T., Arlow, D. H., Vazquez, F., Mootha, V. K.Puigserver, P. 2007. mTOR controls mitochondrial oxidative function through a YY1-PGC-1alpha transcriptional complex. *Nature,* 450**,** 736-40.

D'aubenton Carafa, Y., Brody, E.Thermes, C. 1990. Prediction of rho-independent Escherichia coli transcription terminators. A statistical analysis of their RNA stem-loop structures. *J Mol Biol,* 216**,** 835-58.

Dairaghi, D. J., Shadel, G. S.Clayton, D. A. 1995. Addition of a 29 residue carboxyl-terminal tail converts a simple HMG box-containing protein into a transcriptional activator. *J Mol Biol,* 249**,** 11-28.

Dalakas, M. C., Illa, I., Pezeshkpour, G. H., Laukaitis, J. P., Cohen, B.Griffin, J. L. 1990. Mitochondrial myopathy caused by long-term zidovudine therapy. *N Engl J Med,* 322**,** 1098-105.

Dalla Rosa, I., Goffart, S., Wurm, M., Wiek, C., Essmann, F., Sobek, S., Schroeder, P., Zhang, H., Krutmann, J., Hanenberg, H., Schulze-Osthoff, K., Mielke, C., Pommier, Y., Boege, F.Christensen, M. O. 2009. Adaptation of topoisomerase I paralogs to nuclear and mitochondrial DNA. *Nucleic Acids Res,* 37**,** 6414-28.

Danielson, S. R., Carelli, V., Tan, G., Martinuzzi, A., Schapira, A. H., Savontaus, M. L.Cortopassi, G. A. 2005. Isolation of transcriptomal changes attributable to LHON mutations and the cybridization process. *Brain,* 128**,** 1026-37.

Davey, K. M., Parboosingh, J. S., Mcleod, D. R., Chan, A., Casey, R., Ferreira, P., Snyder, F. F., Bridge, P. J.Bernier, F. P. 2006. Mutation of DNAJC19, a human homologue of yeast inner mitochondrial membrane co-chaperones, causes DCMA syndrome, a novel autosomal recessive Barth syndrome-like condition. *J Med Genet,* 43**,** 385-93.

Davies, S. M., Rackham, O., Shearwood, A. M., Hamilton, K. L., Narsai, R., Whelan, J.Filipovska, A. 2009. Pentatricopeptide repeat domain protein 3 associates with the mitochondrial small ribosomal subunit and regulates translation. *FEBS Lett,* 583**,** 1853-8.

Davis, A. F., Ropp, P. A., Clayton, D. A.Copeland, W. C. 1996. Mitochondrial DNA polymerase gamma is expressed and translated in the absence of mitochondrial DNA maintenance and replication. *Nucleic Acids Res,* 24**,** 2753-9.

De Lonlay, P., Valnot, I., Barrientos, A., Gorbatyuk, M., Tzagoloff, A., Taanman, J. W., Benayoun, E., Chretien, D., Kadhom, N., Lombes, A., De Baulny, H. O., Niaudet, P., Munnich, A., Rustin, P.Rotig, A. 2001. A mutant mitochondrial respiratory chain assembly protein causes complex III deficiency in patients with tubulopathy, encephalopathy and liver failure. *Nat Genet,* 29**,** 57-60.

De Meirleir, L., Seneca, S., Lissens, W., De Clercq, I., Eyskens, F., Gerlo, E., Smet, J.Van Coster, R. 2004. Respiratory chain complex V deficiency due to a mutation in the assembly gene ATP12. *J Med Genet,* 41**,** 120-4.

De Meirleir, L., Seneca, S., Lissens, W., Schoentjes, E.Desprechins, B. 1995. Bilateral striatal necrosis with a novel point mutation in the mitochondrial ATPase 6 gene. *Pediatr Neurol,* 13**,** 242-6.

De Paepe, B., Smet, J., Lammens, M., Seneca, S., Martin, J. J., De Bleecker, J., De Meirleir, L., Lissens, W.Van Coster, R. 2009. Immunohistochemical analysis of the oxidative phosphorylation complexes in skeletal muscle from patients with mitochondrial DNA encoded tRNA gene defects. *J Clin Pathol,* 62**,** 172-6.

De Rasmo, D., Signorile, A., Roca, E.Papa, S. 2009. cAMP response element-binding protein (CREB) is imported into mitochondria and promotes protein synthesis. *FEBS J,* 276**,** 4325-33.

Degoul, F., Diry, M., Rodriguez, D., Robain, O., Francois, D., Ponsot, G., Marsac, C.Desguerre, I. 1995. Clinical, biochemical, and molecular analysis of a maternally inherited case of Leigh syndrome (MILS) associated with the mtDNA T8993G point mutation. *J Inherit Metab Dis,* 18**,** 682-8.

Delerive, P., Wu, Y., Burris, T. P., Chin, W. W.Suen, C. S. 2002. PGC-1 functions as a transcriptional coactivator for the retinoid X receptors. *J Biol Chem,* 277**,** 3913-7.

Demir, O.Aksan Kurnaz, I. 2006. An integrated model of glucose and galactose metabolism regulated by the GAL genetic switch. *Comput Biol Chem,* 30**,** 179-92.

Dennis, G., Jr., Sherman, B. T., Hosack, D. A., Yang, J., Gao, W., Lane, H. C.Lempicki, R. A. 2003. DAVID: Database for Annotation, Visualization, and Integrated Discovery. *Genome Biol,* 4**,** P3.

Deponte, M.Hell, K. 2009. Disulphide bond formation in the intermembrane space of mitochondria. *J Biochem,* 146**,** 599-608.

Desreumaux, P., Dubuquoy, L., Nutten, S., Peuchmaur, M., Englaro, W., Schoonjans, K., Derijard, B., Desvergne, B., Wahli, W., Chambon, P., Leibowitz, M. D., Colombel, J. F.Auwerx, J. 2001. Attenuation of colon inflammation through activators of the retinoid X receptor (RXR)/peroxisome proliferator-activated receptor gamma (PPARgamma) heterodimer. A basis for new therapeutic strategies. *J Exp Med,* 193**,** 827-38.

Diaz, F., Bayona-Bafaluy, M. P., Rana, M., Mora, M., Hao, H.Moraes, C. T. 2002. Human mitochondrial DNA with large deletions repopulates organelles faster than full-length genomes under relaxed copy number control. *Nucleic Acids Res,* 30**,** 4626-33.

Dimauro, S., Bonilla, E., Zeviani, M., Nakagawa, M.Devivo, D. C. 1985. Mitochondrial myopathies. *Ann Neurol,* 17**,** 521-38.

Dimauro, S.Schon, E. A. 2001. Mitochondrial DNA mutations in human disease. *Am J Med Genet,* 106**,** 18-26.

Downs, K. M.Davies, T. 1993. Staging of gastrulating mouse embryos by morphological landmarks in the dissecting microscope. *Development,* 118**,** 1255-66.

Dubeau, F., De Stefano, N., Zifkin, B. G., Arnold, D. L.Shoubridge, E. A. 2000. Oxidative phosphorylation defect in the brains of carriers of the tRNAleu(UUR) A3243G mutation in a MELAS pedigree. *Ann Neurol,* 47**,** 179-85.

Dubuquoy, L., Dharancy, S., Nutten, S., Pettersson, S., Auwerx, J.Desreumaux, P. 2002. Role of peroxisome proliferator-activated receptor gamma and retinoid X receptor heterodimer in hepatogastroenterological diseases. *Lancet,* 360**,** 1410-8.

Durham, S. E., Samuels, D. C.Chinnery, P. F. 2006. Is selection required for the accumulation of somatic mitochondrial DNA mutations in post-mitotic cells? *Neuromuscul Disord,* 16**,** 381-6.

Durham, S. E., Samuels, D. C., Cree, L. M.Chinnery, P. F. 2007. Normal levels of wild-type mitochondrial DNA maintain cytochrome c oxidase activity for two pathogenic mitochondrial DNA mutations but not for m.3243A-->G. *Am J Hum Genet,* 81**,** 189-95.

Edgar, R., Domrachev, M.Lash, A. E. 2002. Gene Expression Omnibus: NCBI gene expression and hybridization array data repository. *Nucleic Acids Res,* 30**,** 207-10.

Ekstrand, M. I., Falkenberg, M., Rantanen, A., Park, C. B., Gaspari, M., Hultenby, K., Rustin, P., Gustafsson, C. M.Larsson, N. G. 2004. Mitochondrial transcription factor A regulates mtDNA copy number in mammals. *Hum Mol Genet,* 13**,** 935-44.

Elliott, H. R., Samuels, D. C., Eden, J. A., Relton, C. L.Chinnery, P. F. 2008. Pathogenic mitochondrial DNA mutations are common in the general population. *Am J Hum Genet,* 83**,** 254-60.

Elpeleg, O., Miller, C., Hershkovitz, E., Bitner-Glindzicz, M., Bondi-Rubinstein, G., Rahman, S., Pagnamenta, A., Eshhar, S.Saada, A. 2005. Deficiency of the ADP-forming succinyl-CoA synthase activity is associated with encephalomyopathy and mitochondrial DNA depletion. *Am J Hum Genet,* 76**,** 1081-6.

Elson, J. L., Samuels, D. C., Johnson, M. A., Turnbull, D. M.Chinnery, P. F. 2002. The length of cytochrome c oxidase-negative segments in muscle fibres in patients with mtDNA myopathy. *Neuromuscul Disord,* 12**,** 858-64.

Elson, J. L., Samuels, D. C., Turnbull, D. M.Chinnery, P. F. 2001. Random intracellular drift explains the clonal expansion of mitochondrial DNA mutations with age. *Am J Hum Genet,* 68**,** 802-6.

Elson, J. L., Swalwell, H., Blakely, E. L., Mcfarland, R., Taylor, R. W.Turnbull, D. M. 2009. Pathogenic mitochondrial tRNA mutations--which mutations are inherited and why? *Hum Mutat,* 30**,** E984-92.

Embley, T. M., Van Der Giezen, M., Horner, D. S., Dyal, P. L., Bell, S.Foster, P. G. 2003. Hydrogenosomes, mitochondria and early eukaryotic evolution. *IUBMB Life,* 55**,** 387-95.

Enders, G. C.May, J. J., 2nd 1994. Developmentally regulated expression of a mouse germ cell nuclear antigen examined from embryonic day 11 to adult in male and female mice. *Dev Biol,* 163**,** 331-40.

Enns, G. M., Bai, R. K., Beck, A. E.Wong, L. J. 2006. Molecular-clinical correlations in a family with variable tissue mitochondrial DNA T8993G mutant load. *Mol Genet Metab,* 88**,** 364-71.

Enns, G. M., Hoppel, C. L., Dearmond, S. J., Schelley, S., Bass, N., Weisiger, K., Horoupian, D.Packman, S. 2005. Relationship of primary mitochondrial respiratory chain dysfunction to fiber type abnormalities in skeletal muscle. *Clin Genet,* 68**,** 337-48.

Evans, R. M., Barish, G. D.Wang, Y. X. 2004. PPARs and the complex journey to obesity. *Nat Med,* 10**,** 355-61.

Fabrizi, G. M., Cardaioli, E., Grieco, G. S., Cavallaro, T., Malandrini, A., Manneschi, L., Dotti, M. T., Federico, A.Guazzi, G. 1996. The A to G transition at nt 3243 of the mitochondrial tRNALeu(UUR) may cause an MERRF syndrome. *J Neurol Neurosurg Psychiatry,* 61**,** 47-51.

Falkenberg, M., Gaspari, M., Rantanen, A., Trifunovic, A., Larsson, N. G.Gustafsson, C. M. 2002. Mitochondrial transcription factors B1 and B2 activate transcription of human mtDNA. *Nat Genet,* 31**,** 289-94.

Fan, W., Waymire, K. G., Narula, N., Li, P., Rocher, C., Coskun, P. E., Vannan, M. A., Narula, J., Macgregor, G. R.Wallace, D. C. 2008. A mouse model of mitochondrial disease reveals germline selection against severe mtDNA mutations. *Science,* 319**,** 958-62.

Fearnley, I. M.Walker, J. E. 1992. Conservation of sequences of subunits of mitochondrial complex I and their relationships with other proteins. *Biochim Biophys Acta,* 1140**,** 105-34.

Fell, D. A. 1992. Metabolic control analysis: a survey of its theoretical and experimental development. *Biochem J,* 286 (Pt 2)**,** 313-30.

Felsenstein, J. 1974. The evolutionary advantage of recombination. *Genetics,* 78**,** 737-56.

Feng, D. F., Cho, G.Doolittle, R. F. 1997. Determining divergence times with a protein clock: update and reevaluation. *Proc Natl Acad Sci U S A,* 94**,** 13028-33.

Ferlin, T., Landrieu, P., Rambaud, C., Fernandez, H., Dumoulin, R., Rustin, P.Mousson, B. 1997. Segregation of the G8993 mutant mitochondrial DNA through generations and embryonic tissues in a family at risk of Leigh syndrome. *J Pediatr,* 131**,** 447-9.

Fernandez-Vizarra, E., Tiranti, V.Zeviani, M. 2009. Assembly of the oxidative phosphorylation system in humans: what we have learned by studying its defects. *Biochim Biophys Acta,* 1793**,** 200-11.

Ferrer-Martinez, A., Montell, E., Montori-Grau, M., Garcia-Martinez, C., Gomez-Foix, A. M., Roberts, M. A., Mansourian, R.Mace, K. 2006. Long-term cultured human myotubes decrease contractile gene expression and regulate apoptosis-related genes. *Gene,* 384**,** 145-53.

Fink, L., Kohlhoff, S., Stein, M. M., Hanze, J., Weissmann, N., Rose, F., Akkayagil, E., Manz, D., Grimminger, F., Seeger, W.Bohle, R. M. 2002. cDNA array hybridization after laser-assisted microdissection from nonneoplastic tissue. *Am J Pathol,* 160**,** 81-90.

Fisher, R. P.Clayton, D. A. 1988. Purification and characterization of human mitochondrial transcription factor 1. *Mol Cell Biol,* 8**,** 3496-509.

Fisher, R. P., Lisowsky, T., Parisi, M. A.Clayton, D. A. 1992. DNA wrapping and bending by a mitochondrial high mobility group-like transcriptional activator protein. *J Biol Chem,* 267**,** 3358-67.

Fleige, S., Walf, V., Huch, S., Prgomet, C., Sehm, J.Pfaffl, M. W. 2006. Comparison of relative mRNA quantification models and the impact of RNA integrity in quantitative real-time RT-PCR. *Biotechnol Lett,* 28**,** 1601-13.

Frey, T. G.Mannella, C. A. 2000. The internal structure of mitochondria. *Trends Biochem Sci,* 25**,** 319-24.

Freyer, C., Cree, L. M., Mourier, A., Stewart, J. B., Koolmeister, C., Milenkovic, D., Wai, T., Floros, V. I., Hagstrom, E., Chatzidaki, E. E., Wiesner, R. J., Samuels, D. C., Larsson, N. G.Chinnery, P. F. 2012. Variation in germline mtDNA heteroplasmy is determined prenatally but modified during subsequent transmission. *Nat Genet,* 44**,** 1282-5.

Fridovich, I. 1997. Superoxide anion radical (O2-.), superoxide dismutases, and related matters. *J Biol Chem,* 272**,** 18515-7.

Friedrich, T. 2001. Complex I: a chimaera of a redox and conformation-driven proton pump? *J Bioenerg Biomembr,* 33**,** 169-77.

Fryer, A., Appleton, R., Sweeney, M. G., Rosenbloom, L.Harding, A. E. 1994. Mitochondrial DNA 8993 (NARP) mutation presenting with a heterogeneous phenotype including 'cerebral palsy'. *Arch Dis Child,* 71**,** 419-22.

Fujita, P. A., Rhead, B., Zweig, A. S., Hinrichs, A. S., Karolchik, D., Cline, M. S., Goldman, M., Barber, G. P., Clawson, H., Coelho, A., Diekhans, M., Dreszer, T. R., Giardine, B. M., Harte, R. A., Hillman-Jackson, J., Hsu, F., Kirkup, V., Kuhn, R. M., Learned, K., Li, C. H., Meyer, L. R., Pohl, A., Raney, B. J., Rosenbloom, K. R., Smith, K. E., Haussler, D.Kent, W. J. 2011. The UCSC Genome Browser database: update 2011. *Nucleic Acids Res,* 39**,** D876-82.

Fuste, J. M., Wanrooij, S., Jemt, E., Granycome, C. E., Cluett, T. J., Shi, Y., Atanassova, N., Holt, I. J., Gustafsson, C. M.Falkenberg, M. 2010. Mitochondrial RNA polymerase is needed for activation of the origin of light-strand DNA replication. *Mol Cell,* 37**,** 67-78.

Futami, K., Shimamoto, A.Furuichi, Y. 2007. Mitochondrial and nuclear localization of human Pif1 helicase. *Biol Pharm Bull,* 30**,** 1685-92.

Galkin, A. S., Grivennikova, V. G.Vinogradov, A. D. 1999. -->H+/2e- stoichiometry in NADH-quinone reductase reactions catalyzed by bovine heart submitochondrial particles. *FEBS Lett,* 451**,** 157-61.

Galpin, A. J., Raue, U., Jemiolo, B., Trappe, T. A., Harber, M. P., Minchev, K.Trappe, S. 2012. Human skeletal muscle fiber type specific protein content. *Anal Biochem,* 425**,** 175-82.

Gamez, J., Playan, A., Andreu, A. L., Bruno, C., Navarro, C., Cervera, C., Arbos, M. A., Schwartz, S., Enriquez, J. A.Montoya, J. 1998. Familial multiple symmetric lipomatosis associated with the A8344G mutation of mitochondrial DNA. *Neurology,* 51**,** 258-60.

Gaur, R., Grasso, D., Datta, P. P., Krishna, P. D., Das, G., Spencer, A., Agrawal, R. K., Spremulli, L.Varshney, U. 2008. A single mammalian mitochondrial translation initiation factor functionally replaces two bacterial factors. *Mol Cell,* 29**,** 180-90.

Genuario, R.Wong, T. W. 1993. Stimulation of DNA polymerase gamma by a mitochondrial single-strand DNA binding protein. *Cell Mol Biol Res,* 39**,** 625-34.

Ghezzi, D., Goffrini, P., Uziel, G., Horvath, R., Klopstock, T., Lochmuller, H., D'adamo, P., Gasparini, P., Strom, T. M., Prokisch, H., Invernizzi, F., Ferrero, I.Zeviani, M. 2009. SDHAF1, encoding a LYR complex-II specific assembly factor, is mutated in SDH-defective infantile leukoencephalopathy. *Nat Genet,* 41**,** 654-6.

Ghosh, S. S., Fahy, E., Bodis-Wollner, I., Sherman, J.Howell, N. 1996. Longitudinal study of a heteroplasmic 3460 Leber hereditary optic neuropathy family by multiplexed primer-extension analysis and nucleotide sequencing. *Am J Hum Genet,* 58**,** 325-34.

Giguere, V. 2008. Transcriptional control of energy homeostasis by the estrogen-related receptors. *Endocr Rev,* 29**,** 677-96.

Giles, R. E., Blanc, H., Cann, H. M.Wallace, D. C. 1980. Maternal inheritance of human mitochondrial DNA. *Proc Natl Acad Sci U S A,* 77**,** 6715-9.

Gilkerson, R. W., Selker, J. M.Capaldi, R. A. 2003. The cristal membrane of mitochondria is the principal site of oxidative phosphorylation. *FEBS Lett,* 546**,** 355-8.

Gille, G.Reichmann, H. 2011. Iron-dependent functions of mitochondria--relation to neurodegeneration. *J Neural Transm,* 118**,** 349-59.

Goldsworthy, S. M., Stockton, P. S., Trempus, C. S., Foley, J. F.Maronpot, R. R. 1999. Effects of fixation on RNA extraction and amplification from laser capture microdissected tissue. *Mol Carcinog,* 25**,** 86-91.

Goto, Y., Nonaka, I.Horai, S. 1990. A mutation in the tRNA(Leu)(UUR) gene associated with the MELAS subgroup of mitochondrial encephalomyopathies. *Nature,* 348**,** 651-3.

Gray, H.Wong, T. W. 1992. Purification and identification of subunit structure of the human mitochondrial DNA polymerase. *J Biol Chem,* 267**,** 5835-41.

Gray, M. W. 1998. Rickettsia, typhus and the mitochondrial connection. *Nature,* 396**,** 109-10.

Greer, E. L., Oskoui, P. R., Banko, M. R., Maniar, J. M., Gygi, M. P., Gygi, S. P.Brunet, A. 2007. The energy sensor AMP-activated protein kinase directly regulates the mammalian FOXO3 transcription factor. *J Biol Chem,* 282**,** 30107-19.

Gresser, M. J., Myers, J. A.Boyer, P. D. 1982. Catalytic site cooperativity of beef heart mitochondrial F1 adenosine triphosphatase. Correlations of initial velocity, bound intermediate, and oxygen exchange measurements with an alternating three-site model. *J Biol Chem,* 257**,** 12030-8.

Grimm, J., Mueller, A., Hefti, F.Rosenthal, A. 2004. Molecular basis for catecholaminergic neuron diversity. *Proc Natl Acad Sci U S A,* 101**,** 13891-6.

Grohmann, K., Amairic, F., Crews, S.Attardi, G. 1978. Failure to detect "cap" structures in mitochondrial DNA-coded poly(A)-containing RNA from HeLa cells. *Nucleic Acids Res,* 5**,** 637-51.

Guan, M. X., Yan, Q., Li, X., Bykhovskaya, Y., Gallo-Teran, J., Hajek, P., Umeda, N., Zhao, H., Garrido, G., Mengesha, E., Suzuki, T., Del Castillo, I., Peters, J. L., Li, R., Qian, Y., Wang, X., Ballana, E., Shohat, M., Lu, J., Estivill, X., Watanabe, K.Fischel-Ghodsian, N. 2006. Mutation in TRMU related to transfer RNA modification modulates the phenotypic expression of the deafness-associated mitochondrial 12S ribosomal RNA mutations. *Am J Hum Genet,* 79**,** 291-302.

Guo, D.Catchpoole, D. R. 2003. Isolation of intact RNA following cryosection of archived frozen tissue. *Biotechniques,* 34**,** 48-50.

Guo, W., Worley, K., Adams, V., Mason, J., Sylvester-Jackson, D., Zhang, Y. H., Towbin, J. A., Fogt, D. D., Madu, S., Wheeler, D. A.Et Al. 1993. Genomic scanning for expressed sequences in Xp21 identifies the glycerol kinase gene. *Nat Genet,* 4**,** 367-72.

Guzy, R. D.Schumacker, P. T. 2006. Oxygen sensing by mitochondria at complex III: the paradox of increased reactive oxygen species during hypoxia. *Exp Physiol,* 91**,** 807-19.

Hackenbrock, C. R., Chazotte, B.Gupte, S. S. 1986. The random collision model and a critical assessment of diffusion and collision in mitochondrial electron transport. *J Bioenerg Biomembr,* 18**,** 331-68.

Hammans, S. R., Sweeney, M. G., Brockington, M., Lennox, G. G., Lawton, N. F., Kennedy, C. R., Morgan-Hughes, J. A.Harding, A. E. 1993. The mitochondrial DNA transfer RNA(Lys)A-->G(8344) mutation and the syndrome of myoclonic

epilepsy with ragged red fibres (MERRF). Relationship of clinical phenotype to proportion of mutant mitochondrial DNA. *Brain,* 116 (Pt 3)**,** 617-32.

Hammans, S. R., Sweeney, M. G., Hanna, M. G., Brockington, M., Morgan-Hughes, J. A.Harding, A. E. 1995. The mitochondrial DNA transfer RNALeu(UUR) A-->G(3243) mutation. A clinical and genetic study. *Brain,* 118 (Pt 3)**,** 721-34.

Hammarsund, M., Wilson, W., Corcoran, M., Merup, M., Einhorn, S., Grander, D.Sangfelt, O. 2001. Identification and characterization of two novel human mitochondrial elongation factor genes, hEFG2 and hEFG1, phylogenetically conserved through evolution. *Hum Genet,* 109**,** 542-50.

Handschin, C., Rhee, J., Lin, J., Tarr, P. T.Spiegelman, B. M. 2003. An autoregulatory loop controls peroxisome proliferator-activated receptor gamma coactivator 1alpha expression in muscle. *Proc Natl Acad Sci U S A,* 100**,** 7111-6.

Handschin, C.Spiegelman, B. M. 2006. Peroxisome proliferator-activated receptor gamma coactivator 1 coactivators, energy homeostasis, and metabolism. *Endocr Rev,* 27**,** 728-35.

Hansen, P. J.Fear, J. M. 2011. Cheating death at the dawn of life: developmental control of apoptotic repression in the preimplantation embryo. *Biochem Biophys Res Commun,* 413**,** 155-8.

Hao, J., Shen, W., Yu, G., Jia, H., Li, X., Feng, Z., Wang, Y., Weber, P., Wertz, K., Sharman, E.Liu, J. 2010. Hydroxytyrosol promotes mitochondrial biogenesis and mitochondrial function in 3T3-L1 adipocytes. *J Nutr Biochem,* 21**,** 634-44.

Haque, M. E., Grasso, D.Spremulli, L. L. 2008. The interaction of mammalian mitochondrial translational initiation factor 3 with ribosomes: evolution of terminal extensions in IF3mt. *Nucleic Acids Res,* 36**,** 589-97.

Hardie, D. G. 2007. AMP-activated/SNF1 protein kinases: conserved guardians of cellular energy. *Nat Rev Mol Cell Biol,* 8**,** 774-85.

Harding, A. E., Sweeney, M. G., Govan, G. G.Riordan-Eva, P. 1995. Pedigree analysis in Leber hereditary optic neuropathy families with a pathogenic mtDNA mutation. *Am J Hum Genet,* 57**,** 77-86.

Harmel, J., Ruzzenente, B., Terzioglu, M., Spahr, H., Falkenberg, M.Larsson, N. G. 2013. The leucine-rich pentatricopeptide repeat containing (LRPPRC) protein does not activate transcription in mammalian mitochondria. *J Biol Chem*.

Harris, J. K., Kelley, S. T., Spiegelman, G. B.Pace, N. R. 2003. The genetic core of the universal ancestor. *Genome Res,* 13**,** 407-12.

Hauswirth, W. W.Laipis, P. J. 1982. Mitochondrial DNA polymorphism in a maternal lineage of Holstein cows. *Proc Natl Acad Sci U S A,* 79**,** 4686-90.

Haut, S., Brivet, M., Touati, G., Rustin, P., Lebon, S., Garcia-Cazorla, A., Saudubray, J. M., Boutron, A., Legrand, A.Slama, A. 2003. A deletion in the human QP-C gene causes a complex III deficiency resulting in hypoglycaemia and lactic acidosis. *Hum Genet,* 113**,** 118-22.

He, X., Sun, C., Wang, F., Shan, A., Guo, T., Gu, W., Cui, B.Ning, G. 2012. Peri-implantation lethality in mice lacking the PGC-1-related coactivator protein. *Dev Dyn,* 241**,** 975-83.

Heddi, A., Lestienne, P., Wallace, D. C.Stepien, G. 1993. Mitochondrial DNA expression in mitochondrial myopathies and coordinated expression of nuclear genes involved in ATP production. *J Biol Chem,* 268**,** 12156-63.

Heddi, A., Lestienne, P., Wallace, D. C.Stepien, G. 1994. Steady state levels of mitochondrial and nuclear oxidative phosphorylation transcripts in Kearns-Sayre syndrome. *Biochim Biophys Acta,* 1226**,** 206-12.

Heddi, A., Stepien, G., Benke, P. J.Wallace, D. C. 1999. Coordinate induction of energy gene expression in tissues of mitochondrial disease patients. *J Biol Chem,* 274**,** 22968-76.

Hellebrekers, D. M., Wolfe, R., Hendrickx, A. T., De Coo, I. F., De Die, C. E., Geraedts, J. P., Chinnery, P. F.Smeets, H. J. 2012. PGD and heteroplasmic mitochondrial DNA point mutations: a systematic review estimating the chance of healthy offspring. *Hum Reprod Update,* 18**,** 341-9.

Helm, M. 2006. Post-transcriptional nucleotide modification and alternative folding of RNA. *Nucleic Acids Res,* 34**,** 721-33.

Helm, M., Brule, H., Friede, D., Giege, R., Putz, D.Florentz, C. 2000. Search for characteristic structural features of mammalian mitochondrial tRNAs. *RNA,* 6**,** 1356-79.

Herrnstadt, C.Howell, N. 2004. An evolutionary perspective on pathogenic mtDNA mutations: haplogroup associations of clinical disorders. *Mitochondrion,* 4**,** 791-8.

Ho, P. C., Gupta, P., Tsui, Y. C., Ha, S. G., Huq, M.Wei, L. N. 2008. Modulation of lysine acetylation-stimulated repressive activity by Erk2-mediated phosphorylation of RIP140 in adipocyte differentiation. *Cell Signal,* 20**,** 1911-9.

Hock, M. B.Kralli, A. 2009. Transcriptional control of mitochondrial biogenesis and function. *Annu Rev Physiol,* 71**,** 177-203.

Holt, I. J. 2009. Mitochondrial DNA replication and repair: all a flap. *Trends Biochem Sci,* 34**,** 358-65.

Holt, I. J., Harding, A. E.Morgan-Hughes, J. A. 1988. Deletions of muscle mitochondrial DNA in patients with mitochondrial myopathies. *Nature,* 331**,** 717-9.

Holt, I. J., Harding, A. E., Petty, R. K.Morgan-Hughes, J. A. 1990. A new mitochondrial disease associated with mitochondrial DNA heteroplasmy. *Am J Hum Genet,* 46**,** 428-33.

Holt, I. J., Lorimer, H. E.Jacobs, H. T. 2000. Coupled leading- and lagging-strand synthesis of mammalian mitochondrial DNA. *Cell,* 100**,** 515-24.

Holt, I. J., Miller, D. H.Harding, A. E. 1989. Genetic heterogeneity and mitochondrial DNA heteroplasmy in Leber's hereditary optic neuropathy. *J Med Genet,* 26**,** 739-43.

Holzmann, J., Frank, P., Loffler, E., Bennett, K. L., Gerner, C.Rossmanith, W. 2008. RNase P without RNA: identification and functional reconstitution of the human mitochondrial tRNA processing enzyme. *Cell,* 135**,** 462-74.

Horvath, R., Fu, K., Johns, T., Genge, A., Karpati, G.Shoubridge, E. A. 1998. Characterization of the mitochondrial DNA abnormalities in the skeletal muscle of patients with inclusion body myositis. *J Neuropathol Exp Neurol,* 57**,** 396-403.

Horvath, R., Schoser, B. G., Muller-Hocker, J., Volpel, M., Jaksch, M.Lochmuller, H. 2005. Mutations in mtDNA-encoded cytochrome c oxidase subunit genes causing isolated myopathy or severe encephalomyopathy. *Neuromuscul Disord,* 15**,** 851-7.

Hoskins, D. D.Mackenzie, C. G. 1961. Solubilization and electron transfer flavoprtein requirement of mitochondrial sarcosine dehydrogenase and dimethylglycine dehydrogenase. *J Biol Chem,* 236**,** 177-83.

Hotta, O., Inoue, C. N., Miyabayashi, S., Furuta, T., Takeuchi, A.Taguma, Y. 2001. Clinical and pathologic features of focal segmental glomerulosclerosis with mitochondrial tRNALeu(UUR) gene mutation. *Kidney Int,* 59**,** 1236-43.

Houstek, J., Klement, P., Hermanska, J., Houstkova, H., Hansikova, H., Van Den Bogert, C.Zeman, J. 1995. Altered properties of mitochondrial ATP-synthase in

patients with a T-->G mutation in the ATPase 6 (subunit a) gene at position 8993 of mtDNA. *Biochim Biophys Acta,* 1271**,** 349-57.

Howell, N., Bindoff, L. A., Mccullough, D. A., Kubacka, I., Poulton, J., Mackey, D., Taylor, L.Turnbull, D. M. 1991. Leber hereditary optic neuropathy: identification of the same mitochondrial ND1 mutation in six pedigrees. *Am J Hum Genet,* 49**,** 939-50.

Howell, N., Ghosh, S. S., Fahy, E.Bindoff, L. A. 2000. Longitudinal analysis of the segregation of mtDNA mutations in heteroplasmic individuals. *J Neurol Sci,* 172**,** 1-6.

Howell, N., Halvorson, S., Kubacka, I., Mccullough, D. A., Bindoff, L. A.Turnbull, D. M. 1992a. Mitochondrial gene segregation in mammals: is the bottleneck always narrow? *Hum Genet,* 90**,** 117-20.

Howell, N., Kubacka, I., Smith, R., Frerman, F., Parks, J. K.Parker, W. D., Jr. 1996. Association of the mitochondrial 8344 MERRF mutation with maternally inherited spinocerebellar degeneration and Leigh disease. *Neurology,* 46**,** 219-22.

Howell, N., Mccullough, D.Bodis-Wollner, I. 1992b. Molecular genetic analysis of a sporadic case of Leber hereditary optic neuropathy. *Am J Hum Genet,* 50**,** 443-6.

Howell, N., Xu, M., Halvorson, S., Bodis-Wollner, I.Sherman, J. 1994. A heteroplasmic LHON family: tissue distribution and transmission of the 11778 mutation. *Am J Hum Genet,* 55**,** 203-6.

Huang, C. C., Chen, R. S., Chen, C. M., Wang, H. S., Lee, C. C., Pang, C. Y., Hsu, H. S., Lee, H. C.Wei, Y. H. 1994. MELAS syndrome with mitochondrial tRNA(Leu(UUR)) gene mutation in a Chinese family. *J Neurol Neurosurg Psychiatry,* 57**,** 586-9.

Huang, C. C., Chen, R. S., Chu, N. S., Pang, C. Y.Wei, Y. H. 1996. Random mitotic segregation of mitochondrial DNA in MELAS syndrome. *Acta Neurol Scand,* 93**,** 198-202.

Huang, W., Yu, M., Jiao, Y., Ma, J., Ma, M., Wang, Z., Wu, H.Tan, D. 2011. Mitochondrial transcription termination factor 2 binds to entire mitochondrial DNA and negatively regulates mitochondrial gene expression. *Acta Biochim Biophys Sin (Shanghai),* 43**,** 472-9.

Hudson, G., Amati-Bonneau, P., Blakely, E. L., Stewart, J. D., He, L., Schaefer, A. M., Griffiths, P. G., Ahlqvist, K., Suomalainen, A., Reynier, P., Mcfarland, R., Turnbull, D. M., Chinnery, P. F.Taylor, R. W. 2008. Mutation of OPA1 causes

dominant optic atrophy with external ophthalmoplegia, ataxia, deafness and multiple mitochondrial DNA deletions: a novel disorder of mtDNA maintenance. *Brain,* 131**,** 329-37.

Hudson, G., Yu-Wai-Man, P., Griffiths, P. G., Caporali, L., Salomao, S. S., Berezovsky, A., Carelli, V., Zeviani, M.Chinnery, P. F. 2010. Variation in OPA1 does not explain the incomplete penetrance of Leber hereditary optic neuropathy. *Mol Vis,* 16**,** 2760-4.

Hudson, G., Yu-Wai-Man, P., Griffiths, P. G., Horvath, R., Carelli, V., Zeviani, M.Chinnery, P. F. 2011. Variation in MAPT is not a contributing factor to the incomplete penetrance in LHON. *Mitochondrion,* 11**,** 620-2.

Huss, J. M., Torra, I. P., Staels, B., Giguere, V.Kelly, D. P. 2004. Estrogen-related receptor alpha directs peroxisome proliferator-activated receptor alpha signaling in the transcriptional control of energy metabolism in cardiac and skeletal muscle. *Mol Cell Biol,* 24**,** 9079-91.

Hyvarinen, A. K., Kumanto, M. K., Marjavaara, S. K.Jacobs, H. T. 2010. Effects on mitochondrial transcription of manipulating mTERF protein levels in cultured human HEK293 cells. *BMC Mol Biol,* 11**,** 72.

Hyvarinen, A. K., Pohjoismaki, J. L., Holt, I. J.Jacobs, H. T. 2011. Overexpression of MTERFD1 or MTERFD3 impairs the completion of mitochondrial DNA replication. *Mol Biol Rep,* 38**,** 1321-8.

Hyvarinen, A. K., Pohjoismaki, J. L., Reyes, A., Wanrooij, S., Yasukawa, T., Karhunen, P. J., Spelbrink, J. N., Holt, I. J.Jacobs, H. T. 2007. The mitochondrial transcription termination factor mTERF modulates replication pausing in human mitochondrial DNA. *Nucleic Acids Res,* 35**,** 6458-74.

Iwanishi, M., Obata, T., Yamada, S., Maegawa, H., Tachikawa-Ide, R., Ugi, S., Hasegawa, M., Kojima, H., Oguni, T., Toudo, R.Et Al. 1995. Clinical and laboratory characteristics in the families with diabetes and a mitochondrial tRNA(LEU(UUR)) gene mutation. *Diabetes Res Clin Pract,* 29**,** 75-82.

Iwata, S., Lee, J. W., Okada, K., Lee, J. K., Iwata, M., Rasmussen, B., Link, T. A., Ramaswamy, S.Jap, B. K. 1998. Complete structure of the 11-subunit bovine mitochondrial cytochrome bc1 complex. *Science,* 281**,** 64-71.

Jager, S., Handschin, C., St-Pierre, J.Spiegelman, B. M. 2007. AMP-activated protein kinase (AMPK) action in skeletal muscle via direct phosphorylation of PGC-1alpha. *Proc Natl Acad Sci U S A,* 104**,** 12017-22.

Jansen, J. J., Maassen, J. A., Van Der Woude, F. J., Lemmink, H. A., Van Den Ouweland, J. M., T' Hart, L. M., Smeets, H. J., Bruijn, J. A.Lemkes, H. H. 1997. Mutation in mitochondrial tRNA(Leu(UUR)) gene associated with progressive kidney disease. *J Am Soc Nephrol,* 8**,** 1118-24.

Jemt, E., Farge, G., Backstrom, S., Holmlund, T., Gustafsson, C. M.Falkenberg, M. 2011. The mitochondrial DNA helicase TWINKLE can assemble on a closed circular template and support initiation of DNA synthesis. *Nucleic Acids Res,* 39**,** 9238-49.

Jenuth, J. P., Peterson, A. C., Fu, K.Shoubridge, E. A. 1996. Random genetic drift in the female germline explains the rapid segregation of mammalian mitochondrial DNA. *Nat Genet,* 14**,** 146-51.

Jia, L., Dienhart, M., Schramp, M., Mccauley, M., Hell, K.Stuart, R. A. 2003. Yeast Oxa1 interacts with mitochondrial ribosomes: the importance of the C-terminal region of Oxa1. *EMBO J,* 22**,** 6438-47.

Jia, L., Kaur, J.Stuart, R. A. 2009. Mapping of the Saccharomyces cerevisiae Oxa1-mitochondrial ribosome interface and identification of MrpL40, a ribosomal protein in close proximity to Oxa1 and critical for oxidative phosphorylation complex assembly. *Eukaryot Cell,* 8**,** 1792-802.

Jimenez-Menendez, N., Fernandez-Millan, P., Rubio-Cosials, A., Arnan, C., Montoya, J., Jacobs, H. T., Bernado, P., Coll, M., Uson, I.Sola, M. 2010. Human mitochondrial mTERF wraps around DNA through a left-handed superhelical tandem repeat. *Nat Struct Mol Biol,* 17**,** 891-3.

Jin, H., May, M., Tranebjaerg, L., Kendall, E., Fontan, G., Jackson, J., Subramony, S. H., Arena, F., Lubs, H., Smith, S., Stevenson, R., Schwartz, C.Vetrie, D. 1996. A novel X-linked gene, DDP, shows mutations in families with deafness (DFN-1), dystonia, mental deficiency and blindness. *Nat Genet,* 14**,** 177-80.

Johnson, A. A.Johnson, K. A. 2001. Exonuclease proofreading by human mitochondrial DNA polymerase. *J Biol Chem,* 276**,** 38097-107.

Johnson, A. A., Tsai, Y., Graves, S. W.Johnson, K. A. 2000. Human mitochondrial DNA polymerase holoenzyme: reconstitution and characterization. *Biochemistry,* 39**,** 1702-8.

Juvonen, V., Nikoskelainen, E., Lamminen, T., Penttinen, M., Aula, P.Savontaus, M. L. 1997. Tissue distribution of the ND4/11778 mutation in heteroplasmic lineages with Leber hereditary optic neuropathy. *Hum Mutat,* 9**,** 412-7.

Kadowaki, M.Kanazawa, T. 2003. Amino acids as regulators of proteolysis. *J Nutr,* 133**,** 2052S-2056S.

Kanehisa, M.Goto, S. 2000. KEGG: kyoto encyclopedia of genes and genomes. *Nucleic Acids Res,* 28**,** 27-30.

Kao, L. P., Ovchinnikov, D.Wolvetang, E. 2012. The effect of ethidium bromide and chloramphenicol on mitochondrial biogenesis in primary human fibroblasts. *Toxicol Appl Pharmacol,* 261**,** 42-9.

Kaplanova, V., Zeman, J., Hansikova, H., Cerna, L., Houst'kova, H., Misovicova, N.Houstek, J. 2004. Segregation pattern and biochemical effect of the G3460A mtDNA mutation in 27 members of LHON family. *J Neurol Sci,* 223**,** 149-55.

Karlberg, O., Canback, B., Kurland, C. G.Andersson, S. G. 2000. The dual origin of the yeast mitochondrial proteome. *Yeast,* 17**,** 170-87.

Kasiviswanathan, R.Copeland, W. C. 2011. Ribonucleotide discrimination and reverse transcription by the human mitochondrial DNA polymerase. *J Biol Chem,* 286**,** 31490-500.

Kaufman, B. A., Durisic, N., Mativetsky, J. M., Costantino, S., Hancock, M. A., Grutter, P.Shoubridge, E. A. 2007. The mitochondrial transcription factor TFAM coordinates the assembly of multiple DNA molecules into nucleoid-like structures. *Mol Biol Cell,* 18**,** 3225-36.

Kaukonen, J., Juselius, J. K., Tiranti, V., Kyttala, A., Zeviani, M., Comi, G. P., Keranen, S., Peltonen, L.Suomalainen, A. 2000. Role of adenine nucleotide translocator 1 in mtDNA maintenance. *Science,* 289**,** 782-5.

Kilbride, S. M.Prehn, J. H. 2012. Central roles of apoptotic proteins in mitochondrial function. *Oncogene*.

Kim, J., Lee, J. H.Iyer, V. R. 2008. Global identification of Myc target genes reveals its direct role in mitochondrial biogenesis and its E-box usage in vivo. *PLoS One,* 3**,** e1798.

Kimura, T., Yomogida, K., Iwai, N., Kato, Y.Nakano, T. 1999. Molecular cloning and genomic organization of mouse homologue of Drosophila germ cell-less and its expression in germ lineage cells. *Biochem Biophys Res Commun,* 262**,** 223-30.

King, M. P.Attardi, G. 1989. Human cells lacking mtDNA: repopulation with exogenous mitochondria by complementation. *Science,* 246**,** 500-3.

Kirby, D. M., Mcfarland, R., Ohtake, A., Dunning, C., Ryan, M. T., Wilson, C., Ketteridge, D., Turnbull, D. M., Thorburn, D. R.Taylor, R. W. 2004. Mutations of the mitochondrial ND1 gene as a cause of MELAS. *J Med Genet,* 41**,** 784-9.

Klingenberg, M. 1970. Localization of the glycerol-phosphate dehydrogenase in the outer phase of the mitochondrial inner membrane. *Eur J Biochem,* 13**,** 247-52.

Klingenspor, M. 2003. Cold-induced recruitment of brown adipose tissue thermogenesis. *Exp Physiol,* 88**,** 141-8.

Ko, C. H., Lam, C. W., Tse, P. W., Kong, C. K., Chan, A. K.Wong, L. J. 2001. De novo mutation in the mitochondrial tRNALeu(UUR) gene (A3243G) with rapid segregation resulting in MELAS in the offspring. *J Paediatr Child Health,* 37**,** 87-90.

Koc, E. C.Spremulli, L. L. 2002. Identification of mammalian mitochondrial translational initiation factor 3 and examination of its role in initiation complex formation with natural mRNAs. *J Biol Chem,* 277**,** 35541-9.

Koo, B., Becker, L. E., Chuang, S., Merante, F., Robinson, B. H., Macgregor, D., Tein, I., Ho, V. B., Mcgreal, D. A., Wherrett, J. R.Et Al. 1993. Mitochondrial encephalomyopathy, lactic acidosis, stroke-like episodes (MELAS): clinical, radiological, pathological, and genetic observations. *Ann Neurol,* 34**,** 25-32.

Koppen, M.Langer, T. 2007. Protein degradation within mitochondria: versatile activities of AAA proteases and other peptidases. *Crit Rev Biochem Mol Biol,* 42**,** 221-42.

Korhonen, J. A., Pham, X. H., Pellegrini, M.Falkenberg, M. 2004. Reconstitution of a minimal mtDNA replisome in vitro. *EMBO J,* 23**,** 2423-9.

Kraytsberg, Y., Kudryavtseva, E., Mckee, A. C., Geula, C., Kowall, N. W.Khrapko, K. 2006. Mitochondrial DNA deletions are abundant and cause functional impairment in aged human substantia nigra neurons. *Nat Genet,* 38**,** 518-20.

Krishnan, K. J., Reeve, A. K., Samuels, D. C., Chinnery, P. F., Blackwood, J. K., Taylor, R. W., Wanrooij, S., Spelbrink, J. N., Lightowlers, R. N.Turnbull, D. M. 2008. What causes mitochondrial DNA deletions in human cells? *Nat Genet,* 40**,** 275-9.

Kruse, B., Narasimhan, N.Attardi, G. 1989. Termination of transcription in human mitochondria: identification and purification of a DNA binding protein factor that promotes termination. *Cell,* 58**,** 391-7.

Kukat, C., Wurm, C. A., Spahr, H., Falkenberg, M., Larsson, N. G.Jakobs, S. 2011. Super-resolution microscopy reveals that mammalian mitochondrial nucleoids have a uniform size and frequently contain a single copy of mtDNA. *Proc Natl Acad Sci U S A,* 108**,** 13534-9.

Kunishige, M., Mitsui, T., Akaike, M., Kawajiri, M., Shono, M., Kawai, H.Matsumoto, T. 2003. Overexpressions of myoglobin and antioxidant enzymes in ragged-red fibers of skeletal muscle from patients with mitochondrial encephalomyopathy. *Muscle Nerve,* 28**,** 484-92.

Kunishige, M., Mitsui, T., Akaike, M., Shono, M., Kawai, H.Saito, S. 1996. Localization and amount of myoglobin and myoglobin mRNA in ragged-red fiber of patients with mitochondrial encephalomyopathy. *Muscle Nerve,* 19**,** 175-82.

Lagouge, M., Argmann, C., Gerhart-Hines, Z., Meziane, H., Lerin, C., Daussin, F., Messadeq, N., Milne, J., Lambert, P., Elliott, P., Geny, B., Laakso, M., Puigserver, P.Auwerx, J. 2006. Resveratrol improves mitochondrial function and protects against metabolic disease by activating SIRT1 and PGC-1alpha. *Cell,* 127**,** 1109-22.

Lai, L., Leone, T. C., Zechner, C., Schaeffer, P. J., Kelly, S. M., Flanagan, D. P., Medeiros, D. M., Kovacs, A.Kelly, D. P. 2008. Transcriptional coactivators PGC-1alpha and PGC-lbeta control overlapping programs required for perinatal maturation of the heart. *Genes Dev,* 22**,** 1948-61.

Laipis, P. J., Van De Walle, M. J.Hauswirth, W. W. 1988. Unequal partitioning of bovine mitochondrial genotypes among siblings. *Proc Natl Acad Sci U S A,* 85**,** 8107-10.

Lane, N.Martin, W. 2010. The energetics of genome complexity. *Nature,* 467**,** 929-34.

Lang, J. E., Magbanua, M. J., Scott, J. H., Makrigiorgos, G. M., Wang, G., Federman, S., Esserman, L. J., Park, J. W.Haqq, C. M. 2009. A comparison of RNA amplification techniques at sub-nanogram input concentration. *BMC Genomics,* 10**,** 326.

Lanza, I. R., Zabielski, P., Klaus, K. A., Morse, D. M., Heppelmann, C. J., Bergen, H. R., 3rd, Dasari, S., Walrand, S., Short, K. R., Johnson, M. L., Robinson, M. M., Schimke, J. M., Jakaitis, D. R., Asmann, Y. W., Sun, Z.Nair, K. S. 2012. Chronic caloric restriction preserves mitochondrial function in senescence without increasing mitochondrial biogenesis. *Cell Metab,* 16**,** 777-88.

Larsson, N. G.Clayton, D. A. 1995. Molecular genetic aspects of human mitochondrial disorders. *Annu Rev Genet,* 29**,** 151-78.

Larsson, N. G., Oldfors, A., Holme, E.Clayton, D. A. 1994. Low levels of mitochondrial transcription factor A in mitochondrial DNA depletion. *Biochem Biophys Res Commun,* 200**,** 1374-81.

Larsson, N. G., Tulinius, M. H., Holme, E., Oldfors, A., Andersen, O., Wahlstrom, J.Aasly, J. 1992. Segregation and manifestations of the mtDNA tRNA(Lys) A-->G(8344) mutation of myoclonus epilepsy and ragged-red fibers (MERRF) syndrome. *Am J Hum Genet,* 51**,** 1201-12.

Laursen, B. S., Sorensen, H. P., Mortensen, K. K.Sperling-Petersen, H. U. 2005. Initiation of protein synthesis in bacteria. *Microbiol Mol Biol Rev,* 69**,** 101-23.

Lebon, S., Chol, M., Benit, P., Mugnier, C., Chretien, D., Giurgea, I., Kern, I., Girardin, E., Hertz-Pannier, L., De Lonlay, P., Rotig, A., Rustin, P.Munnich, A. 2003. Recurrent de novo mitochondrial DNA mutations in respiratory chain deficiency. *J Med Genet,* 40**,** 896-9.

Lebrasseur, N. K., Cote, G. M., Miller, T. A., Fielding, R. A.Sawyer, D. B. 2003. Regulation of neuregulin/ErbB signaling by contractile activity in skeletal muscle. *Am J Physiol Cell Physiol,* 284**,** C1149-55.

Lee, D. Y.Clayton, D. A. 1998. Initiation of mitochondrial DNA replication by transcription and R-loop processing. *J Biol Chem,* 273**,** 30614-21.

Lehtonen, R., Kiuru, M., Vanharanta, S., Sjoberg, J., Aaltonen, L. M., Aittomaki, K., Arola, J., Butzow, R., Eng, C., Husgafvel-Pursiainen, K., Isola, J., Jarvinen, H., Koivisto, P., Mecklin, J. P., Peltomaki, P., Salovaara, R., Wasenius, V. M., Karhu, A., Launonen, V., Nupponen, N. N.Aaltonen, L. A. 2004. Biallelic inactivation of fumarate hydratase (FH) occurs in nonsyndromic uterine leiomyomas but is rare in other tumors. *Am J Pathol,* 164**,** 17-22.

Lelliott, C. J., Medina-Gomez, G., Petrovic, N., Kis, A., Feldmann, H. M., Bjursell, M., Parker, N., Curtis, K., Campbell, M., Hu, P., Zhang, D., Litwin, S. E., Zaha, V. G., Fountain, K. T., Boudina, S., Jimenez-Linan, M., Blount, M., Lopez, M., Meirhaeghe, A., Bohlooly, Y. M., Storlien, L., Stromstedt, M., Snaith, M., Oresic, M., Abel, E. D., Cannon, B.Vidal-Puig, A. 2006. Ablation of PGC-1beta results in defective mitochondrial activity, thermogenesis, hepatic function, and cardiac performance. *PLoS Biol,* 4**,** e369.

Leonardsson, G., Steel, J. H., Christian, M., Pocock, V., Milligan, S., Bell, J., So, P. W., Medina-Gomez, G., Vidal-Puig, A., White, R.Parker, M. G. 2004. Nuclear receptor corepressor RIP140 regulates fat accumulation. *Proc Natl Acad Sci U S A,* 101**,** 8437-42.

Leone, T. C., Lehman, J. J., Finck, B. N., Schaeffer, P. J., Wende, A. R., Boudina, S., Courtois, M., Wozniak, D. F., Sambandam, N., Bernal-Mizrachi, C., Chen, Z., Holloszy, J. O., Medeiros, D. M., Schmidt, R. E., Saffitz, J. E., Abel, E. D., Semenkovich, C. F.Kelly, D. P. 2005. PGC-1alpha deficiency causes multi-system energy metabolic derangements: muscle dysfunction, abnormal weight control and hepatic steatosis. *PLoS Biol,* 3**,** e101.

Lerin, C., Rodgers, J. T., Kalume, D. E., Kim, S. H., Pandey, A.Puigserver, P. 2006. GCN5 acetyltransferase complex controls glucose metabolism through transcriptional repression of PGC-1alpha. *Cell Metab,* 3**,** 429-38.

Levinger, L., Morl, M.Florentz, C. 2004. Mitochondrial tRNA 3' end metabolism and human disease. *Nucleic Acids Res,* 32**,** 5430-41.

Li, K.Williams, R. S. 1997. Tetramerization and single-stranded DNA binding properties of native and mutated forms of murine mitochondrial single-stranded DNA-binding proteins. *J Biol Chem,* 272**,** 8686-94.

Liao, H. X.Spremulli, L. L. 1990. Identification and initial characterization of translational initiation factor 2 from bovine mitochondria. *J Biol Chem,* 265**,** 13618-22.

Lien, L. M., Lee, H. C., Wang, K. L., Chiu, J. C., Chiu, H. C.Wei, Y. H. 2001. Involvement of nervous system in maternally inherited diabetes and deafness (MIDD) with the A3243G mutation of mitochondrial DNA. *Acta Neurol Scand,* 103**,** 159-65.

Lightowlers, R. N.Chrzanowska-Lightowlers, Z. M. 2008. PPR (pentatricopeptide repeat) proteins in mammals: important aids to mitochondrial gene expression. *Biochem J,* 416**,** e5-6.

Lill, R., Hoffmann, B., Molik, S., Pierik, A. J., Rietzschel, N., Stehling, O., Uzarska, M. A., Webert, H., Wilbrecht, C.Muhlenhoff, U. 2012. The role of mitochondria in cellular iron-sulfur protein biogenesis and iron metabolism. *Biochim Biophys Acta,* 1823**,** 1491-508.

Lim, S. E., Longley, M. J.Copeland, W. C. 1999. The mitochondrial p55 accessory subunit of human DNA polymerase gamma enhances DNA binding, promotes processive DNA synthesis, and confers N-ethylmaleimide resistance. *J Biol Chem,* 274**,** 38197-203.

Lin, J., Puigserver, P., Donovan, J., Tarr, P.Spiegelman, B. M. 2002. Peroxisome proliferator-activated receptor gamma coactivator 1beta (PGC-1beta), a novel PGC-1-related transcription coactivator associated with host cell factor. *J Biol Chem,* 277**,** 1645-8.

Lin, M. T.Beal, M. F. 2006. Mitochondrial dysfunction and oxidative stress in neurodegenerative diseases. *Nature,* 443**,** 787-95.

Linder, T., Park, C. B., Asin-Cayuela, J., Pellegrini, M., Larsson, N. G., Falkenberg, M., Samuelsson, T.Gustafsson, C. M. 2005. A family of putative transcription termination factors shared amongst metazoans and plants. *Curr Genet,* 48**,** 265-9.

Ling, M., Merante, F., Chen, H. S., Duff, C., Duncan, A. M.Robinson, B. H. 1997. The human mitochondrial elongation factor tu (EF-Tu) gene: cDNA sequence, genomic localization, genomic structure, and identification of a pseudogene. *Gene,* 197**,** 325-36.

Liou, C. W., Huang, C. C., Chee, E. C., Jong, Y. J., Tsai, J. L., Pang, C. Y., Lee, H. C.Wei, Y. H. 1994. MELAS syndrome: correlation between clinical features and molecular genetic analysis. *Acta Neurol Scand,* 90**,** 354-9.

Litonin, D., Sologub, M., Shi, Y., Savkina, M., Anikin, M., Falkenberg, M., Gustafsson, C. M.Temiakov, D. 2010. Human mitochondrial transcription revisited: only TFAM and TFB2M are required for transcription of the mitochondrial genes in vitro. *J Biol Chem,* 285**,** 18129-33.

Liu, M.Spremulli, L. 2000. Interaction of mammalian mitochondrial ribosomes with the inner membrane. *J Biol Chem,* 275**,** 29400-6.

Liu, P.Demple, B. 2010. DNA repair in mammalian mitochondria: Much more than we thought? *Environ Mol Mutagen,* 51**,** 417-26.

Liu, P., Qian, L., Sung, J. S., De Souza-Pinto, N. C., Zheng, L., Bogenhagen, D. F., Bohr, V. A., Wilson, D. M., 3rd, Shen, B.Demple, B. 2008. Removal of oxidative DNA damage via FEN1-dependent long-patch base excision repair in human cell mitochondria. *Mol Cell Biol,* 28**,** 4975-87.

Lodeiro, M. F., Uchida, A., Bestwick, M., Moustafa, I. M., Arnold, J. J., Shadel, G. S.Cameron, C. E. 2012. Transcription from the second heavy-strand promoter of human mtDNA is repressed by transcription factor A in vitro. *Proc Natl Acad Sci U S A,* 109**,** 6513-8.

Lodi, R., Montagna, P., Iotti, S., Zaniol, P., Barboni, P., Puddu, P.Barbiroli, B. 1994. Brain and muscle energy metabolism studied in vivo by 31P-magnetic resonance spectroscopy in NARP syndrome. *J Neurol Neurosurg Psychiatry,* 57**,** 1492-6.

Loeffen, J., Smeitink, J., Triepels, R., Smeets, R., Schuelke, M., Sengers, R., Trijbels, F., Hamel, B., Mullaart, R.Van Den Heuvel, L. 1998. The first nuclear-encoded

complex I mutation in a patient with Leigh syndrome. *Am J Hum Genet,* 63**,** 1598-608.

Longley, M. J., Clark, S., Yu Wai Man, C., Hudson, G., Durham, S. E., Taylor, R. W., Nightingale, S., Turnbull, D. M., Copeland, W. C.Chinnery, P. F. 2006. Mutant POLG2 disrupts DNA polymerase gamma subunits and causes progressive external ophthalmoplegia. *Am J Hum Genet,* 78**,** 1026-34.

Longley, M. J., Prasad, R., Srivastava, D. K., Wilson, S. H.Copeland, W. C. 1998. Identification of 5'-deoxyribose phosphate lyase activity in human DNA polymerase gamma and its role in mitochondrial base excision repair in vitro. *Proc Natl Acad Sci U S A,* 95**,** 12244-8.

Lopez-Lluch, G., Hunt, N., Jones, B., Zhu, M., Jamieson, H., Hilmer, S., Cascajo, M. V., Allard, J., Ingram, D. K., Navas, P.De Cabo, R. 2006. Calorie restriction induces mitochondrial biogenesis and bioenergetic efficiency. *Proc Natl Acad Sci U S A,* 103**,** 1768-73.

Lowell, B. B.Shulman, G. I. 2005. Mitochondrial dysfunction and type 2 diabetes. *Science,* 307**,** 384-7.

Lowell, B. B.Spiegelman, B. M. 2000. Towards a molecular understanding of adaptive thermogenesis. *Nature,* 404**,** 652-60.

Lu, C. Y., Tso, D. J., Yang, T., Jong, Y. J.Wei, Y. H. 2002. Detection of DNA mutations associated with mitochondrial diseases by Agilent 2100 bioanalyzer. *Clin Chim Acta,* 318**,** 97-105.

Lu, C. Y., Wang, E. K., Lee, H. C., Tsay, H. J.Wei, Y. H. 2003. Increased expression of manganese-superoxide dismutase in fibroblasts of patients with CPEO syndrome. *Mol Genet Metab,* 80**,** 321-9.

Luft, R., Ikkos, D., Palmieri, G., Ernster, L.Afzelius, B. 1962. A case of severe hypermetabolism of nonthyroid origin with a defect in the maintenance of mitochondrial respiratory control: a correlated clinical, biochemical, and morphological study. *J Clin Invest,* 41**,** 1776-804.

Lythgow, K. T., Hudson, G., Andras, P.Chinnery, P. F. 2011. A critical analysis of the combined usage of protein localization prediction methods: Increasing the number of independent data sets can reduce the accuracy of predicted mitochondrial localization. *Mitochondrion,* 11**,** 444-9.

Ma, J.Spremulli, L. L. 1996. Expression, purification, and mechanistic studies of bovine mitochondrial translational initiation factor 2. *J Biol Chem,* 271**,** 5805-11.

Ma, L.Spremulli, L. L. 1995. Cloning and sequence analysis of the human mitochondrial translational initiation factor 2 cDNA. *J Biol Chem,* 270**,** 1859-65.

Ma, Y. S., Chen, Y. C., Lu, C. Y., Liu, C. Y.Wei, Y. H. 2005. Upregulation of matrix metalloproteinase 1 and disruption of mitochondrial network in skin fibroblasts of patients with MERRF syndrome. *Ann N Y Acad Sci,* 1042**,** 55-63.

Macdonald, M. J. 1981. High content of mitochondrial glycerol-3-phosphate dehydrogenase in pancreatic islets and its inhibition by diazoxide. *J Biol Chem,* 256**,** 8287-90.

Maglott, D. R., Katz, K. S., Sicotte, H.Pruitt, K. D. 2000. NCBI's LocusLink and RefSeq. *Nucleic Acids Res,* 28**,** 126-8.

Mahrous, E., Yang, Q.Clarke, H. J. 2012. Regulation of mitochondrial DNA accumulation during oocyte growth and meiotic maturation in the mouse. *Reproduction,* 144**,** 177-85.

Mak, S. C., Chi, C. S., Liu, C. Y., Pang, C. Y.Wei, Y. H. 1996. Leigh syndrome associated with mitochondrial DNA 8993 T-->G mutation and ragged-red fibers. *Pediatr Neurol,* 15**,** 72-5.

Makela-Bengs, P., Suomalainen, A., Majander, A., Rapola, J., Kalimo, H., Nuutila, A.Pihko, H. 1995. Correlation between the clinical symptoms and the proportion of mitochondrial DNA carrying the 8993 point mutation in the NARP syndrome. *Pediatr Res,* 37**,** 634-9.

Makino, M., Horai, S., Goto, Y.Nonaka, I. 2000. Mitochondrial DNA mutations in Leigh syndrome and their phylogenetic implications. *J Hum Genet,* 45**,** 69-75.

Malarkey, C. S., Bestwick, M., Kuhlwilm, J. E., Shadel, G. S.Churchill, M. E. 2012. Transcriptional activation by mitochondrial transcription factor A involves preferential distortion of promoter DNA. *Nucleic Acids Res,* 40**,** 614-24.

Malena, A., Loro, E., Di Re, M., Holt, I. J.Vergani, L. 2009. Inhibition of mitochondrial fission favours mutant over wild-type mitochondrial DNA. *Hum Mol Genet,* 18**,** 3407-16.

Man, P. Y., Griffiths, P. G., Brown, D. T., Howell, N., Turnbull, D. M.Chinnery, P. F. 2003. The epidemiology of Leber hereditary optic neuropathy in the North East of England. *Am J Hum Genet,* 72**,** 333-9.

Mandel, H., Szargel, R., Labay, V., Elpeleg, O., Saada, A., Shalata, A., Anbinder, Y., Berkowitz, D., Hartman, C., Barak, M., Eriksson, S.Cohen, N. 2001. The

deoxyguanosine kinase gene is mutated in individuals with depleted hepatocerebral mitochondrial DNA. *Nat Genet,* 29**,** 337-41.

Mannella, C. A., Marko, M., Penczek, P., Barnard, D.Frank, J. 1994. The internal compartmentation of rat-liver mitochondria: tomographic study using the high-voltage transmission electron microscope. *Microsc Res Tech,* 27**,** 278-83.

Marchington, D. R., Hartshorne, G. M., Barlow, D.Poulton, J. 1997. Homopolymeric tract heteroplasmy in mtDNA from tissues and single oocytes: support for a genetic bottleneck. *Am J Hum Genet,* 60**,** 408-16.

Marchington, D. R., Macaulay, V., Hartshorne, G. M., Barlow, D.Poulton, J. 1998. Evidence from human oocytes for a genetic bottleneck in an mtDNA disease. *Am J Hum Genet,* 63**,** 769-75.

Margulis, L. 1971. Symbiosis and evolution. *Sci Am,* 225**,** 48-57.

Martin, J. L., Brown, C. E., Matthews-Davis, N.Reardon, J. E. 1994. Effects of antiviral nucleoside analogs on human DNA polymerases and mitochondrial DNA synthesis. *Antimicrob Agents Chemother,* 38**,** 2743-9.

Martin, M., Cho, J., Cesare, A. J., Griffith, J. D.Attardi, G. 2005. Termination factor-mediated DNA loop between termination and initiation sites drives mitochondrial rRNA synthesis. *Cell,* 123**,** 1227-40.

Martin, W.Schnarrenberger, C. 1997. The evolution of the Calvin cycle from prokaryotic to eukaryotic chromosomes: a case study of functional redundancy in ancient pathways through endosymbiosis. *Curr Genet,* 32**,** 1-18.

Martinuzzi, A., Bartolomei, L., Carrozzo, R., Mostacciuolo, M., Carbonin, C., Toso, V., Ciafaloni, E., Shanske, S., Dimauro, S.Angelini, C. 1992. Correlation between clinical and molecular features in two MELAS families. *J Neurol Sci,* 113**,** 222-9.

Mason, P. A.Lightowlers, R. N. 2003. Why do mammalian mitochondria possess a mismatch repair activity? *FEBS Lett,* 554**,** 6-9.

Massa, V., Fernandez-Vizarra, E., Alshahwan, S., Bakhsh, E., Goffrini, P., Ferrero, I., Mereghetti, P., D'adamo, P., Gasparini, P.Zeviani, M. 2008. Severe infantile encephalomyopathy caused by a mutation in COX6B1, a nucleus-encoded subunit of cytochrome c oxidase. *Am J Hum Genet,* 82**,** 1281-9.

Masters, B. S., Stohl, L. L.Clayton, D. A. 1987. Yeast mitochondrial RNA polymerase is homologous to those encoded by bacteriophages T3 and T7. *Cell,* 51**,** 89-99.

Masuda, N., Ohnishi, T., Kawamoto, S., Monden, M.Okubo, K. 1999. Analysis of chemical modification of RNA from formalin-fixed samples and optimization of molecular biology applications for such samples. *Nucleic Acids Res,* 27**,** 4436-43.

Mcconnell, J. M.Petrie, L. 2004. Mitochondrial DNA turnover occurs during preimplantation development and can be modulated by environmental factors. *Reprod Biomed Online,* 9**,** 418-24.

Mccormack, J. G., Halestrap, A. P.Denton, R. M. 1990. Role of calcium ions in regulation of mammalian intramitochondrial metabolism. *Physiol Rev,* 70**,** 391-425.

Mcculloch, V., Seidel-Rogol, B. L.Shadel, G. S. 2002. A human mitochondrial transcription factor is related to RNA adenine methyltransferases and binds S-adenosylmethionine. *Mol Cell Biol,* 22**,** 1116-25.

Mcculloch, V.Shadel, G. S. 2003. Human mitochondrial transcription factor B1 interacts with the C-terminal activation region of h-mtTFA and stimulates transcription independently of its RNA methyltransferase activity. *Mol Cell Biol,* 23**,** 5816-24.

Mcfarland, R., Elson, J. L., Taylor, R. W., Howell, N.Turnbull, D. M. 2004. Assigning pathogenicity to mitochondrial tRNA mutations: when "definitely maybe" is not good enough. *Trends Genet,* 20**,** 591-6.

Mcgee, S. L.Hargreaves, M. 2004. Exercise and myocyte enhancer factor 2 regulation in human skeletal muscle. *Diabetes,* 53**,** 1208-14.

Mckenzie, M., Lazarou, M., Thorburn, D. R.Ryan, M. T. 2006. Mitochondrial respiratory chain supercomplexes are destabilized in Barth Syndrome patients. *J Mol Biol,* 361**,** 462-9.

Mclaren, A. 2003. Primordial germ cells in the mouse. *Dev Biol,* 262**,** 1-15.

Meier, S., Neupert, W.Herrmann, J. M. 2005. Proline residues of transmembrane domains determine the sorting of inner membrane proteins in mitochondria. *J Cell Biol,* 170**,** 881-8.

Metodiev, M. D., Lesko, N., Park, C. B., Camara, Y., Shi, Y., Wibom, R., Hultenby, K., Gustafsson, C. M.Larsson, N. G. 2009. Methylation of 12S rRNA is necessary for in vivo stability of the small subunit of the mammalian mitochondrial ribosome. *Cell Metab,* 9**,** 386-97.

Michikawa, Y., Mazzucchelli, F., Bresolin, N., Scarlato, G.Attardi, G. 1999. Aging-dependent large accumulation of point mutations in the human mtDNA control region for replication. *Science,* 286**,** 774-9.

Mikelsaar, R. 1983. Human mitochondrial genome and the evolution of methionine transfer ribonucleic acids. *J Theor Biol,* 105**,** 221-32.

Miller, C., Saada, A., Shaul, N., Shabtai, N., Ben-Shalom, E., Shaag, A., Hershkovitz, E.Elpeleg, O. 2004. Defective mitochondrial translation caused by a ribosomal protein (MRPS16) mutation. *Ann Neurol,* 56**,** 734-8.

Minczuk, M., He, J., Duch, A. M., Ettema, T. J., Chlebowski, A., Dzionek, K., Nijtmans, L. G., Huynen, M. A.Holt, I. J. 2011. TEFM (c17orf42) is necessary for transcription of human mtDNA. *Nucleic Acids Res,* 39**,** 4284-99.

Mitchell, A. L., Elson, J. L., Howell, N., Taylor, R. W.Turnbull, D. M. 2006. Sequence variation in mitochondrial complex I genes: mutation or polymorphism? *J Med Genet,* 43**,** 175-9.

Miura, S., Kawanaka, K., Kai, Y., Tamura, M., Goto, M., Shiuchi, T., Minokoshi, Y.Ezaki, O. 2007. An increase in murine skeletal muscle peroxisome proliferator-activated receptor-gamma coactivator-1alpha (PGC-1alpha) mRNA in response to exercise is mediated by beta-adrenergic receptor activation. *Endocrinology,* 148**,** 3441-8.

Mkaouar-Rebai, E., Chaari, W., Younes, S., Bousoffara, R., Sfar, M. T.Fakhfakh, F. 2009. Maternally inherited Leigh syndrome: T8993G mutation in a Tunisian family. *Pediatr Neurol,* 40**,** 437-42.

Montoya, J., Christianson, T., Levens, D., Rabinowitz, M.Attardi, G. 1982. Identification of initiation sites for heavy-strand and light-strand transcription in human mitochondrial DNA. *Proc Natl Acad Sci U S A,* 79**,** 7195-9.

Montoya, J., Gaines, G. L.Attardi, G. 1983. The pattern of transcription of the human mitochondrial rRNA genes reveals two overlapping transcription units. *Cell,* 34**,** 151-9.

Montoya, J., Ojala, D.Attardi, G. 1981. Distinctive features of the 5'-terminal sequences of the human mitochondrial mRNAs. *Nature,* 290**,** 465-70.

Mootha, V. K., Handschin, C., Arlow, D., Xie, X., St Pierre, J., Sihag, S., Yang, W., Altshuler, D., Puigserver, P., Patterson, N., Willy, P. J., Schulman, I. G., Heyman, R. A., Lander, E. S.Spiegelman, B. M. 2004. Erralpha and Gabpa/b specify PGC-1alpha-dependent oxidative phosphorylation gene expression that is altered in diabetic muscle. *Proc Natl Acad Sci U S A,* 101**,** 6570-5.

Moraes, C. T., Kenyon, L.Hao, H. 1999. Mechanisms of human mitochondrial DNA maintenance: the determining role of primary sequence and length over function. *Mol Biol Cell,* 10**,** 3345-56.

Morovvati, S., Nakagawa, M., Sato, Y., Hamada, K., Higuchi, I.Osame, M. 2002. Phenotypes and mitochondrial DNA substitutions in families with A3243G mutation. *Acta Neurol Scand,* 106**,** 104-8.

Mostaqul Huq, M. D., Gupta, P., Tsai, N. P., White, R., Parker, M. G.Wei, L. N. 2006. Suppression of receptor interacting protein 140 repressive activity by protein arginine methylation. *EMBO J,* 25**,** 5094-104.

Mourier, T., Hansen, A. J., Willerslev, E.Arctander, P. 2001. The Human Genome Project reveals a continuous transfer of large mitochondrial fragments to the nucleus. *Mol Biol Evol,* 18**,** 1833-7.

Muller-Hocker, J., Schneiderbanger, K., Stefani, F. H.Kadenbach, B. 1992. Progressive loss of cytochrome c oxidase in the human extraocular muscles in ageing--a cytochemical-immunohistochemical study. *Mutat Res,* 275**,** 115-24.

Muller, H. J. 1964. The Relation of Recombination to Mutational Advance. *Mutat Res,* 106**,** 2-9.

Muller, M. 1993. The hydrogenosome. *J Gen Microbiol,* 139**,** 2879-89.

Munoz-Malaga, A., Bautista, J., Salazar, J. A., Aguilera, I., Garcia, R., Chinchon, I., Segura, M. D., Campos, Y.Arenas, J. 2000. Lipomatosis, proximal myopathy, and the mitochondrial 8344 mutation. A lipid storage myopathy? *Muscle Nerve,* 23**,** 538-42.

Murakami, E., Feng, J. Y., Lee, H., Hanes, J., Johnson, K. A.Anderson, K. S. 2003. Characterization of novel reverse transcriptase and other RNA-associated catalytic activities by human DNA polymerase gamma: importance in mitochondrial DNA replication. *J Biol Chem,* 278**,** 36403-9.

Musumeci, O., Andreu, A. L., Shanske, S., Bresolin, N., Comi, G. P., Rothstein, R., Schon, E. A.Dimauro, S. 2000. Intragenic inversion of mtDNA: a new type of pathogenic mutation in a patient with mitochondrial myopathy. *Am J Hum Genet,* 66**,** 1900-4.

Nagaike, T., Suzuki, T., Katoh, T.Ueda, T. 2005. Human mitochondrial mRNAs are stabilized with polyadenylation regulated by mitochondria-specific poly(A) polymerase and polynucleotide phosphorylase. *J Biol Chem,* 280**,** 19721-7.

Nagaike, T., Suzuki, T., Tomari, Y., Takemoto-Hori, C., Negayama, F., Watanabe, K.Ueda, T. 2001. Identification and characterization of mammalian mitochondrial tRNA nucleotidyltransferases. *J Biol Chem,* 276**,** 40041-9.

Nagao, A., Suzuki, T.Suzuki, T. 2007. Aminoacyl-tRNA surveillance by EF-Tu in mammalian mitochondria. *Nucleic Acids Symp Ser (Oxf)***,** 41-2.

Nakada, K., Inoue, K., Ono, T., Isobe, K., Ogura, A., Goto, Y. I., Nonaka, I.Hayashi, J. I. 2001. Inter-mitochondrial complementation: Mitochondria-specific system preventing mice from expression of disease phenotypes by mutant mtDNA. *Nat Med,* 7**,** 934-40.

Nass, M. M. 1969. Mitochondrial DNA. I. Intramitochondrial distribution and structural relations of single- and double-length circular DNA. *J Mol Biol,* 42**,** 521-8.

Naviaux, R. K.Nguyen, K. V. 2004. POLG mutations associated with Alpers' syndrome and mitochondrial DNA depletion. *Ann Neurol,* 55**,** 706-12.

Nekhaeva, E., Bodyak, N. D., Kraytsberg, Y., Mcgrath, S. B., Van Orsouw, N. J., Pluzhnikov, A., Wei, J. Y., Vijg, J.Khrapko, K. 2002. Clonally expanded mtDNA point mutations are abundant in individual cells of human tissues. *Proc Natl Acad Sci U S A,* 99**,** 5521-6.

Ngo, H. B., Kaiser, J. T.Chan, D. C. 2011. The mitochondrial transcription and packaging factor Tfam imposes a U-turn on mitochondrial DNA. *Nat Struct Mol Biol,* 18**,** 1290-6.

Nikoskelainen, E. K., Marttila, R. J., Huoponen, K., Juvonen, V., Lamminen, T., Sonninen, P.Savontaus, M. L. 1995. Leber's "plus": neurological abnormalities in patients with Leber's hereditary optic neuropathy. *J Neurol Neurosurg Psychiatry,* 59**,** 160-4.

Nishigaki, Y., Tadesse, S., Bonilla, E., Shungu, D., Hersh, S., Keats, B. J., Berlin, C. I., Goldberg, M. F., Vockley, J., Dimauro, S.Hirano, M. 2003. A novel mitochondrial tRNA(Leu(UUR)) mutation in a patient with features of MERRF and Kearns-Sayre syndrome. *Neuromuscul Disord,* 13**,** 334-40.

Nishino, I., Spinazzola, A.Hirano, M. 1999. Thymidine phosphorylase gene mutations in MNGIE, a human mitochondrial disorder. *Science,* 283**,** 689-92.

Nisoli, E., Tonello, C., Cardile, A., Cozzi, V., Bracale, R., Tedesco, L., Falcone, S., Valerio, A., Cantoni, O., Clementi, E., Moncada, S.Carruba, M. O. 2005. Calorie restriction promotes mitochondrial biogenesis by inducing the expression of eNOS. *Science,* 310**,** 314-7.

Niwano, K., Arai, M., Koitabashi, N., Hara, S., Watanabe, A., Sekiguchi, K., Tanaka, T., Iso, T.Kurabayashi, M. 2006. Competitive binding of CREB and ATF2 to cAMP/ATF responsive element regulates eNOS gene expression in endothelial cells. *Arterioscler Thromb Vasc Biol,* 26**,** 1036-42.

Nogawa, T., Sung, W. K., Jagiello, G. M.Bowne, W. 1988. A quantitative analysis of mitochondria during fetal mouse oogenesis. *J Morphol,* 195**,** 225-34.

Nolan, T., Hands, R. E.Bustin, S. A. 2006a. Quantification of mRNA using real-time RT-PCR. *Nat Protoc,* 1**,** 1559-82.

Nolan, T., Hands, R. E., Ogunkolade, W.Bustin, S. A. 2006b. SPUD: a quantitative PCR assay for the detection of inhibitors in nucleic acid preparations. *Anal Biochem,* 351**,** 308-10.

Nolden, M., Ehses, S., Koppen, M., Bernacchia, A., Rugarli, E. I.Langer, T. 2005. The m-AAA protease defective in hereditary spastic paraplegia controls ribosome assembly in mitochondria. *Cell,* 123**,** 277-89.

Nozaki, Y., Matsunaga, N., Ishizawa, T., Ueda, T.Takeuchi, N. 2008. HMRF1L is a human mitochondrial translation release factor involved in the decoding of the termination codons UAA and UAG. *Genes Cells,* 13**,** 429-38.

Ogilvie, I., Kennaway, N. G.Shoubridge, E. A. 2005. A molecular chaperone for mitochondrial complex I assembly is mutated in a progressive encephalopathy. *J Clin Invest,* 115**,** 2784-92.

Ohinata, Y., Payer, B., O'carroll, D., Ancelin, K., Ono, Y., Sano, M., Barton, S. C., Obukhanych, T., Nussenzweig, M., Tarakhovsky, A., Saitou, M.Surani, M. A. 2005. Blimp1 is a critical determinant of the germ cell lineage in mice. *Nature,* 436**,** 207-13.

Ohinata, Y., Sano, M., Shigeta, M., Yamanaka, K.Saitou, M. 2008. A comprehensive, non-invasive visualization of primordial germ cell development in mice by the Prdm1-mVenus and Dppa3-ECFP double transgenic reporter. *Reproduction,* 136**,** 503-14.

Ojala, D., Montoya, J.Attardi, G. 1981. tRNA punctuation model of RNA processing in human mitochondria. *Nature,* 290**,** 470-4.

Oliveira, M. T.Kaguni, L. S. 2011. Reduced stimulation of recombinant DNA polymerase gamma and mitochondrial DNA (mtDNA) helicase by variants of mitochondrial single-stranded DNA-binding protein (mtSSB) correlates with defects in mtDNA replication in animal cells. *J Biol Chem,* 286**,** 40649-58.

Olivo, P., Van De Walle, M., Laipis, P.Hauswirth, W. 1983. Nucleotide sequence evidence for rapid genotypic shifts in the bovinemitochondrial DNA D-loop. *Nature,* 306**,** 400-402.

Olson, B. L., Hock, M. B., Ekholm-Reed, S., Wohlschlegel, J. A., Dev, K. K., Kralli, A.Reed, S. I. 2008. SCFCdc4 acts antagonistically to the PGC-1alpha transcriptional coactivator by targeting it for ubiquitin-mediated proteolysis. *Genes Dev,* 22**,** 252-64.

Olsson, C., Zethelius, B., Lagerstrom-Fermer, M., Asplund, J., Berne, C.Landegren, U. 1998. Level of heteroplasmy for the mitochondrial mutation A3243G correlates with age at onset of diabetes and deafness. *Hum Mutat,* 12**,** 52-8.

Oltvai, Z. N., Milliman, C. L.Korsmeyer, S. J. 1993. Bcl-2 heterodimerizes in vivo with a conserved homolog, Bax, that accelerates programmed cell death. *Cell,* 74**,** 609-19.

Onishi, H., Hanihara, T., Sugiyama, N., Kawanishi, C., Iseki, E., Maruyama, Y., Yamada, Y., Kosaka, K., Yagishita, S., Sekihara, H.Satoh, S. 1998. Pancreatic exocrine dysfunction associated with mitochondrial tRNA(Leu)(UUR) mutation. *J Med Genet,* 35**,** 255-7.

Orren, D. K., Dianov, G. L.Bohr, V. A. 1996. The human CSB (ERCC6) gene corrects the transcription-coupled repair defect in the CHO cell mutant UV61. *Nucleic Acids Res,* 24**,** 3317-22.

Osawa, S., Jukes, T. H., Watanabe, K.Muto, A. 1992. Recent evidence for evolution of the genetic code. *Microbiol Rev,* 56**,** 229-64.

Ostergaard, E., Christensen, E., Kristensen, E., Mogensen, B., Duno, M., Shoubridge, E. A.Wibrand, F. 2007. Deficiency of the alpha subunit of succinate-coenzyme A ligase causes fatal infantile lactic acidosis with mitochondrial DNA depletion. *Am J Hum Genet,* 81**,** 383-7.

Ott, M., Prestele, M., Bauerschmitt, H., Funes, S., Bonnefoy, N.Herrmann, J. M. 2006. Mba1, a membrane-associated ribosome receptor in mitochondria. *EMBO J,* 25**,** 1603-10.

Ozawa, M., Nonaka, I.Goto, Y. 1998. Single muscle fiber analysis in patients with 3243 mutation in mitochondrial DNA: comparison with the phenotype and the proportion of mutant genome. *J Neurol Sci,* 159**,** 170-5.

Pagliarini, D. J., Calvo, S. E., Chang, B., Sheth, S. A., Vafai, S. B., Ong, S. E., Walford, G. A., Sugiana, C., Boneh, A., Chen, W. K., Hill, D. E., Vidal, M., Evans, J. G.,

Thorburn, D. R., Carr, S. A.Mootha, V. K. 2008. A mitochondrial protein compendium elucidates complex I disease biology. *Cell,* 134**,** 112-23.

Palade, G. E. 1952. The fine structure of mitochondria. *Anat Rec,* 114**,** 427-51.

Papadopoulou, L. C., Sue, C. M., Davidson, M. M., Tanji, K., Nishino, I., Sadlock, J. E., Krishna, S., Walker, W., Selby, J., Glerum, D. M., Coster, R. V., Lyon, G., Scalais, E., Lebel, R., Kaplan, P., Shanske, S., De Vivo, D. C., Bonilla, E., Hirano, M., Dimauro, S.Schon, E. A. 1999. Fatal infantile cardioencephalomyopathy with COX deficiency and mutations in SCO2, a COX assembly gene. *Nat Genet,* 23**,** 333-7.

Parisi, M. A.Clayton, D. A. 1991. Similarity of human mitochondrial transcription factor 1 to high mobility group proteins. *Science,* 252**,** 965-9.

Park, C. B., Asin-Cayuela, J., Camara, Y., Shi, Y., Pellegrini, M., Gaspari, M., Wibom, R., Hultenby, K., Erdjument-Bromage, H., Tempst, P., Falkenberg, M., Gustafsson, C. M.Larsson, N. G. 2007. MTERF3 is a negative regulator of mammalian mtDNA transcription. *Cell,* 130**,** 273-85.

Paschen, S. A., Waizenegger, T., Stan, T., Preuss, M., Cyrklaff, M., Hell, K., Rapaport, D.Neupert, W. 2003. Evolutionary conservation of biogenesis of beta-barrel membrane proteins. *Nature,* 426**,** 862-6.

Pastores, G. M., Santorelli, F. M., Shanske, S., Gelb, B. D., Fyfe, B., Wolfe, D.Willner, J. P. 1994. Leigh syndrome and hypertrophic cardiomyopathy in an infant with a mitochondrial DNA point mutation (T8993G). *Am J Med Genet,* 50**,** 265-71.

Payer, B., Chuva De Sousa Lopes, S. M., Barton, S. C., Lee, C., Saitou, M.Surani, M. A. 2006. Generation of stella-GFP transgenic mice: a novel tool to study germ cell development. *Genesis,* 44**,** 75-83.

Payne, B. A., Wilson, I. J., Hateley, C. A., Horvath, R., Santibanez-Koref, M., Samuels, D. C., Price, D. A.Chinnery, P. F. 2011. Mitochondrial aging is accelerated by anti-retroviral therapy through the clonal expansion of mtDNA mutations. *Nat Genet,* 43**,** 806-10.

Pecina, P., Houstkova, H., Hansikova, H., Zeman, J.Houstek, J. 2004. Genetic defects of cytochrome c oxidase assembly. *Physiol Res,* 53 Suppl 1**,** S213-23.

Pedersen, R. A., Wu, K.Balakier, H. 1986. Origin of the inner cell mass in mouse embryos: cell lineage analysis by microinjection. *Dev Biol,* 117**,** 581-95.

Pepling, M. E., Sundman, E. A., Patterson, N. L., Gephardt, G. W., Medico, L., Jr.Wilson, K. I. 2010. Differences in oocyte development and estradiol sensitivity among mouse strains. *Reproduction,* 139**,** 349-57.

Perez, E., Bourguet, W., Gronemeyer, H.De Lera, A. R. 2012. Modulation of RXR function through ligand design. *Biochim Biophys Acta,* 1821**,** 57-69.

Perkins, G., Renken, C., Martone, M. E., Young, S. J., Ellisman, M.Frey, T. 1997. Electron tomography of neuronal mitochondria: three-dimensional structure and organization of cristae and membrane contacts. *J Struct Biol,* 119**,** 260-72.

Petros, J. A., Baumann, A. K., Ruiz-Pesini, E., Amin, M. B., Sun, C. Q., Hall, J., Lim, S., Issa, M. M., Flanders, W. D., Hosseini, S. H., Marshall, F. F.Wallace, D. C. 2005. mtDNA mutations increase tumorigenicity in prostate cancer. *Proc Natl Acad Sci U S A,* 102**,** 719-24.

Petruzzella, V., Moraes, C. T., Sano, M. C., Bonilla, E., Dimauro, S.Schon, E. A. 1994. Extremely high levels of mutant mtDNAs co-localize with cytochrome c oxidase-negative ragged-red fibers in patients harboring a point mutation at nt 3243. *Hum Mol Genet,* 3**,** 449-54.

Pfaffl, M. W., Horgan, G. W.Dempfle, L. 2002. Relative expression software tool (REST) for group-wise comparison and statistical analysis of relative expression results in real-time PCR. *Nucleic Acids Res,* 30**,** e36.

Pfaffl, M. W., Tichopad, A., Prgomet, C.Neuvians, T. P. 2004. Determination of stable housekeeping genes, differentially regulated target genes and sample integrity: BestKeeper--Excel-based tool using pair-wise correlations. *Biotechnol Lett,* 26**,** 509-15.

Pfeiffer, T., Schuster, S.Bonhoeffer, S. 2001. Cooperation and competition in the evolution of ATP-producing pathways. *Science,* 292**,** 504-7.

Phasukkijwatana, N., Chuenkongkaew, W. L., Suphavilai, R., Luangtrakool, K., Kunhapan, B.Lertrit, P. 2006. Transmission of heteroplasmic G11778A in extensive pedigrees of Thai Leber hereditary optic neuropathy. *J Hum Genet,* 51**,** 1110-7.

Piao, L., Li, Y., Kim, S. J., Byun, H. S., Huang, S. M., Hwang, S. K., Yang, K. J., Park, K. A., Won, M., Hong, J., Hur, G. M., Seok, J. H., Shong, M., Cho, M. H., Brazil, D. P., Hemmings, B. A.Park, J. 2009. Association of LETM1 and MRPL36 contributes to the regulation of mitochondrial ATP production and necrotic cell death. *Cancer Res,* 69**,** 3397-404.

Picca, A., Pesce, V., Fracasso, F., Joseph, A. M., Leeuwenburgh, C.Lezza, A. M. 2013. Aging and calorie restriction oppositely affect mitochondrial biogenesis through TFAM binding at both origins of mitochondrial DNA replication in rat liver. *PLoS One,* 8**,** e74644.

Piccolo, G., Banfi, P., Azan, G., Rizzuto, R., Bisson, R., Sandona, D.Bellomo, G. 1991. Biological markers of oxidative stress in mitochondrial myopathies with progressive external ophthalmoplegia. *J Neurol Sci,* 105**,** 57-60.

Piccolo, G., Focher, F., Verri, A., Spadari, S., Banfi, P., Gerosa, E.Mazzarello, P. 1993. Myoclonus epilepsy and ragged-red fibers: blood mitochondrial DNA heteroplasmy in affected and asymptomatic members of a family. *Acta Neurol Scand,* 88**,** 406-9.

Piechota, J., Tomecki, R., Gewartowski, K., Szczesny, R., Dmochowska, A., Kudla, M., Dybczynska, L., Stepien, P. P.Bartnik, E. 2006. Differential stability of mitochondrial mRNA in HeLa cells. *Acta Biochim Pol,* 53**,** 157-68.

Piko, L.Taylor, K. D. 1987. Amounts of mitochondrial DNA and abundance of some mitochondrial gene transcripts in early mouse embryos. *Dev Biol,* 123**,** 364-74.

Pitceathly, R. D., Rahman, S.Hanna, M. G. 2012. Single deletions in mitochondrial DNA--molecular mechanisms and disease phenotypes in clinical practice. *Neuromuscul Disord,* 22**,** 577-86.

Pohjoismaki, J. L.Goffart, S. 2011. Of circles, forks and humanity: Topological organisation and replication of mammalian mitochondrial DNA. *Bioessays,* 33**,** 290-9.

Popot, J. L.De Vitry, C. 1990. On the microassembly of integral membrane proteins. *Annu Rev Biophys Biophys Chem,* 19**,** 369-403.

Porto, F. B., Mack, G., Sterboul, M. J., Lewin, P., Flament, J., Sahel, J.Dollfus, H. 2001. Isolated late-onset cone-rod dystrophy revealing a familial neurogenic muscle weakness, ataxia, and retinitis pigmentosa syndrome with the T8993G mitochondrial mutation. *Am J Ophthalmol,* 132**,** 935-7.

Poulsen, J. B., Andersen, K. R., Kjaer, K. H., Durand, F., Faou, P., Vestergaard, A. L., Talbo, G. H., Hoogenraad, N., Brodersen, D. E., Justesen, J.Martensen, P. M. 2011. Human 2'-phosphodiesterase localizes to the mitochondrial matrix with a putative function in mitochondrial RNA turnover. *Nucleic Acids Res,* 39**,** 3754-70.

Powelka, A. M., Seth, A., Virbasius, J. V., Kiskinis, E., Nicoloro, S. M., Guilherme, A., Tang, X., Straubhaar, J., Cherniack, A. D., Parker, M. G.Czech, M. P. 2006.

Suppression of oxidative metabolism and mitochondrial biogenesis by the transcriptional corepressor RIP140 in mouse adipocytes. *J Clin Invest,* 116**,** 125-36.

Prezant, T. R., Agapian, J. V., Bohlman, M. C., Bu, X., Oztas, S., Qiu, W. Q., Arnos, K. S., Cortopassi, G. A., Jaber, L., Rotter, J. I.Et Al. 1993. Mitochondrial ribosomal RNA mutation associated with both antibiotic-induced and non-syndromic deafness. *Nat Genet,* 4**,** 289-94.

Pritchard, L.Kell, D. B. 2002. Schemes of flux control in a model of Saccharomyces cerevisiae glycolysis. *Eur J Biochem,* 269**,** 3894-904.

Pruitt, K. D., Tatusova, T., Klimke, W.Maglott, D. R. 2009. NCBI Reference Sequences: current status, policy and new initiatives. *Nucleic Acids Res,* 37**,** D32-6.

Puddu, P., Barboni, P., Mantovani, V., Montagna, P., Cerullo, A., Bragliani, M., Molinotti, C.Caramazza, R. 1993. Retinitis pigmentosa, ataxia, and mental retardation associated with mitochondrial DNA mutation in an Italian family. *Br J Ophthalmol,* 77**,** 84-8.

Puigserver, P., Rhee, J., Lin, J., Wu, Z., Yoon, J. C., Zhang, C. Y., Krauss, S., Mootha, V. K., Lowell, B. B.Spiegelman, B. M. 2001. Cytokine stimulation of energy expenditure through p38 MAP kinase activation of PPARgamma coactivator-1. *Mol Cell,* 8**,** 971-82.

Puigserver, P., Wu, Z., Park, C. W., Graves, R., Wright, M.Spiegelman, B. M. 1998. A cold-inducible coactivator of nuclear receptors linked to adaptive thermogenesis. *Cell,* 92**,** 829-39.

Pyle, A., Taylor, R. W., Durham, S. E., Deschauer, M., Schaefer, A. M., Samuels, D. C.Chinnery, P. F. 2007. Depletion of mitochondrial DNA in leucocytes harbouring the 3243A->G mtDNA mutation. *J Med Genet,* 44**,** 69-74.

Rahman, S., Poulton, J., Marchington, D.Suomalainen, A. 2001. Decrease of 3243 A-->G mtDNA mutation from blood in MELAS syndrome: a longitudinal study. *Am J Hum Genet,* 68**,** 238-40.

Rajasimha, H. K., Chinnery, P. F.Samuels, D. C. 2008. Selection against pathogenic mtDNA mutations in a stem cell population leads to the loss of the 3243A-->G mutation in blood. *Am J Hum Genet,* 82**,** 333-43.

Richter, C., Gogvadze, V., Laffranchi, R., Schlapbach, R., Schweizer, M., Suter, M., Walter, P.Yaffee, M. 1995. Oxidants in mitochondria: from physiology to diseases. *Biochim Biophys Acta,* 1271**,** 67-74.

Ringel, R., Sologub, M., Morozov, Y. I., Litonin, D., Cramer, P.Temiakov, D. 2011. Structure of human mitochondrial RNA polymerase. *Nature,* 478**,** 269-73.

Rizzuto, R., Brini, M., Murgia, M.Pozzan, T. 1993. Microdomains with high Ca2+ close to IP3-sensitive channels that are sensed by neighboring mitochondria. *Science,* 262**,** 744-7.

Robberson, D. L., Kasamatsu, H.Vinograd, J. 1972. Replication of mitochondrial DNA. Circular replicative intermediates in mouse L cells. *Proc Natl Acad Sci U S A,* 69**,** 737-41.

Robinson, B. H., Petrova-Benedict, R., Buncic, J. R.Wallace, D. C. 1992. Nonviability of cells with oxidative defects in galactose medium: a screening test for affected patient fibroblasts. *Biochem Med Metab Biol,* 48**,** 122-6.

Rockl, K. S., Witczak, C. A.Goodyear, L. J. 2008. Signaling mechanisms in skeletal muscle: acute responses and chronic adaptations to exercise. *IUBMB Life,* 60**,** 145-53.

Roger, A. J. 1999. Reconstructing Early Events in Eukaryotic Evolution. *Am Nat,* 154**,** S146-S163.

Roise, D., Theiler, F., Horvath, S. J., Tomich, J. M., Richards, J. H., Allison, D. S.Schatz, G. 1988. Amphiphilicity is essential for mitochondrial presequence function. *EMBO J,* 7**,** 649-53.

Rojo, E. E., Guiard, B., Neupert, W.Stuart, R. A. 1998. Sorting of D-lactate dehydrogenase to the inner membrane of mitochondria. Analysis of topogenic signal and energetic requirements. *J Biol Chem,* 273**,** 8040-7.

Rokas, A. 2008. The origins of multicellularity and the early history of the genetic toolkit for animal development. *Annu Rev Genet,* 42**,** 235-51.

Rorbach, J.Minczuk, M. 2012. The post-transcriptional life of mammalian mitochondrial RNA. *Biochem J,* 444**,** 357-73.

Rorbach, J., Nicholls, T. J.Minczuk, M. 2011. PDE12 removes mitochondrial RNA poly(A) tails and controls translation in human mitochondria. *Nucleic Acids Res,* 39**,** 7750-63.

Rorbach, J., Richter, R., Wessels, H. J., Wydro, M., Pekalski, M., Farhoud, M., Kuhl, I., Gaisne, M., Bonnefoy, N., Smeitink, J. A., Lightowlers, R. N.Chrzanowska-Lightowlers, Z. M. 2008. The human mitochondrial ribosome recycling factor is essential for cell viability. *Nucleic Acids Res,* 36**,** 5787-99.

Rosenberg, M. J., Agarwala, R., Bouffard, G., Davis, J., Fiermonte, G., Hilliard, M. S., Koch, T., Kalikin, L. M., Makalowska, I., Morton, D. H., Petty, E. M., Weber, J. L., Palmieri, F., Kelley, R. I., Schaffer, A. A.Biesecker, L. G. 2002. Mutant deoxynucleotide carrier is associated with congenital microcephaly. *Nat Genet,* 32**,** 175-9.

Ross, O. A., Mccormack, R., Maxwell, L. D., Duguid, R. A., Quinn, D. J., Barnett, Y. A., Rea, I. M., El-Agnaf, O. M., Gibson, J. M., Wallace, A., Middleton, D.Curran, M. D. 2003. mt4216C variant in linkage with the mtDNA TJ cluster may confer a susceptibility to mitochondrial dysfunction resulting in an increased risk of Parkinson's disease in the Irish. *Exp Gerontol,* 38**,** 397-405.

Rossen, L., Norskov, P., Holmstrom, K.Rasmussen, O. F. 1992. Inhibition of PCR by components of food samples, microbial diagnostic assays and DNA-extraction solutions. *Int J Food Microbiol,* 17**,** 37-45.

Rossmanith, W.Holzmann, J. 2009. Processing mitochondrial (t)RNAs: new enzyme, old job. *Cell Cycle,* 8**,** 1650-3.

Rotig, A. 2011. Human diseases with impaired mitochondrial protein synthesis. *Biochim Biophys Acta,* 1807**,** 1198-205.

Rouzier, C., Bannwarth, S., Chaussenot, A., Chevrollier, A., Verschueren, A., Bonello-Palot, N., Fragaki, K., Cano, A., Pouget, J., Pellissier, J. F., Procaccio, V., Chabrol, B.Paquis-Flucklinger, V. 2012. The MFN2 gene is responsible for mitochondrial DNA instability and optic atrophy 'plus' phenotype. *Brain,* 135**,** 23-34.

Rozen, S.Skaletsky, H. 2000. Primer3 on the WWW for general users and for biologist programmers. *Methods Mol Biol,* 132**,** 365-86.

Rubio-Cosials, A., Sidow, J. F., Jimenez-Menendez, N., Fernandez-Millan, P., Montoya, J., Jacobs, H. T., Coll, M., Bernado, P.Sola, M. 2011. Human mitochondrial transcription factor A induces a U-turn structure in the light strand promoter. *Nat Struct Mol Biol,* 18**,** 1281-9.

Rusanen, H., Majamaa, K.Hassinen, I. E. 2000. Increased activities of antioxidant enzymes and decreased ATP concentration in cultured myoblasts with the 3243A-->G mutation in mitochondrial DNA. *Biochim Biophys Acta,* 1500**,** 10-6.

Rusanen, H., Majamaa, K., Tolonen, U., Remes, A. M., Myllyla, R.Hassinen, I. E. 1995. Demyelinating polyneuropathy in a patient with the tRNA(Leu)(UUR) mutation at base pair 3243 of the mitochondrial DNA. *Neurology,* 45**,** 1188-92.

Rutter, J., Winge, D. R.Schiffman, J. D. 2010. Succinate dehydrogenase - Assembly, regulation and role in human disease. *Mitochondrion,* 10**,** 393-401.

Ruzicka, F. J.Beinert, H. 1977. A new iron-sulfur flavoprotein of the respiratory chain. A component of the fatty acid beta oxidation pathway. *J Biol Chem,* 252**,** 8440-5.

Rytinki, M. M.Palvimo, J. J. 2008. SUMOylation modulates the transcription repressor function of RIP140. *J Biol Chem,* 283**,** 11586-95.

Saada, A. 2004. Deoxyribonucleotides and disorders of mitochondrial DNA integrity. *DNA Cell Biol,* 23**,** 797-806.

Saada, A., Shaag, A.Elpeleg, O. 2003. mtDNA depletion myopathy: elucidation of the tissue specificity in the mitochondrial thymidine kinase (TK2) deficiency. *Mol Genet Metab,* 79**,** 1-5.

Saada, A., Shaag, A., Mandel, H., Nevo, Y., Eriksson, S.Elpeleg, O. 2001. Mutant mitochondrial thymidine kinase in mitochondrial DNA depletion myopathy. *Nat Genet,* 29**,** 342-4.

Sabour, D., Arauzo-Bravo, M. J., Hubner, K., Ko, K., Greber, B., Gentile, L., Stehling, M.Scholer, H. R. 2011. Identification of genes specific to mouse primordial germ cells through dynamic global gene expression. *Hum Mol Genet,* 20**,** 115-25.

Sahin, E., Colla, S., Liesa, M., Moslehi, J., Muller, F. L., Guo, M., Cooper, M., Kotton, D., Fabian, A. J., Walkey, C., Maser, R. S., Tonon, G., Foerster, F., Xiong, R., Wang, Y. A., Shukla, S. A., Jaskelioff, M., Martin, E. S., Heffernan, T. P., Protopopov, A., Ivanova, E., Mahoney, J. E., Kost-Alimova, M., Perry, S. R., Bronson, R., Liao, R., Mulligan, R., Shirihai, O. S., Chin, L.Depinho, R. A. 2011. Telomere dysfunction induces metabolic and mitochondrial compromise. *Nature,* 470**,** 359-65.

Saitoh, A., Haas, R. H., Naviaux, R. K., Salva, N. G., Wong, J. K.Spector, S. A. 2008. Impact of nucleoside reverse transcriptase inhibitors on mitochondrial DNA and RNA in human skeletal muscle cells. *Antimicrob Agents Chemother,* 52**,** 2825-30.

Saitou, M., Barton, S. C.Surani, M. A. 2002. A molecular programme for the specification of germ cell fate in mice. *Nature,* 418**,** 293-300.

Sakuta, R., Goto, Y., Horai, S., Ogino, T., Yoshinaga, H., Ohtahara, S.Nonaka, I. 1992. Mitochondrial DNA mutation and Leigh's syndrome. *Ann Neurol,* 32**,** 597-8.

Sallevelt, S. C., Dreesen, J. C., Drusedau, M., Spierts, S., Coonen, E., Van Tienen, F. H., Van Golde, R. J., De Coo, I. F., Geraedts, J. P., De Die-Smulders, C. E.Smeets, H. J. 2013. Preimplantation genetic diagnosis in mitochondrial DNA disorders: challenge and success. *J Med Genet,* 50**,** 125-32.

Samuels, D. C., Wonnapinij, P., Cree, L. M.Chinnery, P. F. 2010. Reassessing evidence for a postnatal mitochondrial genetic bottleneck. *Nat Genet,* 42**,** 471-2; author reply 472-3.

Sanchez, M. I., Mercer, T. R., Davies, S. M., Shearwood, A. M., Nygard, K. K., Richman, T. R., Mattick, J. S., Rackham, O.Filipovska, A. 2011. RNA processing in human mitochondria. *Cell Cycle,* 10**,** 2904-16.

Santorelli, F. M., Shanske, S., Macaya, A., Devivo, D. C.Dimauro, S. 1993. The mutation at nt 8993 of mitochondrial DNA is a common cause of Leigh's syndrome. *Ann Neurol,* 34**,** 827-34.

Scaglia, F.Wong, L. J. 2008. Human mitochondrial transfer RNAs: role of pathogenic mutation in disease. *Muscle Nerve,* 37**,** 150-71.

Scarpulla, R. C. 2008. Transcriptional paradigms in mammalian mitochondrial biogenesis and function. *Physiol Rev,* 88**,** 611-38.

Schaefer, A. M., Mcfarland, R., Blakely, E. L., He, L., Whittaker, R. G., Taylor, R. W., Chinnery, P. F.Turnbull, D. M. 2008. Prevalence of mitochondrial DNA disease in adults. *Ann Neurol,* 63**,** 35-9.

Schafer, E., Dencher, N. A., Vonck, J.Parcej, D. N. 2007. Three-dimensional structure of the respiratory chain supercomplex I1III2IV1 from bovine heart mitochondria. *Biochemistry,* 46**,** 12579-85.

Schafer, E., Seelert, H., Reifschneider, N. H., Krause, F., Dencher, N. A.Vonck, J. 2006. Architecture of active mammalian respiratory chain supercomplexes. *J Biol Chem,* 281**,** 15370-5.

Schagger, H., De Coo, R., Bauer, M. F., Hofmann, S., Godinot, C.Brandt, U. 2004. Significance of respirasomes for the assembly/stability of human respiratory chain complex I. *J Biol Chem,* 279**,** 36349-53.

Schagger, H.Pfeiffer, K. 2000. Supercomplexes in the respiratory chains of yeast and mammalian mitochondria. *EMBO J,* 19**,** 1777-83.

Scheper, G. C., Van Der Klok, T., Van Andel, R. J., Van Berkel, C. G., Sissler, M., Smet, J., Muravina, T. I., Serkov, S. V., Uziel, G., Bugiani, M., Schiffmann, R., Krageloh-Mann, I., Smeitink, J. A., Florentz, C., Van Coster, R., Pronk, J.

C.Van Der Knaap, M. S. 2007. Mitochondrial aspartyl-tRNA synthetase deficiency causes leukoencephalopathy with brain stem and spinal cord involvement and lactate elevation. *Nat Genet,* 39**,** 534-9.

Schleicher, M., Shepherd, B. R., Suarez, Y., Fernandez-Hernando, C., Yu, J., Pan, Y., Acevedo, L. M., Shadel, G. S.Sessa, W. C. 2008. Prohibitin-1 maintains the angiogenic capacity of endothelial cells by regulating mitochondrial function and senescence. *J Cell Biol,* 180**,** 101-12.

Schreiber, S. N., Knutti, D., Brogli, K., Uhlmann, T.Kralli, A. 2003. The transcriptional coactivator PGC-1 regulates the expression and activity of the orphan nuclear receptor estrogen-related receptor alpha (ERRalpha). *J Biol Chem,* 278**,** 9013-8.

Schroeder, A., Mueller, O., Stocker, S., Salowsky, R., Leiber, M., Gassmann, M., Lightfoot, S., Menzel, W., Granzow, M.Ragg, T. 2006. The RIN: an RNA integrity number for assigning integrity values to RNA measurements. *BMC Mol Biol,* 7**,** 3.

Schulz, C., Lytovchenko, O., Melin, J., Chacinska, A., Guiard, B., Neumann, P., Ficner, R., Jahn, O., Schmidt, B.Rehling, P. 2011. Tim50's presequence receptor domain is essential for signal driven transport across the TIM23 complex. *J Cell Biol,* 195**,** 643-56.

Schwartz, M.Vissing, J. 2002. Paternal inheritance of mitochondrial DNA. *N Engl J Med,* 347**,** 576-80.

Scocca, J. R.Shapiro, T. A. 2008. A mitochondrial topoisomerase IA essential for late theta structure resolution in African trypanosomes. *Mol Microbiol,* 67**,** 820-9.

Scott, W., Stevens, J.Binder-Macleod, S. A. 2001. Human skeletal muscle fiber type classifications. *Phys Ther,* 81**,** 1810-6.

Seibel, P., Flierl, A., Kottlors, M.Reichmann, H. 1994. A rapid and sensitive PCR screening method for point mutations associated with mitochondrial encephalomyopathies. *Biochem Biophys Res Commun,* 200**,** 938-42.

Seidel-Rogol, B. L., Mcculloch, V.Shadel, G. S. 2003. Human mitochondrial transcription factor B1 methylates ribosomal RNA at a conserved stem-loop. *Nat Genet,* 33**,** 23-4.

Seidel-Rogol, B. L.Shadel, G. S. 2002. Modulation of mitochondrial transcription in response to mtDNA depletion and repletion in HeLa cells. *Nucleic Acids Res,* 30**,** 1929-34.

Selby, C. P.Sancar, A. 1997. Cockayne syndrome group B protein enhances elongation by RNA polymerase II. *Proc Natl Acad Sci U S A,* 94**,** 11205-9.

Shadel, G. S. 2004. Coupling the mitochondrial transcription machinery to human disease. *Trends Genet,* 20**,** 513-9.

Shang, J.Clayton, D. A. 1994. Human mitochondrial transcription termination exhibits RNA polymerase independence and biased bipolarity in vitro. *J Biol Chem,* 269**,** 29112-20.

Sharma, M. R., Koc, E. C., Datta, P. P., Booth, T. M., Spremulli, L. L.Agrawal, R. K. 2003. Structure of the mammalian mitochondrial ribosome reveals an expanded functional role for its component proteins. *Cell,* 115**,** 97-108.

Sharma, N. K., Reyes, A., Green, P., Caron, M. J., Bonini, M. G., Gordon, D. M., Holt, I. J.Santos, J. H. 2012. Human telomerase acts as a hTR-independent reverse transcriptase in mitochondria. *Nucleic Acids Res,* 40**,** 712-25.

Shen, W., Wei, Y., Dauk, M., Tan, Y., Taylor, D. C., Selvaraj, G.Zou, J. 2006. Involvement of a glycerol-3-phosphate dehydrogenase in modulating the NADH/NAD+ ratio provides evidence of a mitochondrial glycerol-3-phosphate shuttle in Arabidopsis. *Plant Cell,* 18**,** 422-41.

Shoffner, J. M., Fernhoff, P. M., Krawiecki, N. S., Caplan, D. B., Holt, P. J., Koontz, D. A., Takei, Y., Newman, N. J., Ortiz, R. G., Polak, M.Et Al. 1992. Subacute necrotizing encephalopathy: oxidative phosphorylation defects and the ATPase 6 point mutation. *Neurology,* 42**,** 2168-74.

Shoffner, J. M., Lott, M. T., Lezza, A. M., Seibel, P., Ballinger, S. W.Wallace, D. C. 1990. Myoclonic epilepsy and ragged-red fiber disease (MERRF) is associated with a mitochondrial DNA tRNA(Lys) mutation. *Cell,* 61**,** 931-7.

Shoffner, J. M., Lott, M. T., Voljavec, A. S., Soueidan, S. A., Costigan, D. A.Wallace, D. C. 1989. Spontaneous Kearns-Sayre/chronic external ophthalmoplegia plus syndrome associated with a mitochondrial DNA deletion: a slip-replication model and metabolic therapy. *Proc Natl Acad Sci U S A,* 86**,** 7952-6.

Shoubridge, E. A. 2001. Cytochrome c oxidase deficiency. *Am J Med Genet,* 106**,** 46-52.

Shutt, T. E., Lodeiro, M. F., Cotney, J., Cameron, C. E.Shadel, G. S. 2010. Core human mitochondrial transcription apparatus is a regulated two-component system in vitro. *Proc Natl Acad Sci U S A,* 107**,** 12133-8.

Sicheritz-Ponten, T., Kurland, C. G.Andersson, S. G. 1998. A phylogenetic analysis of the cytochrome b and cytochrome c oxidase I genes supports an origin of mitochondria from within the Rickettsiaceae. *Biochim Biophys Acta,* 1365**,** 545-51.

Silvestri, G., Ciafaloni, E., Santorelli, F. M., Shanske, S., Servidei, S., Graf, W. D., Sumi, M.Dimauro, S. 1993. Clinical features associated with the A-->G transition at nucleotide 8344 of mtDNA ("MERRF mutation"). *Neurology,* 43**,** 1200-6.

Simon, D. K., Pulst, S. M., Sutton, J. P., Browne, S. E., Beal, M. F.Johns, D. R. 1999. Familial multisystem degeneration with parkinsonism associated with the 11778 mitochondrial DNA mutation. *Neurology,* 53**,** 1787-93.

Sirrenberg, C., Bauer, M. F., Guiard, B., Neupert, W.Brunner, M. 1996. Import of carrier proteins into the mitochondrial inner membrane mediated by Tim22. *Nature,* 384**,** 582-5.

Smits, P., Mattijssen, S., Morava, E., Van Den Brand, M., Van Den Brandt, F., Wijburg, F., Pruijn, G., Smeitink, J., Nijtmans, L., Rodenburg, R.Van Den Heuvel, L. 2010a. Functional consequences of mitochondrial tRNA Trp and tRNA Arg mutations causing combined OXPHOS defects. *Eur J Hum Genet,* 18**,** 324-9.

Smits, P., Smeitink, J.Van Den Heuvel, L. 2010b. Mitochondrial translation and beyond: processes implicated in combined oxidative phosphorylation deficiencies. *J Biomed Biotechnol,* 2010**,** 737385.

Smits, P., Smeitink, J. A., Van Den Heuvel, L. P., Huynen, M. A.Ettema, T. J. 2007. Reconstructing the evolution of the mitochondrial ribosomal proteome. *Nucleic Acids Res,* 35**,** 4686-703.

Soleimanpour-Lichaei, H. R., Kuhl, I., Gaisne, M., Passos, J. F., Wydro, M., Rorbach, J., Temperley, R., Bonnefoy, N., Tate, W., Lightowlers, R.Chrzanowska-Lightowlers, Z. 2007. mtRF1a is a human mitochondrial translation release factor decoding the major termination codons UAA and UAG. *Mol Cell,* 27**,** 745-57.

Sologub, M., Litonin, D., Anikin, M., Mustaev, A.Temiakov, D. 2009. TFB2 is a transient component of the catalytic site of the human mitochondrial RNA polymerase. *Cell,* 139**,** 934-44.

Sparaco, M., Rosoklija, G., Tanji, K., Sciacco, M., Latov, N., Dimauro, S.Bonilla, E. 1993. Immunolocalization of heat shock proteins in ragged-red fibers of patients with mitochondrial encephalomyopathies. *Neuromuscul Disord,* 3**,** 71-6.

Spelbrink, J. N., Li, F. Y., Tiranti, V., Nikali, K., Yuan, Q. P., Tariq, M., Wanrooij, S., Garrido, N., Comi, G., Morandi, L., Santoro, L., Toscano, A., Fabrizi, G. M., Somer, H., Croxen, R., Beeson, D., Poulton, J., Suomalainen, A., Jacobs, H. T., Zeviani, M.Larsson, C. 2001. Human mitochondrial DNA deletions associated with mutations in the gene encoding Twinkle, a phage T7 gene 4-like protein localized in mitochondria. *Nat Genet,* 28**,** 223-31.

Spelbrink, J. N., Toivonen, J. M., Hakkaart, G. A., Kurkela, J. M., Cooper, H. M., Lehtinen, S. K., Lecrenier, N., Back, J. W., Speijer, D., Foury, F.Jacobs, H. T. 2000. In vivo functional analysis of the human mitochondrial DNA polymerase POLG expressed in cultured human cells. *J Biol Chem,* 275**,** 24818-28.

Spierings, D., Mcstay, G., Saleh, M., Bender, C., Chipuk, J., Maurer, U.Green, D. R. 2005. Connected to death: the (unexpurgated) mitochondrial pathway of apoptosis. *Science,* 310**,** 66-7.

Spinazzola, A., Viscomi, C., Fernandez-Vizarra, E., Carrara, F., D'adamo, P., Calvo, S., Marsano, R. M., Donnini, C., Weiher, H., Strisciuglio, P., Parini, R., Sarzi, E., Chan, A., Dimauro, S., Rotig, A., Gasparini, P., Ferrero, I., Mootha, V. K., Tiranti, V.Zeviani, M. 2006. MPV17 encodes an inner mitochondrial membrane protein and is mutated in infantile hepatic mitochondrial DNA depletion. *Nat Genet,* 38**,** 570-5.

Srivastava, S., Diaz, F., Iommarini, L., Aure, K., Lombes, A.Moraes, C. T. 2009. PGC-1alpha/beta induced expression partially compensates for respiratory chain defects in cells from patients with mitochondrial disorders. *Hum Mol Genet,* 18**,** 1805-12.

Steffann, J., Gigarel, N., Corcos, J., Bonniere, M., Encha-Razavi, F., Sinico, M., Prevot, S., Dumez, Y., Yamgnane, A., Frydman, R., Munnich, A.Bonnefont, J. P. 2007. Stability of the m.8993T->G mtDNA mutation load during human embryofetal development has implications for the feasibility of prenatal diagnosis in NARP syndrome. *J Med Genet,* 44**,** 664-9.

Stewart, J. B., Freyer, C., Elson, J. L., Wredenberg, A., Cansu, Z., Trifunovic, A.Larsson, N. G. 2008. Strong purifying selection in transmission of mammalian mitochondrial DNA. *PLoS Biol,* 6**,** e10.

Stewart, J. D. 2008. *Nuclear mitochondrial interactions in human disease.* Doctor of Philosophy, Newcastle University.

Stewart, J. D., Schoeler, S., Sitarz, K. S., Horvath, R., Hallmann, K., Pyle, A., Yu-Wai-Man, P., Taylor, R. W., Samuels, D. C., Kunz, W. S.Chinnery, P. F. 2011. POLG mutations cause decreased mitochondrial DNA repopulation rates following induced depletion in human fibroblasts. *Biochim Biophys Acta,* 1812**,** 321-5.

Storici, F., Bebenek, K., Kunkel, T. A., Gordenin, D. A.Resnick, M. A. 2007. RNA-templated DNA repair. *Nature,* 447**,** 338-41.

Stuart, J. A.Brown, M. F. 2006. Mitochondrial DNA maintenance and bioenergetics. *Biochim Biophys Acta,* 1757**,** 79-89.

Stuart, R. 2002. Insertion of proteins into the inner membrane of mitochondria: the role of the Oxa1 complex. *Biochim Biophys Acta,* 1592**,** 79-87.

Sugimoto, M.Abe, K. 2007. X chromosome reactivation initiates in nascent primordial germ cells in mice. *PLoS Genet,* 3**,** e116.

Sun, F., Huo, X., Zhai, Y., Wang, A., Xu, J., Su, D., Bartlam, M.Rao, Z. 2005. Crystal structure of mitochondrial respiratory membrane protein complex II. *Cell,* 121**,** 1043-57.

Suomalainen, A.Kaukonen, J. 2001. Diseases caused by nuclear genes affecting mtDNA stability. *Am J Med Genet,* 106**,** 53-61.

Suski, C.Marians, K. J. 2008. Resolution of converging replication forks by RecQ and topoisomerase III. *Mol Cell,* 30**,** 779-89.

Sutovsky, P., Moreno, R. D., Ramalho-Santos, J., Dominko, T., Simerly, C.Schatten, G. 1999. Ubiquitin tag for sperm mitochondria. *Nature,* 402**,** 371-2.

Suzuki, T., Nagao, A.Suzuki, T. 2011. Human mitochondrial tRNAs: biogenesis, function, structural aspects, and diseases. *Annu Rev Genet,* 45**,** 299-329.

Suzuki, Y., Holmes, J. B., Cerritelli, S. M., Sakhuja, K., Minczuk, M., Holt, I. J.Crouch, R. J. 2010. An upstream open reading frame and the context of the two AUG codons affect the abundance of mitochondrial and nuclear RNase H1. *Mol Cell Biol,* 30**,** 5123-34.

Sweeney, M. G., Davis, M. B., Lashwood, A., Brockington, M., Toscano, A.Harding, A. E. 1992. Evidence against an X-linked locus close to DXS7 determining visual loss susceptibility in British and Italian families with Leber hereditary optic neuropathy. *Am J Hum Genet,* 51**,** 741-8.

Szczesny, R. J., Borowski, L. S., Brzezniak, L. K., Dmochowska, A., Gewartowski, K., Bartnik, E.Stepien, P. P. 2010. Human mitochondrial RNA turnover caught in flagranti: involvement of hSuv3p helicase in RNA surveillance. *Nucleic Acids Res,* 38**,** 279-98.

T Hart, L. M., Jansen, J. J., Lemkes, H. H., De Knijff, P.Maassen, J. A. 1996. Heteroplasmy levels of a mitochondrial gene mutation associated with diabetes mellitus decrease in leucocyte DNA upon aging. *Hum Mutat,* 7**,** 193-7.

Takaku, H., Minagawa, A., Takagi, M.Nashimoto, M. 2003. A candidate prostate cancer susceptibility gene encodes tRNA 3' processing endoribonuclease. *Nucleic Acids Res,* 31**,** 2272-8.

Takeuchi, N., Kawakami, M., Ueda, T., Spremulli, L. L.Watanabe, K. 1997. Mitochondrial methionyl-tRNA transformylase from bovine liver. *Nucleic Acids Symp Ser***,** 195-6.

Tanaka, A., Kiyosawa, M., Mashima, Y.Tokoro, T. 1998. A family with Leber's hereditary optic neuropathy with mitochondrial DNA heteroplasmy related to disease expression. *J Neuroophthalmol,* 18**,** 81-3.

Tanaka, T., Yamamoto, J., Iwasaki, S., Asaba, H., Hamura, H., Ikeda, Y., Watanabe, M., Magoori, K., Ioka, R. X., Tachibana, K., Watanabe, Y., Uchiyama, Y., Sumi, K., Iguchi, H., Ito, S., Doi, T., Hamakubo, T., Naito, M., Auwerx, J., Yanagisawa, M., Kodama, T.Sakai, J. 2003. Activation of peroxisome proliferator-activated receptor delta induces fatty acid beta-oxidation in skeletal muscle and attenuates metabolic syndrome. *Proc Natl Acad Sci U S A,* 100**,** 15924-9.

Tangrea, M. A., Mukherjee, S., Gao, B., Markey, S. P., Du, Q., Armani, M., Kreitman, M. S., Rosenberg, A. M., Wallis, B. S., Eberle, F. C., Duncan, F. C., Hanson, J. C., Chuaqui, R. F., Rodriguez-Canales, J.Emmert-Buck, M. R. 2011. Effect of immunohistochemistry on molecular analysis of tissue samples: implications for microdissection technologies. *J Histochem Cytochem,* 59**,** 591-600.

Tatuch, Y., Christodoulou, J., Feigenbaum, A., Clarke, J. T., Wherret, J., Smith, C., Rudd, N., Petrova-Benedict, R.Robinson, B. H. 1992. Heteroplasmic mtDNA mutation (T----G) at 8993 can cause Leigh disease when the percentage of abnormal mtDNA is high. *Am J Hum Genet,* 50**,** 852-8.

Taylor, R. W., Mcdonnell, M. T., Blakely, E. L., Chinnery, P. F., Taylor, G. A., Howell, N., Zeviani, M., Briem, E., Carrara, F.Turnbull, D. M. 2003. Genotypes from patients indicate no paternal mitochondrial DNA contribution. *Ann Neurol,* 54**,** 521-4.

Taylor, R. W., Schaefer, A. M., Barron, M. J., Mcfarland, R.Turnbull, D. M. 2004. The diagnosis of mitochondrial muscle disease. *Neuromuscul Disord,* 14**,** 237-45.

Taylor, R. W.Turnbull, D. M. 2005. Mitochondrial DNA mutations in human disease. *Nat Rev Genet,* 6**,** 389-402.

Temperley, R., Richter, R., Dennerlein, S., Lightowlers, R. N.Chrzanowska-Lightowlers, Z. M. 2010. Hungry codons promote frameshifting in human mitochondrial ribosomes. *Science,* 327**,** 301.

Teyssier, C., Ma, H., Emter, R., Kralli, A.Stallcup, M. R. 2005. Activation of nuclear receptor coactivator PGC-1alpha by arginine methylation. *Genes Dev,* 19**,** 1466-73.

Thundathil, J., Filion, F.Smith, L. C. 2005. Molecular control of mitochondrial function in preimplantation mouse embryos. *Mol Reprod Dev,* 71**,** 405-13.

Tielens, A. G., Rotte, C., Van Hellemond, J. J.Martin, W. 2002. Mitochondria as we don't know them. *Trends Biochem Sci,* 27**,** 564-72.

Timmis, J. N., Ayliffe, M. A., Huang, C. Y.Martin, W. 2004. Endosymbiotic gene transfer: organelle genomes forge eukaryotic chromosomes. *Nat Rev Genet,* 5**,** 123-35.

Tiranti, V., Hoertnagel, K., Carrozzo, R., Galimberti, C., Munaro, M., Granatiero, M., Zelante, L., Gasparini, P., Marzella, R., Rocchi, M., Bayona-Bafaluy, M. P., Enriquez, J. A., Uziel, G., Bertini, E., Dionisi-Vici, C., Franco, B., Meitinger, T.Zeviani, M. 1998. Mutations of SURF-1 in Leigh disease associated with cytochrome c oxidase deficiency. *Am J Hum Genet,* 63**,** 1609-21.

Tiranti, V., Savoia, A., Forti, F., D'apolito, M. F., Centra, M., Rocchi, M.Zeviani, M. 1997. Identification of the gene encoding the human mitochondrial RNA polymerase (h-mtRPOL) by cyberscreening of the Expressed Sequence Tags database. *Hum Mol Genet,* 6**,** 615-25.

Tokunaga, M., Mita, S., Murakami, T., Kumamoto, T., Uchino, M., Nonaka, I.Ando, M. 1994. Single muscle fiber analysis of mitochondrial myopathy, encephalopathy, lactic acidosis, and stroke-like episodes (MELAS). *Ann Neurol,* 35**,** 413-9.

Tomecki, R., Dmochowska, A., Gewartowski, K., Dziembowski, A.Stepien, P. P. 2004. Identification of a novel human nuclear-encoded mitochondrial poly(A) polymerase. *Nucleic Acids Res,* 32**,** 6001-14.

Tondera, D., Grandemange, S., Jourdain, A., Karbowski, M., Mattenberger, Y., Herzig, S., Da Cruz, S., Clerc, P., Raschke, I., Merkwirth, C., Ehses, S., Krause, F., Chan, D. C., Alexander, C., Bauer, C., Youle, R., Langer, T.Martinou, J. C. 2009. SLP-2 is required for stress-induced mitochondrial hyperfusion. *EMBO J,* 28**,** 1589-600.

Torroni, A., Achilli, A., Macaulay, V., Richards, M.Bandelt, H. J. 2006. Harvesting the fruit of the human mtDNA tree. *Trends Genet,* 22**,** 339-45.

Torroni, A., Huoponen, K., Francalacci, P., Petrozzi, M., Morelli, L., Scozzari, R., Obinu, D., Savontaus, M. L.Wallace, D. C. 1996. Classification of European mtDNAs from an analysis of three European populations. *Genetics,* 144**,** 1835-50.

Tovar, J., Fischer, A.Clark, C. G. 1999. The mitosome, a novel organelle related to mitochondria in the amitochondrial parasite Entamoeba histolytica. *Mol Microbiol,* 32**,** 1013-21.

Tovar, J., Leon-Avila, G., Sanchez, L. B., Sutak, R., Tachezy, J., Van Der Giezen, M., Hernandez, M., Muller, M.Lucocq, J. M. 2003. Mitochondrial remnant organelles of Giardia function in iron-sulphur protein maturation. *Nature,* 426**,** 172-6.

Toyooka, Y., Tsunekawa, N., Takahashi, Y., Matsui, Y., Satoh, M.Noce, T. 2000. Expression and intracellular localization of mouse Vasa-homologue protein during germ cell development. *Mech Dev,* 93**,** 139-49.

Traff, J., Holme, E., Ekbom, K.Nilsson, B. Y. 1995. Ekbom's syndrome of photomyoclonus, cerebellar ataxia and cervical lipoma is associated with the tRNA(Lys) A8344G mutation in mitochondrial DNA. *Acta Neurol Scand,* 92**,** 394-7.

Tranebjaerg, L., Hamel, B. C., Gabreels, F. J., Renier, W. O.Van Ghelue, M. 2000. A de novo missense mutation in a critical domain of the X-linked DDP gene causes the typical deafness-dystonia-optic atrophy syndrome. *Eur J Hum Genet,* 8**,** 464-7.

Trifunovic, A., Wredenberg, A., Falkenberg, M., Spelbrink, J. N., Rovio, A. T., Bruder, C. E., Bohlooly, Y. M., Gidlof, S., Oldfors, A., Wibom, R., Tornell, J., Jacobs, H. T.Larsson, N. G. 2004. Premature ageing in mice expressing defective mitochondrial DNA polymerase. *Nature,* 429**,** 417-23.

Tsuboi, M., Morita, H., Nozaki, Y., Akama, K., Ueda, T., Ito, K., Nierhaus, K. H.Takeuchi, N. 2009. EF-G2mt is an exclusive recycling factor in mammalian mitochondrial protein synthesis. *Mol Cell,* 35**,** 502-10.

Tsukihara, T., Aoyama, H., Yamashita, E., Tomizaki, T., Yamaguchi, H., Shinzawa-Itoh, K., Nakashima, R., Yaono, R.Yoshikawa, S. 1995. Structures of metal sites of oxidized bovine heart cytochrome c oxidase at 2.8 A. *Science,* 269**,** 1069-74.

Tulinius, M. H., Houshmand, M., Larsson, N. G., Holme, E., Oldfors, A., Holmberg, E.Wahlstrom, J. 1995. De novo mutation in the mitochondrial ATP synthase subunit 6 gene (T8993G) with rapid segregation resulting in Leigh syndrome in the offspring. *Hum Genet,* 96**,** 290-4.

Twig, G., Elorza, A., Molina, A. J., Mohamed, H., Wikstrom, J. D., Walzer, G., Stiles, L., Haigh, S. E., Katz, S., Las, G., Alroy, J., Wu, M., Py, B. F., Yuan, J., Deeney, J. T., Corkey, B. E.Shirihai, O. S. 2008. Fission and selective fusion govern mitochondrial segregation and elimination by autophagy. *EMBO J,* 27**,** 433-46.

Tyynismaa, H., Sembongi, H., Bokori-Brown, M., Granycome, C., Ashley, N., Poulton, J., Jalanko, A., Spelbrink, J. N., Holt, I. J.Suomalainen, A. 2004. Twinkle helicase is essential for mtDNA maintenance and regulates mtDNA copy number. *Hum Mol Genet,* 13**,** 3219-27.

Uusimaa, J., Moilanen, J. S., Vainionpaa, L., Tapanainen, P., Lindholm, P., Nuutinen, M., Lopponen, T., Maki-Torkko, E., Rantala, H.Majamaa, K. 2007. Prevalence, segregation, and phenotype of the mitochondrial DNA 3243A>G mutation in children. *Ann Neurol,* 62**,** 278-87.

Uziel, G., Moroni, I., Lamantea, E., Fratta, G. M., Ciceri, E., Carrara, F.Zeviani, M. 1997. Mitochondrial disease associated with the T8993G mutation of the mitochondrial ATPase 6 gene: a clinical, biochemical, and molecular study in six families. *J Neurol Neurosurg Psychiatry,* 63**,** 16-22.

Uzumcu, M.Zachow, R. 2007. Developmental exposure to environmental endocrine disruptors: consequences within the ovary and on female reproductive function. *Reprod Toxicol,* 23**,** 337-52.

Valente, L., Tiranti, V., Marsano, R. M., Malfatti, E., Fernandez-Vizarra, E., Donnini, C., Mereghetti, P., De Gioia, L., Burlina, A., Castellan, C., Comi, G. P., Savasta, S., Ferrero, I.Zeviani, M. 2007. Infantile encephalopathy and defective mitochondrial DNA translation in patients with mutations of mitochondrial elongation factors EFG1 and EFTu. *Am J Hum Genet,* 80**,** 44-58.

Valerio, A., Bertolotti, P., Delbarba, A., Perego, C., Dossena, M., Ragni, M., Spano, P., Carruba, M. O., De Simoni, M. G.Nisoli, E. 2011. Glycogen synthase kinase-3 inhibition reduces ischemic cerebral damage, restores impaired mitochondrial biogenesis and prevents ROS production. *J Neurochem,* 116**,** 1148-59.

Valnot, I., Osmond, S., Gigarel, N., Mehaye, B., Amiel, J., Cormier-Daire, V., Munnich, A., Bonnefont, J. P., Rustin, P.Rotig, A. 2000. Mutations of the SCO1 gene in mitochondrial cytochrome c oxidase deficiency with neonatal-onset hepatic failure and encephalopathy. *Am J Hum Genet,* 67**,** 1104-9.

Van De Glind, G., De Vries, M., Rodenburg, R., Hol, F., Smeitink, J.Morava, E. 2007. Resting muscle pain as the first clinical symptom in children carrying the MTTK A8344G mutation. *Eur J Paediatr Neurol,* 11**,** 243-6.

Van Der Walt, J. M., Dementieva, Y. A., Martin, E. R., Scott, W. K., Nicodemus, K. K., Kroner, C. C., Welsh-Bohmer, K. A., Saunders, A. M., Roses, A. D., Small, G. W., Schmechel, D. E., Murali Doraiswamy, P., Gilbert, J. R., Haines, J. L., Vance, J. M.Pericak-Vance, M. A. 2004. Analysis of European mitochondrial haplogroups with Alzheimer disease risk. *Neurosci Lett,* 365**,** 28-32.

Van Der Walt, J. M., Nicodemus, K. K., Martin, E. R., Scott, W. K., Nance, M. A., Watts, R. L., Hubble, J. P., Haines, J. L., Koller, W. C., Lyons, K., Pahwa, R., Stern, M. B., Colcher, A., Hiner, B. C., Jankovic, J., Ondo, W. G., Allen, F. H., Jr., Goetz, C. G., Small, G. W., Mastaglia, F., Stajich, J. M., Mclaurin, A. C., Middleton, L. T., Scott, B. L., Schmechel, D. E., Pericak-Vance, M. A.Vance, J. M. 2003. Mitochondrial polymorphisms significantly reduce the risk of Parkinson disease. *Am J Hum Genet,* 72**,** 804-11.

Van Eijsden, R. G., Eijssen, L. M., Lindsey, P. J., Van Den Burg, C. M., De Wit, L. E., Rubio-Gozalbo, M. E., De Die, C. E., Ayoubi, T., Sluiter, W., De Coo, I. F.Smeets, H. J. 2008. Termination of damaged protein repair defines the occurrence of symptoms in carriers of the m.3243A > G tRNA(Leu) mutation. *J Med Genet,* 45**,** 525-34.

Van Goethem, G., Dermaut, B., Lofgren, A., Martin, J. J.Van Broeckhoven, C. 2001. Mutation of POLG is associated with progressive external ophthalmoplegia characterized by mtDNA deletions. *Nat Genet,* 28**,** 211-2.

Van Oven, M.Kayser, M. 2009. Updated comprehensive phylogenetic tree of global human mitochondrial DNA variation. *Hum Mutat,* 30**,** E386-94.

Van Remmen, H., Ikeno, Y., Hamilton, M., Pahlavani, M., Wolf, N., Thorpe, S. R., Alderson, N. L., Baynes, J. W., Epstein, C. J., Huang, T. T., Nelson, J., Strong, R.Richardson, A. 2003. Life-long reduction in MnSOD activity results in increased DNA damage and higher incidence of cancer but does not accelerate aging. *Physiol Genomics,* 16**,** 29-37.

Van Tienen, F. H., Lindsey, P. J., Van Der Kallen, C. J.Smeets, H. J. 2010. Prolonged Nrf1 overexpression triggers adipocyte inflammation and insulin resistance. *J Cell Biochem,* 111**,** 1575-85.

Van Tuyle, G. C.Pavco, P. A. 1985. The rat liver mitochondrial DNA-protein complex: displaced single strands of replicative intermediates are protein coated. *J Cell Biol,* 100**,** 251-7.

Vattemi, G., Mechref, Y., Marini, M., Tonin, P., Minuz, P., Grigoli, L., Guglielmi, V., Klouckova, I., Chiamulera, C., Meneguzzi, A., Di Chio, M., Tedesco, V., Lovato, L., Degan, M., Arcaro, G., Lechi, A., Novotny, M. V.Tomelleri, G. 2011. Increased protein nitration in mitochondrial diseases: evidence for vessel wall involvement. *Mol Cell Proteomics,* 10**,** M110 002964.

Vawter, M. P., Tomita, H., Meng, F., Bolstad, B., Li, J., Evans, S., Choudary, P., Atz, M., Shao, L., Neal, C., Walsh, D. M., Burmeister, M., Speed, T., Myers, R., Jones, E. G., Watson, S. J., Akil, H.Bunney, W. E. 2006. Mitochondrial-related gene expression changes are sensitive to agonal-pH state: implications for brain disorders. *Mol Psychiatry,* 11**,** 615, 663-79.

Vercauteren, K., Gleyzer, N.Scarpulla, R. C. 2008. PGC-1-related coactivator complexes with HCF-1 and NRF-2beta in mediating NRF-2(GABP)-dependent respiratory gene expression. *J Biol Chem,* 283**,** 12102-11.

Vergnolle, M. A., Baud, C., Golovanov, A. P., Alcock, F., Luciano, P., Lian, L. Y.Tokatlidis, K. 2005. Distinct domains of small Tims involved in subunit interaction and substrate recognition. *J Mol Biol,* 351**,** 839-49.

Vermeulen, J., De Preter, K., Lefever, S., Nuytens, J., De Vloed, F., Derveaux, S., Hellemans, J., Speleman, F.Vandesompele, J. 2011. Measurable impact of RNA quality on gene expression results from quantitative PCR. *Nucleic Acids Res,* 39**,** e63.

Vilarinho, L., Santorelli, F. M., Rosas, M. J., Tavares, C., Melo-Pires, M.Dimauro, S. 1997. The mitochondrial A3243G mutation presenting as severe cardiomyopathy. *J Med Genet,* 34**,** 607-9.

Virbasius, C. A., Virbasius, J. V.Scarpulla, R. C. 1993a. NRF-1, an activator involved in nuclear-mitochondrial interactions, utilizes a new DNA-binding domain conserved in a family of developmental regulators. *Genes Dev,* 7**,** 2431-45.

Virbasius, J. V., Virbasius, C. A.Scarpulla, R. C. 1993b. Identity of GABP with NRF-2, a multisubunit activator of cytochrome oxidase expression, reveals a cellular role for an ETS domain activator of viral promoters. *Genes Dev,* 7**,** 380-92.

Visch, H. J., Rutter, G. A., Koopman, W. J., Koenderink, J. B., Verkaart, S., De Groot, T., Varadi, A., Mitchell, K. J., Van Den Heuvel, L. P., Smeitink, J. A.Willems, P. H. 2004. Inhibition of mitochondrial Na+-Ca2+ exchange restores agonist-induced ATP production and Ca2+ handling in human complex I deficiency. *J Biol Chem,* 279**,** 40328-36.

Vogel, R. O., Janssen, R. J., Ugalde, C., Grovenstein, M., Huijbens, R. J., Visch, H. J., Van Den Heuvel, L. P., Willems, P. H., Zeviani, M., Smeitink, J. A.Nijtmans, L.

G. 2005. Human mitochondrial complex I assembly is mediated by NDUFAF1. *FEBS J,* 272**,** 5317-26.

Vogtle, F. N., Wortelkamp, S., Zahedi, R. P., Becker, D., Leidhold, C., Gevaert, K., Kellermann, J., Voos, W., Sickmann, A., Pfanner, N.Meisinger, C. 2009. Global analysis of the mitochondrial N-proteome identifies a processing peptidase critical for protein stability. *Cell,* 139**,** 428-39.

Volod'ko, N. V., L'vova M, A., Starikovskaia, E. B., Derbeneva, O. A., Bychkov, I., Mikhailovskaia, I. E., Pogozheva, I. V., Fedotov, F. F., Soyan, G. V., Procaccio, V., Wallace, D. C.Sukernik, R. I. 2006. [Spectrum of pathogenic mtDNA mutations in Leber hereditary optic neuropathy families from Siberia]. *Genetika,* 42**,** 89-97.

Von Heijne, G. 1986. Why mitochondria need a genome. *FEBS Lett,* 198**,** 1-4.

Voos, W.Rottgers, K. 2002. Molecular chaperones as essential mediators of mitochondrial biogenesis. *Biochim Biophys Acta,* 1592**,** 51-62.

Wai, T., Teoli, D.Shoubridge, E. A. 2008. The mitochondrial DNA genetic bottleneck results from replication of a subpopulation of genomes. *Nat Genet,* 40**,** 1484-8.

Walker, U. A.Schon, E. A. 1998. Neurotrophin-4 is up-regulated in ragged-red fibers associated with pathogenic mitochondrial DNA mutations. *Ann Neurol,* 43**,** 536-40.

Wallace, D. C., Singh, G., Lott, M. T., Hodge, J. A., Schurr, T. G., Lezza, A. M., Elsas, L. J., 2ndNikoskelainen, E. K. 1988. Mitochondrial DNA mutation associated with Leber's hereditary optic neuropathy. *Science,* 242**,** 1427-30.

Wanders, R. J., Ruiter, J. P., L, I. J., Waterham, H. R.Houten, S. M. 2010. The enzymology of mitochondrial fatty acid beta-oxidation and its application to follow-up analysis of positive neonatal screening results. *J Inherit Metab Dis,* 33**,** 479-94.

Wang, C., Li, Z., Lu, Y., Du, R., Katiyar, S., Yang, J., Fu, M., Leader, J. E., Quong, A., Novikoff, P. M.Pestell, R. G. 2006. Cyclin D1 repression of nuclear respiratory factor 1 integrates nuclear DNA synthesis and mitochondrial function. *Proc Natl Acad Sci U S A,* 103**,** 11567-72.

Wang, J. C. 2002. Cellular roles of DNA topoisomerases: a molecular perspective. *Nat Rev Mol Cell Biol,* 3**,** 430-40.

Wang, Y.Bogenhagen, D. F. 2006. Human mitochondrial DNA nucleoids are linked to protein folding machinery and metabolic enzymes at the mitochondrial inner membrane. *J Biol Chem,* 281**,** 25791-802.

Wang, Z. G., White, P. S.Ackerman, S. H. 2001. Atp11p and Atp12p are assembly factors for the F(1)-ATPase in human mitochondria. *J Biol Chem,* 276**,** 30773-8.

Wani, A. A., Rangrez, A. Y., Kumar, H., Bapat, S. A., Suresh, C. G., Barnabas, S., Patole, M. S.Shouche, Y. S. 2008. Analysis of reactive oxygen species and antioxidant defenses in complex I deficient patients revealed a specific increase in superoxide dismutase activity. *Free Radic Res,* 42**,** 415-27.

Wanrooij, P. H., Uhler, J. P., Simonsson, T., Falkenberg, M.Gustafsson, C. M. 2010. G-quadruplex structures in RNA stimulate mitochondrial transcription termination and primer formation. *Proc Natl Acad Sci U S A,* 107**,** 16072-7.

Wanrooij, S., Fuste, J. M., Farge, G., Shi, Y., Gustafsson, C. M.Falkenberg, M. 2008. Human mitochondrial RNA polymerase primes lagging-strand DNA synthesis in vitro. *Proc Natl Acad Sci U S A,* 105**,** 11122-7.

Wanrooij, S., Goffart, S., Pohjoismaki, J. L., Yasukawa, T.Spelbrink, J. N. 2007. Expression of catalytic mutants of the mtDNA helicase Twinkle and polymerase POLG causes distinct replication stalling phenotypes. *Nucleic Acids Res,* 35**,** 3238-51.

Watmough, N. J.Frerman, F. E. 2010. The electron transfer flavoprotein: ubiquinone oxidoreductases. *Biochim Biophys Acta,* 1797**,** 1910-6.

Weidner, U., Geier, S., Ptock, A., Friedrich, T., Leif, H.Weiss, H. 1993. The gene locus of the proton-translocating NADH: ubiquinone oxidoreductase in Escherichia coli. Organization of the 14 genes and relationship between the derived proteins and subunits of mitochondrial complex I. *J Mol Biol,* 233**,** 109-22.

Wenz, T., Diaz, F., Hernandez, D.Moraes, C. T. 2009. Endurance exercise is protective for mice with mitochondrial myopathy. *J Appl Physiol,* 106**,** 1712-9.

Wenz, T., Diaz, F., Spiegelman, B. M.Moraes, C. T. 2008. Activation of the PPAR/PGC-1alpha pathway prevents a bioenergetic deficit and effectively improves a mitochondrial myopathy phenotype. *Cell Metab,* 8**,** 249-56.

Wenz, T., Wang, X., Marini, M.Moraes, C. T. 2011. A metabolic shift induced by a PPAR panagonist markedly reduces the effects of pathogenic mitochondrial tRNA mutations. *J Cell Mol Med,* 15**,** 2317-25.

Wenz, T., Williams, S. L., Bacman, S. R.Moraes, C. T. 2010. Emerging therapeutic approaches to mitochondrial diseases. *Dev Disabil Res Rev,* 16**,** 219-29.

Weraarpachai, W., Antonicka, H., Sasarman, F., Seeger, J., Schrank, B., Kolesar, J. E., Lochmuller, H., Chevrette, M., Kaufman, B. A., Horvath, R.Shoubridge, E. A. 2009. Mutation in TACO1, encoding a translational activator of COX I, results in cytochrome c oxidase deficiency and late-onset Leigh syndrome. *Nat Genet,* 41**,** 833-7.

White, R., Morganstein, D., Christian, M., Seth, A., Herzog, B.Parker, M. G. 2008. Role of RIP140 in metabolic tissues: connections to disease. *FEBS Lett,* 582**,** 39-45.

White, S. L., Collins, V. R., Wolfe, R., Cleary, M. A., Shanske, S., Dimauro, S., Dahl, H. H.Thorburn, D. R. 1999a. Genetic counseling and prenatal diagnosis for the mitochondrial DNA mutations at nucleotide 8993. *Am J Hum Genet,* 65**,** 474-82.

White, S. L., Shanske, S., Mcgill, J. J., Mountain, H., Geraghty, M. T., Dimauro, S., Dahl, H. H.Thorburn, D. R. 1999b. Mitochondrial DNA mutations at nucleotide 8993 show a lack of tissue- or age-related variation. *J Inherit Metab Dis,* 22**,** 899-914.

Wiesinger, H. 2001. Arginine metabolism and the synthesis of nitric oxide in the nervous system. *Prog Neurobiol,* 64**,** 365-91.

Wijers, S. L., Schrauwen, P., Saris, W. H.Van Marken Lichtenbelt, W. D. 2008. Human skeletal muscle mitochondrial uncoupling is associated with cold induced adaptive thermogenesis. *PLoS One,* 3**,** e1777.

Wikstrom, J. D., Twig, G.Shirihai, O. S. 2009. What can mitochondrial heterogeneity tell us about mitochondrial dynamics and autophagy? *Int J Biochem Cell Biol,* 41**,** 1914-27.

Wilichowski, E., Korenke, G. C., Ruitenbeek, W., De Meirleir, L., Hagendorff, A., Janssen, A. J., Lissens, W.Hanefeld, F. 1998. Pyruvate dehydrogenase complex deficiency and altered respiratory chain function in a patient with Kearns-Sayre/MELAS overlap syndrome and A3243G mtDNA mutation. *J Neurol Sci,* 157**,** 206-13.

Woese, C. R., Kandler, O.Wheelis, M. L. 1990. Towards a natural system of organisms: proposal for the domains Archaea, Bacteria, and Eucarya. *Proc Natl Acad Sci U S A,* 87**,** 4576-9.

Wollen Steen, K., Doseth, B., M, P. W., Akbari, M., Kang, D., Falkenberg, M.Slupphaug, G. 2012. mtSSB may sequester UNG1 at mitochondrial ssDNA

and delay uracil processing until the dsDNA conformation is restored. *DNA Repair (Amst),* 11**,** 82-91.

Wong, L. J. 2007. Pathogenic mitochondrial DNA mutations in protein-coding genes. *Muscle Nerve,* 36**,** 279-93.

Wong, L. J., Wong, H.Liu, A. 2002. Intergenerational transmission of pathogenic heteroplasmic mitochondrial DNA. *Genet Med,* 4**,** 78-83.

Wong, T. W.Clayton, D. A. 1985. In vitro replication of human mitochondrial DNA: accurate initiation at the origin of light-strand synthesis. *Cell,* 42**,** 951-8.

Wu, Z., Puigserver, P., Andersson, U., Zhang, C., Adelmant, G., Mootha, V., Troy, A., Cinti, S., Lowell, B., Scarpulla, R. C.Spiegelman, B. M. 1999. Mechanisms controlling mitochondrial biogenesis and respiration through the thermogenic coactivator PGC-1. *Cell,* 98**,** 115-24.

Wydro, M., Bobrowicz, A., Temperley, R. J., Lightowlers, R. N.Chrzanowska-Lightowlers, Z. M. 2010. Targeting of the cytosolic poly(A) binding protein PABPC1 to mitochondria causes mitochondrial translation inhibition. *Nucleic Acids Res,* 38**,** 3732-42.

Xin, H., Woriax, V., Burkhart, W.Spremulli, L. L. 1995. Cloning and expression of mitochondrial translational elongation factor Ts from bovine and human liver. *J Biol Chem,* 270**,** 17243-9.

Xu, F., Morin, C., Mitchell, G., Ackerley, C.Robinson, B. H. 2004. The role of the LRPPRC (leucine-rich pentatricopeptide repeat cassette) gene in cytochrome oxidase assembly: mutation causes lowered levels of COX (cytochrome c oxidase) I and COX III mRNA. *Biochem J,* 382**,** 331-6.

Xu, Y., Krishnan, A., Wan, X. S., Majima, H., Yeh, C. C., Ludewig, G., Kasarskis, E. J.St Clair, D. K. 1999. Mutations in the promoter reveal a cause for the reduced expression of the human manganese superoxide dismutase gene in cancer cells. *Oncogene,* 18**,** 93-102.

Yakubovskaya, E., Mejia, E., Byrnes, J., Hambardjieva, E.Garcia-Diaz, M. 2010. Helix unwinding and base flipping enable human MTERF1 to terminate mitochondrial transcription. *Cell,* 141**,** 982-93.

Yang, C., Curth, U., Urbanke, C.Kang, C. 1997. Crystal structure of human mitochondrial single-stranded DNA binding protein at 2.4 A resolution. *Nat Struct Biol,* 4**,** 153-7.

Yang, M. Y., Bowmaker, M., Reyes, A., Vergani, L., Angeli, P., Gringeri, E., Jacobs, H. T.Holt, I. J. 2002. Biased incorporation of ribonucleotides on the mitochondrial L-strand accounts for apparent strand-asymmetric DNA replication. *Cell,* 111**,** 495-505.

Yasukawa, T., Reyes, A., Cluett, T. J., Yang, M. Y., Bowmaker, M., Jacobs, H. T.Holt, I. J. 2006. Replication of vertebrate mitochondrial DNA entails transient ribonucleotide incorporation throughout the lagging strand. *EMBO J,* 25**,** 5358-71.

Yasukawa, T., Yang, M. Y., Jacobs, H. T.Holt, I. J. 2005. A bidirectional origin of replication maps to the major noncoding region of human mitochondrial DNA. *Mol Cell,* 18**,** 651-62.

Young, J. C., Hoogenraad, N. J.Hartl, F. U. 2003. Molecular chaperones Hsp90 and Hsp70 deliver preproteins to the mitochondrial import receptor Tom70. *Cell,* 112**,** 41-50.

Yu-Wai-Man, P.Chinnery, P. F. 2012. Dysfunctional mitochondrial maintenance: what breaks the circle of life? *Brain,* 135**,** 9-11.

Yu-Wai-Man, P., Griffiths, P. G., Gorman, G. S., Lourenco, C. M., Wright, A. F., Auer-Grumbach, M., Toscano, A., Musumeci, O., Valentino, M. L., Caporali, L., Lamperti, C., Tallaksen, C. M., Duffey, P., Miller, J., Whittaker, R. G., Baker, M. R., Jackson, M. J., Clarke, M. P., Dhillon, B., Czermin, B., Stewart, J. D., Hudson, G., Reynier, P., Bonneau, D., Marques, W., Jr., Lenaers, G., Mcfarland, R., Taylor, R. W., Turnbull, D. M., Votruba, M., Zeviani, M., Carelli, V., Bindoff, L. A., Horvath, R., Amati-Bonneau, P.Chinnery, P. F. 2010. Multi-system neurological disease is common in patients with OPA1 mutations. *Brain,* 133**,** 771-86.

Zeharia, A., Shaag, A., Pappo, O., Mager-Heckel, A. M., Saada, A., Beinat, M., Karicheva, O., Mandel, H., Ofek, N., Segel, R., Marom, D., Rotig, A., Tarassov, I.Elpeleg, O. 2009. Acute infantile liver failure due to mutations in the TRMU gene. *Am J Hum Genet,* 85**,** 401-7.

Zhang, H., Barcelo, J. M., Lee, B., Kohlhagen, G., Zimonjic, D. B., Popescu, N. C.Pommier, Y. 2001. Human mitochondrial topoisomerase I. *Proc Natl Acad Sci U S A,* 98**,** 10608-13.

Zhang, H., Gao, P., Fukuda, R., Kumar, G., Krishnamachary, B., Zeller, K. I., Dang, C. V.Semenza, G. L. 2007. HIF-1 inhibits mitochondrial biogenesis and cellular respiration in VHL-deficient renal cell carcinoma by repression of C-MYC activity. *Cancer Cell,* 11**,** 407-20.

Zhang, H.Pommier, Y. 2008. Mitochondrial topoisomerase I sites in the regulatory D-loop region of mitochondrial DNA. *Biochemistry,* 47**,** 11196-203.

Zhang, Y.Spremulli, L. L. 1998. Identification and cloning of human mitochondrial translational release factor 1 and the ribosome recycling factor. *Biochim Biophys Acta,* 1443**,** 245-50.

Zheng, L., Zhou, M., Guo, Z., Lu, H., Qian, L., Dai, H., Qiu, J., Yakubovskaya, E., Bogenhagen, D. F., Demple, B.Shen, B. 2008. Human DNA2 is a mitochondrial nuclease/helicase for efficient processing of DNA replication and repair intermediates. *Mol Cell,* 32**,** 325-36.

Zhu, D. P., Economou, E. P., Antonarakis, S. E.Maumenee, I. H. 1992. Mitochondrial DNA mutation and heteroplasmy in type I Leber hereditary optic neuropathy. *Am J Med Genet,* 42**,** 173-9.

Ziebarth, T. D., Gonzalez-Soltero, R., Makowska-Grzyska, M. M., Nunez-Ramirez, R., Carazo, J. M.Kaguni, L. S. 2010. Dynamic effects of cofactors and DNA on the oligomeric state of human mitochondrial DNA helicase. *J Biol Chem,* 285**,** 14639-47.

Zollo, O., Tiranti, V.Sondheimer, N. 2012. Transcriptional requirements of the distal heavy-strand promoter of mtDNA. *Proc Natl Acad Sci U S A,* 109**,** 6508-12.